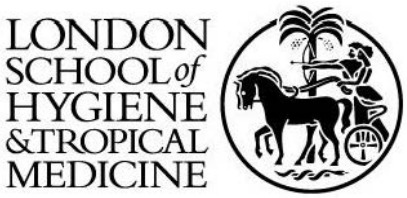


# Investigation of *Campylobacter jejuni* Modulation of Host Defence Mechanisms in Human Intestinal Epithelial Cells

**Geunhye Hong**

Thesis submitted in accordance with the requirements for the degree of
Doctor of Philosophy
of the
University of London

July 2023

**Department of Infection Biology**

**Faculty of Infectious and Tropical Diseases**

**LONDON SCHOOL OF HYGIENE & TROPICAL MEDICINE**

Funding details - No funding received

## Declaration

I, Geunhye Hong, confirm that the work presented in this thesis is my own. Where information has been derived from other sources, I confirm that this has been indicated in the thesis.

## Abstract

*Campylobacter jejuni* is one of the major bacterial causes of foodborne gastroenteritis worldwide. Despite this health burden, how *C. jejuni* interacts with the intrinsic defence mechanisms of intestinal epithelial cells (IECs) remains elusive. To address this, an initial investigation into how *C. jejuni* counteracts reactive oxygen species (ROS) was undertaken. *C. jejuni* was shown to differentially regulate ROS production in T84 and Caco-2 IECs. *C. jejuni* downregulated NAPDH oxidase (NOX1), a key ROS-generating enzyme in IECs. Furthermore, inhibition of NOX1 by either diphenyleneiodonium chloride (DPI) or siRNA transfection reduced *C. jejuni* pathogenesis within IECs. Both DPI treatment and siRNA transfection resulted in reduced fibronectin, a glycoprotein in extracellular matrix. These findings provide mechanistic insight into how *C. jejuni* modulates the ROS-related host defence mechanisms. A further investigation was performed into the potential mechanism of *C. jejuni*-mediated inflammation. Intestinal inflammation is associated with the unfolded protein response (UPR), a pathway involved in ER homeostasis. *C. jejuni* was shown to activate the PERK, IRE1α and ATF6 pathways in IECs in a strain- and cell line-dependent manner. Capsular polysaccharide, flagella and FlpA adhesin were shown to have a role during PERK pathway activation. The impact of the UPR on *C. jejuni* pathogenesis in IECs was also investigated. Pre-treatment with thapsigargin reduced *C. jejuni* intracellular survival whilst pre-treatment with UPR inhibitors increased intracellular *C. jejuni* numbers in IECs. The relationship between the UPR and inflammation was further investigated. *C. jejuni*-mediated interleukin-8 (IL-8) secretion was decreased with pre-treatment with the PERK inhibitor GSK2656157 and the IRE1α kinase/RNase inhibitor KIRA6. In contrast, pre-treatment with the IRE1α RNase inhibitor STF-083010 increased *C. jejuni*-mediated IL-8 secretion. In addition, *C. jejuni*-mediated UPR activation was independent of the increase in intracellular free calcium. These findings will form the basis for understanding the mechanisms of *C. jejuni*-induced UPR and UPR-mediated inflammation. Collectively, this study investigating *C. jejuni*-induced NOX1 modulation and UPR activation in human IECs provides exploration of survival mechanisms of *C. jejuni* within human IECs and pathogenic mechanisms which may lead to *C. jejuni*-induced inflammatory diarrhoea.

## Table of Contents

## Acknowledgement

Firstly, I would like to express my deepest gratitude to my PhD supervisors, Professor Nick Dorrell and Dr Ozan Gundogdu for giving me the opportunity to work on this project. Thank you Nick for all the guidance and support during my PhD journey. Thank you Ozan for all the guidance, encouragement and for treating me to endless of nice flat whites and raspberry bakewells. I would also like to thank Dr Abdi Elmi for his constructive advice and providing me cell culture training. Thank you Abdi for your support and inspiration.

It has been an amazing experience working with both past and present members of the *Campylobacter* research group. I would like to extend my sincere thanks to my lab mates Dr Janie Liaw, Dr Cadi Davies and Zahra Omole. I cannot thank you enough for walking with me throughout this journey. Your friendship and support have added a lot to this journey and my life. I would also like to thank Dr Banaz Star-Shirko, Dr Fauzy Nasher and Dr Sherif Abouelhadid for their help and support.

I am also thankful to Professor Brendan Wren and everyone from the Wren group I have worked with and from whom I have learned so much. I would particularly like to thank Dr Vanessa Terra and Dr Catherine Hall for their help and support. I would also like to thank Dr Marta Mauri for her advice on siRNA transfection and Dr Anna D. Grabowska at Medical University of Warsaw for her advice and guidance on mutant construction.

Words cannot express my gratitude to my parents Hwagyun Hong and Sugyeong Jeong for their unconditional love and unlimited support which keep me motivated and confident. Deepest thanks to my sister Minhye Hong and my brother-in-law Jung Hyun Kim for their support throughout this journey. Many thanks to Mocha for being such a good dog and always cheering me up. I would also like to thank my partner Sungwhan Park for his support and for always being there for me. Special thanks to my friend Min Jung Kim who has always supported and encouraged me. I would also like to thank Fr Mun Kwon Hyun and Sr Paulina for their prayers and support.

# List of abbreviations

| | |
|---|---|
| -/- | Knockout |
| % | Percentage |
| °C | Degree Celsius |
| x g | Times gravity |
| 5’ | 5 prime |
| 3’ | 3 prime |
| α | Alpha |
| β | Beta |
| µg | Microgram |
| µM | Micromolar |
| ADP | Adenosine diphosphate |
| ALPK1 | Alpha-kinase 1 |
| APR | Acute phase response |
| ATF4 | Activating transcription factor 4 |
| ATF6 | Activating transcription factor 6 |
| ATP | Adenosine triphosphate |
| BA | Blood agar |
| BCA | Bicinchoninic acid |
| BiP | Binding-immunoglobulin protein |
| BMDM | Bone marrow-derived macrophages |
| bp | Base pair |
| BSA | Bovine serum albumin |
| BSS | Buffered saline solution |
| $Ca^{2+}$ | Calcium ion |
| CARD | Caspase recruitment domains |
| CAT | Catalase |
| CCV | *Campylobacter*-containing vacuole |
| cDNA | Complementary deoxyribonucleic acid |
| CDT | Cytolethal distending toxin |
| CFU | Colony-forming units |
| CHOP | C/EBP homologous protein |
| Cia | *Campylobacter* invasion antigen |
| $Cm^r$ | Chloramphenicol resistance |

| | |
|---|---|
| $CO_2$ | Carbon dioxide |
| CREBH | Cyclic AMP-responsive element-binding protein H |
| $C_T$ | Threshold cycle |
| DAMP | Damage-associated molecular pattern |
| DEPC | Diethyl pyrocarbonate |
| DMEM/F-12 | Dulbecco's modified Eagle's medium and Ham's F-12 medium |
| DNA | Deoxyribonucleic acid |
| DNase | Deoxyribonuclease |
| dNTP | Deoxynucleoside triphosphate |
| DPI | Diphenylene iodonium |
| DTT | Dithiothreitol |
| EBF | Electroporation buffer |
| ECDC | European Centre for Disease Prevention and Control |
| EDTA | Ethylenediaminetetraacetic acid |
| EFSA | European Food Safety Authority |
| EGF | Epidermal growth factor |
| EGFR | Epidermal growth factor receptor |
| eIF2α | Eukaryotic translation initiation factor 2α |
| ELISA | Enzyme-linked immunosorbent assay |
| ENaC | Epithelial sodium channel |
| ER | Endoplasmic reticulum |
| ERAD | ER-associated degradation |
| ERK | Extracellular signal-regulated kinase |
| $Ery^r$ | Erythromycin resistance |
| FAD | Flavin adenine dinucleotide |
| FAK | Focal adhesion kinase |
| FBS | Foetal bovine serum |
| FPR | Formyl peptide receptor |
| FSA | Food Standards Agency |
| g | Gram |
| GADD34 | Growth arrest and DNA damage inducible 34 |
| GAPDH | Glyceraldehyde 3-phosphate dehydrogenase |
| GBS | Guillain-Barré syndrome |
| gDNA | Genomic deoxyribonucleic acid |
| GTP | Guanosine triphosphate |
| GRP78 | Glucose-regulated protein 78 |

| | |
|---|---|
| $H_2O_2$ | Hydrogen peroxide |
| HCMV | Human cytomegalovirus |
| HIC | High income countries |
| HRP | Horseradish peroxidase |
| IBS | Irritable bowel syndrome |
| IEC | Intestinal epithelial cell |
| iE-DAP | intracellular γ-D-glutamyl-meso-diaminopimelic acid |
| IFN | Interferon |
| IKK | IκB kinase |
| IL-6 | Interleukin-6 |
| IL-8 | Interleukin-8 |
| IL-12 | Interleukin-12 |
| IL-17 | Interleukin-17 |
| IL-25 | Interleukin-25 |
| IQGAP1 | IQ motif containing GTPase activating protein 1 |
| IRE1α | Inositol-requiring enzyme 1α |
| IRF3 | Interferon regulatory factor 3 |
| IRF7 | Interferon regulatory factor 7 |
| JEV | Japanese encephalitis virus |
| JNK | c-Jun N-terminal kianse |
| $Kan^r$ | Kanamycin resistance |
| kb | Kilobase |
| kDa | Kilodalton |
| L1 | Left fragment |
| LB | Lysogeny broth |
| LDH | Lactate dehydrogenase |
| LGP2 | Laboratory of genetics and physiology 2 |
| LMIC | Low- and middle-income countries |
| LOS | Lipooligosaccharide |
| LPS | Lipopolysaccharide |
| M | Molar |
| mA | Milliampere |
| MAPK | Mitogen-activated protein kinase |
| MAVS | Mitochondrial antiviral signaling proteins |
| M cells | Microfold cells |
| MDA5 | Melanoma differentiation-associated gene 5 |

| | |
|---|---|
| MDP | Muramyl dipeptide |
| $MgCl_2$ | Magnesium chloride |
| ml | Millilitre |
| MLA | Maintenance of lipid asymmetry |
| mM | Millimolar |
| MOI | Multiplicity of infection |
| mRNA | Messenger ribonucleic acid |
| miRNA | MicroRNA |
| Myd88 | Myeloid differentiation primary response protein 88 |
| N | Normality |
| $N_2$ | Nitrogen |
| $Na^+$ | Sodium ion |
| NaCl | Sodium chloride |
| NCTC | National Collection of Type Cultures |
| NF-κB | Nuclear factor kappa light chain enhancer of activated B cells |
| NADPH | Nicotinamide adenine dinucleotide phosphate |
| nm | Nanometer |
| nM | Nanomolar |
| NMR | Nuclear magnetic resonance |
| NOD | Nucleotide-binding oligomerization domain |
| NOX | Nicotinamide adenine dinucleotide phosphate oxidase |
| NOXA1 | Nicotinamide adenine dinucleotide phosphate oxidase activator 1 |
| NOXO1 | Nicotinamide adenine dinucleotide phosphate oxidase organizer 1 |
| NLRP3 | NOD-, LRR- and pyrin domain-containing protein 3 |
| $O_2$ | Oxygen |
| $O_2^-$ | Superoxide |
| OD | Optical density |
| OMV | Outer membrane vesicle |
| PBS | Phosphate buffered saline |
| PCR | Polymerase chain reaction |
| PDGF | Platelet-derived growth factor (PDGF) |
| PERK | Protein kinase R-like ER kinase |
| PI3K | Phosphatidylinositol-3-kinase |
| PRR | Pattern recognition receptor |
| PTEN | Phosphatase and tensin homologue deleted on chromosome 10 |
| PTP | Protein tyrosine phosphatase |

| | |
|---|---|
| qRT-PCR | Quantitative reverse transcription polymerase chain reaction |
| R1 | Right fragment |
| RIDD | Regulated IRE1-dependent degradation |
| RIG-I | Retinoic acid-inducible gene I |
| RIPK2 | Receptor-interacting protein kinase 2 |
| RLR | Retinoic acid-inducible gene I-like receptor |
| RNA | Ribonucleic acid |
| RNase | Ribonuclease |
| ROS | Reactive oxygen species |
| rpm | Revolutions per minute |
| RT-PCR | Reverse transcription polymerase chain reaction |
| S1P | Site 1 protease |
| S2P | Site 2 protease |
| siRNA | Small interfering RNA |
| SOC | Super optimal broth |
| SOD | Superoxide dismutase |
| SOE PCR | Splicing by overlap extension polymerase chain reaction |
| T3SS | Type III secretion system |
| T4SS | Type IV secretion system |
| T5SS | Type V secretion system |
| T6SS | Type VI secretion system |
| T7SS | Type VII secretion system |
| TAE | Tris-acetate-ethylenediaminetetraacetic acid |
| TAK | Transforming growth factor β-activated kinase 1 |
| Tg | Thapsigargin |
| TGF | Transforming growth factor |
| TIFA | TRAF-interacting protein with forkhead-associated domain |
| TIR | Toll/IL-R |
| TIRAP | Toll/IL-R domain-containing adapter protein |
| TLR1 | Toll-like receptor 1 |
| TLR2 | Toll-like receptor 2 |
| TLR3 | Toll-like receptor 3 |
| TLR4 | Toll-like receptor 4 |
| TLR5 | Toll-like receptor 5 |
| TLR6 | Toll-like receptor 6 |
| TLR7 | Toll-like receptor 7 |

| | |
|---|---|
| TLR8 | Toll-like receptor 8 |
| TLR9 | Toll-like receptor 9 |
| Tm | Melting temperature |
| TMB | tetramethylbenzidine |
| TNF-α | Tumour necrosis factor-alpha |
| TRAF2 | Tumour necrosis factor receptor associated factor 2 |
| TRIF | Toll/IL-R domain-containing adapter protein-inducing interferon-beta |
| TRAM | TRIF-related adapter molecule |
| Tris-HCl | Tris(hydroxymethyl)aminomethane hydrochloride |
| TXNIP | Thioredoxin-interacting protein |
| U | Unit |
| UK | United Kingdom |
| UPR | Unfolded protein response |
| USA | United States of America |
| V | Volt |
| v/v | Volume per volume |
| VBNC | Viable but non-culturable cells |
| w/v | Weight per volume |
| XBP1 | X-box-binding protein 1 |

# CHAPTER ONE: Introduction

## 1.1. *Campylobacter jejuni*

### 1.1.1. General characteristics

*Campylobacter jejuni* belongs to the genus *Campylobacter*, the family *Campylobacteraceae*, and the order *Campylobacterales* in the class *Epsilonproteobacteria* (Vandamme et al., 2015). *C. jejuni* is a major bacterial causative agent of human gastroenteritis worldwide (Kaakoush et al., 2015). A Gram-negative bacterium, *C. jejuni* is motile by use of either a single polar flagellum or bipolar flagella with size ranges from 0.2 to 0.8 μm wide by 0.5 to 5 μm long (Vandamme, 2000). *C. jejuni* mainly displays a spiral- or a curved, rod-shaped morphology but can become viable but non-culturable (VBNC) coccoid under unfavourable environmental conditions (Beumer, de Vries, & Rombouts, 1992). *C. jejuni* is microaerophilic and grows optimally in 5% $O_2$, 10% $CO_2$ and 85% $N_2$ (Lindsay Davis & DiRita, 2008). *C. jejuni* is able to grow at temperatures ranging from 30°C to 45°C, but the optimum growth temperature ranges from 37°C to 42°C which is the core body temperature of human and avian species respectively (Lindsay Davis & DiRita, 2008; Park, 2002). Short-chain fatty acids, citric acid cycle intermediates and certain amino acids are the major energy source for *C. jejuni* (Stahl, Butcher, & Stintzi, 2012).

### 1.1.2. Disease

Upon exposure to an infectious dose of as little as 500-800 colony forming units (CFU), *Campylobacter* can cause watery or bloody diarrhoea, muscle and joint pain, vomiting, abdominal pain and fever (Black et al., 1988; FSA, 2021; Kaakoush et al., 2015). These clinical symptoms can vary depending on socioeconomic status. In high income countries (HIC), infected people experience inflammatory and bloody diarrhoea (FSA, 2021). Whereas, asymptomatic infection is more common in low- and middle-income countries (LMIC) which might be due to developed immunity from previous exposures to *C. jejuni* (Havelaar et al., 2009). However, children in LMICs are frequently infected with *C. jejuni* which can lead to developmental deficits and even death (Amour et al., 2016; Platts-Mills & Kosek, 2014).

As the infection is usually self-limiting, antibiotics are only used to treat severe illness and immunocompromised people (FSA, 2021). Immunocompromised or elderly people may require hospitalisation and even die due to the illness. Campylobacteriosis can also lead to post-infectious irritable bowel syndrome (IBS) (Spiller & Garsed, 2009). A previous study showed that approximately 9-13% of *C. jejuni*-infected people developed IBS (Spiller & Garsed, 2009; Thornley et al., 2001). In addition, campylobacteriosis is associated with the rare but severe complication, Gullain-Barré syndrome (GBS) and Miller-Fisher syndrome which are autoimmune diseases of the peripheral nervous system (Nowshin Papri et al., 2021).

### 1.1.3. Epidemiology and Transmission

*C. jejuni* is the leading bacterial cause of human intestinal illness worldwide resulting in significant economic burden costing the United Kingdom (UK) approximately £1.8 billion annually (FSA, 2013; Kaakoush et al., 2015). According to the Food Standards Agency (FSA), there are around 300,000 cases of human campylobacteriosis each year in the UK (FSA, 2021). The UK infection rate of *Campylobacter* in 2019 was 88.1 cases per 100,000 population in 2019 (EFSA & ECDC, 2021). In European countries, 220,682 confirmed cases (59.7 cases per 100,000 population) of human campylobacteriosis were reported in 2019 (EFSA & ECDC, 2021). In 2018, *Campylobacter* was responsible for the most GP presentations and hospital admissions of diarrhoea followed by norovirus and *Clostridium perfringens* in the UK (FSA, 2020). *Campylobacter* also resulted in the highest number of hospitalisations in the EU in 2019 compared with other foodborne pathogens (EFSA & ECDC, 2021). The pattern of human campylobacteriosis displays seasonality with the highest peak during the summer and the lowest peak during the winter (FSA, 2021). In addition, the age/gender group with highest infection in the UK is male aged between 50 and 59 (FSA, 2021).

The major route of transmission of human *Campylobacter* infection is cross-contamination or consumption of raw or undercooked poultry especially chicken meat (Kaakoush et al., 2015). A recent study showed that chicken meat is responsible for approximately 70% of human campylobacteriosis (FSA, 2019). Testing conducted on UK chicken retailers between April and June 2019 indicated that 37.4% of chickens were carrying between 10 to 1,000 CFU/g of *Campylobacter* and 3.6% of chickens were carrying more than 1,000 CFU/g (FSA, 2019). There are also other routes of transmission, such as contact with animals and consumption of unpasteurised milk, contaminated ruminant meat or untreated water (Kaakoush et al., 2015). In addition, contact with pet store puppies has been associated with outbreaks of extensively drug-resistant *C. jejuni* (Francois Watkins et al., 2021).

## 1.2. *C. jejuni* virulence determinants

### 1.2.1. Flagella

*C. jejuni* possesses uni- or bi-polar flagella allowing bacterial motility. *C. jejuni* flagella are comprised of a basal body and filament which are connected by a hook (Hughes & Chevance, 2008; Young, Davis, & DiRita, 2007). The filament consists of major flagellin FlaA and minor flagellin FlaB proteins (Guerry, 2007). Expression of these flagellar components is highly regulated by the $\sigma^{28}$ and $\sigma^{54}$ sigma factors which are encoded by *fliA* and *rpoN* respectively (Hendrixson, Akerley, & DiRita, 2001). The $\sigma^{28}$ sigma factor regulates expression of *flaA* and the $\sigma^{54}$ sigma factor regulates expression of *flaB* and genes encoding the basal body and hook proteins (Guerry et al., 1991). FlgSR is a well-characterised two-component regulatory system in flagellar biogenesis (Burnham & Hendrixson, 2018). Upon signalling, cytoplasmic FlgS undergoes autophosphorylation and activates a response regulator FlgR. Phosphorylated FlgR activates a RNA polymerase associated with the $\sigma^{54}$ sigma factor. Both FlgSR and the $\sigma^{54}$ sigma factor are involved in expression of the $\sigma^{28}$ sigma factor (Boll & Hendrixson, 2013). Flagellar Type III secretion system (T3SS) transports flagellar proteins to localise flagella in *C. jejuni*. In addition, expression of flagellar T3SS components is required for the $\sigma^{54}$ sigma factor-dependent gene expression. Interaction between flagellin and flagellar proteins FliW and FliS is important for biogenesis of flagellin (Radomska et al., 2017). It was also noted that *flgS* and *flgR* as well as *motA* which encodes the motor stator exhibited phase variation which is caused during replication where slipped-strand mispairing is frequent in regions harbouring homopolymeric sequences (Burnham & Hendrixson, 2018; Hendrixson, 2006; Parkhill et al., 2000). *C. jejuni* facilitates motility by wrapping one of polar filaments around helical shaped cell body and changes directions by wrapping and unwrapping polar filaments (Cohen et al., 2020).

*C. jejuni* flagella is a key determinant for intestinal colonisation and invasion (Grant et al., 1993; Ren et al., 2018). Previous studies have demonstrated that *C. jejuni* flagellar T3SS secretes *Campylobacter* invasion antigen (Cia) proteins (CiaC and CiaD), and flagellin protein FlaC to facilitate bacterial invasion to host cell (Neal-McKinney & Konkel, 2012; Negretti et al., 2021; Song et al., 2004). Chemotaxis is important for *C. jejuni* adaptation to various environments especially in host cells and *C. jejuni* flagella are involved in this process (Chandrashekhar, Kassem, & Rajashekara, 2017). A two-component regulatory system in *C. jejuni* chemotaxis is comprised of CheA and CheY which are histidine kinase and response regulator proteins respectively. When a membrane-bound CheA detects a chemoeffector, CheA autophosphorylates and phosphorylates CheY. Then interaction between phosphorylated CheY and flagellar motor proteins FliM and FliN regulates the rotational direction of flagella. *C. jejuni* chemorepellents include most constituents of bile and chemoattractants include mucin, L-fucose, a range of amino acids (e.g. L-aspartate, L-cysteine, L-glutamate, L-serine) and organic acids (pyruvate, succinate and fumarate) (Chandrashekhar, Kassem, & Rajashekara, 2017). Furthermore,

studies demonstrated flagella play an important role in biofilm formation (Reeser et al., 2007; Ren et al., 2018).

Bacterial flagellum is one of the main pathogen-associated molecular patterns detected by host immune systems. However, *C. jejuni* flagella evade Toll-like receptor 5 (TLR5) surveillance by mutation in the TLR5 epitope (Andersen-Nissen et al., 2005). A previous study on the atomic structure of *C. jejuni* flagella revealed that the TLR5 epitope within the *C. jejuni* flagella showed weaker interaction with the adjacent filament which is different from the TLR5 epitopes of other enteric bacterial flagella (Kreutzberger et al., 2020).

### 1.2.2. Lipooligosaccharide

Most Gram-negative bacteria possess lipopolysaccharide (LPS) which is comprised of lipid A, core polysaccharide structure and O-antigen. *C. jejuni* has lipooligosaccharide (LOS) which is structurally similar to LPS but lacking O-antigen (Hameed et al., 2020; Moran, 1997). *C. jejuni* LOS has a role in antibiotic resistance, serum resistance, and adherence and invasion to host cells (Hameed et al., 2020). Genes involved in synthesis of LOS inner core structure are conserved among *C. jejuni* strains. Whereas genes for the outer core structure exhibit inter-strain variation resulting in variable outer core structures among *C. jejuni* strains (Hameed et al., 2020). *C. jejuni* LOS synthesis genes are phase variable which contributes to intra-strain variation in LOS structure (Dorrell et al., 2001; Parkhill et al., 2000). Studies revealed that *C. jejuni*-mediated autoimmune disease GBS is associated with phase variation of LOS synthesis genes (Guerry et al., 2002; Linton et al., 2000). Both *wlaN* and *cgtA* encoding a beta-1,3 galactosyltransferase and a *N*-acetylgalactosaminyltransferase respectively, are hypervariable resulting in production of different outer core structures similar to GM1, GM2 or GM3 gangliosides (Guerry et al., 2002; Linton et al., 2000).

### 1.2.3. Capsular polysaccharide

Sequencing analysis of *C. jejuni* NCTC 11168 genome first revealed the presence of a capsular polysaccharide gene cluster (Karlyshev et al., 1999; Karlyshev et al., 2000; Parkhill et al., 2000). Electron microscopy further allowed visualisation of the *C. jejuni* capsule following staining with Alcian blue dye (Karlyshev, McCrossan, & Wren, 2001). In early studies, it was thought that heat stable LOS accounted for Penner serotyping of *C. jejuni* (Aspinall et al., 1993; Nam Shin et al., 1997). However, after the finding of capsular polysaccharide of *C. jejuni*, it has been shown that Penner serotyping is actually based on capsular polysaccharide (Karlyshev et al., 2000; Penner, Hennessy, & Congi, 1983). Whole genome DNA microarray analysis demonstrated the region of capsular polysaccharide of *C. jejuni* is conserved within strains with the same serotype confirming *C. jejuni* Penner serotyping is based on the capsule (Dorrell et al., 2001). In addition to genes involved in synthesis of flagella and LOS, capsular polysaccharide gene clusters are phase variable which might be

reflected by environment stimuli and host responses (Bacon et al., 2001). *C. jejuni* capsule plays a role in invasion of intestinal epithelial cells (IECs), serum resistance and host immune responses involving TLR activation and interleukin-17 (IL-17) release (Bacon et al., 2001; Maue et al., 2013).

### 1.2.4. Glycosylation

*C. jejuni* possesses two types of glycosylation system, *O*-linked and *N*-linked glycosylation (Szymanski et al., 2003). *O*-linked glycosylation is involved in post-translational modification of *C. jejuni* flagella. Serine and threonine residues in surfaced exposed region of *C. jejuni* 81-176 flagellin are modified by addition of pseudaminic acid (Thibault et al., 2001). There is variation in the flagellar glycosylation locus between *C. jejuni* strains. *C. jejuni* NCTC 11168 contains seven motility accessory factor genes (*maf*) which are likely involved in flagellin modification (Karlyshev et al., 2002). *C. jejuni* 81-176 lacks two *maf* genes and several post-translational modification genes, such as *neuB2* (*Cj1327*) and *neuC2* (*Cj1328*) which are found in *C. jejuni* NCTC 11168 and *C. coli* (Guerry et al., 2006; Logan et al., 2002).

In contrast, genes for *N*-linked glycosylation are conserved within *Campylobacter* genus (Szymanski et al., 2003). Genes in protein glycosylation (*pgl*) locus encode the proteins that are responsible for *N*-linked glycosylation of *C. jejuni* proteins (Szymanski et al., 1999). Enzymes encoded by the *pgl* locus are involved in glycan synthesis and transferring this to the asparagine residue in the Asn-Xaa-Ser/Thr sequon. PglB is an oligosaccharyltransferase which is essential for *N*-linked glycosylation (Linton et al., 2005; Szymanski et al., 2003). Studies have demonstrated potential roles for *N*-glycosylation in bacterial fitness and host-bacteria interactions (Alemka et al., 2013; Karlyshev et al., 2004; Wacker et al., 2002). Mutation of *pglB* failed to protect *C. jejuni* from gut proteases and resulted in reduced growth. This indicates *N*-linked glycoproteins on the surface of *C. jejuni* enhance bacterial survival within the host gut (Alemka et al., 2013). In addition, disruption of *pglB* resulted in reduced reactivity against *C. jejuni* antiserum suggesting immunogenicity of glycan site of glycoproteins (Wacker et al., 2002). It is also shown that *N*-glycosylation is an important factor for efficient adherence to human IECs and colonisation in a chick model (Karlyshev et al., 2004). Because of the ability of *pgl* system to transfer various glycan structures to a protein in site-specific way, *C. jejuni* PglB has been used for development of glycoconjugate vaccines (Kay, Cuccui, & Wren, 2019).

### 1.2.5. Cytolethal distending toxin

A novel toxin activity of *Escherichia coli* was first discovered in 1987 (Johnson & Lior, 1987b). Johnson and Lior observed a distinct toxin activity which resulted in distended cell morphology of Chinese hamster ovary cells infected with *E. coli* and they termed this toxin cytolethal distending toxin (CDT) (Johnson & Lior, 1987b). Further studies demonstrated that other enteric pathogens *Shigella dysenteriae* and the majority of *C. jejuni* strains also possesses CDT (Johnson & Lior, 1987a, 1988). CDT is an $AB_2$ holotoxin composed of three subunits, CdtA, CdtB and CdtC which are encoded by *cdtA*, *cdtB* and *cdtC*

respectively (Lara-Tejero & Galan, 2001; Pickett et al., 1996). All three components are required to exhibit maximal toxicity against host cells (Lee et al., 2003). Binding of CDT to host cells is facilitated by CdtA and CdtC which bind to cholesterol-rich lipid rafts (Boesze-Battaglia et al., 2009). CdtB exhibits deoxyribonuclease (DNase) I-like enzymatic activity which damages host DNA resulting in $G_2$/M phase arrest (He et al., 2019; Whitehouse et al., 1998). *In vitro* studies showed membrane-associated and/or secreted CDT activates pro-inflammatory cytokine IL-8 in human IECs (Hickey et al., 2000; Zheng et al., 2008). *In vivo* studies using NF-κB-deficient mice demonstrated that *C. jejuni* CDT is associated with host immune responses and severity of intestinal disease (Fox et al., 2004).

#### 1.2.6. Outer membrane vesicles

Outer membrane vesicles (OMVs) are spherical nanoparticles generated from the outer membrane of Gram-negative bacteria. The size of OMV ranges from 20 to 300 nm and secreted OMVs can fuse with membranes of target cells delivering contents into the target cells (Avila-Calderón et al., 2021). A bile acid sodium taurocholate modulates *C. jejuni* OMV biogenesis by regulating expression of components of the maintenance of lipid asymmetry (MLA) pathway (Davies et al., 2019). Proteomic analysis revealed that *C. jejuni* OMVs contain lipoproteins, *N*-linked glycoproteins including an adhesin Peb3, serine proteases Cj0511, Cj1365c and HtrA and CDT (Elmi et al., 2016; Elmi et al., 2012; Lindmark et al., 2009). OMV-associated Cj1365c and HtrA are involved in cleavage of E-cadherin and occludin which enhances *C. jejuni* invasiveness into human IECs (Elmi et al., 2016). *C. jejuni* OMVs are implicated in induction of proinflammation in human IECs showing increased expression of IL-8, IL-6, tumour necrosis factor-alpha (TNF-α) and beta defensin-3 (Elmi et al., 2012). Lindmark et al. demonstrated OMV-associated CDT resulted in cell cycle arrest and cellular distension indicating OMV-mediated delivery of active CDT into the target cells (Lindmark et al., 2009).

### 1.3. Mechanism of *C. jejuni* pathogenesis

#### 1.3.1. Adherence

The lack of convenient and inexpensive animal models which reproduce human gastroenteritis has limited the understanding of *C. jejuni* pathogenesis (Newell, 2001; Young, Davis, & DiRita, 2007). However, recent development of mouse models with genetic manipulation, antibiotic treatment or zinc- or protein-deficient diet mimic human diarrhoeal disease and these novel mouse models provides the better understanding of *C. jejuni* pathogenesis (Giallourou et al., 2018; Stahl et al., 2014).

Bacterial adherence to host cells is an essential step for successful colonisation and pathogenesis and is mediated by interactions between bacteria and host cells (Pizarro-Cerdá & Cossart, 2006). Surface structures fimbriae and pili in other enteric bacteria such as *E. coli* and *Salmonella* promote adherence to and invasion of host cells (Nougayrède, Fernandes, & Donnenberg, 2003; Zhang et al., 2000). Even though genes encoding pili synthesis are absent in *C. jejuni* (Young, Davis, & DiRita, 2007), *C. jejuni* possesses other surface structures to facilitate adherence to host cells, such as adhesins which bind to structures of the host extracellular matrix (Konkel et al., 2020). The extracellular matrix is comprised of collagen which maintains the integrity of the extracellular matrix and laminin and integrin which connect cells with the extracellular matrix and neighbouring cells (Bosman & Stamenkovic, 2003). External stimuli-induced integrin clustering and occupancy result in accumulation of signalling molecules which allows transduction of cellular signalling regulating cytoskeletal rearrangements (DeMali, Wennerberg, & Burridge, 2003). For example, integrin recognises fibronectin (an extracellular adhesive glycoprotein) and their interaction induces actin polymerisation (Miyamoto et al., 1998). Studies revealed that *C. jejuni* adhesins, FlpA, CadF, JlpA, PEB1, CapA and CapC play an important role in adherence to host cells (Ashgar et al., 2007; Del Rocio Leon-Kempis et al., 2006; Flanagan et al., 2009; Konkel et al., 1997; Mehat et al., 2018; Pei et al., 1998). FlpA and CadF possess fibronectin-binding domains which bind to fibronectin (Konkel et al., 1997; Konkel, Larson, & Flanagan, 2010). A lipoprotein JlpA binds to heat shock protein 90α of host cells leading to inflammation (Jin et al., 2001; Jin et al., 2003). PEB1 is an ABC transporter component which binds to aspartate/glutamate residues (Pei et al., 1998). CapA is an autotransporter protein which is shown to facilitate adherence to human IECs and chicken colonisation (Ashgar et al., 2007; Flanagan et al., 2009). Another autotransporter protein CapC has also been shown to be involved in binding to human IECs (Mehat et al., 2018). In addition to adhesins, *C. jejuni* capsule, LOS and flagella are also involved in adhesion to and further internalisation into host cells (Bacon et al., 2001; Grant et al., 1993; Hameed et al., 2020).

Mechanisms of *C. jejuni* interaction with host cells are associated with inter-strain variation in *C. jejuni*. *capA* encoding CapA is not found in all *C. jejuni* strains indicating different *C. jejuni* strains possess different strategies of adherence to host cells (Ashgar et al., 2007; Flanagan et al., 2009). Similarly,

CDT is not conserved among different *C. jejuni* strains (Jain et al., 2008). A previous study has demonstrated that CDT-positive and CDT-negative *C. jejuni* strains exhibited differences in adhesion and invasion efficiency in HeLa cells (Jain et al., 2008). Adherence and invasion of CDT-positive *C. jejuni* strains were significantly higher compared to CDT-negative *C. jejuni* strains (Jain et al., 2008). In addition, mice treated with supernatants of CDT-positive strains exhibited severe inflammation in the GI tract while mice treated with supernatants of CDT-negative strains showed mild inflammation (Jain et al., 2008). This study suggest different *C. jejuni* isolates possess unique mechanisms of adhesion and invasion resulting in different pathological outcomes.

### 1.3.2. Invasion

There exist two hypothetical mechanisms of bacterial internalisation termed zipper and trigger mechanisms (O Cróinín & Backert, 2012). The zipper mechanism involves binding of bacterial adhesins to host cells followed by invasion and the trigger mechanism involves secretion of effector proteins by bacterial secretion systems which triggers internalisation into the host cell (O Cróinín & Backert, 2012). *C. jejuni* internalisation exhibits characteristics of both mechanisms and is dependent on lipid rafts in the plasma membrane which are rich in cholesterol and sphingomyelin (Konkel et al., 2013; Rosenberger, Brumell, & Finlay, 2000; Wooldridge, Williams, & Ketley, 1996).

Binding of *C. jejuni* to fibronectin induces a signalling cascade resulting in activation of the small GTPase Rac1 and Cdc42 and cytoskeletal rearrangements (Eucker & Konkel, 2012; Krause-Gruszczynska et al., 2007). Binding to fibronectin activates integrin through integrin occupancy and clustering (Eucker & Konkel, 2012). Then focal adhesion kinase (FAK) is activated through interaction with β1 integrins. Activated FAK undergoes autophosphorylation inducing interaction with c-Src which is a tyrosine kinase. Activated c-Src then phosphorylates paxillin resulting in recruitment of guanine exchange factor Tiam-1 and Dock180 which activates Rac1-mediated actin cytoskeleton rearrangements and lamellipodia formation (Eucker & Konkel, 2012).

Activation of integrin, FAK, and c-Src also phosphorylates and activates epidermal growth factor (EGF) and platelet-derived growth factor (PDGF) receptors (Krause-Gruszczynska et al., 2011; Krause-Gruszczynska et al., 2007). Activation of EGF and PDFG receptors phosphorylates PI-3 kinase followed by stimulation of a guanine nucleotide exchange factor Vav2 which then activates Cdc42. Activated Cdc42 promotes filopodia formation enhancing *C. jejuni* invasion (Krause-Gruszczynska et al., 2011; Krause-Gruszczynska et al., 2007).

Interestingly, Cia proteins which are secreted via the *C. jejuni* flagellar T3SS are found to be involved in invasion (Konkel et al., 1999; Konkel et al., 2004). CiaB is translocated into human IECs and plays a role in the flagellar T3SS secretion which is involved in bacterial internalisation (Konkel et al., 1999). Studies have demonstrated CiaD activates Rac1 in human INT 407 cells (Krause-Gruszczynska et al.,

2007; Negretti et al., 2021). CiaD binds to IQ motif containing GTPase activating protein 1 (IQGAP1) to keep Rac1 active preventing interaction between IQGAP1 and RacGAP1 which reduces Rac1 activation (Negretti et al., 2021). CiaD also activates the extracellular signal-regulated kinase 1/2 (ERK 1/2) which then phosphorylates cortactin which results in actin cytoskeleton rearrangements and promotes internalisation of *C. jejuni* (Samuelson & Konkel, 2013). In addition to CiaD, CiaC facilitates host cytoskeletal rearrangement and is required for maximal invasion into human IECs (Neal-McKinney & Konkel, 2012).

*C. jejuni* transmigrates across a polarised epithelial cell barrier using either a transcellular mechanism or a paracellular mechanism (Backert et al., 2013). The transcellular mechanism is when *C. jejuni* invades the cell from the apical surface and exits at the basolateral surface of a polarised cell. The paracellular mechanism is characterised by *C. jejuni* disturbing tight junction proteins such as claudin and occludin as well as adherens junction proteins such as E-cadherin to migrate between adjacent cells (Backert et al., 2013). *C. jejuni* serine protease HtrA cleaves claudin and E-cadherin upon transmigration (Boehm et al., 2012; Sharafutdinov et al., 2020). In addition, cleavage of occludin and E-cadherin by OMV-associated HtrA and Cj1365c has been reported (Elmi et al., 2016). Transmigration to the basolateral surface of epithelial cells might be beneficial for *C. jejuni* to allow spread to other host cells and to allow protection from antibiotic treatment in the lumen (Backert et al., 2013).

### 1.3.3. Intracellular fate

After invasion of host IECs, *C. jejuni* is hypothesised to reside within a membrane-bound vacuole called the *Campylobacter*-containing vacuole (CCV) (Konkel et al., 1992; Watson & Galán, 2008). CCVs avoid the canonical endocytic pathway and prevent fusion with lysosomes. Early endosomal markers EEA-1, Rab4 and Rab5 are transiently associated with the CCV followed by transient co-localisation of late endosomal marker Rab7. CCVs interact with a late endosomal marker Lamp-1 independent of Rab5 and Rab7 and CCVs do not interact with a lysosomal marker cathepsin B which is a distinct mechanism of the canonical endocytic pathway (Watson & Galán, 2008). CCVs are translocated to the Golgi apparatus and perinuclear region along microtubules and dynein (Watson & Galán, 2008). Interestingly, a previous study demonstrated CiaI secreted by the flagellar T3SS is involved in deviation of CCV from delivery to lysosomes (Buelow et al., 2011). This study showed *ciaI* mutants were more associated with cathepsin D compared to wild-type strain suggesting the potential role of CiaI in survival in IECs. Whereas in macrophages, *C. jejuni* cannot avoid fusion with lysosomes and consequently is rapidly degraded (Watson & Galán, 2008).

### 1.4. Mechanisms of *C. jejuni*-induced diarrhoea

*C. jejuni*-induced diarrhoea appears to be a multifactorial process. During transmigration, *C. jejuni* OMV-associated proteases such as Cj1365c and HtrA disrupt the intestinal barrier by cleaving tight junction proteins such as occludin and claudin-8 as well as adherens junction proteins such as E-cadherin (Elmi et al., 2016; Harrer et al., 2019; Sharafutdinov et al., 2020). Disruption of tight junctions and adherens junctions results in a leaky intestinal barrier preventing fluid absorption. In addition, *C. jejuni* promotes diarrhoea via downregulation of absorptive ion channels of the intestine. The maximum transport capacity of sodium ion ($Na^+$) by epithelial sodium channel (ENaC) was significantly reduced in *C. jejuni*-infected human mucosa compared to negative controls (Bücker et al., 2018). Reduced $Na^+$ transport capacity is associated with downregulation of mRNA expression of ENaC subunits β and γ. Disruption of bile reabsorption is also associated with *C. jejuni*-induced diarrhoea. Bile acids are synthesised in the liver and play an important role in digestion of lipids (Chiang, 2013). 95% of bile acids are reabsorbed in the ileum and returned to the liver. However, failure of reabsorption of bile acids induces diarrhoea by increasing intestinal permeability (Chiang, 2013). de Vries et al. demonstrated bile staining was reduced in *C. jejuni*-infected piglet ileum compared to the uninfected controls indicating inhibition of bile resorption by *C. jejuni* (de Vries et al., 2017). Furthermore, intestinal inflammation can lead to diarrhoea by reducing absorption of $Na^+$ (Musch et al., 2002). Intestinal barrier disruption allows translocation of intestine-resident bacteria to the basolateral side of the epithelium (Stolfi et al., 2022). Translocated luminal bacteria are then detected by pattern recognition receptors (PRR) activating an inflammatory response. As discussed in detail in Section 1.5.3, *C. jejuni* induces inflammation via ligand recognition by TLR2, TLR4 and nucleotide-binding oligomerisation domain (NOD) which may contribute to induction of diarrhoea (Rathinam et al., 2009; Zilbauer et al., 2005; Zilbauer et al., 2007).

## 1.5. Host defence mechanisms against pathogens

### 1.5.1. Mucosal immune system in the gut

As the first line of defence, the intestinal epithelium plays an important role in homeostasis in mucosal immunity (Cerf-Bensussan & Gaboriau-Routhiau, 2010). Gut microbes which reside within the lumen also contribute to gut immunological homeostasis through interactions between gut microbiome and host immune system (Cerf-Bensussan & Gaboriau-Routhiau, 2010). The intestinal epithelial layer consists of intestinal stem cells, absorptive cells (enterocytes and colonocytes), microfold cells (M cells) and specialised secretory cells such as goblet cells, Paneth cells (present only in the small intestine), enteroendocrine cells and tuft cells which secrete mucus, antimicrobial peptides, hormones and IL-25 respectively (Noah, Donahue, & Shroyer, 2011). Mucins secreted from goblet cells and antibacterial peptides such as α-defensins secreted from Paneth cells prevent luminal bacteria from adhering to and invading IECs.

Microvilli-lacking M cells overly Peyer's patches in the small intestine and overly colonic patches in the large intestine (Mabbott et al., 2013). B cell follicles and parafollicular regions of T cells are found in Peyer's patches and colonic patches. These specialised cells function by sampling microorganisms in the gut lumen through transcytosis and further introducing antigens to basolateral dendritic cells and macrophages (Mabbott et al., 2013). Dendritic cells underneath the epithelium can also sample luminal antigens directly. Antigen-loaded dendritic cells then present antigens to naive $CD4^+$ T cells and $IgM^+$ naive B cells in the Peyer's patches. After antigen presentation, IgM + naive B cells proliferate in the compartment between the epithelium and the follicle, then differentiate into IgA plasmablasts. IgA plasmablasts then migrate to the germinal centre of the follicle and undergo affinity maturation with help provided by $CD4^+$ T cells (Biram & Shulman, 2020). After maturation, T cells and B cells travel to mesenteric lymph nodes and then to the intestinal lamina propria. Dendritic cells also migrate to the mesenteric lymph nodes and present antigens to naive lymphocytes to amplify the immune response (Mowat, 2003). In the presence of IL-5 and IL-6 produced by T helper 2 cells, plasmablasts then further differentiate into plasma cells which produce IgA which is the most abundant antibody in the mucosa. IgA forms dimeric secretory IgA and is released to the intestinal lumen (Fukuyama & Kiyono, 2004).

Secretory IgA neutralises bacterial toxins and pathogens by preventing microbial binding to the epithelium and entrapping toxins and pathogens in the mucus layer (Macpherson et al., 2008; Mantis, Rol, & Corthésy, 2011). Secretory IgA plays a role in both the innate and adaptive immune systems. As a component of the innate immune system, glycans of secretory IgA possess a similar structure to glycans on the host cell surface thereby preventing bacterial adherence through competitive inhibition (Mantis, Rol, & Corthésy, 2011). Whereas as a component of adaptive immunity, secretory IgA can bind to pathogens and toxins through fragment antigen-binding (Mantis, Rol, & Corthésy, 2011).

### 1.5.2. Pattern recognition receptors in human intestinal epithelial cells (IECs)

In the innate immune response, pathogen-associated molecular patterns (PAMPs) and damage-associated molecular patterns (DAMPs) are detected by PRRs of the host cells (Lavelle et al., 2010). PRRs include membrane-bound or cytosolic TLRs, cytosolic NOD-like receptors (NLRs) and cytosolic retinoic acid-inducible gene I (RIG-I)-like receptors (RLRs) (Lavelle et al., 2010).

In IECs, TLRs are mainly expressed on the basolateral surface so as to be tolerant to commensal bacteria (Kawai & Akira, 2010). There are two subgroups of TLRs which have distinct localisations and PAMP recognitions (Table 1.1) (Gay et al., 2014; Lavelle et al., 2010). TLRs that are localised on the cell surface include TLR1, TLR2, TLR4, TLR5 and TLR6 and detect different surface structures of microbes. Subcellular TLRs are localised within the intracellular compartments and include TLR3, TLR7, TLR8 and TLR9 and detect nucleic acids of microbes (Gay et al., 2014; Lavelle et al., 2010). Ligand binding of TLR induces dimerisation and rearranges the dimer to facilitate further binding of adapter proteins to Toll/IL-R (TIR) domains of TLR dimers (Table 1.1). Downstream adaptor proteins include TIR domain-containing adapter protein (TIRAP), myeloid differentiation primary response protein 88 (MyD88), TIRAP-inducing interferon (IFN)-β (TRIF) and TRIF-related adaptor molecule (TRAM) (Duan et al., 2022). Interaction between TIR domain of TLR and the adapter proteins activates nuclear factor kappa light chain enhancer of activated B cells (NF-κB) and IFN regulatory factor 3 (IRF3) which induce transcription of proinflammatory cytokines and type I IFNs (Duan et al., 2022). In addition, the adaptor proteins mediate signal transduction of the mitogen-activated protein kinase (MAPK) pathways such as c-Jun N-terminal kinase (JNK), ERK and p38 pathways (Duan et al., 2022).

**Table 1.1. Human TLR members and their ligands and downstream adaptor proteins adapted from Gay et al. (2014) and Lavelle et al. (2010).**

| Dimer form | Localisation | Ligand | Adapter proteins |
|---|---|---|---|
| TLR2-TLR1 | Cell surface | Triacyl lipopeptide of Gram-negative bacteria | TIRAP & Myd88 |
| TLR2-TLR6 | Cell surface | Diacyl lipopeptide of Gram-positive bacteria | TIRAP & Myd88 |
| TLR4-TLR4 | Cell surface | LPS | TIRAP & Myd88, TRAM & TRIF |
| TLR5-TLR5 | Cell surface | Flagellin | Myd88 |
| TLR3-TLR3 | Intracellular endosomes | Double-stranded RNA | TRIF |
| TLR7-TLR7 | Intracellular endosomes | Single-stranded RNA | Myd88 |
| TLR8-TLR8 | Intracellular endosomes | Single-stranded RNA | Myd88 |
| TLR9-TLR9 | Intracellular endosomes | Unmethylated cytosine-phosphate-guanine (CpG) DNA | Myd88 |

NOD1 and NOD2 detect intracellular γ-D-glutamyl-meso-diaminopimelic acid (iE-DAP) and muramyl dipeptide (MDP) respectively which are components of bacterial peptidoglycan (Heim, Stafford, & Nachbur, 2019). Ligand binding to NOD recruits receptor-interacting protein kinase 2 (RIPK2) which then interacts with TNF receptor associated factor 2 (TRAF2). Ubiquitination of RIPK2 recruits transforming growth factor (TGF)-β-activated kinase 1 (TAK1) and IκB kinase (IKK) complexes which activates MAPK and NF-κB pathways resulting in proinflammation (Heim, Stafford, & Nachbur, 2019).

RLRs are intracellular sensors of viral RNA (Rehwinkel & Gack, 2020). There are three members of the RLR family; melanoma differentiation-associated gene 5 (MDA5), laboratory of genetics and physiology 2 (LGP2) and RIG-I. RIG-I and MDA5 possess caspase recruitment domains (CARD) which interact with mitochondrial antiviral signalling protein (MAVS). Interaction between RIG-I/MDA5 and MAVS recruits TRAF3, TRAF6 and IKK complexes which in turn activate IRF3, IRF7 and NF-κB pathway resulting in induction of transcription of type I IFNs and proinflammatory cytokines (Rehwinkel & Gack, 2020). In contrast, LGP2 does not have CARD, so LGP2 negatively regulates activity of RIG-I and MDA5.

### 1.5.3. Innate immune response upon *C. jejuni* infection

*C. jejuni* induces inflammatory responses by two mechanisms which are i) adherence and invasion and ii) CDT activity (Hickey et al., 2000). Inflammation-mediated by *C. jejuni* adherence and invasion is associated with ligand-binding of TLR and NOD receptors (Friis, Keelan, & Taylor, 2009; Rathinam et al., 2009; Zilbauer et al., 2007). A previous study demonstrated TLR2 siRNA transfection resulted in reduction in *C. jejuni*-induced IL-6 secretion in human intestinal epithelial Caco-2 cells indicating involvement of TLR2 in *C. jejuni*-mediated inflammation (Friis, Keelan, & Taylor, 2009). Another study demonstrated deficiency of TLR2, TLR4, Myd88 or TRIF resulted in significant reduction in *C. jejuni*-mediated IL-6 and IL-12 in mice dendritic cells suggesting that *C. jejuni* is detected by TLR2 and TLR4 and signal transduction is mediated by Myd88 and TRIF (Rathinam et al., 2009). Upon internalisation into host cells, *C. jejuni* can also be detected by NOD1 (Bereswill et al., 2017; Zilbauer et al., 2005; Zilbauer et al., 2007). Zilbauer et al. showed NOD1 siRNA transfection led to a reduction in *C. jejuni*-induced expression of IL-8 and human β-defensin 2 in Caco-2 cells indicating role of NOD1 in *C. jejuni*-mediated inflammation (Zilbauer et al., 2005; Zilbauer et al., 2007). In contrast to NOD1, NOD2 appears not to be involved in *C. jejuni*-mediated immune responses in human IECS (Zilbauer et al., 2007). In addition to classical PAMPs, CDT is implicated in *C. jejuni*-mediated inflammation and disease presentation as discussed in Section 1.2.5 (Elmi et al., 2012; Fox et al., 2004; Hickey et al., 2000). A recent study also found alpha-kinase 1 (ALPK1)-dependent NF-κB activation by *C. jejuni* (Cui et al., 2021). *C. jejuni* releases ADP-heptose during bacterial growth which further activates ALPK1 followed by phosphorylation of TRAF-interacting protein with forkhead-associated domain (TIFA). Phosphorylated TIFA then activates NF-κB pathway resulting in inflammation in human IECs (Cui et al., 2021).

### 1.5.4. The roles of reactive oxygen species

Reactive oxygen species (ROS) includes oxygen radicals and non-radicals which are highly reactive molecules produced by the partial reduction of oxygen (Aviello & Knaus, 2017). Due to the ability of ROS to damage proteins, lipids and nucleic acids, ROS production is one of the main host defence mechanisms against invading pathogens (Aviello & Knaus, 2017). The respiratory burst in phagocytes results in rapid ROS production to eliminate intracellular pathogens through oxidative damage (Paiva & Bozza, 2014). Even though IECs produce lower levels of ROS compared to phagocytes, ROS produced in IECs can also exert an antimicrobial effect by induction of an inflammatory response (Burgueño et al., 2019; Holmström & Finkel, 2014; Paiva & Bozza, 2014). In addition, cellular ROS plays an important role in signal transduction by acting as secondary messengers (Zhang et al., 2016). As ROS exhibits both beneficial and deleterious effects on cellular physiology, IECs need to achieve homeostasis of cellular ROS. To protect the cells from the damaging effects of ROS, host IECs possess

antioxidant systems that degrade ROS, such as catalase (CAT), superoxide dismutase (SOD) and glutathione peroxidase. SOD catalyses degradation of superoxide ($O_2^-$) into hydrogen peroxide ($H_2O_2$) which is further decomposed into water ($H_2O$) and oxygen ($O_2$) by CAT. Glutathione peroxidase also degrades $H_2O_2$ into $H_2O$ and oxygen $O_2$ and other organic peroxide into alcohols and $O_2$. In contrast, nicotinamide adenine dinucleotide phosphate oxidase (NADPH oxidase; NOX) and mitochondria are main sources of ROS in human IECS (Aviello & Knaus, 2017).

### 1.5.5. NADPH oxidase (NOX)

NOX is a multi-subunit enzyme which plays an essential role in catalysis of $O_2^-$ production (Brandes, Weissmann, & Schröder, 2014; Sumimoto, Miyano, & Takeya, 2005). The most abundant types of NOX found in IECs are NOX1 and constitutively active NOX4. NOX1 is mainly localised on the plasma membrane and NOX4 is mainly found on the membrane of the endoplasmic reticulum (ER) (Helmcke et al., 2009). The NOX1 complex is comprised of NOX1, p22phox, NOX organiser 1 (NOXO1), NOX activator 1 (NOXA1) and Rho family small GTPase Rac1 (Figure 1.1). NOX1 is the catalytic component of the complex on the plasma membrane and activation is accompanied by recruitment of cytosolic subunits. NOX1 expression promotes translocation of p22phox to the plasma membrane (Brandes, Weissmann, & Schröder, 2014). Upon activation, NOXO1 binds to both NOXA1 and p22phox targeting NOXA1 to the plasma membrane. Guanosine triphosphate (GTP)-bound Rac1 binds to NOXA1 which then facilitates electron flow through flavocytochrome in NOX1. As electron flow is in a GTP-dependent manner, GTP-bound Rac1 is found to be necessary for activity of NOX1 (Nisimoto et al., 2008; Ueyama, Geiszt, & Leto, 2006). Electrons are transferred from NADPH initially to flavin adenine dinucleotide (FAD), then through the heme domain of NOX and finally to $O_2$, generating $O_2^-$ (Nisimoto et al., 2008).

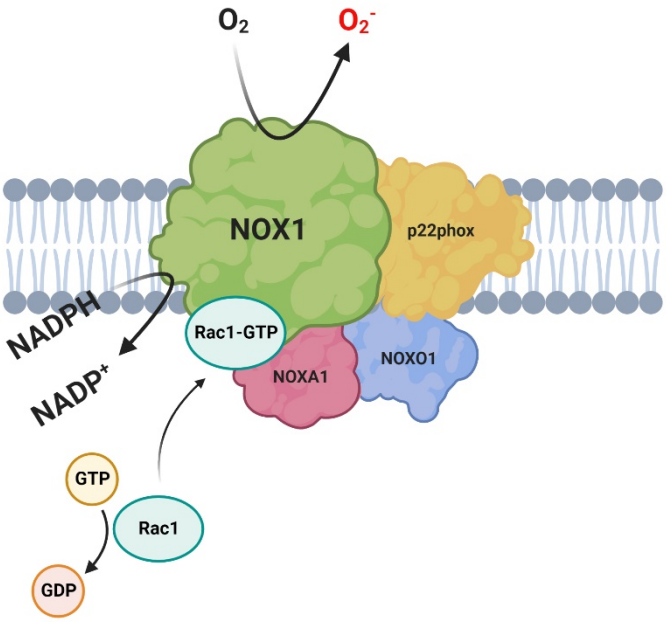


**Figure 1.1. Proposed structure of the NOX1 complex.** Catalytic component of NOX1 is activated by recruitment of membrane-associated p22phox, cytosolic NOX organiser 1 (NOXO1), NOX activator 1 (NOXA1) and Guanosine triphosphate (GTP)-bound active Rac1. Activation of NOX1 results in the formation of superoxide ($O_2^-$) via electron flow from NADPH to NOX1 heme domain. Image from Hong et al. (2023).

### 1.5.6. The roles of NOX1 in physiological processes in IECs

ROS produced by NOX1 in IECs activates wound repair also termed epithelial restitution (Leoni et al., 2013). Migration of epithelial cells is involved in epithelial restitution and is regulated by pro-resolving mediators. Pro-resolving mediators are enzymes derived from fatty acids which participate in resolution of tissue damage and inflammation (Basil & Levy, 2016). Annexin A1 is a calcium-dependent pro-resolving mediator and which activity is mediated by formyl peptide receptors (FPRs). Leoni et al. found ligand binding of FPR induces Rac1-mediated NOX1 activation (Leoni et al., 2013). Phosphatase and tensin homologue deleted on chromosome 10 (PTEN) and protein tyrosine phosphatase (PTP)-PEST dephosphorylate FAK and paxillin which are involved in cellular motility and migration (Tamura et al., 1999). NOX1-produced ROS inhibits PTEN and PTP-PEST resulting in enhanced phosphorylation of FAK and paxillin which promotes epithelial restitution (Leoni et al., 2013).

In addition, cell growth and proliferation are regulated by NOX1-mediated ROS (van der Post, Birchenough, & Held, 2021). Self-renewal of a single layer of mammalian epithelial cells occurs every 4-5 days. Cellular proliferation and differentiation are key processes in self-renewal of epithelium (van

der Flier & Clevers, 2009). Wnt and EGF receptor (EGFR) pathways regulate cellular proliferation and differentiation. Van der Post et al. demonstrated NOX1 knockout ($NOX1^{-/-}$) spheroids exhibited reduced ROS production and reduced phosphorylation of EGFR. The results suggest that NOX1-produced ROS enhances cell proliferation of intestinal stem cells by activating EGFR pathway independent of ligand binding to EGFR (van der Post, Birchenough, & Held, 2021).

NOX1-mediated ROS production also regulates gut microbiota homeostasis (Matziouridou et al., 2018). Matziouridou et al. demonstrated $NOX1^{-/-}$ mice exhibit increased bacterial load in the ileum compared to wild-type mice indicating antimicrobial effect of NOX1 (Matziouridou et al., 2018). In addition, $NOX1^{-/-}$ mice resulted in changes in microbiota composition in the ileum which is similar to composition of cecal microbiota suggesting that NOX1 inhibits translocation of cecal microbiota to the ileum (Matziouridou et al., 2018).

### 1.5.7. Endoplasmic reticulum and the unfolded protein response (UPR)

The ER is the largest membrane-bound organelle in a eukaryotic cell. The ER has essential roles in protein synthesis, folding modification and transport, lipid synthesis, carbohydrate metabolism and $Ca^{2+}$ storage (Schwarz & Blower, 2015). For normal functioning of the ER, regulation of ER homeostasis is important. ER stress can result from the disruption of *N*-glycosylation, disruption of $Ca^{2+}$ homeostasis, elevated rate of protein synthesis, ATP depletion, osmotic stress and redox changes. Due to impaired functioning of the ER, misfolded proteins are accumulated in the ER lumen (Celli & Tsolis, 2014).

The unfolded protein response (UPR) is a highly conserved eukaryotic surveillance system for ER homeostasis which is involved in reduction of ER stress and restoration of ER homeostasis (Celli & Tsolis, 2014; Hetz & Papa, 2018). There are three transmembrane UPR sensors which sense ER stress by detection of unfolded proteins within the ER lumen, i) protein kinase R-like ER kinase (PERK), ii) inositol-requiring enzyme 1α (IRE1α) and iii) activating transcription factor 6 (ATF6) (Figure 1.2). Under homeostatic conditions, binding-immunoglobulin protein (BiP) also known as glucose-regulated protein 78 (GRP78) is bound to the luminal domains of the UPR sensors to maintain their inactive form. During ER stress, increased unfolded proteins bind to BiP which results in disassociation of BiP from the stress sensors leading to conformational change to activate the UPR (Celli & Tsolis, 2014; Hetz & Papa, 2018).

After disassociation of BiP from PERK under ER stress, PERK homodimerises and autophosphorylates (Figure 1.2) (Celli & Tsolis, 2014; Hetz & Papa, 2018). The activated kinase domain in PERK then phosphorylates eukaryotic translation initiation factor 2α (eIF2α). Phosphorylation of eIF2α results in temporal attenuation of global translation by inhibiting 80S ribosome assembly. Activating transcription factor 4 (ATF4) is selectively translated and translocated into the nucleus (Celli & Tsolis, 2014). To recover ER homeostasis, ATF4 upregulates transcription of genes encoding proteins involved in amino

acid transport and metabolism, oxidative stress resistance and ER chaperones. However, severe ER stress and prolonged UPR induce apoptosis as ATF4 induces the transcription of gene encoding C/EBP homologous protein (CHOP) which is involved in the induction of apoptosis (Hetz & Papa, 2018). In addition, ATF4 induces expression of growth arrest and DNA damage inducible 34 (GADD34) which dephosphorylates phosphorylated eIF2α to restore global translation (Márton et al., 2022). For the cells experiencing prolonged ER stress, upregulation of GADD34 is cytotoxic as this increases the amount of proteins entering the ER.

IRE1α has a similar structure to PERK (Hetz & Papa, 2018). There are a serine/threonine kinase and endoribonuclease (RNase) domains in IRE1α. After disassociation of BiP from IRE1α, IRE1α undergoes homodimerisation and autophophosrylation (Figure 1.2). Phosphorylation of IRE1α activates the RNase domain of IRE1α which then cleaves a 26 nucleotide-intron within mRNA of X-box-binding protein 1 (XBP1). Spliced *XBP1* mRNA is then translated into spliced XBP1 which is then translocated into the nucleus inducing expression of genes encoding ER chaperones, autophagy components and ER-associated degradation (ERAD) components involving in degradation of misfolded proteins (Celli & Tsolis, 2014; Hetz & Papa, 2018). In addition, RNase activity of IRE1α degrades ER-localised mRNAs and microRNAs (miRNAs) and this process is termed regulated IRE1-dependent degradation (RIDD) (Maurel et al., 2014).

Detachment of BiP from ATF6 also activates the ATF6 pathway (Figure 1.2). Unlike PERK and IRE1α which undergo homodimerisation and autophosphorylation, activated ATF6 is transported to the Golgi apparatus where site 1 protease (S1P) and site 2 protease (S2P) in the Golgi cleave ATF6 (Celli & Tsolis, 2014; Hetz & Papa, 2018). Then the active amino terminus of ATF6 is translocated into the nucleus resulting in upregulation of genes encoding ER chaperones and ERAD components to enhance ER functioning.

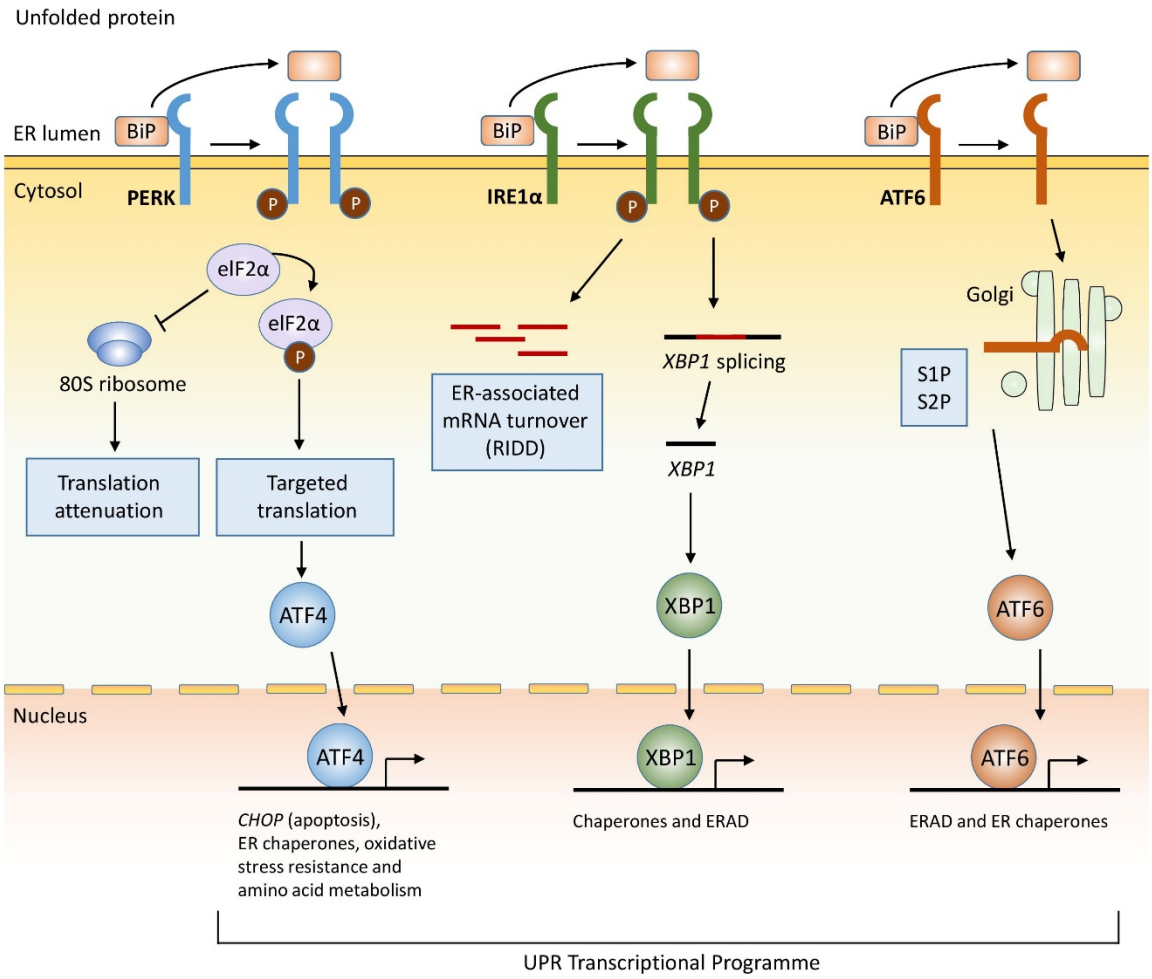


**Figure 1.2. Activation of the unfolded protein response by protein kinase R-like ER kinase (PERK), inositol-requiring enzyme 1α (IRE1α) and activating transcription factor 6 (ATF6) located on the ER membrane.** Under ER stress, BiP is disassociated from each sensor facilitating conformational change to active form. PERK phosphorylates eukaryotic translation initiation factor 2α (eIF2α) which results in attenuation of global translation. Selectively translated activating transcription factor 4 (ATF4) and upregulates genes involved in apoptosis, protein folding and oxidative stress resistance. RNase activity of IRE1α cleaves *XBP1* pre mRNA and translated spliced XBP1 induces expression of gene encoding ER chaperones and ER-associated degradation (ERAD) components. In response to ER detachment, ATF6 is transported to the Golgi apparatus and site 1 protease (S1P) and site 2 protease (S2P) cleave ATF6. The active amino terminus of ATF6 then translocates into the nucleus upregulating genes encoding ERAD components and ER chaperones. Image adapted from Celli & Tsolis (2014).

### 1.5.8. The UPR and inflammation

UPR activation is implicated in proinflammatory responses (Grootjans et al., 2016). In the PERK pathway, global translational inhibition caused by phosphorylation of eIF2α can activate the NF-κB pathway. As IκB has shorter half-life compared to NF-κB, global translation attenuation results in an increased ratio of NF-κB to IκB, leading to activation of the NF-κB pathway (Grootjans et al., 2016). In addition to apoptosis, CHOP is associated with production of proinflammatory cytokine IL-23 in human dendritic cells (Goodall et al., 2010). ATF4 directly binds to the promoter of *IL-6* inducing expression of IL-6. In addition, ATF4 upregulates GADD34 expression which in turn induces transcription of genes encoding type I IFN (Janssens, Pulendran, & Lambrecht, 2014). Along with ATF4, CHOP upregulates ATF5 expression which induces the expression of the gene encoding thioredoxin-interacting protein (TXNIP). TXNIP then activates NOD-, LRR- and pyrin domain-containing protein 3 (NLRP3) inflammasome resulting in the release of proinflammatory cytokine IL-1β (Grootjans et al., 2016; Paerhati et al., 2022).

Activation of the IRE1α pathway is also implicated in inflammation and apoptosis (Fribley, Zhang, & Kaufman, 2009). Phosphorylated IRE1α interacts with TRAF2 and induces inflammation by activating NF-κB and JNK signalling pathways (Celli & Tsolis, 2014; Hu et al., 2006). The interaction between IRE1α and TRAF2 recruits IκB kinase and phosphorylates IκB for degradation inducing activation of NF-κB pathway (Grootjans et al., 2016). In addition, the IRE1α-TRAF2 complex induces autophosphorylation of apoptosis-signalling kinase 1 (ASK1) leading to activation of JNK pathway which phosphorylates proapoptotic BCL-2 family protein Bcl-2-interacting mediator of cell death (BIM) (Fribley, Zhang, & Kaufman, 2009; Szegezdi et al., 2006). Later studies found that NOD1 activity is involved in proinflammation resulting from the interaction between TRAF2 and IRE1α (Keestra-Gounder et al., 2016; Kuss-Duerkop & Keestra-Gounder, 2020). Similar to the PERK pathway, IRE1α activation induces NLRP3 inflammasome. IRE1α-mediated RIDD degrades miR-17 resulting in increased expression of TXNIP which then activates NLRP3 inflammasome (Grootjans et al., 2016).

The cleaved amino terminus of ATF6 can also activate the NF-κB pathway by activating phosphatidylinositol-3-kinase (PI3K)/AKT signalling pathway (Grootjans et al., 2016). In addition, ATF6 interacts with cyclic AMP-responsive element-binding protein H (CREBH) and synergistically upregulates expression of acute phase response (APR) genes which play a role in amplification of inflammatory responses (Stengel et al., 2020; Zhang et al., 2006).

### 1.5.9. Microbial pathogens and UPR activation

UPR activation can be beneficial to host cells by eliminating invading pathogens via activation of the innate immune response (Celli & Tsolis, 2014; Grootjans et al., 2016). However, some invading microbial pathogens can exploit or modulate the UPR to enhance their intracellular life cycle within host cells. Many pathogens exploit a function of the ER to enhance their intracellular replication and survival thereby resulting in UPR activation (Celli & Tsolis, 2014). Viruses induce ER stress-mediated UPR via rearrangement of the ER membrane, disruption of host protein glycosylation and $Ca^{2+}$ depletion by viroporin which oligomerises and forms hydrophilic pores (Jheng, Ho, & Horng, 2014). Some viruses, such as Japanese encephalitis virus (JEV), take advantages of the UPR-mediated RIDD to facilitate replication of viral RNA by degrading host RNA (Bhattacharyya, Sen, & Vrati, 2014). Human cytomegalovirus (HCMV) exploits UPR-induced upregulation of ERAD complex to avoid host immune surveillance by targeting major histocompatibility complex (MHC) class I proteins to degradation.

Similarly, some bacterial pathogens exploit the UPR to enhance their replication and survival within host cells (Celli & Tsolis, 2014). The facultative intracellular bacterium *Brucella melitensis* secretes TcpB which modulates host microtubules and activates the UPR to reorganise the ER structure and to create a niche for intracellular replication and survival in RAW 264.7 murine macrophages (Smith et al., 2013). *S. enterica* also induces the UPR for intracellular replication by exploiting enhanced lipid metabolism (Antoniou et al., 2018). The obligate intracellular bacterium *Chlamydia trachomatis* requires activation of PERK and IRE1α pathways to form a *Chlamydia*-containing vacuole in the ER which is termed *Chlamydia* inclusion (George et al., 2019; George et al., 2017). In contrast, as the UPR can exert detrimental effects on bacterial fitness via activation of immune responses, some bacteria subvert activation of the UPR to avoid deleterious effect. *Legionella pneumophila* glucosyltransferases Lgt1 and Lgt2 are involved in inhibition of translational expression of BiP and CHOP and XBP1 splicing (Sean & Shaeri, 2015). *Streptomyces* spp. secretes trierixin which inhibits IRE1α activation via disruption of XBP1 splicing (Futamura et al., 2007). In addition, the obligate intracellular bacterium *Simkania negevensis* forms ER-associated *Simkania*-containing vacuoles. *S. negevensis* induces the UPR in the early infection and downregulates the UPR in the later infection cycle to promote its fitness in the host cell (Mehlitz et al., 2014).

### 1.5.10. *C. jejuni* and UPR activation

A previous study demonstrated *C. jejuni* cell lysates trigger ER stress and increase in intracellular $Ca^{2+}$ in human monocyte and *C. jejuni* CDT was not responsible for these observations suggesting involvement of other bacterial virulence determinants in induction of ER stress (Canonico et al., 2018). Another study showed *C. jejuni* upregulates *GADD34* and *CHOP* expression in Caco-2 cells and

reduces global translation confirming activation of the PERK pathway (Tentaku et al., 2018). Tentaku et al. also demonstrated *C. jejuni* does not induce expression of ATF6 and XBP1 splicing in Caco-2 cells which indicate that *C. jejuni* does not induce the IRE1α and ATF6 pathways (Tentaku et al., 2018). However, compared to other UPR-activating bacteria, mechanisms of *C. jejuni*-mediated UPR activation and bacterial virulence determinants which are responsible for UPR activation have remained relatively unexplored.

## 1.6. Aims and objectives

The aim of this study was to investigate *C. jejuni*-mediated NOX1 modulation and UPR activation in human IECs.

Objectives and hypotheses:

1. To investigate NOX1-mediated ROS modulation by *C. jejuni* in human IECs.
    a. *C. jejuni* modulates intracellular and extracellular ROS production in human IECs.
    b. *C. jejuni* modulates NOX1 expression in human IECs.
    c. *C. jejuni* modulates activity of small GTPase Rac1 in human IECs.
    d. *C. jejuni* modulates expression of other antioxidant-related genes in human IECs.
    e. Disruption of NOX1 activity affects *C. jejuni* interaction, invasion and intracellular survival in human IECs.
2. To investigate *C. jejuni*-mediated UPR activation and bacterial virulence determinants which are responsible for UPR activation in human IECs.
    a. *C. jejuni* modulates UPR-related gene expression in human IECs.
    b. Mutation of different *C. jejuni* virulence determinants affects *C. jejuni*-mediated UPR activation in human IECs.
3. To investigate the impact of UPR activation on *C. jejuni* pathogenesis and the mechanisms of *C. jejuni*-mediated UPR activation in human IECs.
    a. Thapsigargin-induced UPR affects *C. jejuni* interaction, invasion and intracellular survival in human IECs.
    b. Inhibition of UPR activation affects the number of intracellular *C. jejuni* in human IECs.
    c. Inhibition of UPR activation affects *C. jejuni*-induced IL-8 release in human IECs.
    d. Inhibition of NOD1 affects *C. jejuni*-mediated UPR activation in human IECs.
    e. Inhibition of NOD1 affects *C. jejuni*-induced IL-8 release in human IECs.
    f. Inhibition of an increase in intracellular $Ca^{2+}$ within the cytosol affects *C. jejuni*-mediated UPR activation in human IECs.
    g. Thapsigargin treatment affects NOX1 expression in human IECs.

# CHAPTER TWO: Materials and Methods

## 2.1. Bacterial strains and growth conditions

*C. jejuni* strains used in this study are listed in Table 2.1. For general growth, *C. jejuni* strains were grown on Columbia blood agar (CBA) plates (Oxoid, UK) supplemented with 7% (v/v) horse blood in Alsever's (TCS Microbiology, UK) and *Campylobacter* selective supplement Skirrow (Oxoid) or in *Brucella* broth (BD Diagnostics, UK) shaking at 75 rpm at 37°C under microaerobic conditions (10% $CO_2$, 5% $O_2$ and 85% $N_2$) (Don Whitley Scientific, UK). For growth of *C. jejuni* mutants, kanamycin (50 μg/ml), chloramphenicol (10 μg/ml) or erythromycin (2 μg/ml) were added to CBA based on the selective markers of the individual mutant strain. *Campylobacter* glycerol broth mix was prepared for *C. jejuni* glycerol stocks. *Campylobacter* glycerol broth mix consisted of 1 ml 100% (v/v) glycerol (Sigma-Aldrich, USA) giving a final concentration of 10% (v/v), 1 ml of Foetal Bovine Serum (FBS; Labtech, UK) giving a final concentration of 10% (v/v) and 8 ml of *Brucella* broth. Glycerol stocks were prepared from *C. jejuni* strains grown for 24 hours on CBA plates. 20 μl of bacterial suspension was aliquoted in 0.6 ml microcentrifuge tubes. The cells were snap frozen and stored at -80°C.

*E. coli* DH5α™ Competent Cells (New England BioLabs, UK) were grown on lysogeny broth (LB; Oxoid) agar plates or in LB broth at 37°C under aerobic conditions shaking at 200 rpm (Sanyo, UK). If necessary, *E. coli* cultures were supplemented with ampicillin (100 μg/ml) and chloramphenicol (50 μg/ml).

**Table 2.1. *C. jejuni* strains used in this study.**

| *C. jejuni* strains | Description | References |
|---|---|---|
| 11168H wild-type | A hypermotile derivative of NCTC 11168 wild-type strain which is a human clinical isolate. | (Jones et al., 2004; Karlyshev et al., 2002) |
| 11168H *kpsM* | Capsular polysaccharide mutant of the 11168H strain which was constructed by insertion mutagenesis with kanamycin resistance ($Km^r$) cassette. | Constructed by Dr. Andrey V. Karlyshev (Karlyshev et al., 2000)<br>Obtained from the London School of Hygiene and Tropical Medicine *Campylobacter* Resource Facility http://crf.lshtm.ac.uk/index.htm |
| 11168H *flaA* | Flagellin A (*flaA*) mutant which was constructed by insertion mutagenesis with $Km^r$ cassette. Non-motile however still able to secrete Cia proteins. | Constructed by Dr. Michael A. Jones (Jones et al., 2004)<br>Obtained from the London School of Hygiene and Tropical Medicine *Campylobacter* Resource Facility http://crf.lshtm.ac.uk/index.htm |
| 11168H *htrA* | A serine protease, high temperature requirement protein A (*htrA*) mutant | Constructed by Dr. Andrey V. Karlyshev |

| | | |
|---|---|---|
| | which was constructed by insertion mutagenesis with $Km^r$ cassette. | (Karlyshev et al., 2014) Obtained from the London School of Hygiene and Tropical Medicine *Campylobacter* Resource Facility http://crf.lshtm.ac.uk/index.htm |
| 11168H *cadF* | An adhesin, *Campylobacter* adhesion to fibronectin (*cadF*) mutant which was constructed by insertion mutagenesis with $Km^r$ cassette | Constructed and provided by Dr. Cadi Davies at LSHTM |
| 11168H *flpA* | An adhesin, fibronectin-like protein A (*flpA*) mutant which was constructed by insertion mutagenesis with $Km^r$ cassette | Constructed and provided by Dr. Cadi Davies at LSHTM |
| 11168H *cadF flpA* | *cadF* and *flpA* double mutant which was constructed by insertion of $Km^r$ and erythromycin resistance ($Em^r$) cassettes. | Constructed and provided by Dr. Cadi Davies at LSHTM |
| 11168H *cdtA* | Cytolethal distending toxin subunit A (*cdtA*) mutant which was constructed by insertion mutagenesis with $Km^r$ cassette. | Constructed by Dr. Abdi Elmi at LSHTM (Elmi et al., 2012) Obtained from the London School of Hygiene and Tropical Medicine *Campylobacter* Resource Facility http://crf.lshtm.ac.uk/index.htm |
| 11168H Δ*cdtABC* | *cdt* mutant which was constructed by replacement of the *cdtABC* operon with chloramphenicol resistance ($Cm^r$) cassette. | This study |
| 81-176 wild-type | A human clinical isolate identified during an outbreak of acute enteritis associated with consumption of contaminated milk. The strain possesses two plasmids termed pVir and pTet which contain putative Type IV secretion system (T4SS) genes (Bacon et al., 2000). | (Korlath et al., 1985) |
| 488 wild-type | A human clinical isolate from Brazil which has a Type VI secretion system (T6SS). | (Davies et al., 2019; Liaw et al., 2019) |

## 2.2. Human intestinal epithelial cell culture

### 2.2.1. Cell-lines

Human carcinoma cell line T84 cells (ECACC 88021101) and Caco-2 cells (ECACC 86010202) were used in this study. As T84 cells possess characteristic colonocytes and Caco-2 cells possess characteristic enterocytes throughout differentiation (Devriese et al., 2017), the different cell lines were used to compare phenotypes observed in the cell lines. Human IECs were cultured in complete growth medium consisting of 1:1 mixture of Dulbecco's modified Eagle's medium and Ham's F-12 medium

(DMEM/F-12; Gibco, USA) supplemented with 10% (v/v) FBS, 1% (v/v) non-essential amino acids (Sigma-Aldrich) and 1% penicillin-streptomycin (Sigma-Aldrich). For infection assays, complete growth medium without penicillin-streptomycin was used. Cell lines were grown at 37°C in a 5% $CO_2$ incubator (Sanyo, USA).

### 2.2.2. Thawing frozen IECs and preparation of stock IECs

Human IECs in a cryovial were taken from the liquid nitrogen freezer and thawed in a 37°C water bath for 1 minute. Thawed cells were then transferred to a 25 $cm^2$ cell culture flask containing 10 ml of pre-warmed cell culture medium and the cells were incubated at 37°C in a 5% $CO_2$ incubator. Once cells reached log growth phase, cells were processed for cryopreservation. Cells were washed with pre-warmed phosphate buffered saline (PBS; Gibco, USA) three times and incubated with 3 ml of 0.25% (w/v) trypsin-EDTA (Thermo Fisher Scientific, USA) for 10 minutes at 37°C in a 5% $CO_2$ incubator. Detached cells were resuspended in 10 ml of pre-warmed complete growth medium and centrifuged at 100 x g for 10 minutes. After centrifugation, the supernatant was removed and the pellet was resuspended in 3.5 ml of freezing medium consisted of complete growth medium and 5% (v/v) dimethyl sulfoxide (DMSO; Sigma-Aldrich) as a cryoprotective agent. 1 ml aliquots of cell suspension were transferred to cryovials and incubated in a liquid nitrogen freezer.

### 2.2.3. Seeding IECs on culture plates

Once cells reached log growth phase, cells were washed and harvested as described in Section 2.2.2. Detached cells were resuspended in 10 ml of pre-warmed complete growth medium and centrifuged at 100 x g for 10 minutes. After centrifugation, the supernatant was discarded and the pellet resuspended in 10 ml of pre-warmed complete growth medium. For counting cells, 100 µl of cell suspension was mixed with 100 µl of 0.4% (w/v) trypan blue solution (Thermo Fisher Scientific) and 800 µl of complete growth medium giving a 1:10 dilution. 20 µl of cell suspension with trypan blue was loaded into a haemocytometer (Weber Scientific, UK) avoiding overfilling. The number of viable cells were counted in four outer squares and divided by four giving an average count. Cell density was determined and required volume of cell suspension was calculated using the following equations:

$$\text{Cell density (cells/ml)} = \text{Average cell count x 10 (Dilution factor) x } 10^4$$

$$\text{Volume of one square} = 0.1\ \text{mm}^3 = 10^{-4}\ \text{cm}^3 = 10^{-4}\ \text{ml}$$

$$\text{Volume required (µl)} = \left(\frac{\text{Desired cell density}}{\text{Calculated cell density}}\right) \text{x Required total volume (ml) x 1000}$$

According to the calculation using the equations above, approximately $10^4$, $10^5$ or 2 x $10^5$ cells were seeded into each well of 96-, 24- or 6-well plates respectively. 96-well plates were then incubated overnight at 37°C in a 5% $CO_2$ incubator to allow cells to attach. 24- and 6-well plates were then

incubated for 5-7 days at 37°C in a 5% $CO_2$ incubator and grown up to approximately $10^6$ and 2 x $10^6$ cells respectively. Complete growth medium in each well was replaced with fresh complete growth medium every 2-3 days. 24 hours prior to infection assays, complete growth medium was changed to complete growth medium without penicillin-streptomycin.

2.3. Assays

2.3.1. Growth kinetics

*C. jejuni* was harvested from 24 hour plates and resuspended in 1 ml of PBS. 100 µl of bacterial suspension was added into 900 µl of PBS resulting in a 1:10 dilution. Using a Spectronic™ spectrophotometer (Thermo Fisher Scientific), the optical density at 600 nm ($OD_{600}$) was recorded. Using the equation below, the required volume of the bacterial suspension was calculated and added into a 25 $cm^2$ cell culture flask containing 10 ml of *Brucella* broth resulting in $OD_{600}$ of 0.1 (≈2 x $10^8$ CFU/ml). The inoculated flasks were then incubated with shaking at 75 rpm at 37°C under microaerobic conditions. The $OD_{600}$ of inoculated flasks was recorded at 2, 4, 6, 8, 10, 14, 16, and 24 hours after inoculation.

$$\frac{\text{Required OD at 600 nm}}{\text{10 x OD Reading at 600 nm}} \text{ x Final volume (ml) x 1000}$$
$$= \text{Required volume of bacterial suspension (µl)}$$

2.3.2. Chemical treatment assays

Human IECs were pre-treated with chemicals and/or further incubated with either *C. jejuni* or thapsigargin treatment as described in Table 2.2. After pre-treatment, IECs were washed three times with PBS.

**Table 2.2. Chemicals and experimental conditions used in this study.**

| Chemicals | Company | Description | Experimental condition |
|---|---|---|---|
| Thapsigargin (Tg) | Sigma-Aldrich | An inhibitor of sarco/endoplasmic reticulum $Ca^{2+}$-ATPases (SERCA) resulting in the UPR activation (Sehgal et al., 2017) | 2 µM for 6 hours prior to infection |
| Diphenyleneiodonium chloride (DPI) | Sigma-Aldrich | A broad-spectrum flavoprotein inhibitor including NOX family (Li & Trush, 1998) | 10 µM for 1 hour prior to infection |
| KIRA6 | Selleckchem (Germany) | IRE1α kinase and RNase inhibitor (Ghosh et al., 2014; Mahameed et al., 2019) | 3 µM for 4 hours pre-treatment before and during infection or Tg treatment |
| STF-083010 | Sigma-Aldrich | IRE1α RNase inhibitor (Ghosh et al., 2014) | 100 µM for 4 hours pre-treatment before infection or |

| | | | |
|---|---|---|---|
| | | | Tg treatment |
| GSK2656157 | Selleckchem | ATP-competitive PERK inhibitor (Maly & Papa, 2014) | 3 µM for 4 hours pre-treatment before infection or Tg treatment and during infection or Tg treatment |
| ML130 (Nodinitib-1) | Selleckchem | NOD1 inhibitor (Correa et al., 2011) | 30 µM for 1 hour pre-treatment before infection or Tg treatment and during infection or Tg treatment |
| BAPTA-AM | Invitrogen | Cell-permeable $Ca^{2+}$ chelator (Collatz, Rüdel, & Brinkmeier, 1997) | 5, 10, 20, or 30 µM 1 hour pre-treatment before infection or Tg treatment |

### 2.3.3. *C. jejuni* viability assay under experimental conditions

A loop of *C. jejuni* from a 24 hour incubated CBA plate was inoculated into 1 ml of PBS. Bacterial suspensions with an $OD_{600}$ of 0.2 were prepared in complete growth medium without penicillin-streptomycin using the equation in Section 2.3.1. Bacterial suspensions were treated with chemicals as described in Section 2.3.2. To investigate *C. jejuni* viability with 0.1% (v/v) Triton X-100, *C. jejuni* strains were inoculated in 500 µl of 0.1% (v/v) Triton X-100 and incubated at room temperature for 20 minutes. To investigate *C. jejuni* viability under infection assay conditions, *C. jejuni* strains were inoculated in 1 ml of complete growth medium without penicillin-streptomycin and incubated for 3, 6 and 24 hours at 37°C in a 5% $CO_2$ incubator. After treatment, serial dilutions up to $10^{-8}$ were performed and 10 µl of each dilution was spotted in triplicate on to CBA plates. The plates were incubated under microaerobic atmosphere at 37°C for 48 hours. The CFUs from each spot were enumerated. Three biological replicates were performed for all experiments.

### 2.3.4. Lactate dehydrogenase (LDH) cytotoxicity assay

CyQUANT™ LDH Cytotoxicity Assay (Thermo Scientific) was used to investigate the effect of chemical treatments on the viability of T84 and Caco-2 cells. Human IECs (≈$10^4$ cells/well) were plated in triplicate wells in a clear bottom and black 96-well plate (Corning, USA) followed by incubation at 37°C in a 5% $CO_2$ atmosphere for 18 hours. Complete growth medium was replaced with DMEM/F-12 without phenol red supplemented with 5% (v/v) FBS. 10 µl of DEPC-treated water (Invitrogen, USA) was added to one set of triplicate wells of cells for spontaneous LDH activity controls. For chemical treated samples, chemicals were diluted in 10 µl of DEPC-treated water to give the final concentration as described in Table 2.2. For maximum LDH activity controls, nothing was added at this step. The plate was incubated at 37°C in a 5% $CO_2$ incubator for the designated time as described in Table 2.2. After treatment, 10 µl of 10X Lysis Buffer was added to the set of triplicate wells of maximum LDH activity controls and mixed gently by tapping followed by incubation at 37°C with 5% $CO_2$ for 45 minutes. After incubation, 50 µl of medium from each well was transferred to a new clear bottom and

black 96-well plate. Then 50 µl of reaction mixture was added to each sample and gently mixed. The plate was then incubated at room temperature for 30 minutes protected from light. 50 µl of Stop Solution was then added to each well and mixed gently by tapping. The absorbance at both 490 nm and 680 nm was measured using SpectraMax M3 Multi-Mode Microplate Reader (Molecular Devices, USA). The LDH activity was measured by subtracting the absorbance at 680 nm from the absorbance at 490 nm. Cytotoxicity (%) was calculated by using the equation below.

$$\% \text{ Cytotoxicity} = \frac{\text{Chemical treated LDH activity} - \text{Spontaneous LDH activity}}{\text{Maximum LDH activity} - \text{Spontaneous LDH activity}} \text{ x } 100$$

2.3.5. Trypan blue exclusion assay

To measure viability of human IECs under experimental conditions, a trypan blue exclusion assay was performed. After desired incubation under experimental conditions, 300 µl of 0.25% (w/v) trypsin-EDTA was added into each well and the plates were incubated for 10 minutes at 37°C in a 5% $CO_2$ incubator. After the cells were detached, 1 ml of complete culture medium was added into each well and pipetted to mix well. 50 µl of cell suspension was transferred to 1.5 ml microcentrifuge tubes and mixed with 50 µl of 0.4% (w/v) trypan blue solution. 20 µl of cell suspension with trypan blue solution was loaded to the haemocytometer. The number of viable and dead cells were counted in four outer squares. Percentage viability was calculated based on the enumerated cells.

2.3.6. *C. jejuni* interaction, invasion and intracellular survival assays

T84 or Caco-2 cells (≈$10^6$ cells) in a 24-well plate were washed with pre-warmed PBS three times and a bacterial suspension with an $OD_{600}$ of 0.2 in complete growth medium without penicillin-streptomycin was prepared as described in Section 2.3.1. Then human IECs were infected with 1 ml of bacterial suspension (multiplicity of infection; MOI of 200:1) and incubated for 3 or 24 hours at 37°C in a 5% $CO_2$ incubator. For the interaction (adhesion and invasion) assays, infected human IECs were washed three times with pre-warmed PBS to remove unbound extracellular bacteria. Then 500 µl of 0.1% (v/v) Triton X-100 (Sigma-Aldrich) was added into each well and incubated for 20 min at room temperature. After incubation, each well was pipetted for 1 minute to lyse the IECs. The lysates were then briefly vortexed and 10-fold serial dilutions were performed in a 96-well plate. 10 µl of each dilution was plated onto CBA plates and the plates were incubated for 48 hours at 37°C under microaerobic conditions. The number of *C. jejuni* interacting with IECs was enumerated.

An additional step of treatment with gentamicin (150 µg/ml) for 2 hours at 37°C in a 5% $CO_2$ incubator to kill extracellular bacteria was performed prior to lysis for invasion assays. After incubation with gentamicin, human IECs were washed three times with pre-warmed PBS. The cells were lysed with 0.1% (v/v) Triton X-100 and the lysates were diluted in PBS and plated onto CBA plates as described above.

For intracellular survival assays, after infection with *C. jejuni* for 3 hours, human IECs were incubated with gentamicin (150 μg/ml) for 2 hours at 37°C in a 5% $CO_2$ incubator to kill extracellular bacteria followed by further 18 hours incubation with gentamicin (10 μg/ml) at 37°C in a 5% $CO_2$ incubator. IECs were lysed as described above and 5-fold serial dilution was performed, plated onto blood agar plates for CFU enumeration.

### 2.3.7. Intracellular ROS detection assay

To measure the levels of intracellular ROS produced within human IECs under experimental conditions, 2',7'-dichlorofluorescin diacetate (DCFDA) Cellular ROS Detection Assay Kit (Abcam, UK) was used according to the manufacturer's instructions. Non-fluorescent DCFDA diffuses into the cells and is deacetylated by cellular esterases. Oxidation of this non-fluorescent substrate by ROS produces highly fluorescent DCF. Human IECs (≈2 x $10^4$ CFU/ml) were seeded into a clear bottom and black 96-well plate and incubated overnight to allow cells to attach. Semi-confluent cells were washed with pre-warmed PBS three times and bacterial suspensions with an $OD_{600}$ of 0.2 in DMEM/F-12 without phenol red were prepared as described in Section 2.3.1. 100 μl of bacterial suspension was added into each well giving a MOI of 200:1 and plates were incubated for 3 or 24 hours at 37°C in a 5% $CO_2$ incubator. For positive controls, IECs were treated with 500 μM $H_2O_2$ for 45 minutes. Blank wells contained only DMEM/F-12 without phenol red. 45 minutes prior to completion of the infection, 100 μl of 100 μM DCFDA was added to each well giving a final concentration of 50 μM. The plate was covered with aluminium foil to protect from light and incubated for the final 45 minutes at 37°C in a 5% $CO_2$ incubator. The fluorescence with 485 nm excitation and 535 nm emission were recorded using a SpectraMax M3 Multi-Mode Microplate Reader.

### 2.3.8. Extracellular ROS detection assay

To measure the levels of extracellular $H_2O_2$ produced from human IECs under experimental conditions, Amplex® Red Hydrogen Peroxide/Peroxidase Assay Kit (Invitrogen) was used according to the manufacturer's instructions. Reaction between $H_2O_2$ and Amplex® Red reagent (10-acetyl-3,7-dihydroxyphenoxazine) in the presence of horseradish peroxidase (HRP) produces a fluorescent product called resorufin. Approximately $10^6$ cells of human IECs grown in a 24-well plate were washed with pre-warmed PBS three times and a bacterial suspension with an $OD_{600}$ of 0.2 in DMEM/F-12 without phenol red was prepared as described in Section 2.3.1. 1 ml of bacterial suspension was added into each well of a 24-well plate (MOI 200:1) and incubated for 3 or 24 hours at 37°C in a 5% $CO_2$ incubator. 500 μM of $H_2O_2$ was used for positive controls. After infection, 100 μl of media from each well was transferred to a clear bottom and black 96-well plate. 100 μl of reaction mixture containing DMEM/F-12 without phenol red and 50 μM Amplex® Red reagent was mixed with transferred media. The plate was covered with aluminium foil to protect from light and incubated for 10 minutes at 37°C in a 5%

$CO_2$ incubator. The fluorescence with 530 nm excitation and 590 nm emission were recorded using a SpectraMax M3 Multi-Mode Microplate Reader.

### 2.3.9. Active Rac1 detection assay

To measure the level of GTP-bound Rac1 which is an active form under experimental conditions, G-LISA Rac1 Activation Assay Biochem Kit™ (Cytoskeleton Inc., USA) was used according to the manufacturer's instructions. 24 hours before the infection, T84 or Caco-2 cells grown on a 24-well plate were incubated in DMEM/F-12 with reduced serum (0.1% (v/v) FBS). Serum-starved cells were then infected with *C. jejuni* for 1, 3 or 24 hours (MOI 200:1). Infected or uninfected T84 or Caco-2 cells were washed three times with ice-cold PBS and lysed with 500 µl of the supplied Lysis Buffer containing a protease inhibitor cocktail. Immediately after addition of the Lysis Buffer, lysates were harvested using a cell scraper and transferred to pre-chilled microcentrifuge tubes. The lysates were centrifuged for 1 minute at 10,000 x g at 4°C. After centrifugation, the protein concentration in each lysate was measured using Precision Red™ Advanced Protein Assay Reagent and adjusted to 1 mg/ml. Normalised lysates were snap-frozen and stored at -80°C.

On the day of the assay, 50 µl of lysate was added into designated wells of a provided 96-well Rac1-GTP binding plate. 50 µl of lysis buffer was added as a blank control and 50 µl constitutively active Rac1 (RCCA) provided in the kit was added as a positive control. The plate was incubated with shaking at 400 rpm for 30 minutes at 4°C. After incubation, the solution was removed from the wells and washed twice with 200 µl of Wash Buffer. 200 µl of Antigen Presenting Buffer was added into wells and incubated at room temperature for 2 minutes. The Antigen Presenting Buffer was removed and wells were washed three times with 200 µl of Wash Buffer. 50 µl of anti-Rac1 primary antibody solution was added into wells followed by a 45 minute incubation at room temperature. After incubation, wells were washed three times with 200 µl of Wash Buffer and incubated with 50 µl of Secondary antibody solution for 45 minutes at room temperature. Wells were washed three times with 200 µl of Wash Buffer and incubated with 50 µl of HRP detection reagent for 20 minutes at room temperature. Then 50 µl of HRP Stop Buffer was added and absorbance at 490 nm was recorded using a SpectraMax M3 Multi-Mode Microplate Reader.

### 2.3.10. Interleukin-8 (IL-8) enzyme-linked immunosorbent assay (ELISA)

To measure IL-8 released from T84 cells under experimental conditions, a Human IL-8 Uncoated ELISA kit (Invitrogen) was used according to the manufacturer's instructions. For ELISA, human IECs ($\approx 10^6$ cells) in a 24-well plate were washed with pre-warmed PBS three times and a bacterial suspension with an $OD_{600}$ of 0.2 in complete growth medium without penicillin-streptomycin was prepared as described in Section 2.3.1. Then human IECs were infected with 1 ml of bacterial suspension (MOI of 200:1) and incubated for 6 or 24 hours at 37°C in a 5% $CO_2$ incubator. After infection, culture media

from each well was collected into 1.5 ml microcentrifuge tubes and stored at -80°C before further analysis.

Nunc™ MaxiSorp™ 96-Well flat-bottom microplates (Invitrogen) were used for ELISA. ELISA plates were coated with 100 µl of capture antibody diluted in Coating Buffer and incubated overnight at 4°C. After overnight incubation, each well was washed three times with 230 µl of Wash Buffer (0.05 % (v/v) Tween in PBS). 200 µl of 1X ELISA/ELISPOT Diluent was added into each well and the plate then incubated at room temperature for 1 hour with shaking. The plate was then washed once with Wash Buffer and 2-fold serial dilutions of the standard were performed. 100 µl of 1X ELISA/ELISPOT Diluent was added as a blank. Experimental samples stored at -80°C were thawed and 100 µl of each sample was added into a designated well. The plate was covered with aluminium foil to protect from light and incubated at room temperature for 2 hours with shaking. After incubation, each well was washed three times with Wash Buffer and incubated with 100 µl of Detection Antibody at room temperature for 1 hour with shaking. Then the plate was washed three times with Wash Buffer and incubated with Avidin-horseradish peroxidase (HRP) at room temperature for 30 minutes with shaking. The plate was washed five times with Wash Buffer and incubated with 100 µl of 1X tetramethylbenzidine (TMB) solution at room temperature for 15 minutes with shaking. After incubation, 100 µl of Stop Solution (2N $H_2SO_4$; Sigma-Aldrich) was added into each well. Absorbances at 570 nm and 450 nm were recorded using a SpectraMax M3 Multi-Mode Microplate Reader. The absorbance at 570 nm was subtracted from the absorbance at 450 nm to correct for the optical imperfections in the plate.

#### 2.3.11. Small interfering (si) RNA transfection

On the day of reverse transfection, Caco-2 cells were washed and harvested as described in Section 2.2.2. Detached cells were resuspended in 10 ml of pre-warmed complete growth medium and centrifuged at 100 x g for 10 minutes. After centrifugation, the supernatant was discarded and the pellet resuspended in 10 ml of pre-warmed Opti-MEM® Reduced-Serum Medium (Thermo Fisher Scientific). After counting the cells as described in Section 2.2.3, 500 µl of Caco-2 cells ($10^5$ cells/ml) were seeded in 24-well plates and treated for 24 hours with 30 pmol siRNA from either Nox1 siRNA (sc-43939; Santa Cruz Biotechnology, Inc, USA) or Ambion® Silencer Negative Control #1 siRNA (Invitrogen) for the negative control. For preparation of siRNA transfection reagent complex, 3 µl of 10 µM stock siRNA was diluted with 100 µl of Opti-MEM® Reduced-Serum Medium and mixed with 1.5 µl of Lipofectamine® RNAiMAX Transfection Reagent (Thermo Fisher Scientific). After 24 hours transfection, Opti-MEM® Reduced-Serum Medium was replaced with complete growth medium containing 10% (v/v) FBS. After an additional 48- or 72 hour-incubation, RNA and protein were extracted and further analysed for the efficacy of transfection as described in Sections 2.3.12 and 2.4.2.

A Trypan blue exclusion assay was performed to check cell viability with siRNA transfection as described in Section 2.3.5.

### 2.3.12. Protein extraction from human IECs

For protein extraction assays, human IECs were seeded into a 6-well plate at a density of 2 x $10^5$ cells/well as described in Section 2.2.3. 6-well plates containing cells were incubated for 5-7 days at 37°C in a 5% $CO_2$ incubator and grown up to ≈ 2 x $10^6$ cells. T84 or Caco-2 cells were pre-treated with chemicals as described in Section 2.3.2 or infected with *C. jejuni* (MOI of 200:1) for 24 hours. After infection, T84 or Caco-2 cells were washed three times with 2 ml of ice-cold PBS. Lysis buffer solution was prepared by adding Halt™ Protease & Phosphatase Inhibitor Single-Use Cocktail (Thermo Scientific) into RIPA lysis and extraction buffer (Thermo Fisher Scientific). 250 µl of lysis buffer solution was added into each well and the plate was incubated for 5 minutes at room temperature. Using a cell scraper, the cells were harvested from each well and transferred into 1.5 ml microcentrifuge tube. Cells were lysed by pipetting for 1 minute and vortexed for 1 minute at room temperature. Microcentrifuge tubes containing lysates were centrifuged for 20 minutes at 17,000 x g at 4°C. 10 µl of each supernatant was used in a bicinchoninic acid (BCA) assay to measure protein concentrations as described in Section 2.3.13.

### 2.3.13. Bicinchoninic acid (BCA) assay and protein concentration normalisation

In order to measure protein concentration of each sample lysate, a BCA assay was performed using a Pierce™ Bicinchoninic Acid Protein Assay Kit (Thermo Fisher Scientific) according to the manufacturer's instructions. BCA Working Reagent was prepared by using the following equation.

$$(\text{The number of standards} + \text{The number of unknowns}) \times \text{The number of replicates} \times 0.2 \text{ ml}$$

According to the calculated total volume of Working Reagent, 50 parts of BCA Reagent A was mixed with 1 part of BCA Reagent B. 25 µl of standard with a known concentration of bovine serum albumin and unknown sample lysate were added into a 96-well plate. 200 µl of BCA Working Reagent was added into each well. The plate was incubated protected from light at 37°C in a 5% $CO_2$ incubator for 30 minutes. After incubation, the plate was cooled at room temperature. Absorbance at 595 nm was recorded using a SpectraMax M3 Multi-Mode Microplate Reader. Afterwards, a standard curve was prepared and sample concentrations were calculated. Then samples were diluted to a desired concentration in HyClone™ water (Cytiva, UK) and 4X Laemmli sample buffer (Sigma-Aldrich) and incubated for 5 minutes at 95°C. The protein samples were stored at -20°C until further use.

### 2.3.14. Intracellular $Ca^{2+}$ measurement assay

In order to measure intracellular $Ca^{2+}$ concentration under experimental conditions, T84 cells (≈3 x $10^4$

cells/well) were seeded into a clear bottom and black 96-well plate followed by incubation at 37°C in a 5% $CO_2$ atmosphere for 18 hours to allow the cells to attach to the bottom of the plate. T84 cells were pre-treated with a cell-permeable $Ca^{2+}$ chelator, BAPTA-AM for 1 hour prior to infection with *C. jejuni* or treatment with thapsigargin as described in Section 2.3.2. After pre-treatment, a *C. jejuni* suspension ($OD_{600}$ 0.06) and 2 µM thapsigargin solution were prepared in DMEM/F-12 without phenol red supplemented with 5% (v/v) FBS. T84 cells were infected with *C. jejuni* (MOI of 200:1) or treated with thapsigargin for 3 or 24 hours. After infection or treatment, T84 cells were washed three times with 150 µl of HEPES buffered saline solution (BSS) (PromoCell, Germany). Cell-permeable dye Fura-2, AM (Invitrogen) was used to detect intracellular $Ca^{2+}$. The dye solution was prepared by adding 5 µM Fura-2, AM, 0.05% (v/v) Pluronic F-127 (Invitrogen) and 2.5 mM probenecid (Invitrogen) into HEPES BSS. Pluronic F-127 helps solubilisation of Fura-2, AM and probenecid prevents leakage of Fura-2, AM from the cells. T84 cells were incubated with 100 µl of dye solution for 1 hour protected from light at 37°C in a 5% $CO_2$ incubator. After 1 hour incubation, T84 cells were washed twice with 200 µl of DMEM/F-12 without phenol red and incubated for additional 30 minutes at 37°C in a 5% $CO_2$ incubator for complete de-esterification of Fura-2, AM. At the end of the experiment, for the maximal fluorescence, 0.1% (v/v) Triton X-100 was added to lyse the cells and release intracellular Fura-2, AM from the cells. For the minimal fluorescence, 0.1% (v/v) Triton X-100 was added with subsequent addition of 30 µM BAPTA-AM. Then the two sets of fluorescence with 340 nm excitation and 510 nm emission ($\lambda_1$) and 380 nm excitation and 510 nm emission ($\lambda_2$) were recorded using a SpectraMax M3 Multi-Mode Microplate Reader. Intracellular $Ca^{2+}$ concentration was calculated using the equation below.

$$[Ca^{2+}]_i = K_d \text{ x } Q \text{ x } \frac{(R - R_{min})}{(R_{max} - R)}$$

In the equation, R represents the ratio of fluorescence intensity at $\lambda_1$ and $\lambda_2$. $\lambda_1$ detects $Ca^{2+}$-bound Fura-2 and $\lambda_2$ detects $Ca^{2+}$-free Fura-2. Q is the ratio of the minimal fluorescence intensity and the maximal fluorescence intensity at $\lambda_2$. $K_d$ is the dissociation of constant of the dye. The $K_d$ value of Fura-2 at 37°C is 224 nM (Grynkiewicz, Poenie, & Tsien, 1985). $R_{min}$ is the ratio of minimal fluorescence intensity at $\lambda_1$ and $\lambda_2$ and $R_{max}$ is the ratio of maximal fluorescence intensity at $\lambda_1$ and $\lambda_2$.

## 2.4. Molecular techniques

### 2.4.1. Bacterial genomic DNA (gDNA) extraction

gDNA of *C. jejuni* was extracted using PureLink™ Genomic DNA Mini Kit (Invitrogen) according to the manufacturer's instructions. In order to obtain a *C. jejuni* lysate, *C. jejuni* was harvested from 24 hour plates and resuspended in 180 µl of PureLink™ Genomic Digestion Buffer. 20 µl of Proteinase K was added into the suspension to lyse the cells and mixed by vortexing. The lysate was incubated at 55°C for 1.5 hours with occasional vortexing. 20 µl of RNase A was added after lysis and incubated at

room temperature for 2 minutes. 200 µl of PureLink™ Genomic Lysis/Binding buffer was then added and mixed well. 200 µl of 96% (v/v) ethanol was added and mixed well. 640 µl of the lysate was loaded into the PureLink™ Spin Column and centrifuged at 10,000 x g for 1 minute at room temperature. The spin column was placed into a new collection tube. The column was washed with 500 µl of Wash Buffer 1 and centrifuged at 10,000 x g for 1 minute at room temperature. The column was placed into a new collection tube and 500 µl of Wash Buffer 2 was added into the column followed by centrifugation at 17,000 x g for 3 minutes at room temperature. The spin column was placed into a new 1.5 ml microcentrifuge tube. 100 µl of DEPC-treated water was added and the column was incubated at room temperature for 1 minute. After incubation, the column was centrifuged at 17,000 x g for 1 minute at room temperature. Quantity and quality of bacterial gDNA was checked using a NanoDrop ND-1000 spectrophotometer (Thermo Fisher Scientific).

### 2.4.2. Bacterial and eukaryotic RNA extraction

*C. jejuni* was harvested from 24 hour plates and inoculated in 10 ml of *Brucella* broth, then adjusted to an $OD_{600}$ of 0.1 as described in Section 2.3.1. The inoculated flasks were then incubated for 16 hours with shaking at 75 rpm at 37°C under microaerobic conditions. After incubation, 2 ml of RNAprotect Bacteria Reagent (Qiagen, Germany) was added per 1 ml of bacterial culture, briefly vortexed, incubated for 5 minutes at room temperature then centrifuged at 3,434 x g at 4°C for 10 minutes. The supernatant was discarded and a PureLink™ RNA Mini Kit (Thermo Fisher Scientific) was used for further RNA isolation according to manufacturer's instructions. Lysis Buffer was prepared by adding 100 µl of 99% 2-mercaptoethanol (Sigma-Aldrich) into 6 ml of Lysis Buffer. 500 µl of Lysis Buffer was added to the bacterial pellet and agitated for 1 minute by pipetting. The lysate was vortexed for 2 minutes for homogenisation. 500 µl of 70% (v/v) ethanol was added into the lysate and vortexed. 700 µl of the lysate was transferred into a Spin Cartridge followed by centrifugation at 12,000 x g for 15 seconds at room temperature. The flow-through was discarded and the Spin Cartridge was reinserted into the Collection Tube. This step was repeated for the remaining sample. 700 µl of Wash Buffer 1 was added to the Spin Cartridge followed by centrifugation at 12,000 x g for 15 seconds at room temperature. The flow-through was discarded and the Spin Cartridge was placed into a new Collection Tube. 500 µl of Wash Buffer 2 was added into the Spin Cartridge followed by centrifugation at 12,000 x g for 15 seconds at room temperature. The flow-through was discarded and the Spin Cartridge was reinserted into the Collection Tube. This step was repeated once more. The Spin Cartridge was centrifuged at 12,000 x g for 2 minutes at room temperature to dry the Spin Cartridge. After centrifugation, the Spin Cartridge was inserted into a Recovery Tube and 30 µl of DEPC-treated water added followed by incubation for 1 minute at room temperature, then the Spin Cartridge was centrifuged at 12,000 x g for 2 minutes at room temperature to elute RNA. The concentration and quality of RNA samples were determined using a NanoDrop ND-1000 spectrophotometer. The amount of each RNA sample was

normalised to 2,000 ng in 44 µl of DEPC-treated water.

RNA from human IECs was extracted using PureLink$^{TM}$ RNA Mini Kit. Before extraction, human IECs were washed three times with ice-cold PBS. 500 µl of Lysis Buffer containing 100 µl of 99% 2-mercaptoethanol was added into each well. Human IECs were lysed by pipetting for 1 minute. The lysate was vortexed for 2 minutes for homogenisation and 500 µl of 70% (v/v) ethanol was added into the lysate and vortexed. RNA extraction was then processed as described above.

Each RNA sample was processed for the removal of contaminating DNA within the sample using a TURBO DNA-free kit (Ambion, USA) according to manufacturer's instructions. 5 µl of 10X TURBO DNase Buffer and 1 µl TURBO DNase were added into a RNA sample followed by incubation for 1 hour in a 37°C water bath. After incubation, 5 µl of DNase Inactivation Reagent was added and the sample was centrifuged at 10,000 x g for 1.5 minutes and 10 µl of RNA sample was transferred into a fresh tube. Purified DNase-treated RNA samples were stored at -80°C until further use.

### 2.4.3. Complementary DNA (cDNA) synthesis

10 µl of RNA sample (400 ng) was mixed with 1 µl of random hexamers (50 ng/µl; Invitrogen) and 1 µl of dNTP mix (10 mM; Invitrogen). The sample was incubated at 65°C for 5 minutes and immediately cooled on ice. The sample was then mixed with 4 µl of 5X RT buffer (Invitrogen), 2 µl of 0.1 M DTT (Invitrogen), 2 µl of 25 mM $MgCl_2$ (Thermo Fisher Scientific), 1 µl of RNaseOUT (40 U/µl; Invitrogen) and 1 µl of SuperScript III RT (200 U/µl; Invitrogen). Samples were mixed well and briefly centrifuged. The reaction mixture was incubated at 25°C for 10 minutes followed by a 50 minute incubation at 50°C and a 5 minute incubation at 85°C. The sample was cooled down to 4°C and incubated with 0.5 µl RNase H (5U/µl; Thermo Fisher Scientific) at 37°C for 20 minutes. The cDNA product was stored at -20°C until further use.

### 2.4.4. Polymerase chain reaction (PCR) and gel electrophoresis

Primers used in RT-PCR are listed in Table 2.3. Primers were diluted in DEPC-treated water to a final concentration of 100 pmol/µl and then further diluted to 10 pmol/µl. Each PCR reaction contained 25 µl of 2X MyTaq Red Mix (Bioline, UK), 1 µl of forward primer (10 pmol), 1 µl of reverse primer (10 pmol), 1.5 µl of cDNA and 21.5 µl of DEPC-treated water. One cycle of PCR program performed as:

| | | | |
|---|---|---|---|
| Initial denaturation: | | 95°C for 2 minutes | |
| 36 cycles of | - | Denaturation: | 95°C for 15 seconds |
| | | Annealing*: | 50°C for 20 seconds |
| | | Extension: | 72°C for 30 seconds |

*Annealing temperature is based on the melting temperature (Tm) of primer.

A 1% (w/v) agarose gel was prepared in Tris-acetate-EDTA (TAE) buffer. For detection of XBP1 splicing, a 2% (w/v) agarose gel was prepared. After melting the agar in TAE buffer, GelRed (10,000X; Sigma-Aldrich) was added to 1X final concentration. After the gel was solidified, 25 µl of each PCR product or 4 µl of HyperLadder (100 bp to 1 kb) (Bioline) was loaded into the wells. The gel was run at 120V/400 mA for 1.5 hours. The gel was visualised using an Azure c600 (Azure Biosystems, USA).

**Table 2.3. Primers used RT-PCR and qRT-PCR.**

| Name | Sequence | Tm (° C) | RT-PCR / qRT-PCR | Reference |
|---|---|---|---|---|
| *CHOP* (Forward) | 5'-GGAAACAGAGTGGTCATTCCC-3' | 55.6 | Both | (Di et al., 2016) |
| *CHOP* (Reverse) | 5'-CTGCTTGAGCCGTTCATTCTC-3' | 56.2 | Both | (Di et al., 2016) |
| *XBP1* (Forward) | 5'-ACACGCTTGGGGATGAATGC-3' | 58.5 | RT-PCR | (Yamazaki et al., 2009) |
| *XBP1* (Reverse) | 5'-CCATGGGAAGATGTTCTGGG-3' | 55.5 | RT-PCR | (Yamazaki et al., 2009) |
| Spliced *XBP1* (Forward) | 5'-TGCTGAGTCCGCAGCAGGTG -3' | 62.6 | qRT-PCR | (Misiewicz et al., 2013) |
| Spliced *XBP1* (Reverse) | 5'-GCTGGCAGGCTCTGGGGAAG-3' | 63.3 | qRT-PCR | (Misiewicz et al., 2013) |
| *ATF6* (Forward) | 5'-TCCTCGGTCAGTGGACTCTTA-3' | 56.9 | Both | (Ma et al., 2021) |
| *ATF6* (Reverse) | 5'-CTTGGGCTGAATTGAAGGTTTTG-3' | 55.1 | Both | (Ma et al., 2021) |
| *BIP* (Forward) | 5'-CATCACGCCGTCCTATGTCG-3' | 58.0 | Both | (Liu et al., 2016) |
| *BIP* (Reverse) | 5'-CGTCAAAGACCGTGTTCTCG-3' | 56.0 | Both | (Liu et al., 2016) |
| *NOX1* (Forward) | 5'-CACAAGAAAAATCCTTGGGTCAA-3' | 53.9 | Both | (Manea et al., 2014) |

| | | | | |
|---|---|---|---|---|
| *NOX1* (Reverse) | 5'-GACAGCAGATTGCGACACACA-3' | 58 | Both | (Manea et al., 2014) |
| *CAT* (Forward) | 5'-TGCAAGCTAGTGGCTTCAAAA-3' | 55.3 | qRT-PCR | (Wang & Eskiw, 2019) |
| *CAT* (Reverse) | 5'-TCCAATCATCCGTCAAAACAA-3' | 52.6 | qRT-PCR | (Wang & Eskiw, 2019) |
| *SOD1* (Forward) | 5'-GGCAAAGGTGGAAATGAAGAA-3' | 53.7 | qRT-PCR | (Wang & Eskiw, 2019) |
| *SOD1* (Reverse) | 5'-GGGCCTCAGACTACATCCAAG-3' | 57.1 | qRT-PCR | (Wang & Eskiw, 2019) |
| *GAPDH* (Forward) | 5'-CATCACCATCTTCCAGGAGC-3' | 55.4 | RT-PCR | (Das et al., 2000) |
| *GAPDH* (Reverse) | 5'-GGATGATGTTCTGGAGAGCC-3' | 55.2 | RT-PCR | (Das et al., 2000) |
| *GAPDH* | Hs_GAPDH_1_SG QuantiTect Primer Assay, QT00079247 | - | qRT-PCR | Qiagen |

2.4.5. Quantitative real-time PCR (qRT-PCR)

Each reaction contained 10 µl of SYBR Green PCR Master Mix (Applied Biosystems, USA), 1 µl of combined forward and reverse primers (20 pmol), 1 µl of cDNA and 10 µl of DEPC-treated water. The sequence of each primer is listed in Table 2.3. All reactions were run in triplicate on an ABI-PRISM 7500 instrument (Applied Biosystems) using the following cycling program:

| | | | |
|---|---|---|---|
| Initial holding stage: | | 50°C for 20 seconds | |
| Initial denaturation: | | 95°C for 10 minutes | |
| 40 cycles of | - | Denaturation: | 95°C for 15 seconds |
| | | Annealing and extension: | 60°C for 1 minute |
| Melt curve: | - | 95°C for 15 seconds | |
| | | 60°C for 1 minute | |
| | | 95°C for 30 seconds | |
| | | 60°C for 15 seconds | |

Expression levels of all target genes were normalised to expression of *GAPDH* encoding glyceraldehyde 3-phosphate dehydrogenase determined in the same experiment as an internal control. Relative expression changes were calculated using the comparative threshold cycle ($C_T$) method. A minimum of three biological replicates were analysed, each in technical triplicate. Relative expression changes were

calculated using the comparative $C_T$ cycle ($2^{-\Delta\Delta CT}$) method (Schmittgen & Livak, 2008).

### 2.4.6. *C. jejuni* 11168H *cdtABC* operon mutagenesis

#### 2.4.6.1. Splicing by overlap extension PCR (SOE PCR)

*C. jejuni* 11168H *cdtABC* operon mutant was created by using SOE PCR (Horton et al., 2013). SOE PCR primers were designed to amplify the left fragment (L1) and right fragment (R1) of *C. jejuni* 11168H *cdtABC* operon (Figure 2.1A and Table 2.4). Primer set *cj0080*_up and *cj0079c*_dw amplified the left fragment (amplicon size 588 bp with 563 bp complementary to *C. jejuni* 11168H genome). Primer set *cj0077c*_up2 and *cj0076c*_dw amplified the right fragment (amplicon size 575 bp with 550 bp complementary to *C. jejuni* 11168H genome). 25 bp of primer *cj0077c*_up2 is complementary to 25 bp of primer *cj0079c*_dw and regions of overlap contain a BamHI restriction site (Figure 2.1B).

To amplify L1 and R1 of *C. jejuni cdtABC* operon, each PCR reaction contained 25 µl of 2X HotStarTaq Master Mix (Qiagen), 1 µl of forward primer (10 pmol), 1 µl of reverse primer (10 pmol) and 2 µl of *C. jejuni* 11168H chromosomal DNA (100-500 ng) and 21 µl of DEPC-treated water. One cycle of PCR programme performed as:

| | | | |
|---|---|---|---|
| Initial denaturation: | | 96°C for 2 minutes | |
| 35 cycles of | - | Denaturation: | 96°C for 30 seconds |
| | | Annealing*: | 50°C for 30 seconds |
| | | Extension: | 72°C for 1 minute |
| Final extension: | | 72°C for 5 minutes | |

*Annealing temperature is based on the Tm of primer.

The PCR products were purified using a QIAquick® PCR Purification Kit (Qiagen), the concentration recorded and stored at -20°C for further use. To confirm the amplification of genes of interest, gel electrophoresis was performed as described in Section 2.4.4. A 1% (w/v) agarose gel was used and 10 µl of samples were loaded into each well.

The combined left and right fragment of *C. jejuni* 11168H *cdtABC* operon (L1R1) was amplified using primer *cj0080*_up and primer *cj0076c*_dw (Table 2.4). Each PCR reaction contained 25 µl of 2X HotStarTaq Master Mix, 1 µl of forward primer (10 pmol), 1 µl of reverse primer (10 pmol), 22 µl of DEPC-treated water and total 1 µl of left and right fragment from purified PCR products (1:1 ratio). One cycle of PCR programme performed as:

| | | | |
|---|---|---|---|
| Initial denaturation: | | 96°C for 2 minutes | |
| 35 cycles of | - | Denaturation: | 96°C for 30 seconds |
| | | Annealing*: | 50°C for 30 seconds |
| | | Extension: | 72°C for 3 minutes |

Final extension: 72°C for 5 minutes

*Annealing temperature is based on the Tm of primer.

Then gel electrophoresis was performed as described in Section 2.4.4. The bands of interest in the gel were cut from the gel and purified using a QIAquick® Gel Extraction Kit (Qiagen). Purified PCR products were sequenced to confirm the amplification of combined left and right fragment of *C. jejuni cdtABC* operon. Sequences of cleaned PCR products were compared with the sequence of the desired PCR product (Figure 2.1C).


**Figure 2.1. SOE PCR design.** (A) Diagram of *C. jejuni* 11168H *cdtABC* operon and the primers used for SOE PCR. Obtained from SnapGene Viewer (SnapGene, USA) (B) The region of overlap between the SOE PCR internal primers. (Blue: 5' homology fragment reverse primer, Yellow: 3' homology fragment forward primer; Green: region of overlap between the primers, Red: BamHI restriction site). (C) Expected product of SOE PCR (1,138 bp). (Purple: SOE PCR external primers; 5' homology fragment forward primer and 3' homology fragment reverse primer).

**Table 2.4. Primers used for *C. jejuni* 11168H *cdtABC* operon knockout mutagenesis.**

| Name | Sequence | Tm (°C) | Reference |
|---|---|---|---|
| *cj0080*_up (Forward) | 5'-CTGTAGCTACACCGATAGC-3' | 52 | This study |
| *cj0077c*_up2 (Forward) | 5'-TGACCCGGGATCGATGGATCCGTAGCCACCTTTAACAGCTGCTACC-3' | 70.9 | This study |
| *cj0079c*_dw (Reverse) | 5'-CTACGGATCCATCGATCCCGGGTCACATT | 65.2 | This study |

| | | | |
|---|---|---|---|
| | AAAAACCTTGATATG-3’ | | |
| *cj0076c*_dw (Reverse) | 5’-CTGGAGTAATGCTCATCACG-3’ | 53 | This study |
| *cdtA* (Forward) | 5’-TAGCGGTGCTGATTTAGTACCT-3’ | 55.6 | (Elmi et al., 2017) |
| *cdtA* (Reverse) | 5’-CATCGCCAAATCCTTTGCTATCG-3’ | 56.6 | (Elmi et al., 2017) |
| *cdtB* (Forward) | 5’-GAACAGCCACTCCAACAGGACG-3’ | 60.3 | (Elmi et al., 2017) |
| *cdtB* (Reverse) | 5’-CGATTAGCTCCTACATCAACGCGA-3’ | 58.6 | (Elmi et al., 2017) |
| *cdtC* (Forward) | 5’-GCCTTTGCAACTCCTACTGGAGAT-3’ | 58.9 | (Elmi et al., 2017) |
| *cdtC* (Reverse) | 5’-GCTCCAAAGGTTCCATCTTCTAAG-3’ | 55.5 | (Elmi et al., 2017) |

#### 2.4.6.2. pGEM®-T Easy Vector ligation and transformation of *E. coli*

According to the instructions for pGEM®-T and pGEM®-T Easy Vector Systems (Promega, USA), the purified PCR product L1R1 from Section 2.4.6.1 was ligated into pGEM-T® Easy Vectors by TA cloning. Each reaction contained 5 µl of 2X Rapid Ligation Buffer, 1 µl of pGEM®-T Easy Vector (50ng), 5 µl of PCR product L1R1 and 1 µl of T4 DNA Ligase (3 Weiss units/µl). Each ligation reaction mixture was incubated for 1 hour at room temperature.

Then *E. coli* DH5α™ Competent Cells (New England BioLabs, UK) were transformed with the resultant plasmid termed pAGH1 according to the manufacturers’ instructions. LB plates containing ampicillin/IPTG/X-gal were prepared by adding 14.8 g of LB agar base in 400 ml of distilled water supplemented with 400 µl of ampicillin (100 µg/ml), 800 µl of 5-bromo-4-chloro-3-inodlyl-β-D-galactopyranoside (X-Gal) (2.0% (w/v)), and 64 µl of isopropyl β-D-1-thiogalactopyranoside (IPTG) (1 pmol/µl). The ligation reaction mixture was centrifuged and 2 µl of the ligation reaction mixture was transferred to a 1.5 ml microcentrifuge tube on ice. *E. coli* DH5α™ Competent Cells were thawed and mixed gently by pipetting. 50 µl of competent cells was transferred to the 1.5 ml microcentrifuge tube containing the ligation reaction mixture. The tube was flicked and placed on ice for 20 minutes. Then cells were heat-shocked for 50 seconds in a water bath at 42°C. The tube was immediately returned to ice for 2 minutes. 1 ml of room-temperature super optimal broth (SOC; New England BioLabs) was added to the tube and incubated for 40 minutes in 37°C water bath. After incubation, the transformation culture was centrifuged at 1,000 x g for 10 minutes and the supernatant was discarded. The cells were

resuspended in 200 µl of SOC medium. 100 µl of transformation culture was plated onto a blue-white screening LB agar plate containing ampicillin/IPTG/X-gal and incubated under aerobic conditions at 37˚C for 24 hours.

#### 2.4.6.3. Blue-white screening and confirmation of *E. coli* transformants

Single white colonies which indicated the uptake of pAGH1 were then restreaked onto a fresh LB plate containing ampicillin/IPTG/X-gal and incubated under aerobic conditions at 37˚C for 24 hours. Then single white colonies from this plate were inoculated into 10 ml of LB broth with 5 µl of ampicillin (100 µg/ml) and incubated aerobically at 37˚C for 24 hours with shaking at 75 rpm. Overnight cultures were then centrifuged at 3,434 x g for 10 minutes using a Centrifuge 5810R (Eppendorf, Germany). A QIAprep® Spin Miniprep kit (Qiagen) was used to isolate putative pAGH1 plasmids.

To confirm the ligation of L1R1 into the pGEM-T® Easy Vector, isolated putative pAGH1 plasmids were sequenced, quantified and amplified using primers *cj0080*_up and *cj0076c*_dw (Table 2.4). One cycle of PCR programme performed as:

| | | | |
|---|---|---|---|
| Initial denaturation: | | 96°C for 2 minutes | |
| 35 cycles of | - | Denaturation: | 96°C for 30 seconds |
| | | Annealing*: | 50°C for 30 seconds |
| | | Extension: | 72°C for 3 minutes |
| Final extension: | | 72°C for 5 minutes | |

*Annealing temperature is based on the Tm of primer.

A total of 35 cycles were repeated. Gel electrophoresis was then performed as described in Section 2.4.4. In addition, restriction enzyme digestion on each putative pAGH1 plasmid was performed using BamHI restriction enzyme whose single restriction site was present within L1R1 sequence but not within the pGEM-T® Easy Vector. The reaction mixture with final volume of 20 µl was prepared by mixing 1 µg of pAGH1, 2 µl of 10X NEBuffer 3.1 (New England BioLabs, USA), 1 µl of BamHI (New England BioLabs) in Milli-Q water. The mixture was incubated for 1.5 hours in a 37˚C water bath. After incubation, the BamHI reaction mixture was treated with 1 µl of Antartic Phosphatase (New England BioLabs) and incubated for 30 minutes in a 37˚C water bath. Gel electrophoresis was performed using 50 ng of BamHI digested pAGH1 as described in Section 2.4.4. The bands of interest in the gel were cut from the gel and purified using QIAquick® Gel Extraction Kit (Qiagen). BamHI-digested pAGH1 was purified using QIAquick® PCR Purification Kit, quantified and stored at -20˚C for further use.

#### 2.4.6.4. Insertion of $Cm^r$ cassette into the vector, screening and confirmation of $Cm^r$ cassette insertion into the vector

10 µl of $Cm^r$ cassette (1.2 ng/µl; 804 bp) which encodes chloramphenicol acetyltransferase was digested

with BamHI restriction enzyme as described in Section 2.4.6.3. The digested cassette was purified using a QIAquick® PCR Purification Kit and quantified. For insertion of the $Cm^r$ cassette into pAGH1, the ligation reaction mixture was prepared by combining 50 ng of BamHI-digested pAGH1 and 12 ng of BamHI-digested $Cm^r$ cassette with 2 µl of 10X Buffer-T4 DNA ligase, 10 mM ATP (New England BioLabs) and 1 µl of T4 ligase enzyme (3 Weiss units/µl; New England BioLabs). Both ligation and transformation of *E. coli* DH5α™ Competent Cells were performed as described in Section 2.4.6.2. LB plates containing ampicillin/chrolamphenicol/IPTG/X-gal were prepared as described in Section 2.4.6.2 with addition of 333.3 µl of chloramphenicol (25 µg/ml). The transformed *E. coli* were then plated onto LB plates containing ampicillin/chloramphenicol/IPTG/X-gal and incubated under aerobic conditions at 37˚C for 24 hours.

Single white colonies which indicated uptake of pAGH1 inserted with a $Cm^r$ cassette were then re-streaked onto fresh LB plates containing ampicillin/chloramphenicol/IPTG/X-gal and the plates were incubated under aerobic conditions at 37˚C for 24 hours. Then single white colonies were inoculated into LB broth containing ampicillin/chloramphenicol and incubated aerobically at 37˚C for 24 hours with shaking at 75 rpm. Overnight cultures were centrifuged at 3,434 x g for 10 minutes and a QIAprep® Spin Miniprep kit was used to isolate pAGH1 with a $Cm^r$ cassette. To confirm $Cm^r$ cassette insertion, L1R1/$Cm^r$ cassette fragments from the isolated plasmids were amplified using primers *cj0080*_up and *cj0076c*_dw and gel electrophoresis was performed as described in Section 2.4.4. Purified PCR products were then sequenced to check presence and orientation of the inserted $Cm^r$ cassette. After confirmation of insertion and orientation of the $Cm^r$ cassette, pAGH2 refers to pAGH1/$Cm^r$ cassette with forward orientation.

#### 2.4.6.5. Preparation of *C. jejuni* 11168H competent cells

Competent *C. jejuni* 11168H was prepared by resuspending *C. jejuni* 11168H from a 24 hour plate in 10 ml ice-cold electroporation buffer (EBF; 15% (v/v) glycerol and 10% (w/v) sucrose) in sterile Milli-Q water and centrifuged at 3,434 x g for 10 minutes. The supernatant was discarded and the pellet resuspended in 250 µl of EBF and this step was repeated.

#### 2.4.6.6. Transformation of *C. jejuni* 11168H by electroporation and screening

A mixture for electroporation was prepared by adding 1 µg of pAGH2 into 50 µl of electrocompetent *C. jejuni* 11168H and the mixture was incubated on ice for 5 minutes. The mixture was then transferred to a cold electroporation cuvette (Bio-Rad, USA). Using a Gene Pulser Xcell™ Electroporation System (Bio-Rad), the mixture was pulsed at 25 µFD and 2.5 kV. 100 µl of pre-warmed SOC medium was added into the cuvette, mixed by pipetting, then plated onto a CBA plate without antibiotics. Plates were incubated overnight under microaerobic conditions at 37°C. Cells were then resuspended in 1 ml *Brucella* broth then 200 µl and 400 µl aliquots of this suspension were plated onto CBA plates

containing chloramphenicol (15 µg/ml). Plates were incubated under microaerobic conditions at 37°C for 5 days. *C. jejuni* colonies on the CBA containing chloramphenicol plates were inoculated onto fresh CBA containing chloramphenicol plates and incubated for 2 days under microaerobic conditions.

#### 2.4.6.7. Confirmation of *C. jejuni* 11168H *cdtABC* operon mutant

To confirm presence of L1R1/Cm$^r$ cassette and orientation, gDNA of putative *cdtABC* operon mutant strains and the wild-type strain were extracted as described in Section 2.4.1. PCR was then performed to amplify L1R1/Cm$^r$ cassette of using primers *cj0080*_up and *cj0076c*_dw. One cycle of PCR programme performed as:

| | | | |
|---|---|---|---|
| Initial denaturation: | | 96°C for 2 minutes | |
| 35 cycles of | - | Denaturation: | 96°C for 30 seconds |
| | | Annealing*: | 50°C for 30 seconds |
| | | Extension: | 72°C for 3 minutes |
| Final extension: | | 72°C for 5 minutes | |

*Annealing temperature is based on the Tm of primer.

As a negative control, the *cdtABC* operon from *C. jejuni* 11168H wild-type strain was also amplified using primers *cj0080*_up and *cj0076c*_dw. One cycle of PCR programme performed as:

| | | | |
|---|---|---|---|
| 35 cycles of | - | Denaturation: | 94°C for 15 seconds |
| | | Annealing*: | 50°C for 1 minute |
| | | Extension: | 72°C for 4 minutes |
| Final extension: | | 72°C for 7 minutes | |

*Annealing temperature is based on the Tm of primer.

Then gel electrophoresis was performed as previously described in Section 2.4.4. PCR products were purified using QIAquick® Gel Extraction Kit and sequenced to confirm absence of *cdtABC* operon and presence of L1R1/Cm$^r$ cassette. RNA from *cdtABC* operon mutant strain and wild-type strain was extracted as described in Section 2.4.2 then cDNA was synthesised as described in Section 2.4.3. qRT-PCR was also performed to confirm no expression of *cdtA*, *cdtB* and *cdtC* using the primers listed in Table 2.4.

### 2.4.7. Sodium dodecyl-sulfate polyacrylamide gel electrophoresis (SDS-PAGE) and Western blot

After quantification of protein samples as described in Section 2.3.14, 30 µg of protein samples were separated at 150 V using 4-12% (w/v) NuPAGE™ Bis-Tris gel in 1× NuPAGE™ MES buffer or MOPS buffer (Invitrogen). For detection of human fibronectin, protein samples were separated using NuPAGE™ 3 to 8%, Tris-Acetate gel (Invitrogen). 4 µl of PageRuler Plus Pre-stained Protein Ladder

(Thermo Fisher Scientific) was loaded as a molecular weight standard.

Proteins in SDS-PAGE gels were then transferred to a nitrocellulose membrane using the iBlot® 2 transfer stacks (Life Technologies, USA) using the iBlot® Gel Transfer Device (Invitrogen). P0 program (20 V for 1 min, 23 V for 4 min, 25 V for 2 minutes) was used for the transfer. The membrane was blocked by a 1 hour incubation with shaking at room temperature in 1X PBS containing 2% (w/v) skimmed milk (Sigma-Aldrich). The blocking solution was removed and the membranes were then incubated with primary antibodies overnight at 4°C without shaking. Primary antibodies were diluted in PBS containing 0.1% (v/v) TWEEN 20 (Sigma-Aldrich) and 2% (w/v) skimmed milk. The following primary antibodies were used; human GAPDH (ab181602; Abcam); human NOX1 (ab101027; Abcam or NBP-31546; Novus Biologicals, USA); human CHOP (NB600-1335; Novus Biologicals); human XBP1 (PA5-27650; Thermo Fisher Scientific); human fibronectin (PA1-23693; Thermo Fisher Scientific). After overnight incubation, blots were washed three times with 25 ml of PBS containing 0.1% (v/v) TWEEN 20. Blots were then incubated with secondary antibody for 1 hour shaking at room temperature. For secondary antibody dilution, either goat anti-rabbit IgG 800 or goat anti-mouse IgG 800 (LI-COR Biosciences, USA) was diluted at 1:10,000 in PBS containing 0.1% (v/v) TWEEN 20 and 2% (w/v) skimmed milk depending on host species of primary antibody. After incubation, blots were washed three times with 25 ml of PBS containing 0.1% (v/v) TWEEN 20 followed by a final wash with 25 ml of PBS. Blots were then visualised on a LI-COR Odyssey Classic (LI-COR Biosciences). Quantification of relative protein levels normalised to GAPDH expression was performed using ImageJ software (Schneider, Rasband, & Eliceiri, 2012).

### 2.5. Statistical analysis and graphing

At least three biological replicates were performed in all experiments. Each biological replicate was performed in three technical replicates. For statistical analysis and graphing, GraphPad Prism 8 for Windows (GraphPad Software, USA) was used. One sample *t*-test was performed to compare the mean of each data set with a hypothetical value. Unpaired *t*-test was performed to compare the mean between two independent data sets for significance with * indicating $p < 0.05$, ** indicating $p < 0.01$, *** indicating $p < 0.001$, and **** indicating $p < 0.0001$.

# CHAPTER THREE: Investigation of *C. jejuni* modulation of reactive oxygen species production and NADPH oxidase 1 expression in human intestinal epithelial cells

## 3.1. Preface

### 3.1.1. Aims and objective

NOX-mediated ROS production is an important host cellular defence strategy used to eliminate pathogens upon infection (Aviello & Knaus, 2017; Aviello & Knaus, 2018; Escoll et al., 2016). *E. coli* and *Salmonella enterica* possess OxyR and SoxRS (Nunoshiba et al., 1992; Zheng, Åslund, & Storz, 1998). OxyR and SoxRS recognise $H_2O_2$ and redox-active compounds respectively to induce appropriate cellular responses against oxidative stress (Nunoshiba et al., 1992; Zheng, Åslund, & Storz, 1998). Unlike other enteric pathogens such as *E. coli* and *Salmonella*, *C. jejuni* lacks the classical stress response regulators, OxyR and SoxRS (Burnham & Hendrixson, 2018; Elmi et al., 2021). Instead, *C. jejuni* utilises CosR, PerR and MarR-type regulators RrpA and RrpB to control bacterial responses against oxidative stress (Gundogdu et al., 2015; Gundogdu et al., 2016; Hwang et al., 2011; Palyada et al., 2009). Previous studies have demonstrated that infection with *E. coli*, *Salmonella* and *H. pylori* resulted in NOX1 induction and ROS production from host cells (den Hartog et al., 2016; Elatrech et al., 2015; Kawahara et al., 2005; Kawahara et al., 2016). As *C. jejuni* displays a unique strategy against oxidative stress, *C. jejuni* may also have a distinct mechanism for modulation of host ROS production.

The aim of the work discussed in this chapter was to investigate *C. jejuni* modulation of ROS production and NOX1 expression in human IECs. Intracellular and extracellular ROS from T84 and Caco-2 cells were measured upon *C. jejuni* infection. Transcriptional and protein levels of NOX1 in *C. jejuni*-infected human IECs were measured using qRT-PCR, RT-PCR and Western blotting. *C. jejuni*-mediated modulation of small GTPase Rac1 in IECs was determined to investigate if downregulation of NOX1 is linked to modulation of Rac1 by *C. jejuni*. To further investigate the mechanisms of *C. jejuni*-mediated ROS modulation, transcriptional levels of genes encoding human superoxide dismutase 1 (*SOD1*) and catalase (*CAT*) were measured using qRT-PCR. *C. jejuni* interaction, invasion and intracellular survival with DPI pre-treatment or NOX1 siRNA transfection were examined to investigate the role of NOX1 in *C. jejuni* pathogenesis in human IECs. Key datasets are included in the following publication in Section 3.2 (Hong et al., 2023) with additional data not included in the publication included in this preface.

### 3.1.2. Additional data

#### 3.1.2.1. *C. jejuni* viability at 37°C in a 5% $CO_2$ incubator

As *C. jejuni*-IEC infection assays were performed in complete growth medium without penicillin-streptomycin at 37°C in an incubator with 5% $CO_2$, viability of *C. jejuni* under these experimental conditions was assessed. As Figure 3.1 shows, the experimental conditions at 37°C in a 5% $CO_2$ incubator did not affect the viability of *C. jejuni* 11168H, 81-176 and 488 wild-type strains.

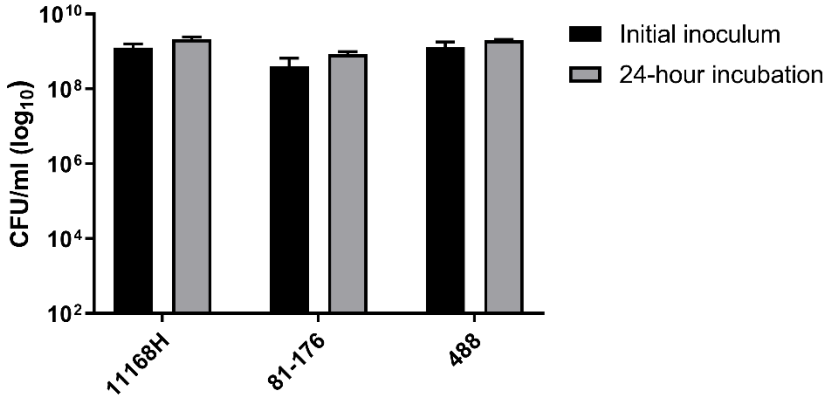


**Figure 3.1. Assessment of *C. jejuni* viability under experimental conditions at 37°C in an incubator with 5% $CO_2$.** *C. jejuni* 11168H, 81-176 or 488 wild-type strains were resuspended in complete growth medium without penicillin-streptomycin and incubated stationary for 24 hours at 37°C in a 5% $CO_2$ incubator. CFU/ml were recorded after incubation. Three biological and three technical replicates were performed for each experiment.

### 3.1.2.2. *C. jejuni* viability with Triton X-100 treatment

For *C. jejuni* interaction, invasion and intracellular survival assays, T84 and Caco-2 cells were treated with 0.1% (v/v) Triton X-100 for 20 minutes at room temperature to lyse the cells and recover *C. jejuni*. Therefore, *C. jejuni* viability with 0.1% (v/v) Triton X-100 treatment was assessed. As Figure 3.2 shows, 0.1% (v/v) Triton X-100 treatment did not affect the viability of *C. jejuni* 11168H, 81-176 and 488 wild-type strains.

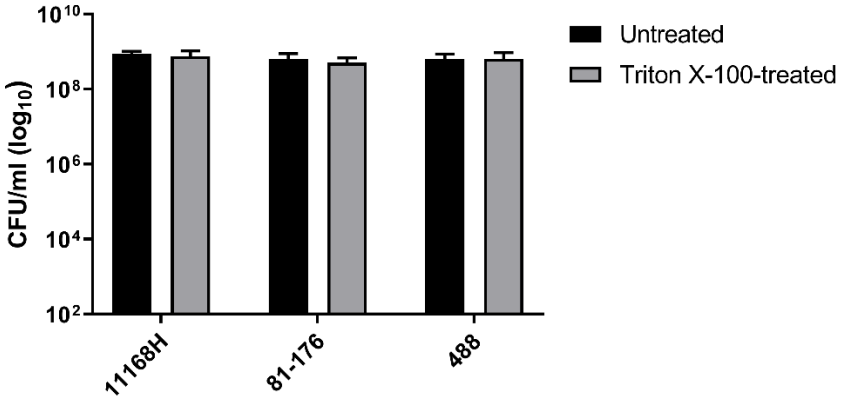


**Figure 3.2. Assessment of *C. jejuni* viability with 0.1% (v/v) Triton X-100 treatment.** *C. jejuni* 11168H, 81-176 or 488 wild-type strains were treated with 0.1% (v/v) Triton X-100 for 20 minutes at room temperature. CFU/ml was recorded after treatment. Three biological and three technical replicates were performed for each experiment.

### 3.1.2.3. Optimisation of NOX1 siRNA transfection in Caco-2 cells

To determine optimal conditions for NOX1 siRNA transfection in Caco-2 cells, NOX1 siRNA transfection with different transfection times and different concentrations of siRNA was performed. As shown in Figure 3.3, 48 hour transfection with 5 pmol NOX1 siRNA did not significantly reduce *NOX1* expression in Caco-2 cells. 48 hour transfection with 10 pmol and 20 pmol NOX1 siRNA resulted in 56.1% and 71.4% mean reduction of *NOX1* expression respectively, compared to scrambled siRNA transfected Caco-2 cells. Caco-2 cells were then transfected for longer with a higher concentration of NOX1 siRNA (30 pmol) resulting in greater reduction of *NOX1* expression. 48 hour, 72 hour and 96 hour transfections with 30 pmol NOX1 siRNA resulted in 92.5%, 90.3% and 77% mean reduction of *NOX1* expression respectively. For further experiments, 72 hour transfection with 30 pmol NOX1 siRNA was performed. Reduction of NOX1 expression shown by protein levels under this transfection condition was confirmed in Figure 7B in the publication (Hong et al., 2023).

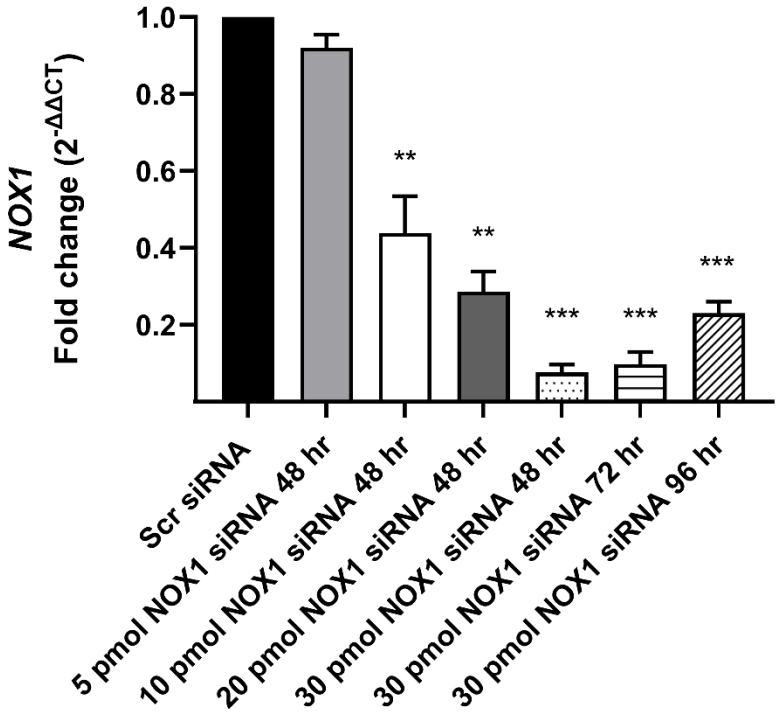


**Figure 3.3. Optimisation of NOX1 siRNA transfection in Caco-2 cells.** qRT-PCR data showing expression of *NOX1*. Caco-2 cells were transfected with 5, 10, 20 or 30 pmol of NOX1 siRNA or scrambled siRNA (Scr siRNA) for 48, 72 or 96 hours at 37°C in an incubator with 5% $CO_2$. *GAPDH* was used as an internal control. Three biological and three technical replicates were performed for each experiment. Asterisks denote a statistically significant difference (** = $p < 0.01$; *** = $p < 0.001$).

#### 3.1.2.4. Fibronectin expression with DPI treatment and NOX1 siRNA transfection

Reductions of *C. jejuni* interactions, invasion and intracellular survival were observed in human IECs after DPI pre-treatment or NOX1 siRNA transfection (Hong et al., 2023). Previous studies had demonstrated a reduction of fibronectin expression in rat renal tubular epithelial cells after DPI treatment (Rhyu et al., 2005) and also in mesangial cells with a pan-NOX inhibitor APX-115 treatment (Cha et al., 2017). As fibronectin has been shown as a key receptor for *C. jejuni* interactions with host cells (Konkel et al., 2020), further investigations were performed to observe if chemical inhibition of NOX1 with DPI and/or silencing NOX1 affected expression of fibronectin (Figure 3.4).

In accordance with previous studies, DPI pre-treatment resulted in a reduction of fibronectin expression in both T84 and Caco-2 cells compared to untreated cells (Figure 3.4A). Similarly, NOX1 siRNA transfected Caco-2 cells exhibited reduced fibronectin expression compared to scrambled siRNA-transfected Caco-2 cells (Figure 3.4B). These results suggest that reduced *C. jejuni* interactions, invasion and intracellular survival with DPI pre-treatment and NOX1 siRNA transfection might be due to reduced fibronectin expression.

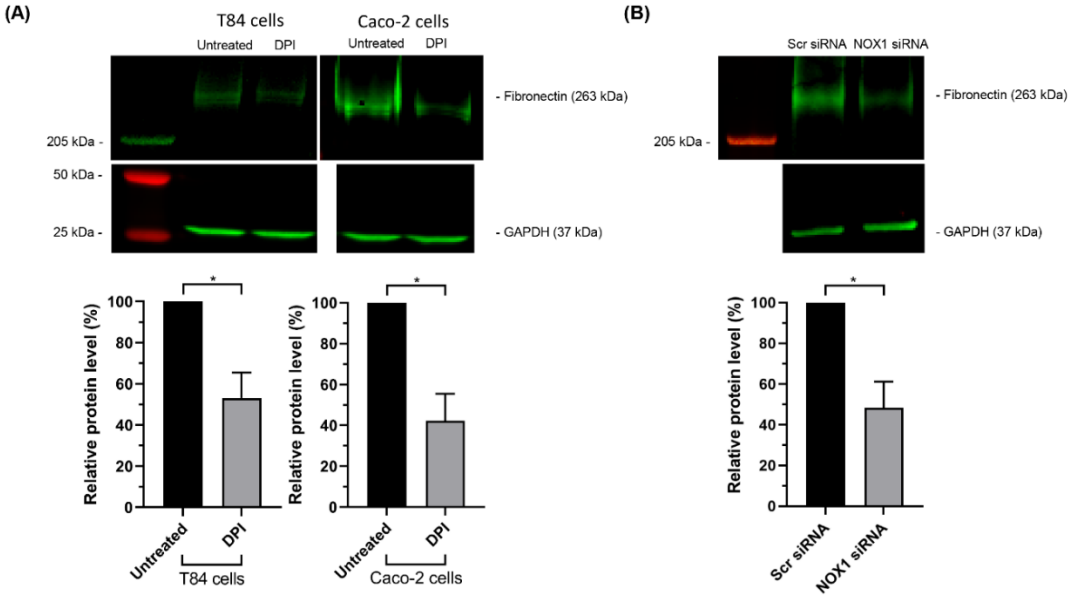


**Figure 3.4. Protein levels of human fibronectin after DPI treatment or NOX1 siRNA transfection.** (A) Western blotting showing human fibronectin in T84 or Caco-2 cells with or without DPI treatment (upper) and relative protein level as a percentage of signal intensity from Western blotting (lower). GAPDH was used as an internal control. (B) Western blotting showing human fibronectin in Caco-2 cells with Scr siRNA or NOX1 siRNA (upper) and relative protein level as a percentage of signal intensity from Western blotting (lower). Three biological and three technical replicates were performed for each experiment. Asterisks denote a statistically significant difference (* = $p < 0.05$).

### 3.2. Publication: *Campylobacter jejuni* modulates reactive oxygen species production and NADPH oxidase 1 expression in human intestinal epithelial cells

Following section contains pre-print Microsoft Word format for the following reference. See Appendix 1 for published PDF format.

Reference: Hong, G., Davies, C., Omole, Z., Liaw, J., Grabowska, A. D., Canonico, B., Corcionivoschi, N., Wren, B. W., Dorrell, N., Elmi, A., and Gundogdu, O. (2023). Campylobacter jejuni Modulates Reactive Oxygen Species Production and NADPH Oxidase 1 Expression in Human Intestinal Epithelial Cells. Cellular microbiology, 2023, 1-14. doi:10.1155/2023/3286330

***Campylobacter jejuni* modulates reactive oxygen species production and NADPH oxidase 1 expression in human intestinal epithelial cells**

Geunhye Hong[1], Cadi Davies[1], Zahra Omole[1], Janie Liaw[1], Anna D. Grabowska[2], Barbara Canonico[3], Nicolae Corcionivoschi[4,5], Brendan Wren[1], Nick Dorrell[1#], Abdi Elmi[1#†] and Ozan Gundogdu[1#†]

[1] Faculty of Infectious and Tropical Diseases, London School of Hygiene & Tropical Medicine, Keppel Street, London, WC1E 7HT, UK.

[2] Department of Biophysics, Physiology and Pathophysiology, Medical University of Warsaw, Warsaw, 02-004, Poland.

[3] Department of Biomolecular Sciences, University of Urbino Carlo Bo, Urbino, 61029, Italy.

[4] Bacteriology Branch, Veterinary Sciences Division, Agri-Food and Biosciences Institute (AFBI), Belfast, BT9 5PX, UK.

[5] Faculty of Bioengineering of Animal Resources, University of Life Sciences King Mihai I from Timisoara, Timisoara, 300645, Romania.

[†]**Joint senior authorship**

[#]**Correspondence**

Nick Dorrell
Faculty of Infectious and Tropical Diseases,
London School of Hygiene & Tropical Medicine,
Keppel Street, London, WC1E 7HT, UK.
Email: nick.dorrell@lshtm.ac.uk

Abdi Elmi
Faculty of Infectious and Tropical Diseases,
London School of Hygiene & Tropical Medicine,
Keppel Street, London, WC1E 7HT, UK.
Email: abdi.elmi@lshtm.ac.uk

Ozan Gundogdu
Faculty of Infectious and Tropical Diseases,
London School of Hygiene & Tropical Medicine,
Keppel Street, London, WC1E 7HT, UK.
Email: ozan.gundogdu@lshtm.ac.uk

**Abstract**

*Campylobacter jejuni* is the major bacterial cause of foodborne gastroenteritis worldwide. Mechanistically, how this pathogen interacts with intrinsic defence machinery of human intestinal epithelial cells (IECs) remains elusive. To address this, we investigated how *C. jejuni* counteracts the intracellular and extracellular reactive oxygen species (ROS) in IECs. Our work shows that *C. jejuni* differentially regulates intracellular and extracellular ROS production in human T84 and Caco-2 cells. *C. jejuni* downregulates the transcription and translation of Nicotinamide adenine dinucleotide phosphate (NAPDH) oxidase (NOX1), a key ROS-generating enzyme in IECs and antioxidant defence genes *CAT* and *SOD1*. Furthermore, inhibition of NOX1 by diphenylene iodonium (DPI) and siRNA reduced *C. jejuni* ability to interact, invade and intracellularly survive within T84 and Caco-2 cells. Collectively, these findings provide mechanistic insight into how *C. jejuni* modulates the IEC defence machinery.

**KEYWORDS**

*Campylobacter jejuni*, Intestinal epithelial cells, NADPH oxidase 1, Reactive oxygen species

## Introduction

Microbial pathogens have evolved to possess subversion strategies to alter the functionality of host cells upon infection (Escoll et al., 2016). These include modulation of host cell functions that involve vesicle trafficking, apoptosis, and immune activation (Asrat et al., 2014; Pedron et al., 2007; Rudel, Kepp, & Kozjak-Pavlovic, 2010). Crucially, these host cell functions are essential for elimination of foreign pathogens. The evolving battle between pathogen and host adds to the complexity of the pathogenesis of infection (Escoll et al., 2016).

*Campylobacter jejuni* is the leading foodborne bacterial cause of human gastroenteritis worldwide (Silva et al., 2011). *C. jejuni* causes watery or bloody diarrhoea, abdominal pain, and fever. *C. jejuni* infection can also lead to Guillain-Barré Syndrome (GBS), a rare but severe post-infectious autoimmune complication of the peripheral nervous system (Kaakoush et al., 2015; Silva et al., 2011; Willison, Jacobs, & van Doorn, 2016). Importantly, campylobacteriosis in low-income countries is associated with child growth impairment and can be fatal in children (Amour et al., 2016). Although *C. jejuni* is a microaerophilic bacterium, its omnipresence in the environment and various hosts is mitigated by regulatory mechanisms against oxidative stress (Gundogdu et al., 2016). Upon adhering and invading human intestinal epithelial cells (IECs), *C. jejuni* manipulates host cytoskeleton regulation to maximise its invasion (Negretti et al., 2021). Following invasion, *C. jejuni* resides in cytoplasmic vacuoles named *Campylobacter* containing vacuoles (CCVs) which can escape the canonical endocytic pathway and avoid fusion with lysosomes (Konkel et al., 1992; Watson & Galán, 2008). These findings demonstrate that modulation and invasion of host IECs are a prerequisite for human intestinal disease caused by *C. jejuni*.

A vital mechanism used by host cells in response to pathogens is the production of reactive oxygen species (ROS) which are highly reactive molecules, such as oxygen radicals and non-radicals, produced by the partial reduction of oxygen (Aviello & Knaus, 2017). When phagocytes such as macrophages detect and engulf pathogens using the respiratory burst, ROS are rapidly generated to eradicate the engulfed pathogens through oxidative damage (Paiva & Bozza, 2014). Interestingly, the level of ROS produced by human IECs is lower in comparison to resident macrophages and blood leukocytes (neutrophils and monocytes), however, ROS in IECs can also exhibit antimicrobial activity by inducing inflammation (Burgueño et al., 2019; Holmström & Finkel, 2014; Paiva & Bozza, 2014). The precarious nature of ROS production by IECs is demonstrated by exhibiting both deleterious and beneficial host effects, thus homeostasis of ROS is essential. To counter the damaging effects of ROS, host IECs possess antioxidant components that neutralise ROS, such as catalase, superoxide dismutase and glutathione peroxidase. Nicotinamide adenine dinucleotide phosphate oxidase (NADPH oxidase; NOX) and mitochondria have central roles as predominant sources of ROS in human IECs (Aviello & Knaus,

2017).

NOX is an essential multicomponent enzyme which catalyses production of superoxide ($O_2^-$) (Brandes, Weissmann, & Schröder, 2014; Sumimoto, Miyano, & Takeya, 2005). In IECs, the most abundant types of NOX are NOX1 and NOX4. Intriguingly, NOX4 is constitutively active, whereas NOX1 is not. The NOX1 complex is composed of NOX1, p22phox, NOX organiser 1 (NOXO1), NOX activator (NOXA1) and small GTPase Rac1. NOX1 is the catalytic subunit of the complex on the plasma membrane and its activation is dependent on supplementary cytosolic subunits. Following this, p22phox is transported to the plasma membrane promoted by NOX1 expression (Brandes, Weissmann, & Schröder, 2014). Upon activation, NOXO1 binds to both NOXA1 and p22phox targeting NOXA1 to the plasma membrane. In turn NOXA1 binds to GTP (guanosine triphosphate)-bound Rac1 and promotes electron flow through flavocytochrome in NOX1 in a GTP-dependent manner. Studies have shown that GTP-bound Rac1 is essential for activity of NOX1 (Nisimoto et al., 2008; Ueyama, Geiszt, & Leto, 2006). Electrons travel from NADPH initially to flavin adenine dinucleotide (FAD), then through the NOX heme groups and finally to oxygen, forming $O_2^-$ (Nisimoto et al., 2008). Notably, NOX1-mediated ROS play important roles in IECs including regulation of growth and proliferation, epithelial wound healing, intestinal host defence, and maintenance of bacterial homeostasis in the GI tract (Juhasz et al., 2017; Lipinski et al., 2019; Matziouridou et al., 2018).

How *C. jejuni* interacts with the inherent defence machinery of human IECs remains unclear. To explore this further, we examined the mechanisms *C. jejuni* uses to counteract the intracellular and extracellular ROS in IECs. Previous findings demonstrated the upregulation of NOX1 in IECs by enteric pathogens such as *Escherichia coli* (Elatrech et al., 2015), *Salmonella* Enteritidis (Kawahara et al., 2016), and *Helicobacter pylori* (den Hartog et al., 2016; Kawahara et al., 2005). *C. jejuni* lacks classical stress response regulators such as OxyR and SoxRS that are found in other enteric bacteria (Burnham & Hendrixson, 2018; Elmi et al., 2020). Instead, it possesses unique strategies to counteract oxidative stress such as CosR, PerR and MarR-type regulators RrpA and RrpB (Gundogdu et al., 2016; Hwang et al., 2011; Palyada et al., 2009). Given these survival properties of *C. jejuni*, we hypothesised that *C. jejuni* may have a distinct host cell modulation mechanisms in play. In this study, we show that diverse *C. jejuni* strains downregulate both intracellular and extracellular ROS production in human IECs by modulating the expression of NOX1. We demonstrate inhibition of NOX1 by diphenylene iodonium (DPI) and siRNA reduced the ability of *C. jejuni* to interact, invade and intracellularly survive within T84 and Caco-2 cells. Our results highlight a unique strategy of *C. jejuni* survival and emphasise the importance of NOX1 in *C. jejuni*-IEC interactions. This represents a distinctive mechanism that *C. jejuni* uses to modulate IEC defence machinery.

## Experimental procedures

### Bacterial strains and growth conditions

*C. jejuni* wild-type strains used in this study are listed in Table S1. For general growth, all *C. jejuni* strains were grown on Columbia Blood Agar (CBA) plates (Oxoid, UK) supplemented with 7% (v/v) horse blood (TCS Microbiology, UK) and *Campylobacter* selective supplement Skirrow (Oxoid) at 37 °C under microaerobic conditions (10% $CO_2$, 5% $O_2$ and 85% $N_2$) (Don Whitley Scientific, UK).

### Human intestinal epithelial cell culture

T84 cells (ECACC 88021101) and Caco-2 cells (ECACC 86010202) were obtained from European Collection of Authenticated Cell Cultures (ECACC). T84 and Caco-2 cells were cultured in a 1:1 mixture of Dulbecco's modified Eagle's medium and Ham's F-12 medium (DMEM/F-12; Thermo Fisher Scientific, USA) with 10% Fetal Bovine Serum (FBS; Labtech, UK), 1% non-essential amino acid (Sigma-Aldrich, USA) and 1% penicillin-streptomycin (Sigma-Aldrich). Both cell lines were cultured at 37°C in a 5% $CO_2$ humidified environment. DMEM/F-12 without penicillin-streptomycin was used for the co-culture assays. DMEM/F-12 without phenol red was used for the ROS detection assays.

### T84 and Caco-2 cells infection assays

Human IECs were counted using hemocytometer (Thermo Fisher Scientific, USA) and for general infection assays, approximately $10^5$ cells were seeded in 24-well tissue culture plates 7 days prior to initiation of the *C. jejuni* infection. The plates were incubated at 37°C in a 5% $CO_2$ atmosphere. For Western blotting, approximately 2 x $10^5$ cells were seeded in 6-well tissue culture plates. Prior to the infection, IECs were washed with phosphate-buffered saline (PBS; Thermo Fisher Scientific) three times and the medium was replaced with DMEM/F-12 without penicillin-streptomycin. *C. jejuni* strains grown on CBA plates for 24 hours were resuspended in PBS and bacterial suspension with appropriate $OD_{600}$ were then incubated with IECs for various time periods giving a multiplicity of infection (MOI) of 200:1. In some experiments, T84 and Caco-2 cells were pre-treated with 10 μM DPI for 1 hour, washed three times with PBS and then infected with *C. jejuni.* As with our previous infection assays (Elmi et al., 2016; Gundogdu et al., 2011), we primarily focus on relatively early time points as many of the transcriptional and translational changes that we observe in the crosstalk between *C. jejuni* and IECs in our *in vitro* assays are ephemeral in nature and so our focus is to detect these subtle deviations that lead to mechanistic impact.

DCFDA measurement of intracellular reactive oxygen species (ROS)

To analyse the levels of intracellular ROS production in human IECs under experiments conditions, DCFDA Cellular ROS Detection Assay Kit (Abcam UK) was used according to the manufacturer's instructions. Briefly, IECs grown in 96-well cell culture plates were washed three times with PBS and incubated with *C. jejuni* for 3 or 24 hours (MOI 200:1). For positive controls, IECs were treated with 500 µM $H_2O_2$ for 45 minutes. 45 minutes prior to completion of the infection, 100 µM 2',7'-dichlorofluorescin diacetate (DCFDA) was added into each well giving a final concentration of 50 µM. After *C. jejuni* infection, the fluorescence was detected using SpectraMax M3 Multi-Mode Microplate Reader (Molecular Devices, USA) with 485 nm excitation and 535 nm emission.

Measurement of extracellular $H_2O_2$

Amplex® Red Hydrogen Peroxide/Peroxidase Assay Kit (Invitrogen, USA) was used to measure extracellular $H_2O_2$ in culture media after incubation with *C. jejuni*. Briefly, Amplex® Red reagent (10-acetyl-3,7-dihydroxyphenoxazine) with horseradish peroxidase (HRP) reacts with $H_2O_2$ in a 1:1 stoichiometry producing a fluorescent product called resorufin. After incubation with *C. jejuni* for 3 or 24 hours, 100 µl of culture media was transferred to a 96-well plate and 100 µl of reaction mixture containing 50 µM Amplex® Red reagent was added followed by incubation for 10 minutes at 37°C in a 5% $CO_2$ humidified environment. Using SpectraMax M3 Multi-Mode Microplate Reader, fluorescence was measured at 530 nm excitation and 590 nm emission.

Real time-quantitative polymerase chain reaction (qRT-PCR) analysis

For qRT-PCR, RNA was isolated from infected and uninfected IECs using PureLink™ RNA Mini Kit (Thermo Fisher Scientific) and contaminating DNA was removed using TURBO DNA-free kit (Ambion, USA) according to manufacturer's instructions. Concentration and purity of RNA samples were determined in a NanoDrop ND-1000 spectrophotometer (Thermo Fisher Scientific). 400 ng of RNA per sample were first denatured at 65°C for 5 minutes and snap cooled on ice. Complementary DNA (cDNA) was generated with random hexamers and SuperScript III Reverse Transcriptase (Thermo Fisher Scientific). Each reaction had 10 µl of SYBR Green PCR Master Mix (Applied Biosystems, USA), 1 µl of primer (20 pmol), 1 µl of cDNA and 10 µl of HyClone™ water (Thermo Fisher Scientific). The sequence of each primer is described in Table S2. All reactions were run in triplicate on an ABI-PRISM 7500 instrument (Applied Biosystems). Relative expression changes were calculated using the

comparative $C_T$ cycle ($2^{-\Delta\Delta CT}$) method (Schmittgen & Livak, 2008). Expression levels of all target genes were normalised to *GAPDH* expression determined in the same sample as an internal control. A minimum of three biological replicates were always analysed, each with three technical replicates.

Semi-quantitative reverse transcription (RT-PCR) analysis

Each PCR reaction had 50 µl of FasTaq PCR master mix (Qiagen, Netherlands), 2 µl of primer (0.4 nmol) described in Table S2 and 1.5 µl of cDNA. For PCR reactions Tetrad-2 Peltier thermal cycler (Bio-Rad, UK) was used. One cycle of PCR programme performs 95°C for 15 seconds after 2 minutes in the first cycle, annealing at 50°C for 20 seconds, and extension at 72°C for 30 seconds. Total 36 cycles were repeated. The PCR products were loaded on the 1% agarose gel and the gel was running for 1 hour at 120V. The gel was imaged using G:BOX Chime XRQ (Syngene, USA). Quantification of relative mRNA level was performed using ImageJ software (Schneider, Rasband, & Eliceiri, 2012).

SDS-PAGE and Western blot analysis

After infection, IECs were washed three times with PBS and lysed with cold RIPA lysis and extraction buffer (Thermo Fisher Scientific) with cOmplete™ Mini EDTA-free Protease Inhibitor Cocktail (Roche, Switzerland) and cleared by centrifugation (4 °C, 13,000 × g, 20 min). Protein concentration was determined using Pierce™ Bicinchoninic acid (BCA) Protein Assay Kit (Thermo Fisher Scientific) according to the manufacturer's instructions. Afterward, samples were diluted to a desired concentration in HyClone™ water and 4X Laemmli sample buffer (Sigma-Aldrich) and incubated for 5 minutes at 95°C. 30 µg of protein samples were separated using 4-12% NuPAGE™ Bis-Tris gel in 1× NuPAGE™ MES buffer or MOPS buffer (Thermo Fisher Scientific). Proteins were transferred from the gel using the iBlot® 2 transfer stacks (Life Technologies, USA) using the iBlot® Gel Transfer Device (Invitrogen). These stacks were integrated with nitrocellulose transfer membrane. After the transfer, membranes were blocked with 1X PBS containing 2% (w/v) milk. Membranes were then probed with primary antibodies overnight as described previously (Elmi et al., 2016). The following primary antibodies were used; GAPDH (ab181602; Abcam); NOX1 (ab101027; Abcam) or NOX1 (NBP-31546; Novus Biologicals). Blots were developed using LI-COR infrared secondary antibody (IRDye 800CW Donkey anti-rabbit IgG) and imaged on a LI-COR Odyssey Classic (LI-COR Biosciences, USA). Quantification of relative protein levels normalised to GAPDH expression was performed using ImageJ software (Schneider, Rasband, & Eliceiri, 2012).

Detection of GTP-bound Active Rac1

The levels of active GTP-bound Rac1 were measured by using Rac1 G-LISA kit (Cytoskeleton Inc., USA) according to the manufacturer's instructions. Briefly, before the infection, IECs were incubated with reduced serum (0.1% FBS) for 24 hours. Infected or uninfected human IECs were washed with 1X PBS and lysed using the supplied 1X Lysis Buffer. Cell lysates were centrifuged for 1 minute at 10,000 x g at 4°C and adjusted to 1 mg/ml for the further process of the assay. As a positive control, constitutively active Rac1 (RCCA) was provided in the kit. Three biological replicates were conducted in all experiments, along with two technical replicates for each assay.

Inhibition of NOX1 with diphenyleneiodonium chloride (DPI)

A stock solution of 3.25 mM DPI (Sigma-Aldrich) in dimethyl sulfoxide (DMSO; Sigma Aldrich) was prepared and stored at -20°C. For treatment, the DPI stock solution was diluted to 10 µM DPI in culture media without antibiotics, then incubated with IECs for 1 hour at 37°C in a 5% $CO_2$ atmosphere. After treatment, IECs were washed with PBS for three times before co-incubation with *C. jejuni* for various time points.

Small interfering (si) RNA transfection

On the day of reverse transfection, 500 µl of Caco-2 cells ($10^5$ cells/ml) were seeded in 24-well plates and treated for 24 hours with 30 pmol siRNA from either NOX1 siRNA (sc-43939; Santa Cruz Biotechnology, Inc, USA) or Ambion® Silencer Negative Control #1 siRNA (Invitrogen) for the negative control. For preparation of siRNA transfection reagent complex, 3 µl of 10 µM stock siRNA was diluted with 100 µl of Opti-MEM® Reduced-Serum Medium (Thermo Fisher Scientific) and mixed with 1.5 µl of Lipofectamine® RNAiMAX Transfection Reagent (Thermo Fisher Scientific). After 24 hours transfection, media was replaced with DMEM/F-12 containing 10% FBS. After additional 48 or 72 hours, RNA and protein were extracted to check efficacy of transfection.

Adhesion, invasion and intracellular survival assay

Adherence, invasion and intracellular assays were performed as described previously with minor modifications (Elmi et al., 2016; Gundogdu et al., 2011). T84 and Caco-2 cells seeded in a 24-well plate were washed three times with PBS and treated with 10 µM DPI for 1 hour or transfected with NOX1 siRNA as described in above. Then IECs were inoculated with *C. jejuni* with $OD_{600}$ 0.2 at a MOI of 200:1 and incubated for 3 hours at 37°C in 5% $CO_2$. For the interaction (adhesion and invasion) assay,

monolayers were washed three times with PBS to remove unbound extracellular bacteria and then lysed with PBS containing 0.1% (v/v) Triton X-100 (Sigma-Aldrich) for 20 min at room temperature. The cell lysates were diluted and plated on blood agar plates to determine the number of interacting bacteria (CFU/ml).

Invasion assays were performed by additional step of treatment of gentamicin (150 μg/ml) for 2 hours to kill extracellular bacteria, washed three times with PBS, lysed and plated as described above. For intracellular survival assays, after infection with *C. jejuni* for 3 hours, T84 and Caco-2 cells were treated with gentamicin (150 μg/ml) for 2 hours to kill extracellular bacteria followed by further 18 hours incubation with gentamicin (10 μg/ml). Cell lysis and inoculation were performed as described above.

Cytotoxicity assay with trypan blue exclusion methods

After treatment with DPI and gentamicin or transfection with siRNA as previously described, IECs were washed three times with PBS and were detached using trypsin-EDTA (Thermo Fisher Scientific) and resuspended with culture media. 50 μl of cell suspension were added into 50 μl of 0.4% Trypan Blue solution (Thermo Fisher Scientific) and the numbers of viable and dead cells were counted using hemocytometer under microscope.

*Campylobacter jejuni* viability test with DPI treatment

T84 cells were treated with 10 μM DPI for 1 hour and the cells were washed three times with PBS. After DPI treatment for 1 hour, *C. jejuni* strains ($OD_{600}$ 0.2) were co-incubated for 1 hour with PBS from the last wash. After incubation, serial dilution was performed and each dilution was spotted on to blood agar plates. The plates were incubated under microaerobic condition at 37°C for 48 hours. CFU of each spot was recorded.

Statistical analysis and graphing

At least three biological replicates were performed in all experiments. Each biological replicate was performed in three technical replicates. For statistical analysis and graphing, GraphPad Prism 8 for Windows (GraphPad Software, USA) was used. One sample *t*-test or unpaired *t*-test were used to compare two data sets for significance with * indicating $p < 0.05$, ** indicating $p < 0.01$, *** indicating $p < 0.001$, and **** indicating $p < 0.0001$.

## Results

### *Campylobacter jejuni* modulates intracellular and extracellular ROS in T84 and Caco-2 cells in a time- and strain-dependent manner.

As *C. jejuni* possesses distinct physiological characteristics compared to more studied enteric pathogens, we assessed the ability of three distinct *C. jejuni* strains to modulate intracellular and extracellular ROS in T84 and Caco-2 cells (Burnham & Hendrixson, 2018). We observed strain-specific ROS modulation at 3- and 24-hours post-infection (Figure 1). All three *C. jejuni* strains reduced the levels of intracellular ROS in T84 and Caco-2 cells compared to the uninfected control (Figure 1A, 1B, 1E, 1F). A similar pattern was observed for extracellular ROS where all *C. jejuni* strains reduced the levels of extracellular ROS in T84 and Caco-2 cells compared to the uninfected control (Figure 1C, 1D, 1G, 1H). A distinct pattern was observed when assessing levels of extracellular ROS for *C. jejuni* 81-176 strain at 3 hours post-infection (Figure 1C and 1G). At this early time point, extracellular ROS is increased in T84 and Caco-2 cells infected with *C. jejuni* 81-176, although we observed similar reduced levels of ROS at 24 hours. As controls, *C. jejuni* infection did not affect viability of both T84 and Caco-2 cells (Figure S1) and levels of ROS were unchanged when *C. jejuni* was resuspended in DMEM in the absence of IECs (Figure S2). Collectively, these results indicate a strain and time-specific pattern linking the ability of different *C. jejuni* strains to modulate intracellular and extracellular ROS levels in T84 and Caco-2 cells.

### *Campylobacter jejuni* modulates intracellular and extracellular ROS in T84 and Caco-2 cells via the downregulation of NOX1 complex.

Given the observed modulation of intracellular and extracellular ROS in T84 and Caco-2 cells, we next explored the mechanism by which *C. jejuni* strains orchestrate ROS modulation. We analysed the transcription and translation of NOX1 which is the main source of ROS production in IECs (Brandes, Weissmann, & Schröder, 2014; Sumimoto, Miyano, & Takeya, 2005). As shown in Figure 2, NOX1 transcription and translation levels were significantly reduced in both T84 (Figure 2A) and Caco-2 cells (Figure 2B) infected with *C. jejuni* when compared to uninfected cells. Notably, at 24 hours post-infection, mRNA levels of *NOX1* in T84 cells are significantly reduced compared with *C. jejuni*-infected Caco-2 cells. We measured the relative levels of mRNA between T84 and Caco-2 cells and identified T84 cells expressed a higher basal level of *NOX1* mRNA compared to Caco-2 cells (Figure 2C). As a result of this higher basal level of *NOX1* mRNA in T84 cells we validated our qRT-PCR data using RT-PCR where less expression of *NOX1* in *C. jejuni*-infected T84 cells was observed (Figure 2D and 2E). Reduction in the translational level of NOX1 in *C. jejuni*-infected T84 cells was confirmed independently by Western blotting (Figure 2F and 2G).

***Campylobacter jejuni* modulates activity of small GTPase Rac1 in T84 and Caco-2 cells in a time-dependent manner.**

To gain further insight into the mechanism that leads to *C. jejuni* modulation of ROS in T84 and Caco-2 cells, we examined the ability of *C. jejuni* to activate Rac1, a member of the Rho family of small GTPases. Rac1 undergoes cycling between active GTP- or inactive GDP-bound form which switches activation of cellular response upon stimuli (Hodge & Ridley, 2016). Although GTP-bound Rac1 is implicated in NOX1 activation in several eukaryotic cell lines (Nisimoto et al., 2008; Ueyama, Geiszt, & Leto, 2006), the contribution of Rac1 in *C. jejuni*-mediated NOX1 modulation is unknown. As shown in Figure 3, active GTP-bound Rac1 is an integral part of the NOX1 complex. Given that *C. jejuni* activates Rac1 in human INT 407 cells via *Campylobacter* invasion antigen D (CiaD) (Krause-Gruszczynska et al., 2007; Negretti et al., 2021), and that Rac1 supports NOX1 activity only in its GTP-bound active form, we examined the abundance of GTP-bound Rac1 to investigate if downregulation of NOX1 is linked to modulation of Rac1 by *C. jejuni*. Interestingly, *C. jejuni* 11168H strain induced Rac1 1- and 3-hours after infection in T84 cells (Figure 4A). After 24 hours infection, Rac1 activity was reduced (though not statistically significant; $p = 0.0714$) (Figure 4A). Similarly, *C. jejuni* 11168H induced Rac1 activity after 1 hour infection in Caco-2 cells (Figure 4B). However, this activity was reduced after 3- and 24-hours infection (Figure 4B). These results suggest that the downregulation of NOX1 by *C. jejuni* is inversely correlated with an increase in Rac1 GTPase activity.

***Campylobacter jejuni* modulates transcription of antioxidant-related genes in T84 and Caco-2 cells**

To gain further insight into the ability of *C. jejuni* to modulate intracellular and extracellular ROS in T84 and Caco-2 cells, we sought to understand if *C. jejuni* modulates the expression of two important antioxidant genes, superoxide dismutase 1 (*SOD1*) and catalase (*CAT*). SOD1 decomposes $O_2^-$ to $H_2O_2$, and CAT breaks down $H_2O_2$ to $H_2O$ and $O_2$ (Aviello & Knaus, 2017). Intriguingly, as shown in Figure 5A and 5B, there is a significant downregulation of the mRNA levels of *CAT* and *SOD1* at 24 hours post-infection in T84 cells. A similar pattern was observed when compared with Caco-2 cells where the expression of *CAT* and *SOD1* at 24 hours post-infection is significantly downregulated (Figure 5C and 5D). In contrast, the expression of *CAT* and *SOD1* at 3 hours post-infection is unaffected. These results may indicate *C. jejuni*-mediated reduction in intracellular and extracellular ROS is independent of modulation of *CAT* and *SOD1*.

**Chemical inhibition of NOX1 activity by DPI impairs *Campylobacter jejuni* interaction, invasion**

**and intracellular survival of T84 and Caco-2 cells *in vitro*.**

Having established that *C. jejuni* significantly reduced the transcription and translation of NOX1 in T84 and Caco-2 cells in a time-dependent manner, and that Rac1 is not only known as a key component of the NOX1 complex, but also implicated in cell dynamic morphology (Nisimoto et al., 2008; Ueyama, Geiszt, & Leto, 2006), we hypothesised Rac1-mediated NOX1 might modulate membrane ruffling and cytoskeleton rearrangement which might in turn affect *C. jejuni* interaction with IECs. Therefore, we investigated the role of NOX1 in *C. jejuni* interaction, invasion and intracellular survival in IECs by transiently pre-treating T84 and Caco-2 cells with DPI (10 μM) which is known to inhibit activity of flavoenzymes including NOX complex (Riganti et al., 2004). First, we demonstrated that DPI reduced ROS in T84 and Caco-2 cells (Figure S3). As shown in Figure 6A, 6C, 6E, pre-treatment of T84 cells by DPI significantly reduced the ability of *C. jejuni* to interact, invade, and survive intracellularly in T84 cells. Similarly, as shown in Figure 6B, 6D and 6F, *C. jejuni* infected with DPI-treated Caco-2 cells showed significant reduction in interaction, invasion, and intracellular survival compared to untreated Caco-2 cells. Since our data revealed *C. jejuni* reduced interaction, invasion and intracellular survival between the control and DPI-treated T84 and Caco-2 cells, we next evaluated the viability of *C. jejuni*, T84 and Caco-2 cells co-incubated with DPI. Treatment with DPI did not affect viability of IECs (Figure S4) or *C. jejuni* (Figure S5). Thus, our observations suggest further inhibition of NOX1 with DPI is detrimental to *C. jejuni* interaction, invasion and intracellular survival in IECs.

**NOX1 silencing by siRNA impairs *Campylobacter jejuni* interaction, invasion and intracellular survival in Caco-2 cells *in vitro.***

As DPI is a pan-NOX inhibitor, we silenced *NOX1* expression in Caco-2 cells by delivering specific small interfering RNA (siRNA) into cultured Caco-2 cells. We used siRNA sequence which target regions of NOX1 for silencing. As a negative control, we used a non-targeting scrambled RNA sequence which is not complementary to the *NOX1* mRNA. As shown in Figure 7A and 7B, transcriptional and translational levels of NOX1 were significantly decreased in cells treated with NOX1 siRNA, relative to that in mock-treated Caco-2 controls. We further confirmed reduced activity of NOX1 by demonstrating significant reduction in extracellular ROS (Figure 7C). We showed that NOX1 siRNA transfection did not affect viability of Caco-2 cells (Figure S6). Based on these results, we further investigated interaction, invasion and intracellular survival of *C. jejuni* within Caco-2 cells (Figure 7D, 7E and 7F). Our result showed significant decrease in *C. jejuni* interaction, invasion and intracellular survival when compared to non-transfected controls. This result highlights a correlation between reduced NOX1 expression with a reduction in *C. jejuni* infection. Taken together, our results demonstrate that NOX1 is a critical host factor for *C. jejuni* interaction, invasion, and intracellular

survival.

**Discussion**

Upon infection, host cells induce a range of cellular responses to remove offending pathogens. However, bacterial pathogens often target host organelle(s), signalling pathway(s) or immune responses to evade host defence mechanisms (Escoll et al., 2016). Disruption of ROS production in host cells by bacterial pathogens has been previously reported (Gallois et al., 2001; Vareechon et al., 2017). *S.* Typhimurium pathogenicity island-2 encoding Type III Secretion System (T3SS) inhibits ROS production in human macrophages by preventing NOX2 assembly (Antoniou et al., 2018; Gallois et al., 2001). In addition, *Pseudomonas aeruginosa* T3SS effector, ExoS disrupts ROS production in human neutrophils by ADP-ribosylating Ras and inhibiting its activity which is essential for NOX2 assembly (Vareechon et al., 2017).

We have characterised the ability of distinct *C. jejuni* strains to modulate intracellular and extracellular ROS from human IECs *in vitro*. ROS production by human IECs is a major defence mechanism, yet how *C. jejuni* evades ROS remains unclear. Our work establishes that in contrast to other enteric pathogens, *C. jejuni* uses a different mechanism involving downregulation of NOX1 expression to modulate ROS in human IECs (den Hartog et al., 2016; Elatrech et al., 2015; Kawahara et al., 2005; Kawahara et al., 2016). We examined three different *C. jejuni* strains using two different human IECs and showed that *C. jejuni* strains modulate intracellular and extracellular ROS from human IECs via the differential regulation of the transcription and translation of NOX1 which is a major ROS source in IECs (Aviello & Knaus, 2017). Interestingly, a previous study demonstrated that *C. jejuni* 81-176 induces extracellular ROS production through NOX1 activation in human ileocecal adenocarcinoma derived HCT-8 cells (Corcionivoschi et al., 2012). To further understand the implications of *C. jejuni* transcriptional and translational downregulation of NOX1 in T84 and Caco-2 cells, we revealed similarities with some other enteropathogens, and also differences amongst others including the *C. jejuni* strain 81-176 (den Hartog et al., 2016; Elatrech et al., 2015; Kawahara et al., 2005; Kawahara et al., 2016). Enteropathogens such as *E. coli*, *Salmonella* spp., and *H. pylori* upregulate expression of *NOX1* and ROS production in infected IECs (den Hartog et al., 2016; Elatrech et al., 2015; Kawahara et al., 2005; Kawahara et al., 2016). Our findings confirmed downregulation of ROS production by *C. jejuni* is strain dependent. In contrast to *C. jejuni* 11168H and 488 strains, *C. jejuni* 81-176 induced extracellular ROS in T84 and Caco-2 cells at 3 hours post-infection. Induction of extracellular ROS by *C. jejuni* 81-176 at this earlier infection time point was also observed previously (Corcionivoschi et al., 2012). We hypothesise *C. jejuni* 81-176 might have additional bacterial determinants which may induce host extracellular ROS independent of NOX1 modulation (*e.g.* the pVir and pTet plasmids which encode

putative T4SS (Bacon et al., 2002; Batchelor et al., 2004). We also noted a difference between the ability of *C. jejuni* strains to regulate expression of NOX1 in T84 and Caco-2 cells. This difference could be due to variations between the two cell lines. Caco-2 cells possess characteristic enterocytes whereas T84 cells possess characteristic colonocytes throughout differentiation (Devriese et al., 2017). In addition, previous studies have shown that reduced *NOX1* mRNA was present in the ileum than in the colon of healthy patients suggesting there is a gradient in NOX1 expression from small intestine to large intestine (Schwerd et al., 2018). In our study, the lower expression of *NOX1* mRNA detected in Caco-2 cells compared to T84 cells was also observed.

As ROS homeostasis in the GI tract is regulated by multiple antioxidant enzymes (Aviello & Knaus, 2017), *C. jejuni*-mediated modulation of CAT and SOD1 at the transcriptional level was investigated. Our data demonstrated C. *jejuni* strains did not affect transcriptional levels of *CAT* and *SOD1* in T84 and Caco-2 cells after 3 hours infection, but they significantly downregulated expression of both genes after 24 hours. To our knowledge, this is the first data on *C. jejuni* modulation of antioxidant-related genes in human IECs *in vitro*. Our observations imply *C. jejuni* might modulate intracellular or extracellular ROS after 3 hours infection without modulating expression of *CAT* and *SOD1*. These results also suggest that there could be additional mechanisms of *C. jejuni*-mediated reduction of ROS because *C. jejuni* was able to reduce ROS after 24 hours infection even though transcription levels of antioxidant-related genes *CAT* and *SOD1* were downregulated. However, we cannot disregard the possibilities that *C. jejuni* might secrete its own antioxidant-related proteins that may mitigate host cellular ROS and/or *C. jejuni* might induce expression of other host antioxidant genes such as mitochondrial superoxide dismutase (SOD2), extracellular superoxide dismutase (SOD3) and glutathione peroxidase (Aviello & Knaus, 2017). A previous study demonstrated *Pseudomonas* pyocyanin decreased expression of human CAT but not SOD1 in the human A549 alveolar type II epithelial cells (O'Malley et al., 2003). *C. jejuni* might produce pyocyanin-like metabolites but this is not yet investigated. In addition, downregulation of genes encoding CAT and SOD1 might be a host cellular strategy to produce ROS for clearance of *C. jejuni*.

Upon adhering to host cells, *C. jejuni* modulates small GTPase Rac1 resulting in actin filament reorganisation to promote invasion. Activation of Rac1 in human embryonic INT 407 cells was observed between 45 minutes and 4 hours after *C. jejuni* infection (Krause-Gruszczynska et al., 2007; Negretti et al., 2021). In accordance with previous studies, we demonstrated *C. jejuni* activates Rac1 at early infection time points. In contrast, a decrease of active Rac1 was detected at the later infection time point. Given the association of the active GTP-bound Rac1 and NOX1 activity, the early activation of Rac1 in IECs suggest that *C. jejuni* uses an intriguing system which we hypothesise could have temporally nonoverlapping mechanisms. The GTP-bound Rac1 observed in early time points may be

linked to the requirement for *C. jejuni* to establish adhesion/invasion utilising a distinct mechanism in its infection cycle. Although the inactive GDP-bound Rac1 observed at the later time point of 24 hours, suggests *C. jejuni* clearly possesses yet to be discovered mechanisms that enable differential regulation of NOX1 relative to modulation of Rac1. We also observe the pattern of active GTP-bound Rac1 in Caco-2 cells that is different to T84 cells. Such a difference may be due to the signalling cues between the cells as well as *C. jejuni* preference to efficiently interact with individual cells by binding, invading, and intracellularly surviving from distinct states during its infection.

The impact of differential regulation of NOX1 on *C. jejuni* interaction, invasion and intracellular survival in human IECs remains unclear. Surprisingly, chemical inhibition of NOX1 significantly reduced the ability of *C. jejuni* to interact, invade, and survive intracellularly in T84 and Caco-2 cells. It is possible that DPI may inadvertently affect local cellular receptors that *C. jejuni* uses to bind human IECs. Since DPI is not a specific inhibitor of NOX1 (Riganti et al., 2004), we repeated these experiments using siRNA silencing of *NOX1* which demonstrated similar findings, suggesting that NOX1 is indirectly necessary for *C. jejuni* interaction, invasion, and intracellular survival. Previous studies have demonstrated that DPI treatment reduced fibronectin expression in rat renal tubular epithelial cells (Rhyu et al., 2005), and a pan-NOX inhibitor APX-115 reduced fibronectin production in mesangial cells (Cha et al., 2017). As fibronectin has been demonstrated as a key host receptor that *C. jejuni* uses to bind and invade human IECs (Konkel et al., 2020), we hypothesise that silencing *NOX1* might also affect expression of a key receptor fibronectin as is the case following DPI treatment, and this might be responsible for the reduced interaction and invasion of *C. jejuni* strains. We hypothesise that *C. jejuni* fine-tunes the modulation of NOX1 in a cell-specific manner, so that there is no impact on its ability to adhere and invade at early infection time points and then subsequently downregulates NOX1 to obtain the potential benefits of ROS reduction for its enhanced survivability at later infection time points. However, the broader non-specificity of DPI and siRNA silencing experiments mean that there could be alternative mechanisms in play.

We have demonstrated that *C. jejuni* modulates intracellular and extracellular ROS in human T84 and Caco-2 cells. Our observations link *C. jejuni* ROS modulation to the transcriptional and translational downregulation of NOX1. These findings also point to a further role of Rac1 in NOX1 modulation and downstream interaction. Based on chemical inhibition and silencing of NOX1 expression and translation, our findings suggest an indirect role of NOX1 for adhesion, invasion and intracellular survival of *C. jejuni*. In this context, further understanding *C. jejuni* determinants that lead to ROS and/or NOX1 modulation in IECs will provide greater insights into how *C. jejuni* manipulate host defence mechanisms and cause diarrhoeal disease.

**Figures**

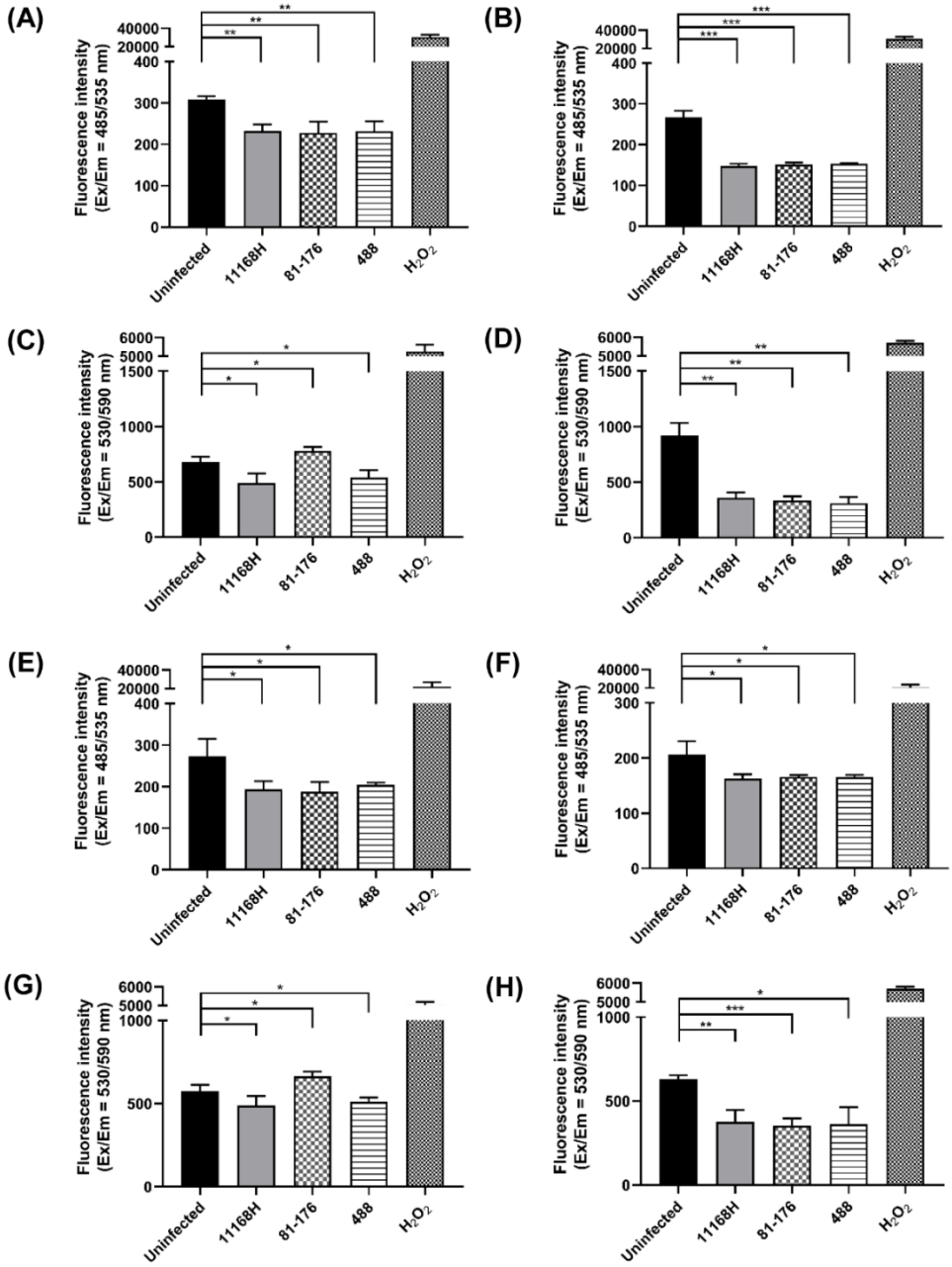


**Figure 1.** Detection of intracellular and extracellular ROS in T84 and Caco-2 cells after infection with *C. jejuni* 11168H, 81-176 or 488 strains. Intracellular ROS in T84 cells after infection with *C. jejuni* for (A) 3 hours or (B) 24 hours and extracellular ROS from T84 cells after infection with *C. jejuni* for (C) 3 hours or (D) 24 hours were measured. Intracellular ROS in Caco-2 cells after infection of *C. jejuni* for (E) 3 hours or (F) 24 hours and extracellular ROS from Caco-2 cells after infection for (G) 3 hours or (H) 24 hours were measured. For detection of intracellular ROS, DCFDA was used. For detection of extracellular ROS, Amplex® Red reagent with HRP were used. $H_2O_2$ was used as a positive control. Experiments were repeated in three biological and three technical replicates. Asterisks denote a statistically significant difference (* = $p < 0.05$; ** = $p < 0.01$; *** = $p < 0.001$).

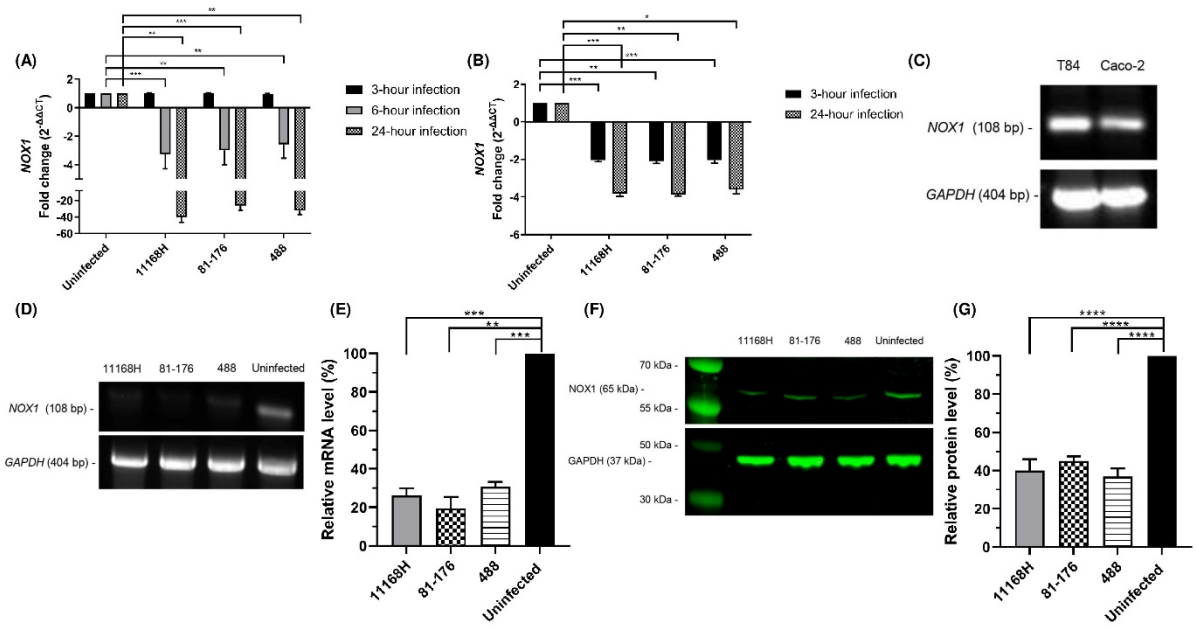


**Figure 2.** *C. jejuni* modulates NOX1 expression in T84 and Caco-2 cells. qRT-PCR showing expression of *NOX1* in (A) T84 and (B) Caco-2 cells. (C) RT-PCR showing expression of *NOX1* in uninfected T84 and Caco-2 cells. *GAPDH* was used as an internal control. (D) RT-PCR showing expression of *NOX1* in T84 cells infected with *C. jejuni* for 24 hours and (E) relative mRNA levels as a percentage from RT-PCR data. (F) Western blotting showing NOX1 in T84 cells infected with *C. jejuni* for 24 hours and (G) relative protein level as a percentage from Western blotting. Asterisks denote a statistically significant difference (* = $p < 0.05$; ** = $p < 0.01$; *** = $p < 0.001$).

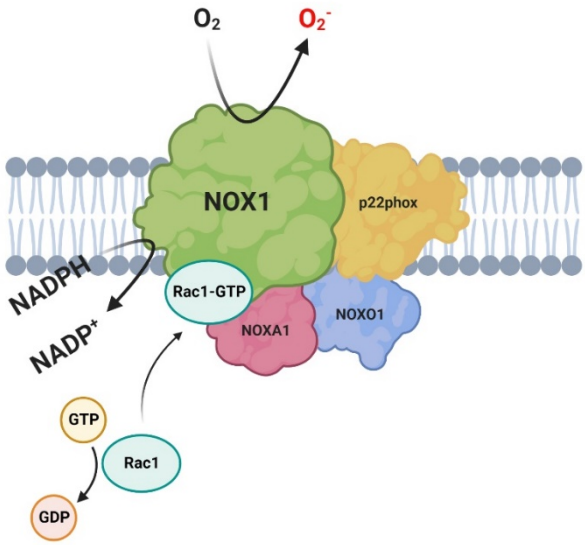


**Figure 3.** Proposed structure of the NOX1 complex consisting of NOX1, p22phox, GTP-bound Rac1, NOXA1 and NOXO1. p22phox and other subcellular subunits are assembled to activate catalytic subunit NOX1 which results in the generation of $O_2^-$ by oxidising NADPH (Brandes, Weissmann, & Schröder, 2014). Created with BioRender.com

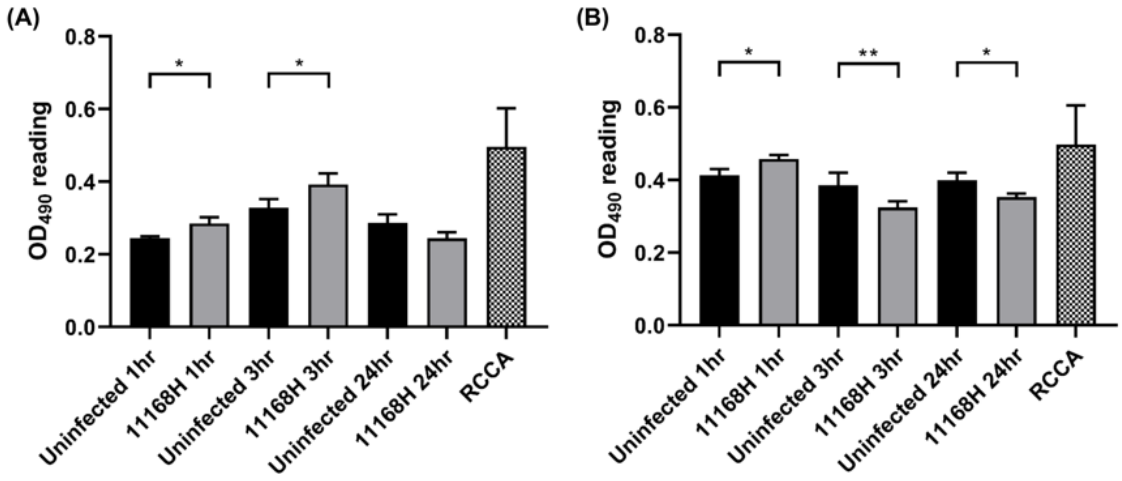


**Figure 4.** *C. jejuni* modulates activity of small GTPase Rac1 in T84 and Caco-2 cells. (A) T84 and (B) Caco-2 cells were infected with *C. jejuni* 11168H strain for 1, 3, and 24 hours and the activation of small GTPase Rac1 in each time point was measured. Constitutively active Rac1 (RCCA) was used as a positive control. Experiments were repeated in three biological and three technical replicates. Asterisks denote a statistically significant difference (* = $p < 0.05$, ** = $p < 0.001$).

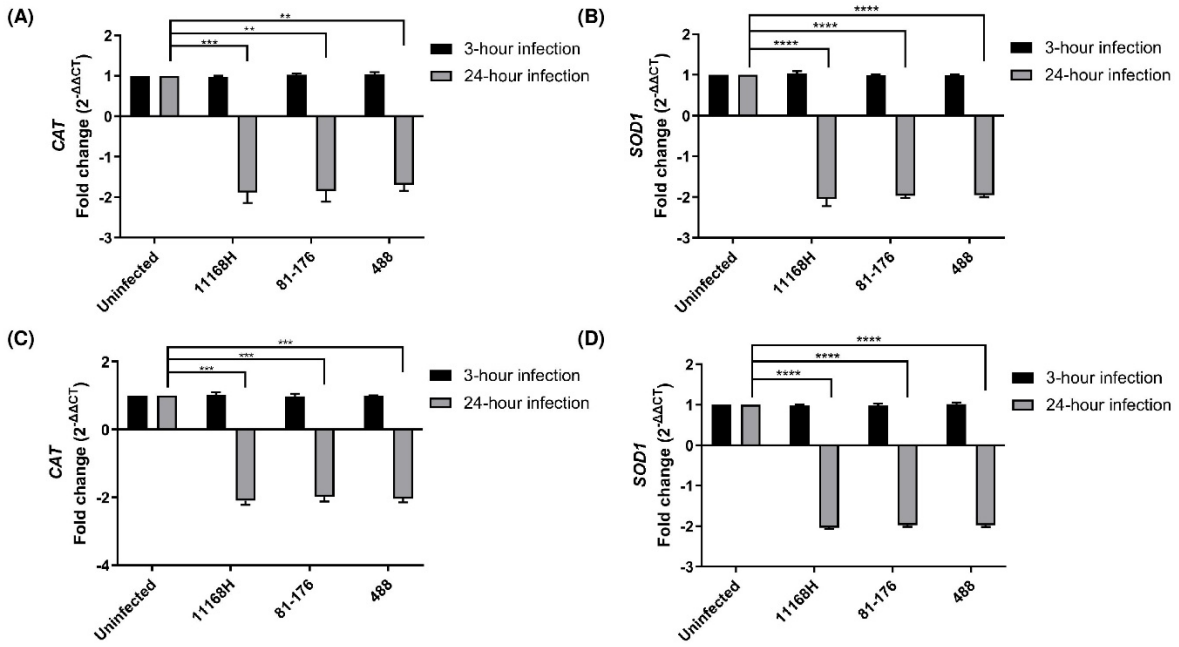


**Figure 5.** qRT-PCR showing expression of human catalase (*CAT*) and superoxide dismutase 1 (*SOD1*) in T84 and Caco-2 cells. (A, B) T84 and (C, D) Caco-2 cells were infected with *C. jejuni* for 3- or 24-hours and transcriptional levels of *CAT* and *SOD1* were measured. *GAPDH* was used as an internal control. Experiments were repeated in three biological and three technical replicates. Asterisks denote a statistically significant difference (** = $p < 0.01$; *** = $p < 0.001$; **** = $p < 0.0001$).

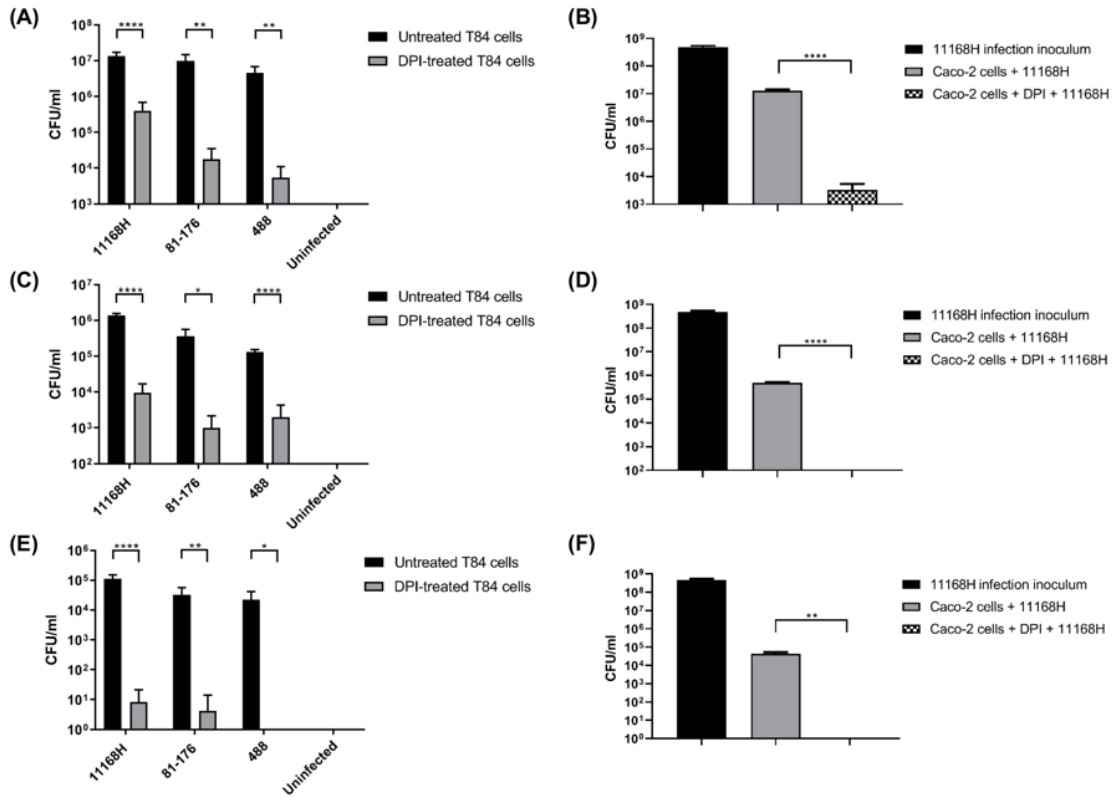


**Figure 6.** The effect of DPI on *C. jejuni* interaction, invasion and intracellular survival. T84 and Caco-2 cells were pre-treated with 10 μM of DPI for 1 hour and infected with *C. jejuni* for 3 hours. (A) T84 and (B) Caco-2 cells were washed with PBS and lysed, and the numbers of interacting bacteria were assessed. (C, D) For invasion assay, after infection with *C. jejuni*, IECs were incubated with gentamicin (150 μg/ml) for 2 hours to kill extracellular bacteria and then lysed, and the numbers of intracellular bacteria were assessed. (E, F) For intracellular survival assay, 2 hours gentamicin treatment was followed by further incubation with gentamicin (10 μg/ml) for 18 hours. Then cells were lysed, and the number of intracellular bacteria were assessed. Experiments were repeated in three biological and three technical replicates. Asterisks denote a statistically significant difference (* = $p < 0.05$; ** = $p < 0.01$; **** = $p < 0.0001$).

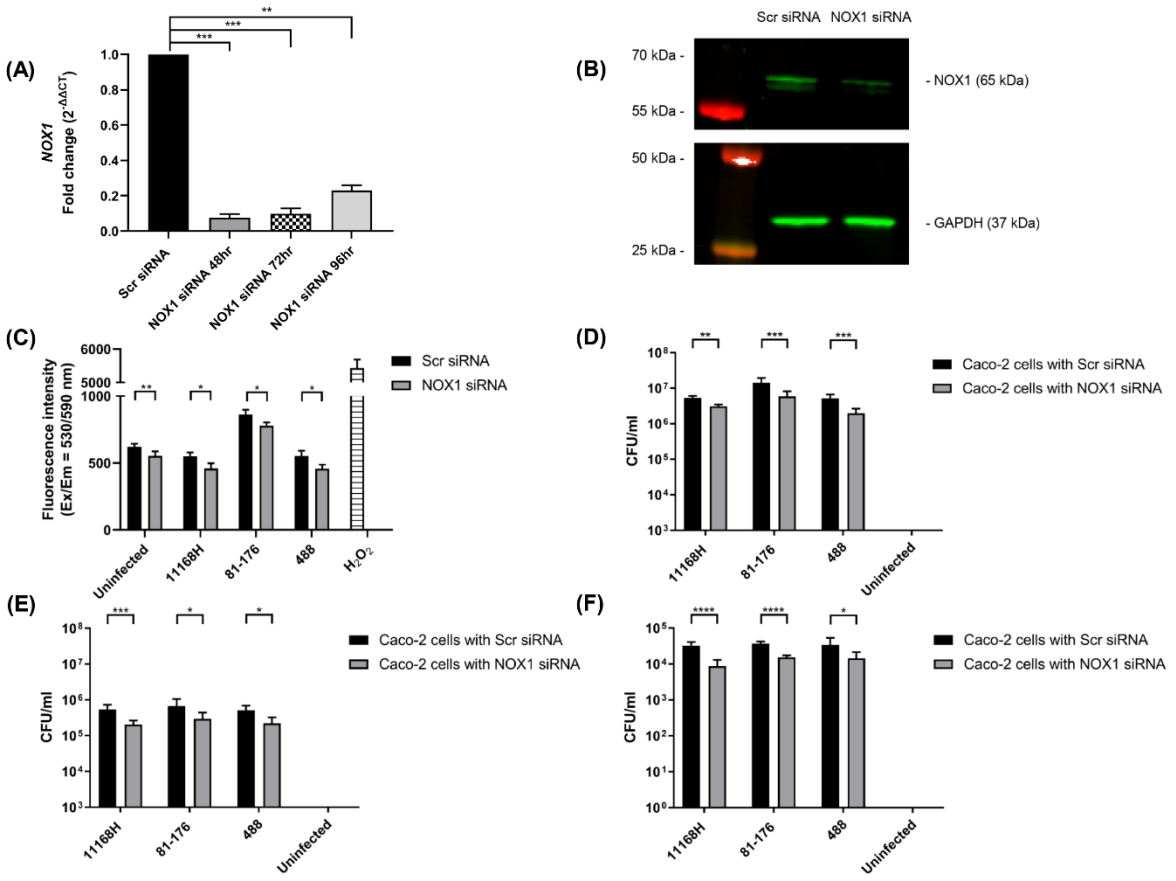


**Figure 7.** The effect of NOX1 silencing on *C. jejuni* interaction, invasion and intracellular survival. Caco-2 cells were transfected with NOX1 siRNA or scrambled siRNA (Scr siRNA). (A) qRT-PCR showing expression of *NOX1* after siRNA transfection. (B) Western blotting showing expression of NOX1 after 72 hours siRNA transfection. (C) Detection of extracellular ROS from Caco-2 cells after 72 hours siRNA transfection followed by co-incubation of *C. jejuni* for 3 hours. (D) After 72 hours siRNA transfection followed by *C. jejuni* infection for 3 hours, Caco-2 cells were washed with PBS and lysed and the numbers of interacting bacteria were assessed or (E) for invasion assay, the cells were incubated with gentamicin (150 µg/ml) for 2 hours to kill extracellular bacteria and then lysed, and the numbers of intracellular bacteria were assessed. (F) For intracellular survival assay, 2 hours gentamicin treatment was followed by further incubation with gentamicin (10 µg/ml) for 18 hours. Then the cells were lysed, and the number of intracellular bacteria determined. Experiments were repeated in three biological and three technical replicates. Asterisks denote a statistically significant difference (* = $p < 0.05$; ** = $p < 0.01$; *** = $p < 0.001$; **** = $p < 0.0001$).

**Supplementary Information**

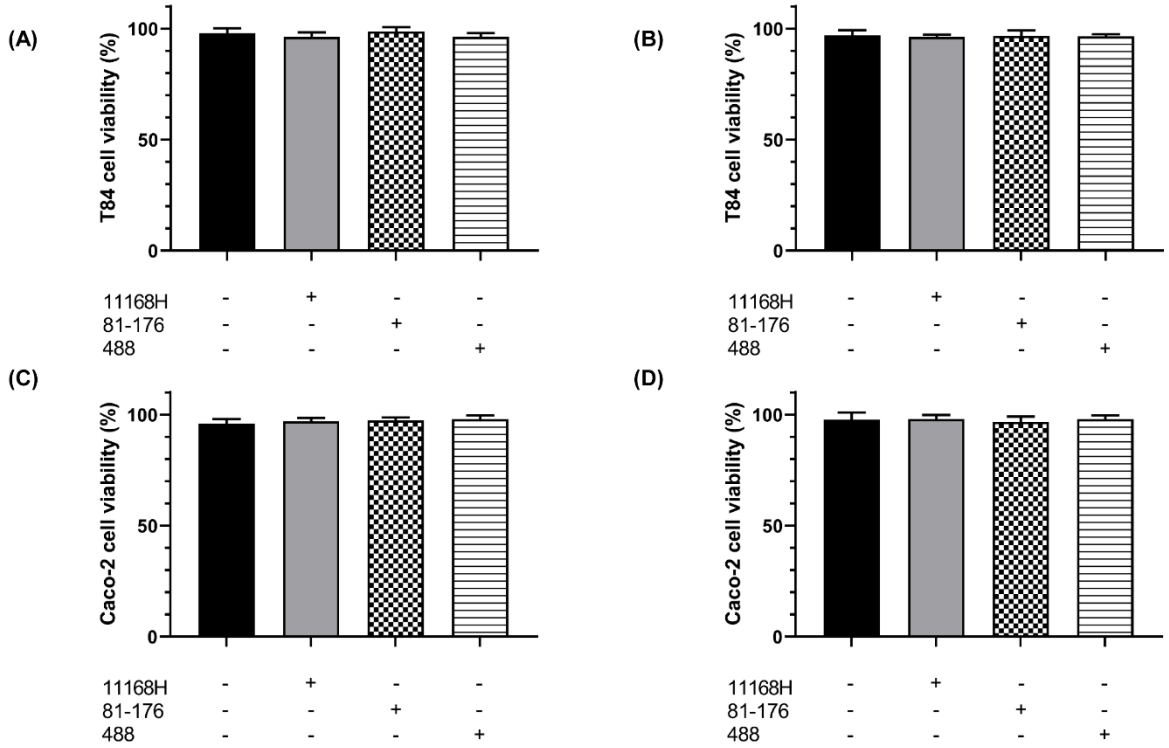


**Figure S1.** Trypan blue exclusion assay. T84 cells were infected with *C. jejuni* for (A) 3 and (B) 24 hours. Caco-2 cells were infected with *C. jejuni* for (C) 3 and (D) 24 hours.

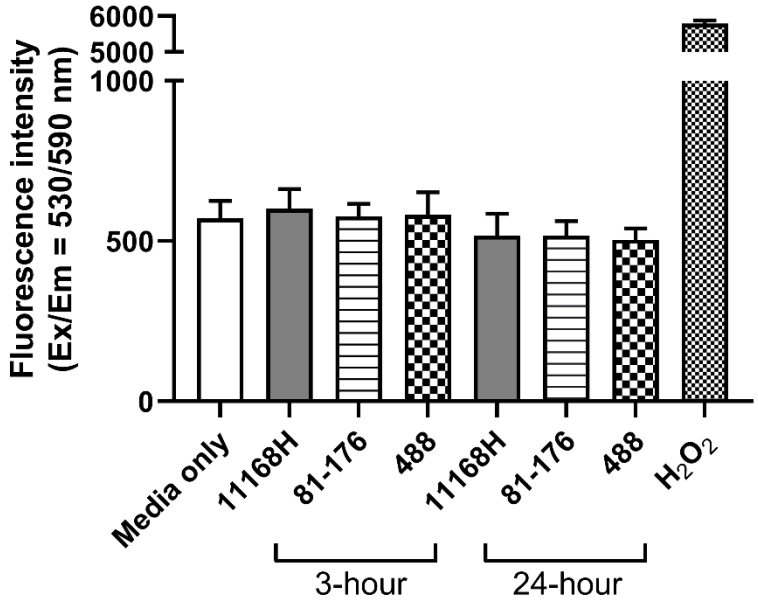


**Figure S2.** Detection of extracellular ROS in DMEM inoculated with *C. jejuni*. *C. jejuni* in DMEM without IECs was incubated for 3 and 24 hours in $CO_2$ incubator. Extracellular ROS was measured after designated incubation. For detection of extracellular ROS, Amplex® Red reagent with HRP were used. For positive controls, $H_2O_2$ was used. Experiments were repeated in triplicate.

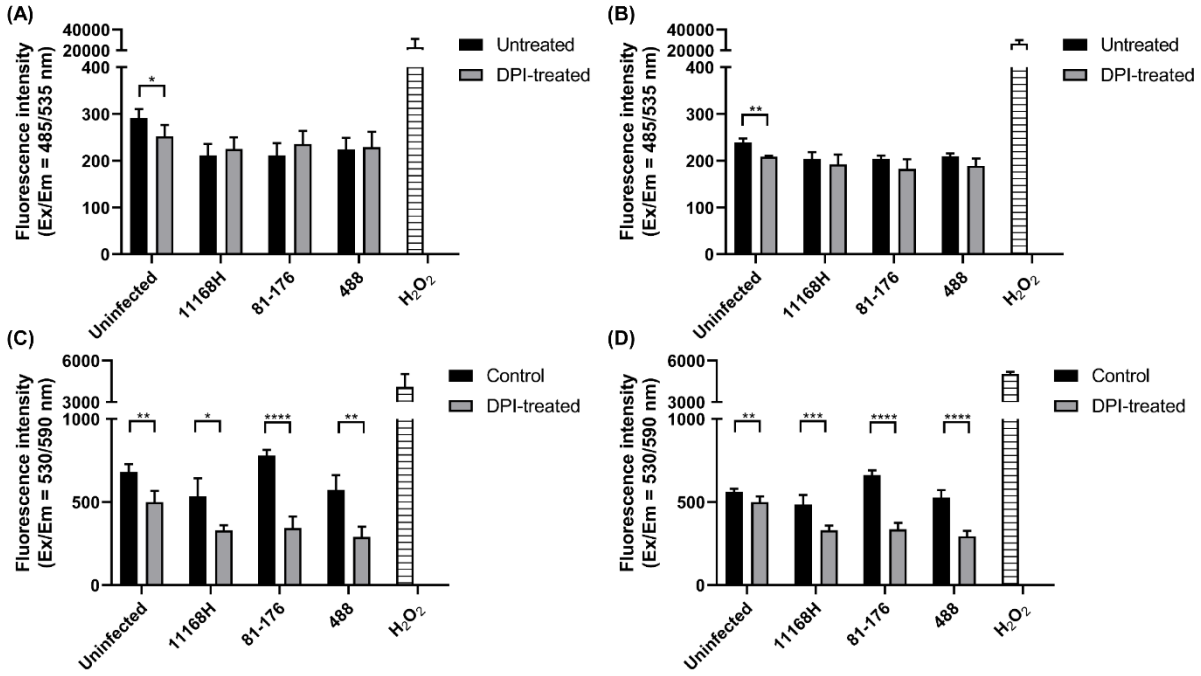


**Figure S3.** Detection of intracellular ROS and extracellular ROS in T84 and Caco-2 cells with or without DPI pre-treatment followed by *C. jejuni* infection. T84 and Caco-2 cells were pre-treated with 10 μM DPI for 1 hour and infected with *C. jejuni*. Intracellular ROS in (A) T84 and (B) Caco-2 cells after co-incubation with *C. jejuni* for 3 hours and extracellular ROS from (C) T84 cells and (D) Caco-2 after co-incubation with *C. jejuni* for 3 hours were measured. For detection of intracellular ROS, DCFDA was used. For detection of extracellular ROS, Amplex® Red reagent with HRP were used. For positive controls, $H_2O_2$ was used. Experiments were repeated in triplicate. Asterisks denote a statistically significant difference (* = $p < 0.05$; ** = $p < 0.01$; *** = $p < 0.001$; **** = $p < 0.0001$).

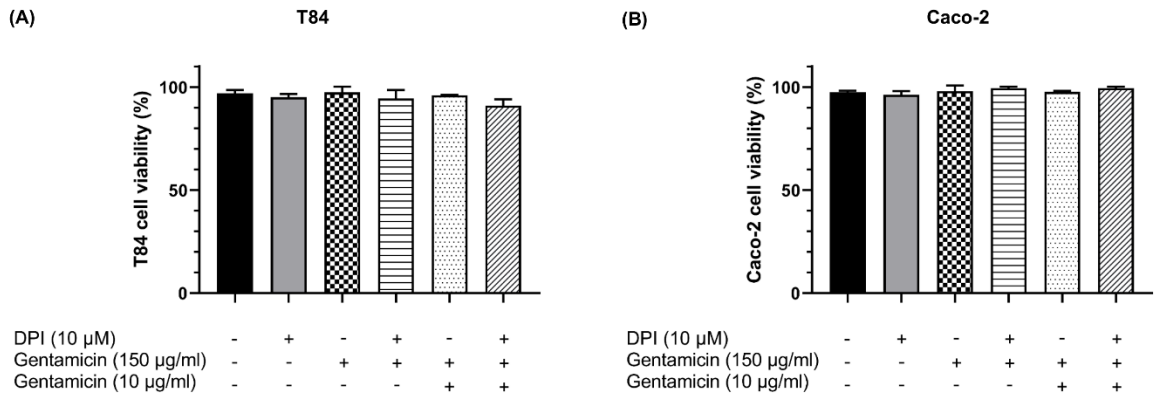


**FIGURE S4.** Assessment of cell viability using trypan blue exclusion assay. (A) T84 and (B) Caco-2 cells were treated with DPI and stained with trypan blue dye to check their viability (%).

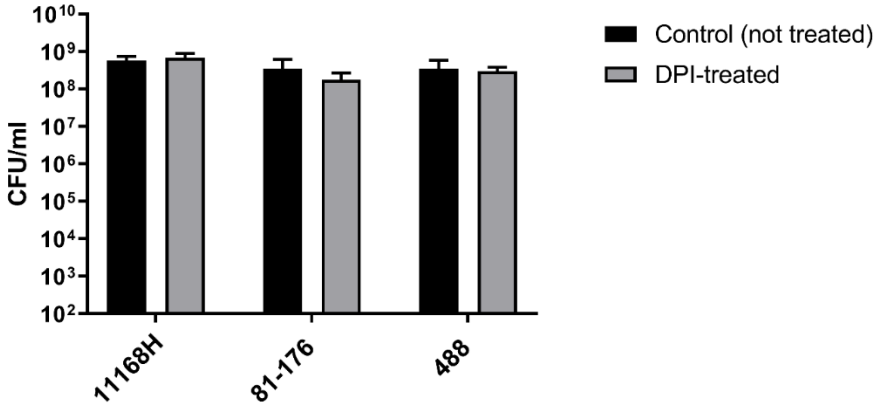


**Figure S5.** *C. jejuni* viability assay with DPI treatment. T84 cells were treated with DPI for 1 hour and the cells were washed three times with PBS. After 1 hour DPI treatment, *C. jejuni* strains were co-incubated for 1 hour with PBS from the last wash and CFU/ml was recorded.

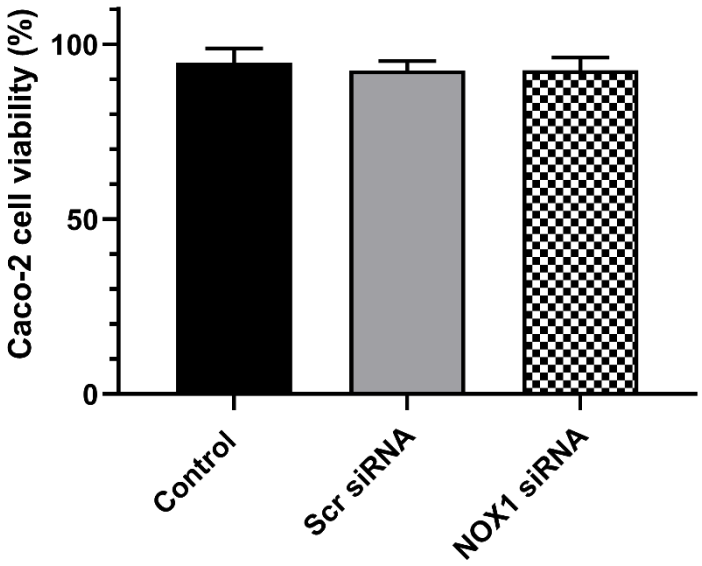


**Figure S6.** Assessment of cell viability using trypan blue exclusion assay. Caco-2 cells were transfected with scrambled siRNA or NOX1 siRNA for 72 hours and stained with trypan blue dye to check their viability (%). Control is without any siRNA transfection.

**Table S1.** *Campylobacter jejuni* strains used in this study

| *C. jejuni* strain | Description | Reference |
|---|---|---|
| 11168H | A hypermotile derivative of NCTC 11168 wild-type strain which is a human clinical isolate. | (Karlyshev et al., 2002; Parkhill et al., 2000) |
| 81-176 | A human clinical isolate identified during an outbreak of acute enteritis associated with consumption of contaminated milk. | (Korlath et al., 1985) |
| 488 | A human clinical isolate from Brazil which has a Type VI Secretion System (T6SS) | (Davies et al., 2019; Liaw et al., 2019) |

**Table S2.** Primers used in this study

| Primer name | Sequences | qRT-PCR/ RT-PCR | Source |
|---|---|---|---|
| *NOX1* | Forward: 5'-CACAAGAAAAATCCTTGGGTCAA-3'<br>Reverse: 5'-GACAGCAGATTGCGACACACA-3' | qRT-PCR and RT-PCR | (Manea et al., 2014) |
| *CAT* | Forward: 5'-TGCAAGCTAGTGGCTTCAAAA-3'<br>Reverse: 5'-TCCAATCATCCGTCAAAACAA-3' | qRT-PCR | (Wang & Eskiw, 2019) |
| *SOD1* | Forward: 5'-GGCAAAGGTGGAAATGAAGAA-3'<br>Reverse: 5'-GGGCCTCAGACTACATCCAAG-3' | qRT-PCR | (Wang & Eskiw, 2019) |
| *GAPDH* | Hs_GAPDH_1_SG QuantiTect Primer Assay, QT00079247 | qRT-PCR | Qiagen |
| *GAPDH* | Forward: 5'-CATCACCATCTTCCAGGAGC-3'<br>Reverse: 5'-GGATGATGTTCTGGAGAGCC-3' | RT-PCR | (Das et al., 2000) |

**ACKNOWLEDGEMENTS**

This manuscript is available as a preprint on bioRxiv (Hong et al., 2022). We would like to acknowledge Marta Mauri for kind advice on siRNA transfection.

# CHAPTER FOUR: Investigation of *C. jejuni*-mediated activation of the unfolded protein response in human intestinal epithelial cells

## 4.1. Introduction

The ER is the largest membrane-bound organelle in eukaryotic cells and plays an important role in protein synthesis and folding, lipid synthesis and $Ca^{2+}$ metabolism (Schwarz & Blower, 2015). Due to the diverse cellular functions of the ER, maintenance of ER homeostasis is crucial (Schwarz & Blower, 2015). The UPR is an ER surveillance response which is activated by ER stress such as hypoxia, $Ca^{2+}$ depletion, glucose depletion or increase of protein folding demand (Hetz & Papa, 2018). The UPR is initially cytoprotective to restore ER homeostasis but prolonged ER stress-induced UPR results in apoptosis (Hetz & Papa, 2018).

Many microbial pathogens can activate the UPR upon infection (Celli & Tsolis, 2014). Viruses have been shown to induce the UPR during their intracellular life cycle (Jheng, Ho, & Horng, 2014). Viruses cause ER stress-induced UPR by rearrangement of the ER membrane, disruption of host protein glycosylation and $Ca^{2+}$ depletion by viroporin (Jheng, Ho, & Horng, 2014). Intracellular bacteria such as *Brucella* spp. and *C. trachomatis* are shown to replicate within host organelles which are derived from the ER membrane which in turn activates the UPR (Celli & Tsolis, 2014). In addition, UPR activation by enteric pathogens such as *E. coli*, *H. pylori* and *V. cholerae* is well-defined (Akazawa et al., 2013; Morinaga et al., 2008). Subtilase cytotoxin produced by Shiga-toxigenic *E. coli* induces all three UPR pathways; PERK, IRE1α and ATF6 pathways by degrading an ER chaperone BiP (Morinaga et al., 2008). *H. pylori* vacuolating cytotoxin VacA which is secreted by Type V secretion system (T5SS) and the secreted antigen HP0175 activate the PERK pathway of the UPR (Akazawa et al., 2013; Halder et al., 2015; Kumar & Dhiman, 2018). Cholera toxin and T3SS effector protein VopQ secreted by *V. cholerae* activate the IRE1α pathway (Banerjee et al., 2021; De Nisco et al., 2021).

Unlike the well-studied UPR activation induced by other enteric bacteria, *C. jejuni*-mediated activation of the UPR has remained relatively less studied. One study has demonstrated that *C. jejuni* induces the PERK pathway only (Aya et al., 2018). However, further investigation is still necessary to elucidate if there is inter-strain variation in UPR activation and to discover the bacterial determinants which are responsible for UPR activation. The aims of the work presented in this chapter was to investigate if *C. jejuni* 11168H, 81-176 and 488 wild-type strains activate the three UPR pathways in human IECs and to ascertain the role of individual *C. jejuni* virulence determinants on UPR activation. To do this, a *C. jejuni cdtABC* operon mutant was constructed and studied along with *cdtA*, *kpsM*, *flaA*, *htrA*, *cadF*, *flpA* mutants and a *cadF flpA* double mutant to identify potential virulence determinants which are involved in *C. jejuni*-mediated UPR activation in human IECs.

## 4.2. Results

### 4.2.1. *C. jejuni* modulates UPR-related gene expression in human IECs

To investigate if there is inter-strain variation in *C. jejuni*-mediated UPR activation, T84 cells were infected with *C. jejuni* 11168H, 81-176 or 488 wild-type strains and transcriptional levels of UPR-related genes were analysed (Figure 4.1 and Figure 4.2). 11168H, 81-176 and 488 significantly upregulated *CHOP* and spliced *XBP1* in T84 cells at 6- and 24-hours post-infection, indicating activation of the PERK and IRE1α pathways respectively (Figure 4.1A, 4.1B and Figure 4.2). Unlike 11168H and 488, 81-176 also upregulated *ATF6* in T84 cells at 6 hours post-infection, suggesting inter-strain variation in activation of the ATF6 pathway (Figure 4.1C). 11168H, 81-176 and 488 downregulated *BiP* in T84 cells at 6 hours post-infection and *BiP* expression was recovered at 24 hours post-infection (Figure 4.1D). Thapsigargin treatment induced *CHOP*, spliced *XBP1*, *ATF6* and *BiP* expression in T84 cells both at 6- and 24-hours post-treatment (Figure 4.1 and Figure 4.2). Similarly, Caco-2 cells infected with 11168H, 81-176 or 488 induced *CHOP* and spliced *XBP1* at 6- and 24-hours post-infection (Figure 4.3A and 4.3B). In contrast to T84 cells, all three *C. jejuni* wild-type strains including 81-176 did not upregulate *ATF6* in Caco-2 cells suggesting activation of the ATF6 pathway is also cell line-dependent (Figure 4.3C). A similar finding in modulation of *BiP* expression was demonstrated in Caco-2 cells. All three *C. jejuni* wild-type strains significantly reduced *BiP* expression in Caco-2 cells at 6 hours post-infection and *BiP* expression was recovered at 24 hours post-infection (Figure 4.3D). Thapsigargin treatment induced *CHOP*, spliced *XBP1*, *ATF6* and *BiP* expression in Caco-2 cells both at 6- and 24-hours post-treatment (Figure 4.3). Upregulation of protein levels of CHOP and spliced XBP1 was demonstrated in T84 and Caco-2 cells infected with 11168H, 81-176 or 488 at 24 hours post-infection (Figure 4.4). Collectively, these data suggest *C. jejuni*-induced UPR is strain-, cell line- and time-dependent.

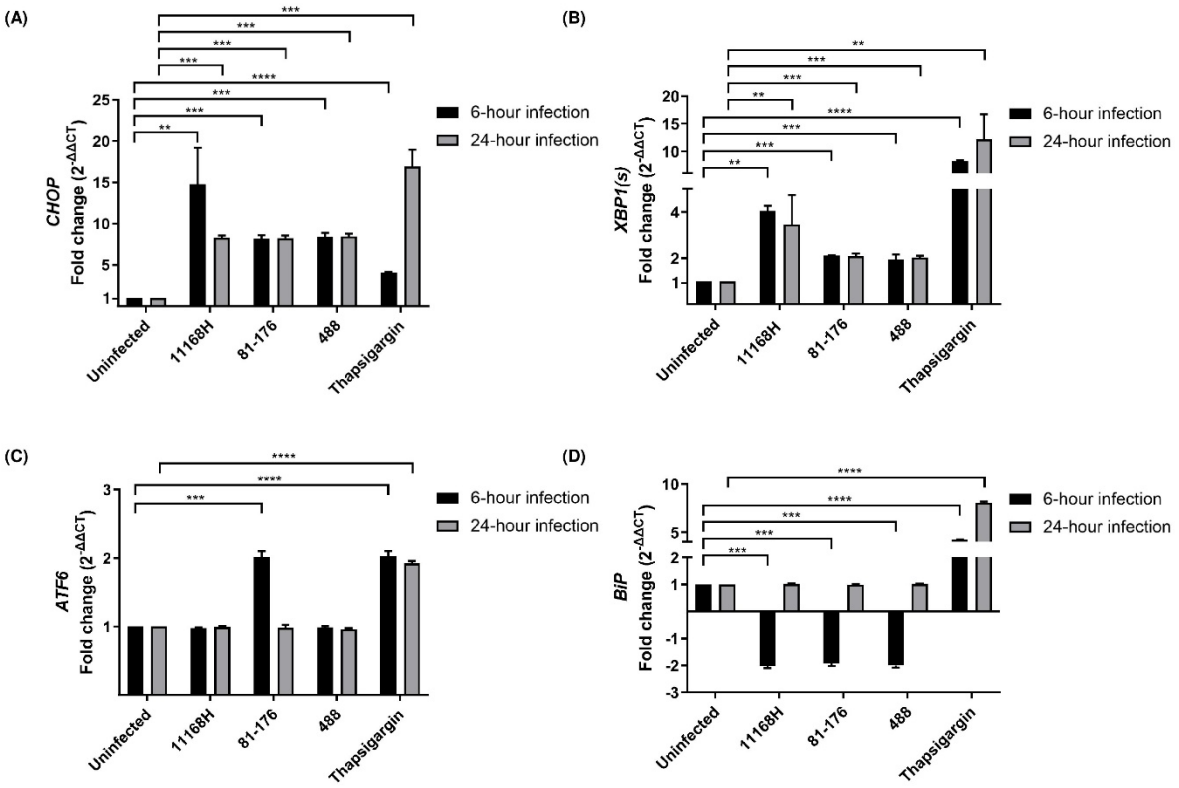


**Figure 4.1. UPR-related gene expression in T84 cells following *C. jejuni* infection.** qRT-PCR showing expression of human (A) *CHOP*, (B) spliced *XBP1* [*XBP1(s)*], (C) *ATF6* and (D) *BiP* in T84 cells infected with *C. jejuni* 11168H, 81-176 or 488 wild-type strains for 6 or 24 hours at 37°C in a 5% $CO_2$ incubator (MOI of 200:1). T84 cells were treated with thapsigargin as a positive control. *GAPDH* was used as an internal control. Three biological and three technical replicates were performed for each experiment. Asterisks denote a statistically significant difference (** = $p < 0.01$; *** = $p < 0.001$; **** = $p < 0.0001$).

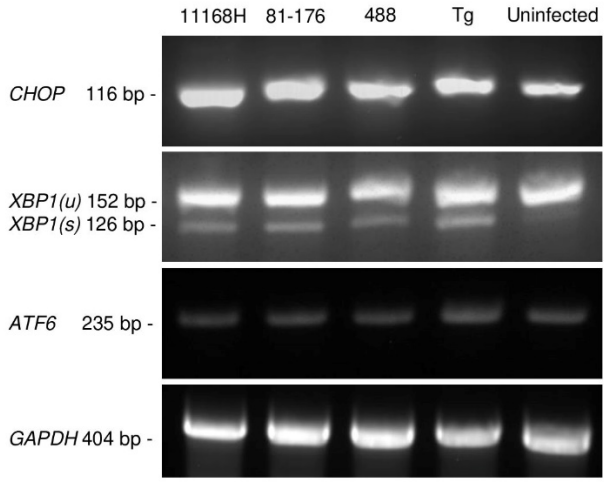


**Figure 4.2. UPR-related gene expression in T84 cells following *C. jejuni* infection.** RT-PCR showing expression of human *CHOP*, unspliced & spliced *XBP1* [*XBP1(u)* & *XBP1(s)*] and *ATF6* in T84 cells infected with *C. jejuni* 11168H, 81-176 or 488 wild-type strains for 24 hours at 37°C in a 5% $CO_2$ incubator (MOI of 200:1). T84 cells were treated with thapsigargin (Tg) as a positive control. *GAPDH* was used as an internal control.

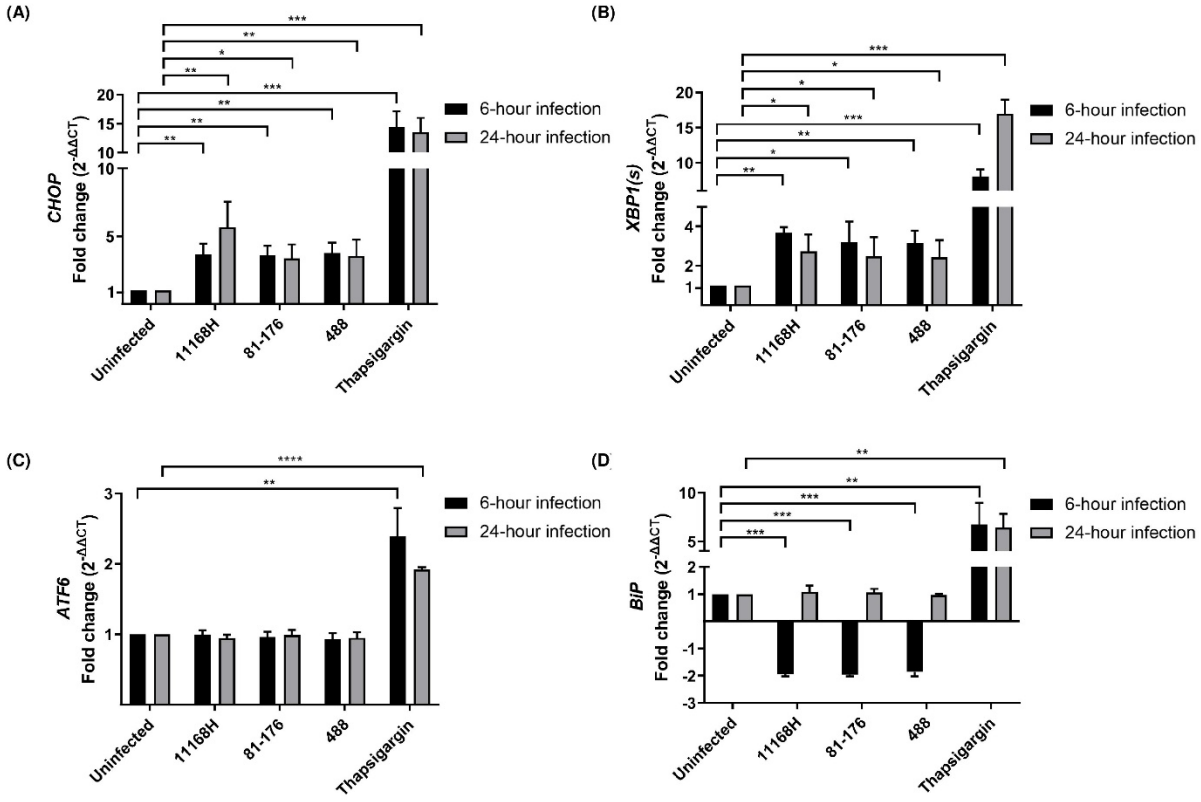


**Figure 4.3. UPR-related gene expression in Caco-2 cells following *C. jejuni* infection.** qRT-PCR showing expression of human (A) *CHOP*, (B) spliced *XBP1* [*XBP1(s)*], (C) *ATF6* and (D) *BiP* in Caco-2 cells infected with *C. jejuni* 11168H, 81-176 or 488 wild-type strains for 6 or 24 hours at 37°C in a 5% $CO_2$ incubator (MOI of 200:1). Caco-2 cells were treated with thapsigargin as a positive control. *GAPDH* was used as an internal control. Three biological and three technical replicates were performed for each experiment. Asterisks denote a statistically significant difference (* = $p < 0.05$; ** = $p < 0.01$; *** = $p < 0.001$; **** = $p < 0.0001$).

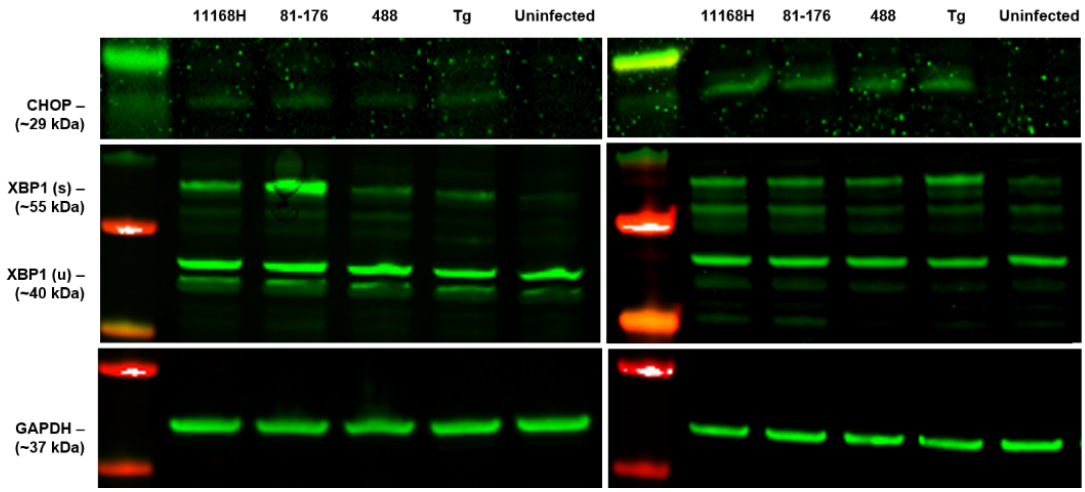


**Figure 4.4. UPR-related gene expression in T84 and Caco-2 cells following *C. jejuni* infection.** Western blotting showing protein levels of human CHOP and both spliced & unspliced forms of XBP1 [XBP1(u) & XBP1(s)] in T84 (left panels) and Caco-2 cells (right panels) infected with *C. jejuni* 11168H, 81-176 or 488 wild-type strains for 24 hours at 37°C in a 5% $CO_2$ incubator (MOI of 200:1). T84 cells were treated with thapsigargin (Tg) as a positive control. GAPDH was used as an internal control.

### 4.2.2. *C. jejuni cdtABC* operon mutagenesis

The *C. jejuni cdtABC* operon encodes CdtA, CdtB and CdtC which are the sub-components of CDT (Lai et al., 2016). After binding of CdtA and CdtC to lipid rafts in the host cell plasma membrane, CdtB internalises into host cells. Within the cytosol, CdtB may translocate from the Golgi complex into the ER. In the nucleus, CdtB triggers DNA double-strand breaks resulting in cell-cycle arrest (Lai et al., 2016). Many bacterial toxins which translocate across the ER are transported from the ER to the cytosol by utilising the UPR-regulated ERAD system (Eshraghi et al., 2014; Guerra et al., 2011; Nowakowska-Gołacka et al., 2019).

To investigate the potential role of *C. jejuni* virulence determinants in UPR activation in human IECs, a *C. jejuni cdtABC* operon knockout mutant was constructed using SOE PCR as described in Chapter 2. Briefly, SOE PCR primers were designed to amplify L1 and R1 of the 11168H *cdtABC* operon and then L1 and R1 were combined and amplified using SOE PCR external primers (Figure 4.5). The purified PCR product L1R1 was ligated into a vector (pGEM-T® Easy Vector) and *E. coli* was transformed with the ligation product termed pAGH1. L1R1 within pAGH1 was amplified and sequenced to confirm the ligation of L1R1 into the vector (Figure 4.6). To confirm the presence of a BamHI single restriction site within L1R1, pAGH1 was digested with BamHI and analysed on an agarose gel (Figure 4.6). As a selective marker for mutagenesis, a BamHI-digested $Cm^r$ cassette (encoding chloramphenicol acetyltransferase) was inserted into BamHI-digested pAGH1. Gel electrophoresis and sequencing confirmed insertion and orientation of the $Cm^r$ cassette. pAGH1 containing the $Cm^r$ cassette in the forward orientation was termed pAGH2 (Figure 4.7). The *C. jejuni* 11168H wild-type strain was then transformed with pAGH2. gDNA of these transformants was extracted and the L1R1/$Cm^r$ cassette was amplified and sequenced to confirm successful construction of a *C. jejuni* 11168H *cdtABC* operon mutant (Figure 4.8).

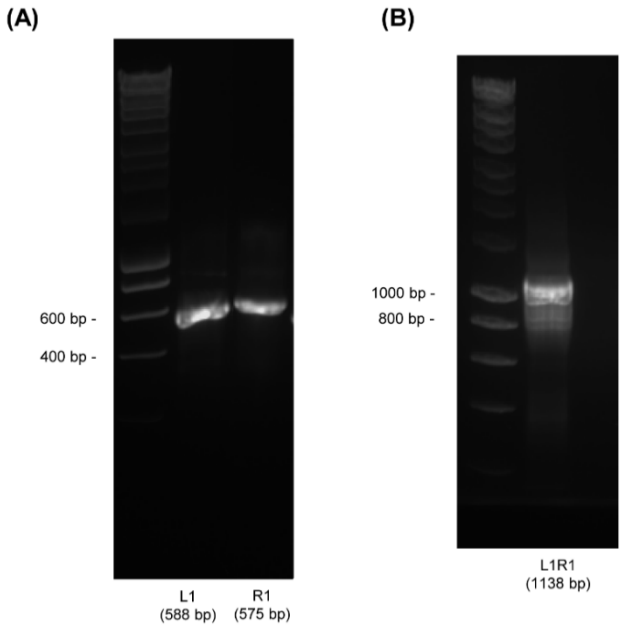


**Figure 4.5. *C. jejuni* 11168H *cdtABC* operon mutagenesis.** PCR verification of amplification of (A) the left fragment (L1) and the right fragment (R1) of *C. jejuni* 11168H *cdtABC* operon and (B) the combined left and right fragment of *C. jejuni* 11168H *cdtABC* operon (L1R1) using SOE PCR external primers.

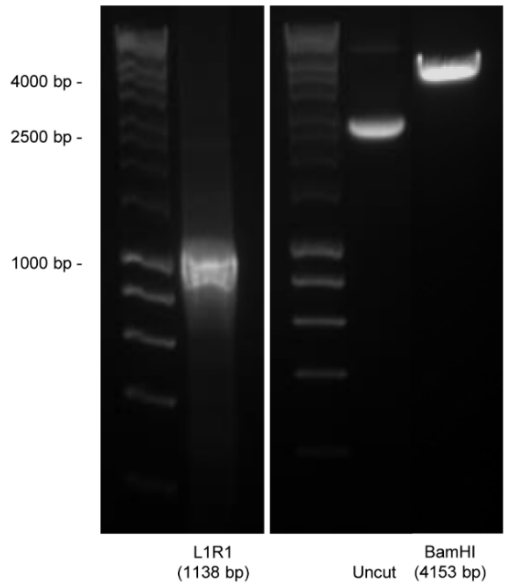


**Figure 4.6. *C. jejuni* 11168H *cdtABC* operon mutagenesis.** PCR verification of vector ligation and *E. coli* transformation. *E. coli* was transformed with the resultant plasmid termed pAGH1 (pGEM-T® Easy Vector ligated with L1R1). L1R1 was amplified within pAGH1 to confirm ligation into the pGEM-T® Easy Vector and pAGH1 was digested with BamHI to confirm the presence of single BamHI restriction site within L1R1.

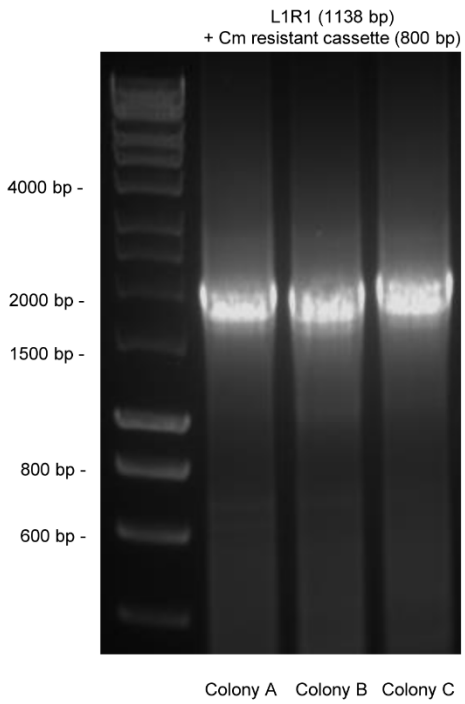


**Figure 4.7. *C. jejuni* 11168H *cdtABC* operon mutagenesis.** PCR verification of $Cm^r$ cassette insertion into L1R1 of pAGH1. $Cm^r$ cassette (encoding chloramphenicol acetyltransferase) was digested with BamHI. BamHI-digested $Cm^r$ cassette was inserted into BamHI-digested pAGH1 and the ligation product termed pAGH2 which refers to pAGH1 with the $Cm^r$ cassette in the forward orientation. After blue-white screening of *E. coli* transformed with pAGH2, L1R1/$Cm^r$ cassette was amplified within pAGH2 using SOE PCR external primers to confirm insertion of $Cm^r$ cassette into the L1R1 fragment.

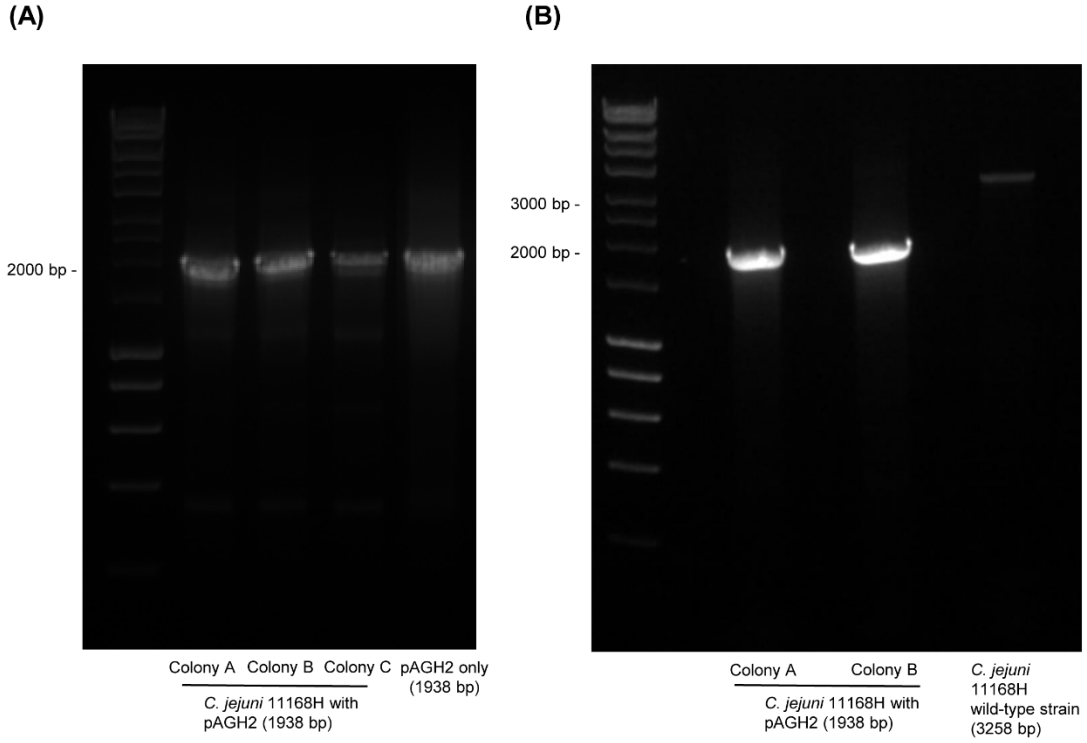


**Figure 4.8. *C. jejuni* 11168H *cdtABC* operon mutagenesis.** PCR verification of *C. jejuni* 11168H transformation with pAGH2 which refers to pAGH1 with the $Cm^r$ cassette in the forward orientation. L1R1/$Cm^r$ cassette was amplified within (A) gDNA of putative *C. jejuni* 11168H transformants and pAGH2 using SOE PCR external primers. As a negative control, the *cdtABC* operon was amplified within (B) gDNA of *C. jejuni* 11168H wild-type strain.

### 4.2.3. Growth kinetics of *C. jejuni* wild-type strain and mutants

Growth kinetics of *C. jejuni* wild-type strains and mutants were chracterised to investigate if there were any significant growth differences (Figure 4.9 and Table 4.1). The 11168H wild-type strain showed a similar growth rate compared to the 81-176 wild-type strain up until 8 hours post-inoculation. However, the 11168H wild-type strain then exhibited a significantly reduced growth rate compared to the 81-176 wild-type strain at 10-, 14-, 16- and 24-hours post-inoculation (Figure 4.9A and Table 4.1). The 11168H wild-type strain showed a higher growth rate compared to the 488 wild-type strain with the exception of timepoints at 2- and 14-hours post-inoculation. The 81-176 wild-type strain exhibited a significantly higher growth rate than the 488 wild-type strain with the exception of timepoints at 2-, 4-, and 6-hours post-inoculation. There were no significant differences in growth rates observed between the 11168H wild-type strain and the 11168H *cdtABC* operon mutant with the exception of a single timepoint at 10 hours post-inoculation (Figure 4.9B and Table 4.1). Compared to the 11168H wild-type strain, the 11168H *cdtA* and *kpsM* mutants showed significantly reduced growth rates until 10 hours post-inoculation and then enhanced growth rates after 14 hours post-inoculation (Figure 4.9C, 4.9D and Table 4.1). The growth rate of the 11168H *flaA* mutant was similar to the 11168H wild-type strain until 8 hours post-inoculation and then enhanced after 10 hours post-inoculation (Figure 4.9E and Table 4.1). The 11168H *htrA*, *cadF,* and *flpA* mutants as well as the *cadF flpA* double mutant all exhibited significantly reduced growth rates compared to the 11168H wild-type strain (Figure 4.9F, 4.9G, 4.9H, 4.9I and Table 4.1).

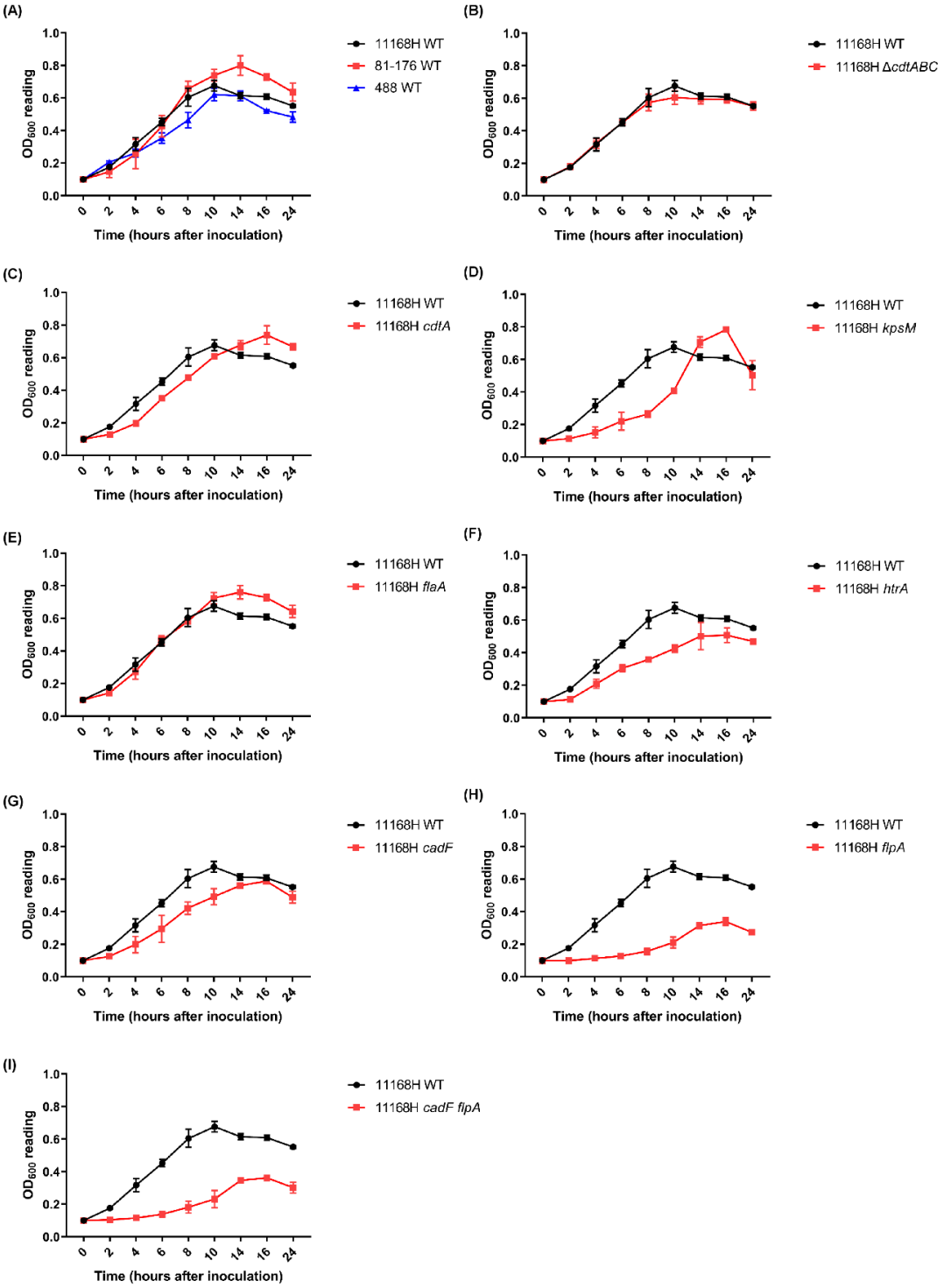


**Figure 4.9. Growth kinetics** of (A) *C. jejuni* 11168H, 81-176 and 488 wild-type strains (WT) and *C. jejuni* 11168H wild-type strain and (B) *cdtABC* operon, (C) *cdtA*, (D) *htrA*, (E) *kpsM*, (F) *flaA*, (G) *cadF*, (H) *flpA* mutants and (I) *cadF flpA* double mutant. *C. jejuni* strains were inoculated in *Brucella* broth resulting in $OD_{600}$ of 0.1. The inoculated flasks were incubated with shaking at 75 rpm at 37°C under microaerobic conditions. The $OD_{600}$ of inoculated flasks was recorded at 2, 4, 6, 8, 10, 14, 16, and 24 hours after inoculation.

**Table 4.1. *p*-values and significant difference of growth kinetics of *C. jejuni* wild-type strains (WT) and 11168H mutants presented in Figure 4.9**

| Time (hours) | (A) 11168H WT vs 81-176 WT | (A) 11168H WT vs 488 WT | (A) 81-176 WT vs 488 WT | (B) 11168H WT vs 11168H Δ*cdtABC* | (C) 11168H WT vs 11168H *cdtA* | (D) 11168H WT vs 11168H *kpsM* | (E) 11168H WT vs 11168H *flaA* | (F) 11168H WT vs 11168H *htrA* | (G) 11168H WT vs 11168H *cadF* | (H) 11168H WT vs 11168H *flpA* | (I) 11168H WT vs 11168H *cadF flpA* |
|---|---|---|---|---|---|---|---|---|---|---|---|
| 2 | 0.1107 | 0.0054 (**) | 0.0181 (*) | 0.6390 | 0.0063 (**) | <0.0001 (****) | 0.0024 (**) | <0.0001 (****) | 0.0005 (***) | <0.0001 (****) | <0.0001 (****) |
| 4 | 0.1953 | 0.0427 (*) | 0.9173 | 0.7772 | 0.0080 (**) | <0.0001 (****) | 0.1054 | 0.0003 (***) | 0.0020 (**) | <0.0001 (****) | <0.0001 (****) |
| 6 | 0.3830 | 0.0004 (***) | 0.1122 | 0.9437 | 0.0009 (***) | <0.0001 (****) | 0.4259 | <0.0001 (****) | 0.0015 (**) | <0.0001 (****) | <0.0001 (****) |
| 8 | 0.1716 | 0.0038 (**) | 0.0070 (**) | 0.2699 | 0.0140 (*) | <0.0001 (****) | 0.4400 | <0.0001 (****) | 0.0006 (***) | <0.0001 (****) | <0.0001 (****) |
| 10 | 0.0330 (*) | 0.0486 (*) | 0.0170 (*) | 0.0079 (**) | 0.0347 (*) | <0.0001 (****) | 0.0558 | <0.0001 (****) | 0.0003 (***) | <0.0001 (****) | <0.0001 (****) |
| 14 | 0.0002 (***) | 0.9279 | 0.0090 (**) | 0.2241 | 0.0092 (**) | 0.0008 (***) | 0.0001 (***) | 0.0118 (*) | 0.0039 (**) | <0.0001 (****) | <0.0001 (****) |
| 16 | <0.0001 (****) | <0.0001 (****) | <0.0001 (****) | 0.2080 | 0.0011 (**) | <0.0001 (****) | <0.0001 (****) | 0.0013 (**) | 0.1134 | <0.0001 (****) | <0.0001 (****) |
| 24 | 0.0057 (**) | 0.0013 (**) | 0.0140 (*) | 0.9887 | <0.0001 (****) | 0.2191 | 0.0002 (***) | <0.0001 (****) | 0.0026 (**) | <0.0001 (****) | <0.0001 (****) |

Asterisks (*) denote a statistically significant difference (* = $p < 0.05$; ** = $p < 0.01$; *** = $p < 0.001$; **** = $p < 0.0001$).

### 4.2.4. Cytotoxicity of *C. jejuni* 11168H wild-type strain and different mutants on T84 IECs

To investigate whether there are differences in cytotoxicity of *C. jejuni* strains on T84 cells, a LDH assay was performed. Compared to the 11168H wild-type strain, the 11168H *cdtABC* operon, *cdtA*, *htrA*, *kpsM*, *flaA* mutants, *cadF flpA* double mutant and the heat-killed 11168H wild-type strain exhibited significantly reduced cytotoxicity on T84 cells (Figure 4.10). However, no significant differences in cytotoxicity were observed between the 11168H wild-type strain and either the *cadF* or *flpA* mutants.

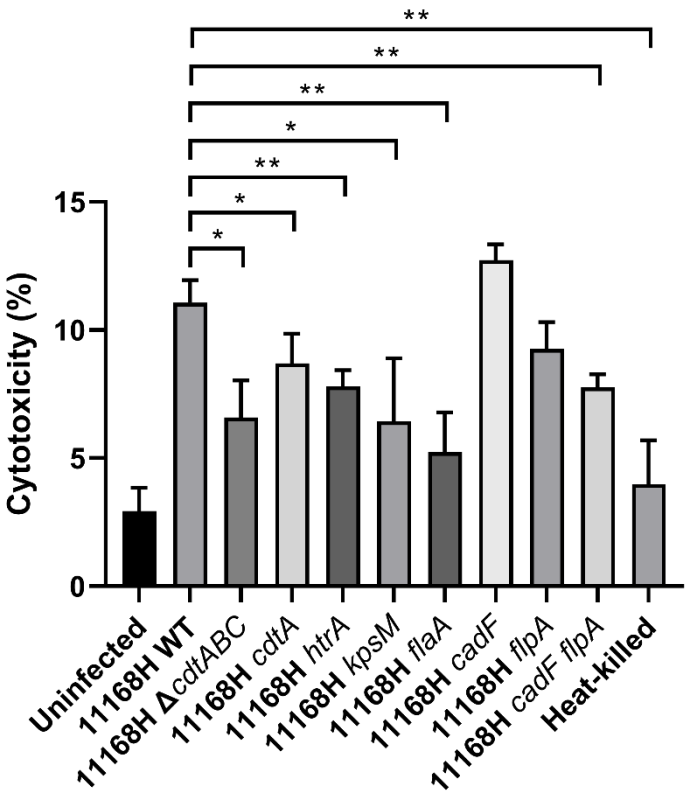


**Figure 4.10. Measurement of cytotoxicity of *C. jejuni* 11168H wild-type strain, mutants and heat-killed 11168H wild-type strain.** T84 cells grown in a 96-well plate were infected with *C. jejuni* strains for 24 hours at 37°C in a 5% $CO_2$ incubator (MOI of 200:1). Medium from each well was then analysed using a LDH assay. Cytotoxicity (%) was calculated as follows; (*C. jejuni* infected LDH activity – spontaneous LDH activity) / (maximum LDH activity – spontaneous LDH activity) x 100. Three biological and three technical replicates were performed for each experiment. Asterisks denote a statistically significant difference (* = $p < 0.05$; ** = $p < 0.01$).

### 4.2.5. Interactions with and invasion of T84 IECs by *C. jejuni* 11168H wild-type strain and different mutants

*C. jejuni* interactions with and invasion of T84 cells were investigated. The 11168H *cdtABC* operon mutant exhibited significantly enhanced interactions compared to the wild-type strain but did not exhibit a significant difference in invasion (Figure 4.11). The 11168H *cdtA*, *htrA*, *kpsM*, *flaA*, *cadF*, *flpA* mutants and *cadF flpA* double mutant showed significant reductions in both interactions with and invasion of T84 cells compared to the wild-type strain. No heat-killed 11168H wild-type strain were recovered on the CBA plate suggesting only viable *C. jejuni* can interact with and invade host cells.

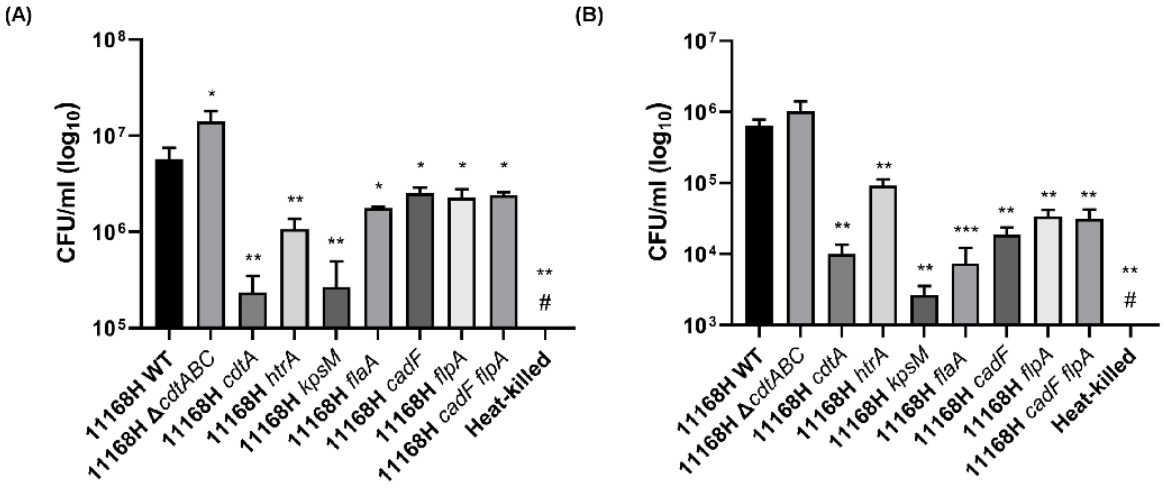


**Figure 4.11. Interactions with and invasion of T84 intestinal epithelial cells by *C. jejuni* 11168H wild-type strain and different mutants.** T84 cells were infected with *C. jejuni* 11168H wild-type strain, 11168H mutants or heat-killed 11168H wild-type strain for 3 hours at 37°C in a 5% $CO_2$ incubator (MOI of 200:1). (A) For interaction assays, T84 cells were then washed with PBS and lysed with 0.1% (v/v) Triton X-100 and CFU/ml were recorded after incubation. (B) For invasion assays, T84 cells were then incubated with gentamicin (150 µg/ml) for 2 hours to kill extracellular bacteria and then lysed with 0.1% (v/v) Triton X-100 and CFU/ml were recorded after incubation. Three biological and three technical replicates were performed for each experiment. # denotes no growth was observed. Asterisks denote a statistically significant difference (* = $p < 0.05$; ** = $p < 0.01$; *** = $p < 0.001$).

### 4.2.6. Induction of IL-8 secretion from T84 cells by *C. jejuni* 11168H wild-type strain and mutants

IL-8 induction by *C. jejuni* strains was measured to investigate whether *C. jejuni* interaction and invasion is correlated to *C. jejuni*-induced IL-8 secretion by T84 cells. To determine IL-8 induction in T84 cells by *C. jejuni* wild-type strain and different mutants, human IL-8 ELISA was performed. There were no significant differences in IL-8 induction between the 11168H wild-type strain and the 11168H *cdtABC* operon, *cdtA* and *cadF* mutants (Figure 4.12). In contrast, 11168H *htrA*, *kpsM*, *flaA*, *flpA* mutants and *cadF flpA* double mutant exhibited significant reduction of IL-8 release compared to the 11168H wild-type strain. The observations indicate *C. jejuni* can induce IL-8 by two main mechanisms which are CDT-dependent and CDT-independent such as active adhesion and/or invasion.

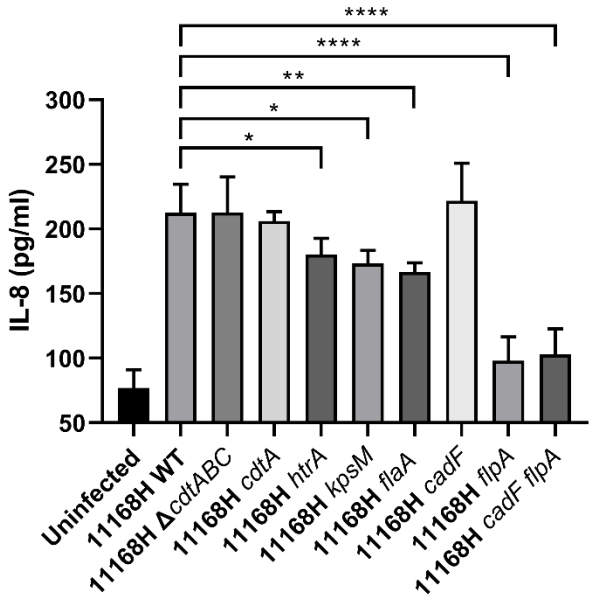


**Figure 4.12. IL-8 release from T84 cells infected with *C. jejuni* 11168H wild-type strain or the mutants.** T84 cells in a 24-well plate were infected with *C. jejuni* for 24 hours at 37°C in a 5% $CO_2$ incubator (MOI of 200:1). Medium from each well was subjected to human IL-8 ELISA to measure the concentrations of IL-8. Three biological and two technical replicates were performed for each experiment. Asterisks denote a statistically significant difference (* = $p < 0.05$; ** = $p < 0.01$; **** = $p < 0.0001$).

### 4.2.7. Activation of PERK and IRE1α pathways in T84 IECs by *C. jejuni* 11168H wild-type strain and mutants

To identify *C. jejuni* virulence determinants which are responsible for UPR activation, T84 cells were infected with either 11168H wild-type strain or different mutants for 24 hours and transcriptional levels of *CHOP* and spliced *XBP1* were analysed (Figure 4.13). Compared to the 11168H wild-type strain, infection with the 11168H *kpsM*, *flaA*, *flpA* mutants and *cadF flpA* double mutant resulted in significantly less upregulated *CHOP* in T84 cells (Figure 4.13A). In contrast, none of these mutants showed significant differences in spliced *XBP1* expression compared to the 11168H wild-type strain (Figure 4.13B and 4.13C). The heat-killed 11168H wild-type strain exhibited impaired upregulation of both *CHOP* and spliced *XBP1* expression compared to the live 11168H wild-type strain suggesting *C. jejuni*-induced UPR requires interactions between live *C. jejuni* and human IECs (Figure 4.13A and 4.13B). Collectively, these data suggest that *C. jejuni* capsule, flagella and FlpA adhesin might be involved in *C. jejuni*-induced UPR. In addition, these observations imply that activation of each UPR pathway is dependent on different *C. jejuni* virulence determinants and there might be other *C. jejuni* virulence determinants that induce the IRE1α pathway.

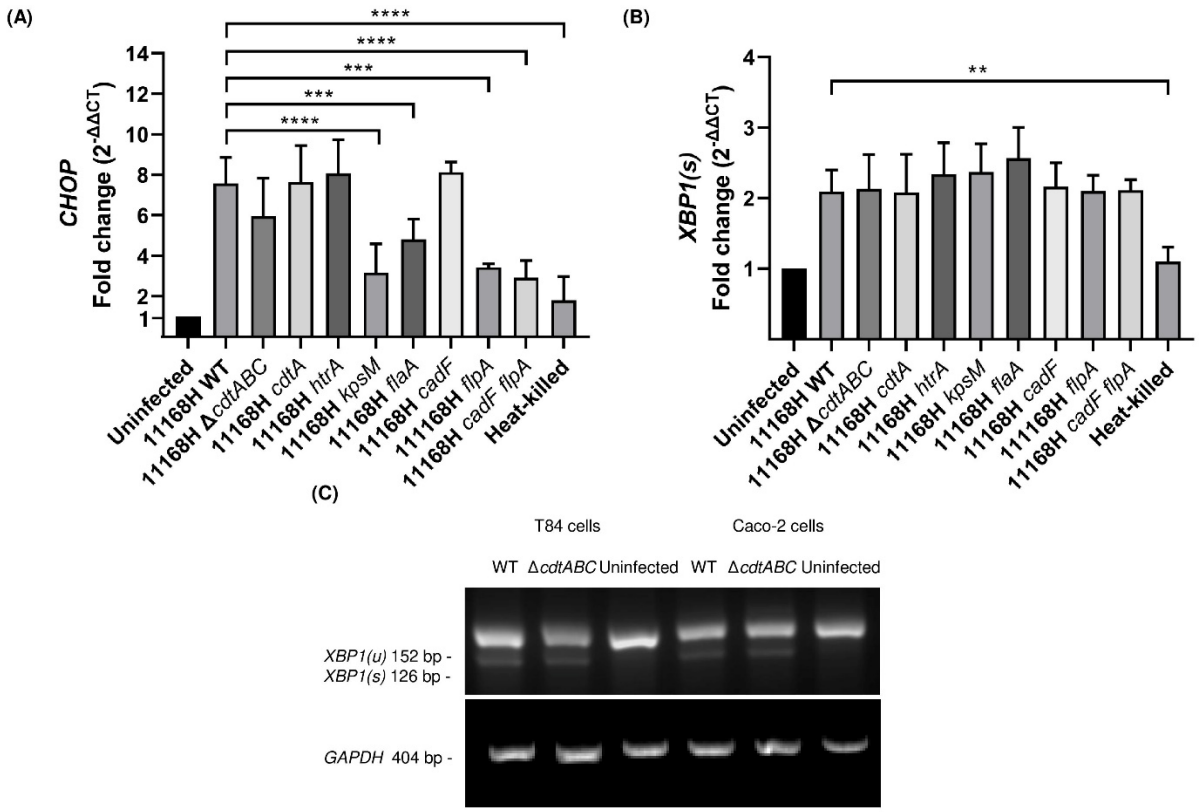


**Figure 4.13. UPR-related gene expression following *C. jejuni* infection.** qRT-PCR showing expression of human (A) *CHOP* and (B) spliced *XBP1* [*XBP1(s)*] in T84 cells infected with either *C. jejuni* 11168H wild-type strain, mutants or heat-killed 11168H wild-type strain for 24 hours at 37°C in a 5% $CO_2$ atmosphere (MOI of 200:1). (C) RT-PCR showing expression of unspliced and spliced *XBP1* [*XBP1(u)* and *XBP1(s)*] in T84 and Caco-2 cells infected with either *C. jejuni* 11168H wild-type strain or *cdtABC* operon mutant for 24 hours at 37°C in a 5% $CO_2$ atmosphere. *GAPDH* was used as an internal control. Three biological and three technical replicates were performed for each experiment. Asterisks denote a statistically significant difference (** = $p < 0.01$; *** = $p < 0.001$; **** = $p < 0.0001$).

## 4.3. Discussion

### 4.3.1. UPR activation by *C. jejuni* in human IECs

UPR activation by *C. jejuni* has not been investigated in the same detail compared to other enteric pathogens. A previous study demonstrated that only the PERK pathway was induced by *C. jejuni* 81-176 in Caco-2 cells (Aya et al., 2018). In contrast, in this study we have demonstrated that 11168H, 81-176 and 488 wild-type strains activated the PERK and IRE1α pathways in both T84 and Caco-2 cells. Amongst the three *C. jejuni* wild-type strains used in this study, only 81-176 induced the ATF6 pathway in T84 cells but not in Caco-2 cells. Such differing data may be due to differences in experimental conditions such as different antibodies and cell lines. Data presented in this study indicates *C. jejuni*-mediated ATF6 pathway activation was both cell line- and strain-dependent. Both the T84 and Caco-2 cells used in this study were originally derived from human colonic adenocarcinoma cells. T84 cells exhibit characteristics of colonocytes, such as shorter microvilli, whereas Caco-2 cells exhibit characteristics of enterocytes upon maturation (Devriese et al., 2017). Small intestinal brush border enzymes are found in Caco-2 cells but not in T84 cells. Monocarboxylate transporter-1 (MCT1) which is a colonocyte biomarker is only expressed in T84 cells. Furthermore, higher TLR4 expression is observed in T84 cells and higher TLR5 expression is detected in Caco-2 cells (Devriese et al., 2017). Such phenotypic variation between the two cell lines might result in differences in host cellular signalling during *C. jejuni* infection. Thus, differential ATF6 pathway activation by *C. jejuni* might be in part due to differences between the two cell lines.

In addition, *C. jejuni*-induced activation of the ATF6 pathway was strain dependent. Genomic analysis has revealed that *C. jejuni* exhibits significant inter-strain variability (Bravo et al., 2021; Dorrell et al., 2001). Most inter-strain diversity of *C. jejuni* was found in the capsule biosynthesis locus, the LOS biosynthesis locus, the flagellin *O*-linked glycosylation locus as well as in the T4SS and T6SS gene clusters (Bravo et al., 2021). 81-176 was originally isolated from an outbreak associated with contaminated milk in the USA (Korlath et al., 1985). 81-176 possesses two plasmids termed pVir and pTet (Bacon et al., 2000). Even though there is little evidence of a full T4SS system, four genes which encode orthologues of *H. pylori* T4SS are found in the pVir plasmid and the *H. pylori cag* Pathogenicity Island contains one of these genes (Bacon et al., 2000, 2002; Kersulyte et al., 2003). *H. pylori* T4SS is involved in translocation of cytotoxin-associated antigen A (CagA) which is responsible for human IL-8 induction (Fischer et al., 2001; Kersulyte et al., 2003). Several studies have investigated the role of the putative *C. jejuni* T4SS encoded on pVir (Bacon et al., 2000, 2002). Adherence and invasion of *C. jejuni* to INT407 cells as well as virulence in a ferret model were significantly reduced by mutation of pVir genes (Bacon et al., 2000, 2002). Mutation in one of the pVir genes involved in *H. pylori* natural

transformation also reduced natural transformation efficiency of 81-176 (Bacon et al., 2000).

A number of bacterial T4SSs including *H. pylori* T4SS are implicated in UPR activation (Celli & Tsolis, 2014). *H. pylori* vacuolating cytotoxin CagA which is translocated by T4SS causes mitochondrial dysfunction through oxidative damage and is responsible for induction of the PERK, IRE1α and ATF6 pathways in human gastric adenocarcinoma-derived AGS and MKN45 cells (Kumar & Dhiman, 2018; Nami et al., 2020). *B. abortus* T4SS effector protein VceC induces the UPR and inflammation through interaction with BiP (de Jong et al., 2013). In addition, *L. pneumophila* effector protein Lpg0519 activates the ATF6 pathway in a T4SS-dependent manner (Ibe, Subramanian, & Mukherjee, 2021). Therefore, further studies are required to investigate if the 81-176 T4SS is responsible for ATF6 pathway activation. We also cannot disregard the possibility that there might be other bacterial virulence determinants of the 81-176 strain which can activate the ATF6 pathway.

Unlike 11168H and 81-176, 488 possesses a functional T6SS associated with roles in oxidative stress response, cytotoxicity and interaction and invasion of chicken intestinal primary cells (Liaw et al., 2019; Robinson et al., 2021). A previous study reported *Pseudomonas aeruginosa* T6SS-mediated UPR activation in human embryonic kidney HEK293T cells (Jiang et al., 2016). *P. aeruginosa* T6SS delivers phospholipase toxin TplE which exerts a lypolytic action on adjacent bacteria. After internalisation into host cells by T6SS, TplE localises to the ER and disrupts the ER structure by lipase activity. ER disruption then results in activation of the PERK and IRE1α pathways followed by autophagy initiation (Jiang et al., 2016). Like *P. aeruginosa* T6SS, *C. jejuni* 488 T6SS might secrete ER-localising and/or ER-disrupting effector proteins which can activate the UPR. It is also possible that structural components of 488 T6SS might be able to induce the UPR in human IECs. Further investigation is required to determine if 488 T6SS is involved in the UPR activation.

In contrast to 488 which is a recently isolated clinical strain, 11168H and 81-176 are the most commonly used *C. jejuni* isolates in the laboratory (Jones et al., 2004; Karlyshev et al., 2002; Korlath et al., 1985). Both *C. jejuni* isolates are fully sequenced and well-studied (Bacon et al., 2002; Gaynor et al., 2004). As 11168H and 81-176 are adapted to the laboratory environments, the use of other fresh clinical *C. jejuni* isolates is required to examine if there is phenotypic differences in UPR activation between the laboratory and fresh clinical isolates.

#### 4.3.2. *C. jejuni* 11168H *cdtABC* operon mutagenesis and phenotypic assays

Translocation of many bacterial AB-toxins from the ER to the cytosol is dependent on the ERAD pathway (Eshraghi et al., 2014; Guerra et al., 2011; Nowakowska-Gołacka et al., 2019). Such toxins include cholera toxin, Shiga toxin and *E. coli* heat-labile enterotoxin (Nowakowska-Gołacka et al.,

2019). Initially, fully folded toxins are translocated to the ER and interact with PDI which catalyses unfolding of toxins. The ERAD system recognises unfolded proteins within the ER, the substrates are retrotranslocated to the ER membrane and released into the cytosol. Then ubiquitin-proteasome degrades misfolded or unfolded substrates. However, toxins can undergo refolding in the cytosol to avoid degradation (Nowakowska-Gołacka et al., 2019). A heterotrimeric AB-type CDT was shown to require the ERAD pathway for intoxication (Eshraghi et al., 2014). As the UPR upregulates expression of genes encoding components of the ERAD pathway (Hetz & Papa, 2018), a *C. jejuni cdtABC* operon mutant was constructed to investigate if *C. jejuni* CDT is responsible for UPR activation in human IECs.

Phenotypic assays were performed using the 11168H wild-type strain, *cdtABC* operon, *cdtA*, *kpsM*, *flaA*, *htrA*, *cadF*, *flpA* mutants and a *cadF flpA* double mutant. Each mutant exhibited distinct growth kinetics which may be due to different metabolic costs resulting from individual mutations. Interestingly, all *C. jejuni* mutants, except the *cdtABC* operon and *cdtA* mutants, exhibited both reduced cytotoxicity and interaction and invasion. A previous study reported *C. jejuni* strains with greater invasiveness result in higher cytotoxicity on T84 cells (Kalischuk, Inglis, & Buret, 2007). In agreement with the previous study, the data shown in this chapter suggests *C. jejuni* cytotoxicity is closely correlated with host cell invasion. The results also indicate that *C. jejuni* CDT exerts cytotoxicity on host cells independent of *C. jejuni* adherence and invasion. While *cdtA* mutant exhibited reduced interaction with T84 cells, *cdtABC* operon mutant exhibited enhanced interaction. Further studies are required to investigate if each mutation affects expression of other genes which are involved in interaction with host cells.

Two mechanisms that *C. jejuni* induces IL-8 secretion from human IECs are adherence and invasion and CDT activity (Hickey et al., 2000). In accordance with a previous study (Hickey et al., 2000), the data presented in this chapter demonstrated that the mutation of either the *cdtABC* operon or *cdtA* did not affect *C. jejuni* whole cell-mediated IL-8 induction from T84 cells. The results suggest *C. jejuni* can induce IL-8 secretion via adherence and invasion which is independent of CDT activity. However, it has been demonstrated that membrane fractions of *cdt* mutants failed to induce IL-8 compared to the membrane fractions of the wild-type strain indicating membrane-bound CDT is involved in IL-8 induction (Hickey et al., 2000). It is now known that *C. jejuni* CDT is secreted via OMVs and extracellular CDT which is closely associated with the OMVs exerts cytotoxicity on human IECs (Elmi et al., 2012; Lindmark et al., 2009). This indicates that *C. jejuni* can induce IL-8 secretion from human IECs via OMV-associated CDT as well as via adherence and invasion.

The *htrA*, *kpsM*, *flaA*, *flpA* mutants and the *cadF flpA* double mutant which all exhibit reduced interaction and invasion, also showed impaired IL-8 induction in T84 cells. These results are in accordance with a previous study which demonstrated that 81-176 *flaA* and *peb1A* mutants with reduced

adherence and invasion resulted in less IL-8 induction from INT407 cells (Hickey et al., 1999). In contrast, another study demonstrated there was no difference in IL-8 expression in Caco-2 and HT-29 cells between the 11168H *kpsM* mutant and the wild-type strain (Zilbauer et al., 2005). Such differing data may be due to phenotypic variation between the cell lines which subsequently results in differential cellular signalling in inflammation.

Whole genome sequencing of each mutant is needed to examine if each mutation does not affect other genes. Western blot is also required to check whether a protein encoded by each mutated gene is still expressed or not. In addition, complementation studies are necessary to confirm the phenotypes of mutants observed in each experiment were due to the mutation of a specific gene.

#### 4.3.3. *C. jejuni* virulence determinants which are responsible for UPR activation

Unlike other UPR-activating bacteria, *C. jejuni* virulence determinants that activate the UPR have yet to be identified. qRT-PCR data presented in this chapter demonstrated that the *cdtABC* operon and *cdtA* mutants did not show any differences in activation of either the PERK or IRE1α pathways compared to the wild-type strain. Given that *C. jejuni* can induce IL-8 secretion via adherence and invasion which is independent of CDT activity (Hickey et al., 2000) and the UPR is closely linked to proinflammation (Garg et al., 2012; Joep et al., 2016), the reason why no differences in UPR activation was observed between the wild-type strain and the *cdt* mutants might be because the UPR is still activated via *C. jejuni* adherence and invasion. Further studies will be necessary to determine if *C. jejuni* OMV-associated CDT is responsible for the UPR activation in human IECs. If *C. jejuni* CDT does not activate the UPR, it is also possible that retrotranslocation of *C. jejuni* CDT might utilise basal level of ERAD components without UPR-induced expression of ERAD components.

In addition, results presented in this chapter showed that *C. jejuni* capsular polysaccharide, flagella and FlpA are involved in activation of the PERK pathway. The observation reemphasises the possibility that PERK pathway activation might be dependent on adherence and invasion of *C. jejuni*. Even though both *cadF* and *flpA* mutants showed reduced interaction and invasion, only the *cadF* mutant displayed similar level of the PERK pathway activation as observed in the wild-type strain. This suggests differential effects of interaction of *C. jejuni* adhesins CadF and FlpA with host IECs on cellular signalling for UPR activation. Furthermore, the *cadF* mutant did not affect IL-8 release but the *flpA* mutant and the *cadF flpA* double mutant both reduced IL-8 secretion. This indicates that *C. jejuni*-mediated IL-8 induction might be correlated to *C. jejuni*-induced UPR activation. Further studies are required to determine whether *C. jejuni*-induced inflammation is linked to the UPR activation.

Similarly, the *htrA* mutant was still able to induce the UPR even though it displayed reduced interaction

and invasion compared to the wild-type strain. A previous study demonstrated that *C. jejuni* OMVs which contain proteases HtrA, Cj0511 and Cj1365c are able to cleave recombinant BiP (Elmi et al., 2017). OMVs from the *htrA* mutant were still able to cleave recombinant BiP whereas OMVs from the *Cj1365c* mutant exhibited reduced BiP cleavage compared to OMVs from the wild-type strain (Elmi et al., 2017). As HtrA is not involved in BiP cleavage as shown in a previous study (Elmi et al., 2017), the *htrA* mutant might still be able to activate the PERK and IRE1α pathways in T84 cells. Unlike HtrA, the Cj1365c protease contains a domain with a sequence identity of 20% with subunit A of the subtilase cytotoxin of *E. coli* (Elmi et al., 2017). The subtilase cytotoxin degrades BiP and induces the activation of all three UPR pathways (Morinaga et al., 2008; Paton et al., 2006). Further experiments using the *Cj1365c* mutant are needed to investigate whether Cj1365c-mediated BiP cleavage is a mechanism of *C. jejuni*-activated UPR. However, it is possible that *C. jejuni*-mediated UPR activation is independent of BiP cleavage. BiP is bound to all three sensors, PERK, IRE1α and ATF6 under homeostatic conditions and detachment of BiP from each sensor activates all three pathways during the ER stress (Hetz & Papa, 2018). *E. coli* subtilase cytotoxin activates all three pathways by degrading BiP (Morinaga et al., 2008; Paton et al., 2006). Unlike *E. coli* which activates all three UPR pathways, the qRT-PCR data presented in this chapter indicated 11168H induced the PERK and IRE1α pathways but not the ATF6 pathway. Therefore, we speculate that *C. jejuni* induces the UPR via other mechanisms.

Interestingly, none of the mutants included in this chapter showed any significant differences in the activation of the IRE1α pathway compared to the wild-type strain. This indicates that different *C. jejuni* virulence determinants are involved in the activation of each UPR pathway. For example, *C. jejuni* LOS might be able to activate the IRE1α pathway. A previous study demonstrated that treatment of RAW264.7 murine macrophage cells with *E. coli* LPS did not induce the PERK pathway but did activate the IRE1α pathway (Nakayama et al., 2010). *C. jejuni* LOS is structurally similar to LPS but it lacks the O-antigen (Hameed et al., 2020). In addition, we cannot exclude the possibility of involvement of OMV-associated CDT in IREα pathway activation. Thus, further studies are required to investigate whether *C. jejuni* LOS and/or OMV-associated CDT are involved in IREα pathway activation. Data presented in this chapter also indicates that live *C. jejuni* is required to activate both the PERK and IRE1α pathways which suggests that the interaction between human IECs and the intact *C. jejuni* membrane proteins and/or live whole cells is necessary for the *C. jejuni*-mediated UPR activation.

## 4.4. Conclusion

In this study, the UPR activation in human IECs by *C. jejuni* wild-type and different mutant strains was investigated. Data presented in this chapter suggests that *C. jejuni*-mediated activation of the ATF6 pathway is strain- and cell line-dependent unlike the activation of the PERK and IREα pathways. In addition, the data indicates the requirement of live *C. jejuni* cells for UPR activation and the involvement of *C. jejuni* capsular polysaccharide, flagella and FlpA in PERK pathway activation. However, none of the 11168H mutants used in this study exhibited differences in activation of the IREα pathway. This study also points to the possibility that *C. jejuni*-mediated UPR might be linked to *C. jejuni*-induced inflammation. Leading from this study, further investigation is necessary to identify bacterial virulence determinants which are responsible for IRE1α pathway activation and to determine whether *C. jejuni*-induced UPR results in inflammation in human IECs.

# CHAPTER FIVE: Further investigation of *C. jejuni*-mediated activation of the unfolded protein response in human intestinal epithelial cells

## 5.1. Introduction

Many microbial pathogens can modulate the UPR as UPR activation can affect their fitness (Jean & Renée, 2014). Japanese encephalitis virus (JEV) induces the IRE1α pathway which upregulates the RIDD pathway (Bhattacharyya, Sen, & Vrati, 2014). JEV exploits the UPR-induced RIDD pathway which degrades host mRNA but not viral RNA resulting in effective viral protein synthesis (Bhattacharyya, Sen, & Vrati, 2014). In addition to viral pathogens, some bacterial pathogens exploit the UPR to benefit bacterial replication within host cells (Jean & Renée, 2014). *B. melitensis* TcpB interacts with microtubules and induces the UPR to reorganise the ER and to enhance intracellular replication within the ER in RAW 264.7 macrophages (Smith et al., 2013). *S. enterica* activates the UPR for intracellular replication by exploiting UPR-induced lipid metabolism (Antoniou et al., 2018). In contrast, some effector proteins of *L. pneumophila* T4SS inhibit upregulation of translational expression of BiP and CHOP and block XBP1 mRNA splicing (Sean & Shaeri, 2015). As the UPR can be either beneficial or detrimental to pathogens, each pathogen exhibits distinct strategies to manipulate the UPR (Jean & Renée, 2014).

The UPR can exert antibacterial effects on microbial pathogens as the UPR is implicated in proinflammation (Grootjans et al., 2016; Jean & Renée, 2014). Phosphorylation of eIF2α by PERK increases the relative ratio of NF-κB over IκB resulting in inflammation (Deng et al., 2004). ATF4 is selectively translated during activation of the PERK pathway and upregulates *IL-6* gene expression (Zhang et al., 2013). IRE1α interacts with TRAF2 to activate the JNK and NF-κB pathways and spliced XBP1 upregulates *TNF* and *IL-6* gene expression (Hu et al., 2006). In addition, ATF6 activates NF-κB-mediated inflammation and ATF6 with CREBH induces genes involved in the acute phase response (Zhang et al., 2006). The UPR-mediated inflammation is detrimental to the invading pathogens; however, at the same time activation of the UPR benefits the intracellular survival of some pathogens, highlighting the complexity of microbial pathogen-mediated UPR modulation.

As a surveillance system for the ER homeostasis, the UPR is activated by various stimuli such as $Ca^{2+}$ depletion or increased protein folding demands (Hetz & Papa, 2018). These stimuli result in an increase in misfolded proteins within the ER lumen which subsequently bind to BiP and trigger the UPR (Hetz & Papa, 2018). In addition to the accumulation of misfolded proteins within the ER lumen, the UPR can be activated by TLR stimulation upon bacterial infection (Kim et al., 2018). In the previous chapter, we demonstrated *C. jejuni* induces the UPR in human IECs. However, the mechanisms of *C. jejuni*-

induced UPR still remain to be elucidated. The aims of the work presented in this chapter were to examine whether the UPR exerts either beneficial or detrimental effects on *C. jejuni* within human IECs as well as to investigate whether *C. jejuni*-activated UPR is correlated to *C. jejuni*-induced inflammation. In addition, a potential mechanism for *C. jejuni*-mediated activation of the UPR in human IECs was investigated. Lastly, a crosstalk between the UPR activation and NOX1 expression was examined.

## 5.2. Results

### 5.2.1. *C. jejuni* viability with chemical treatments

To achieve the aims of the study presented in this chapter, human IECs were treated with different chemicals before and/or during *C. jejuni* infection. Thapsigargin is an inhibitor of SERCA resulting in disruption of $Ca^{2+}$ storage and activation of the UPR (Sehgal et al., 2017). KIRA6 inhibits kinase activity of IRE1α through interaction with the ATP-binding site of IRE1α (Mahameed et al., 2019). KIRA6 can also allosterically inhibit the RNase activity of IRE1α (Ghosh et al., 2014). STF-083010 inhibits the RNase activity of IRE1α through covalent modification (Ghosh et al., 2014). GSK2656157 is an ATP-competitive PERK inhibitor which prevents phosphorylation of PERK (Maly & Papa, 2014). ML130 is a NOD1 inhibitor (Correa et al., 2011) and BAPTA-AM is a cell-permeable $Ca^{2+}$ chelator (Collatz, Rüdel, & Brinkmeier, 1997). As human IECs were to be pre-treated with these chemicals before and/or during *C. jejuni* infection, *C. jejuni* viability during co-incubation with these chemicals was assessed. Treatment with thapsigargin, KIRA6, STF-083010, GSK2656157, ML130 or BAPTA-AM for the timepoints used in each respective assay did not significantly affect the viability of *C. jejuni* 11168H, 81-176 or 488 wild-type strains (Figure 5.1 and Figure 5.2).

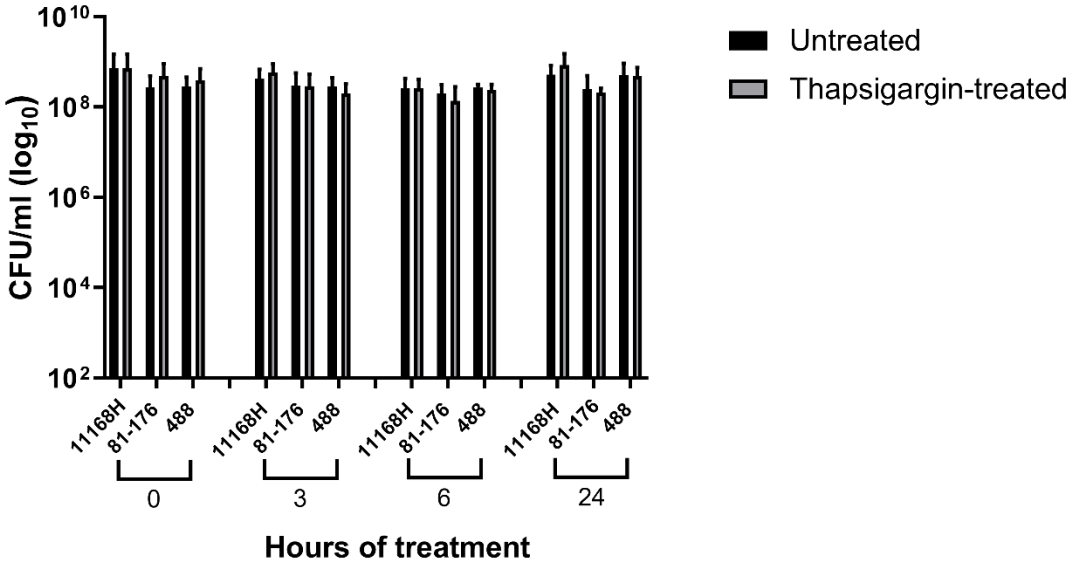


**Figure 5.1. Assessment of *C. jejuni* vability with thapsigargin treatment.** *C. jejuni* 11168H, 81-176 and 488 wild-type strains were treated with 2 μM of thapsigargin for 3-, 6- or 24-hours at 37°C in a 5% $CO_2$ incubator. CFU/ml were recorded after incubation. Three biological and three technical replicates were performed for each experiment.

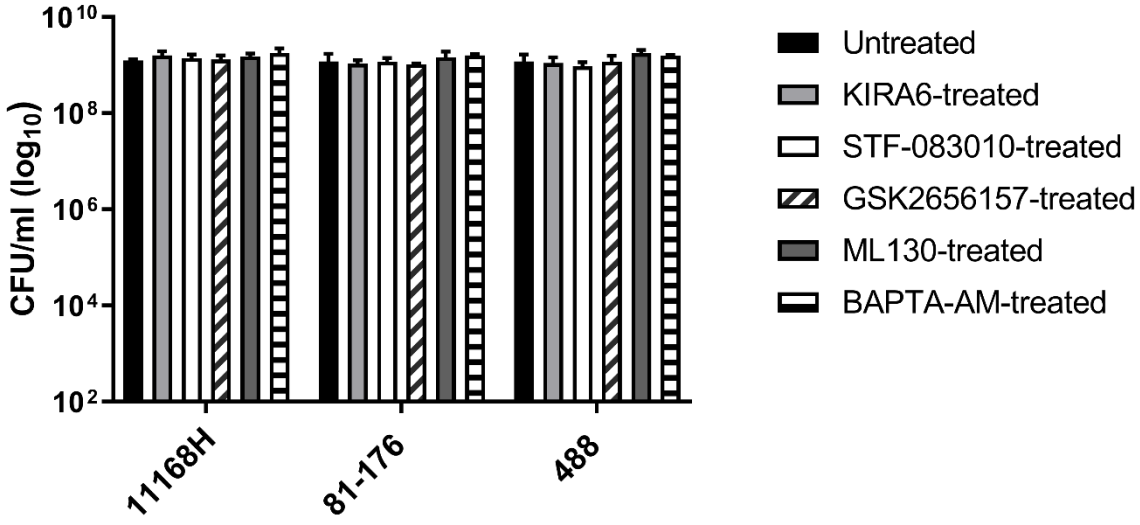


**Figure 5.2. Assessment of *C. jejuni* vability with different chemical treatments.** *C. jejuni* 11168H, 81-176 or 488 wild-type strains were treated with 3 μM of KIRA6, 3 μM of GSK2656157 or 30 μM of ML130 for 24 hours or treated with 100 μM of STF-083010 for 4 hours or 10 μM of BAPTA-AM for 1 hour at 37°C in a 5% $CO_2$ incubator. CFU/ml were recorded after incubation. Three biological and three technical replicates were performed for each experiment.

### 5.2.2. Cytotoxicity of chemical treatments on T84 and Caco-2 IECs

To investigate whether each chemical treatment exerts cytotoxicity on T84 and Caco-2 cells, a LDH assay was performed. 6 hours treatment with thapsigargin significantly increased cytotoxicity by 5.7% and 5.5% on T84 and Caco-2 cells respectively compared to untreated human IECs (Figure 5.3A and 5.3B). Treatment with KIRA6, STF-083010, GSK2656157, ML130 or BAPTA-AM did not result in any significant increases in cytotoxicity on either T84 or Caco-2 cells (Figure 5.3A and 5.3B).

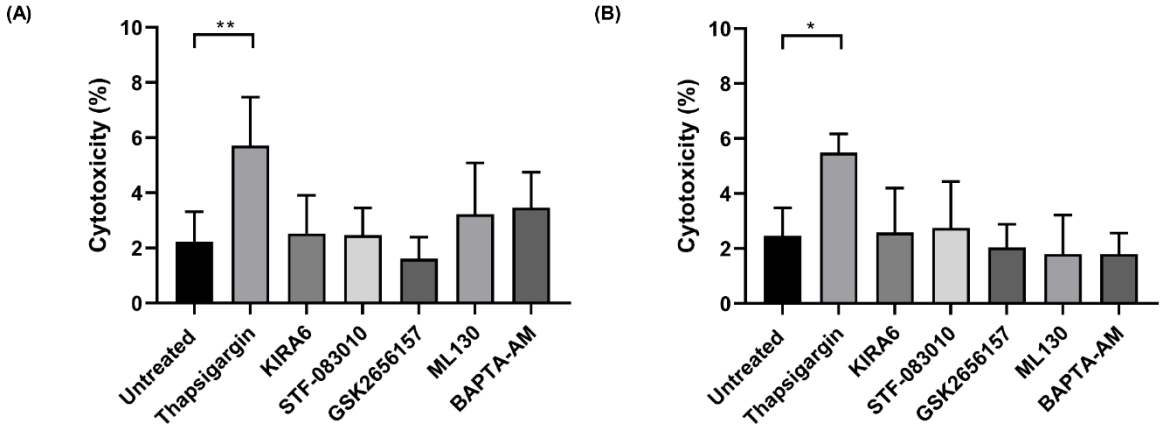


**Figure 5.3. Measurement of cytotoxicity of chemical treatment on T84 and Caco-2 cells.** (A) T84 or (B) Caco-2 cells grown in a 96-well plate were treated with 3 µM of KIRA6, 3 µM of GSK2656157 or 30 µM of ML130 for 24 hours or treated with 2 µM of thapsigargin for 6 hours, 100 µM of STF-083010 for 4 hours or 10 µM of BAPTA-AM for 1 hour at 37°C in a 5% $CO_2$ incubator. Medium from each well was then analysed using a LDH assay. Cytotoxicity (%) was calculated by using the following equation: (*C. jejuni* infected LDH activity – spontaneous LDH activity) / (maximum LDH activity – spontaneous LDH activity) x 100. Three biological and three technical replicates were performed for each experiment. Asterisks denote a statistically significant difference (* = $p < 0.05$; ** = $p < 0.01$).

### 5.2.3. Thapsigargin-induced UPR reduces *C. jejuni* intracellular survival in human IECs

The impact of thapsigargin-induced UPR on *C. jejuni* interaction, invasion and intracellular survival in human IECs was investigated. T84 and Caco-2 cells were pre-treated with thapsigargin for 6 hours, infected with *C. jejuni* and the number of interacting, invading and intracellularly surviving *C. jejuni* were analysed (Figure 5.4). Pre-treatment with thapsigargin did not affect *C. jejuni* interactions with or invasion of T84 or Caco-2 cells (Figure 5.4A, 5.4B, 5.4C and 5.4D). In contrast, intracellular survival of *C. jejuni* in T84 or Caco-2 cells was significantly reduced in thapsigargin-treated human IECs compared to untreated controls (Figure 5.4E and 5.4F). This data suggests the UPR is detrimental to *C. jejuni* intracellular survival within human IECs.

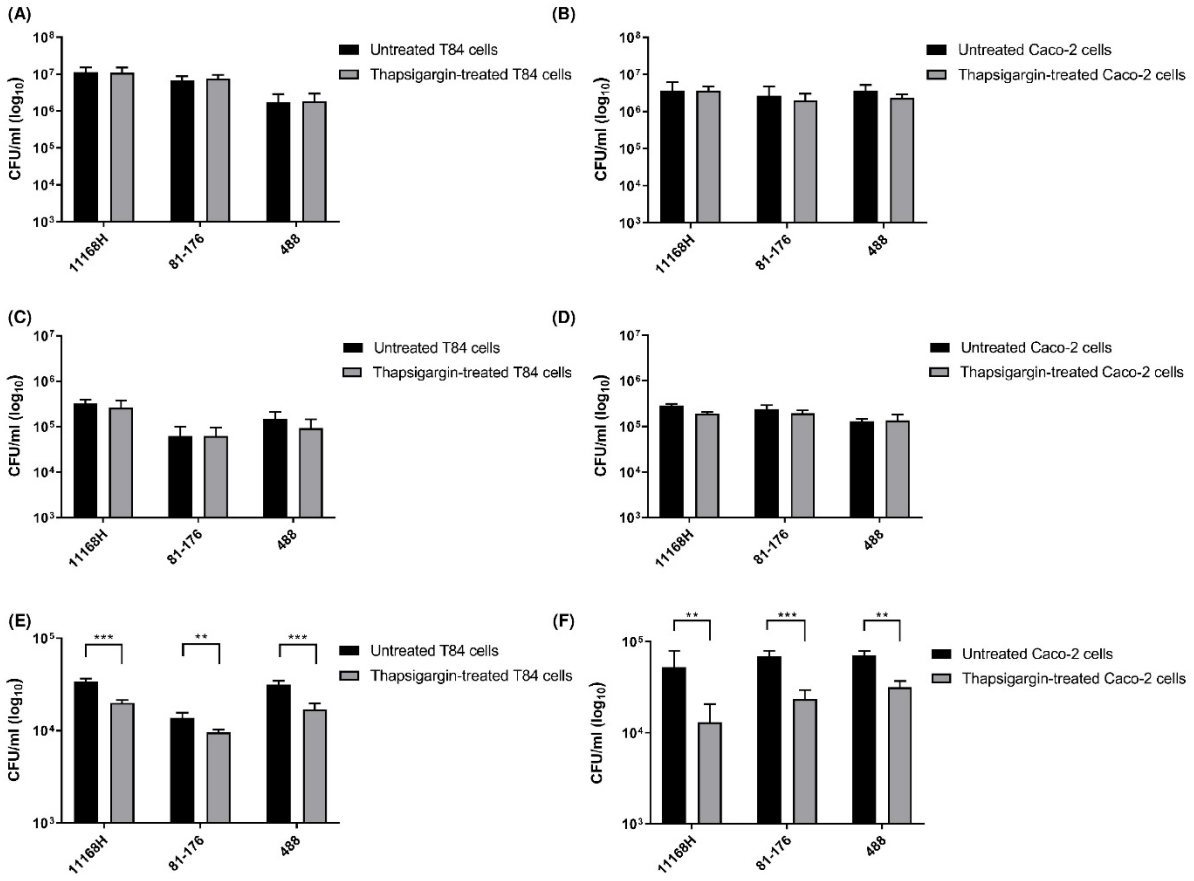


**Figure 5.4**. **The effect of thapsigargin-mediated UPR on *C. jejuni* interaction, invasion and intracellular survival.** T84 or Caco-2 cells were pre-treated with 2 µM of thapsigargin for 6 hours and infected with *C. jejuni* 11168H, 81-176 or 488 wild-type strains for 3 hours at 37°C in a 5% $CO_2$ atmosphere (MOI of 200:1). For interaction assays, (A) T84 or (B) Caco-2 cells were washed with PBS, lysed with 0.1% (v/v) Triton X-100 and CFU/ml were recorded after incubation. For invasion assays, after infection with *C. jejuni*, (C) T84 or (D) Caco-2 cells were incubated with gentamicin (150 µg/ml) for 2 hours to kill extracellular bacteria, then lysed with 0.1% (v/v) Triton X-100 and CFU/ml were recorded after incubation. For intracellular survival assays, the 2 hours gentamicin treatment as for invasion assays was followed by further incubation with gentamicin (10 µg/ml) for 18 hours, then (E) T84 or (F) Caco-2 cells were lysed with 0.1% (v/v) Triton X-100 and CFU/ml were recorded after incubation. Three biological and three technical replicates were performed for each experiment. Asterisks denote a statistically significant difference (** = $p < 0.01$; *** = $p < 0.001$).

### 5.2.4. Treatment with UPR inhibitors downregulates *C. jejuni*-mediated UPR activation in T84 and Caco-2 cells

Thapsigargin activates the UPR by inhibiting SERCA and disturbing $Ca^{2+}$ homeostasis in the ER. As an opposite approach to thapsigargin pre-treatment, human IECs were treated with different UPR inhibitors to investigate the impact of the UPR on intracellular *C. jejuni* within human IECs. qRT-PCR was performed to confirm downregulation of *C. jejuni*- and thapsigargin-mediated UPR activation in T84 and Caco-2 cells treated with the UPR inhibitors (Figure 5.5 and 5.6). Pre-treatment with GSK2656157 significantly reduced *C. jejuni*- and thapsigargin-induced *CHOP* expression in T84 and Caco-2 cells indicating impaired activation of PERK pathway (Figure 5.5A and 5.5C). In addition, pre-treatment with KIRA6 or STF-083010 significantly downregulated *C. jejuni*- and thapsigargin-induced expression of spliced *XBP1* in T84 and Caco-2 cells indicating reduced activation of IRE1α pathway (Figure 5.5B and 5.5D). Reduction of protein levels of CHOP and spliced XBP1 with the UPR inhibitors was confirmed using Western blotting (Figure 5.6).

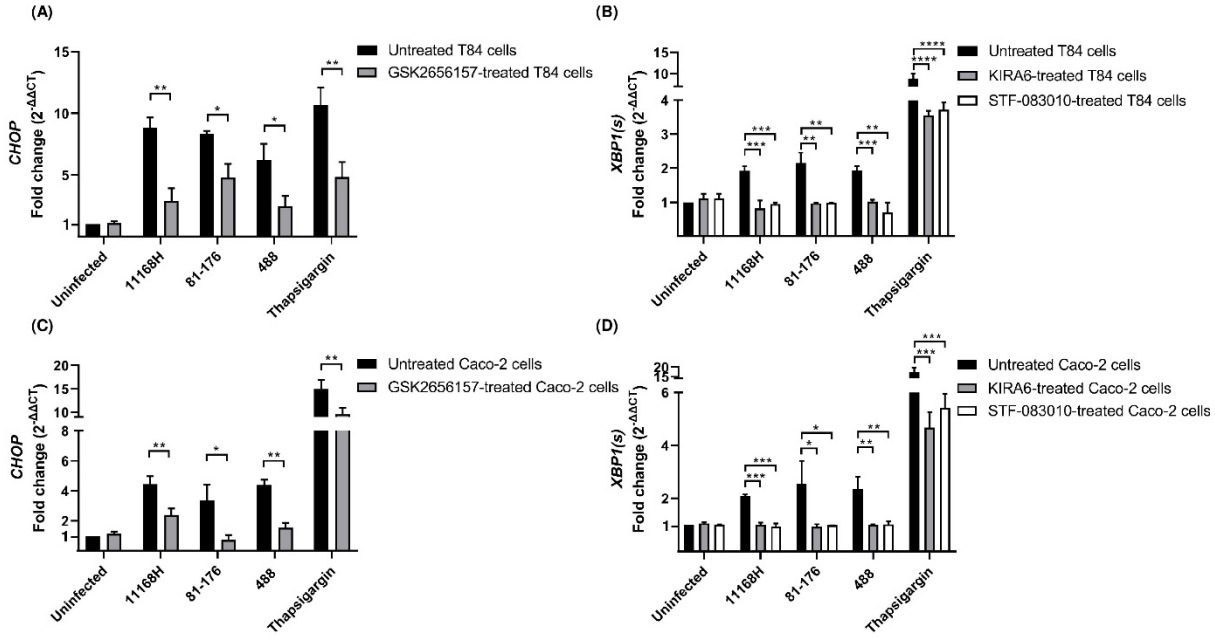


**Figure 5.5. UPR-related gene expression in T84 and Caco-2 cells treated with UPR inhibitors followed by *C. jejuni* infection.** qRT-PCR showing expression of human (A, C) *CHOP* and (B, D) spliced *XBP1* [*XBP1(s)*] in T84 or Caco-2 cells infected with either *C. jejuni* 11168H, 81-176 or 488 wild-type strains (MOI of 200:1) or treated with 2 μM of thapsigargin for 24 hours at 37°C in a 5% $CO_2$ atmosphere. Prior to *C. jejuni* infection or thapsigargin treatment, T84 and Caco-2 cells were treated with 3 μM of KIRA6, 100 μM of STF-083010 or 3 μM of GSK2656157 for 4 hours at 37°C in a 5% $CO_2$ incubator. T84 and Caco-2 cells were further treated with 3 μM of KIRA6 and 3 μM of GSK2656157 during *C. jejuni* infection or thapsigargin treatment. *GAPDH* was used as an internal control. Three biological and three technical replicates were performed for each experiment. Asterisks denote a statistically significant difference (* = $p < 0.05$; ** = $p < 0.01$; *** = $p < 0.001$; **** = $p < 0.0001$).

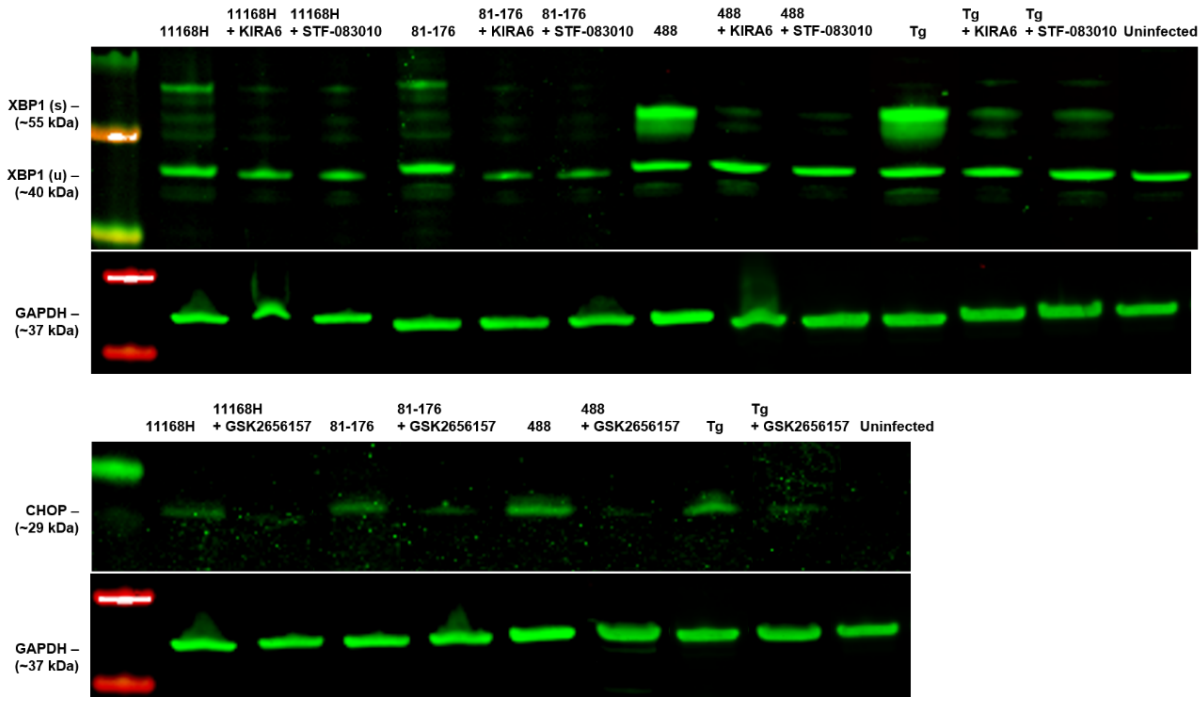


**Figure 5.6. UPR-related protein expression in T84 cells treated with UPR inhibitors followed by *C. jejuni* infection.** Western blotting showing protein levels of both spliced & unspliced forms of XBP1 [XBP1(u) & XBP1(s)] and CHOP in T84 cells infected with *C. jejuni* 11168H, 81-176 or 488 wild-type strains (MOI of 200:1) or treated with 2 µM of thapsigargin (Tg) for 24 hours at 37°C in a 5% $CO_2$ incubator. Prior to *C. jejuni* infection or thapsigargin treatment, T84 and Caco-2 cells were pre-treated with 3 µM of KIRA6, 100 µM of STF-083010 or 3 µM of GSK2656157 for 4 hours at 37°C in a 5% $CO_2$ incubator. T84 and Caco-2 cells were further treated with 3 µM of KIRA6 and 3 µM of GSK2656157 during *C. jejuni* infection or thapsigargin treatment. GAPDH was used as an internal control.

### 5.2.5. Pre-treatment with UPR inhibitors increases the number of intracellular *C. jejuni* in human IECs

Using UPR inhibitors, the impact of the UPR on the number of intracellular *C. jejuni* in human IECs was investigated (Figure 5.7). Compared to untreated human IECs, pre-treatment with KIRA6 and STF-083010 significantly increased the number of intracellular 11168H, 81-176 and 488 in T84 and Caco-2 cells indicating activation of IRE1α pathway is detrimental to intracellular *C. jejuni* survival (Figure 5.7A and 5.7B). Similarly, GSK2656157 pre-treatment significantly increased the number of intracellular 11168H, 81-176 and 488 in T84 and Caco-2 cells suggesting a detrimental impact of PERK pathway on intracellular *C. jejuni* survival in human IECs (Figure 5.7A and 5.7B).

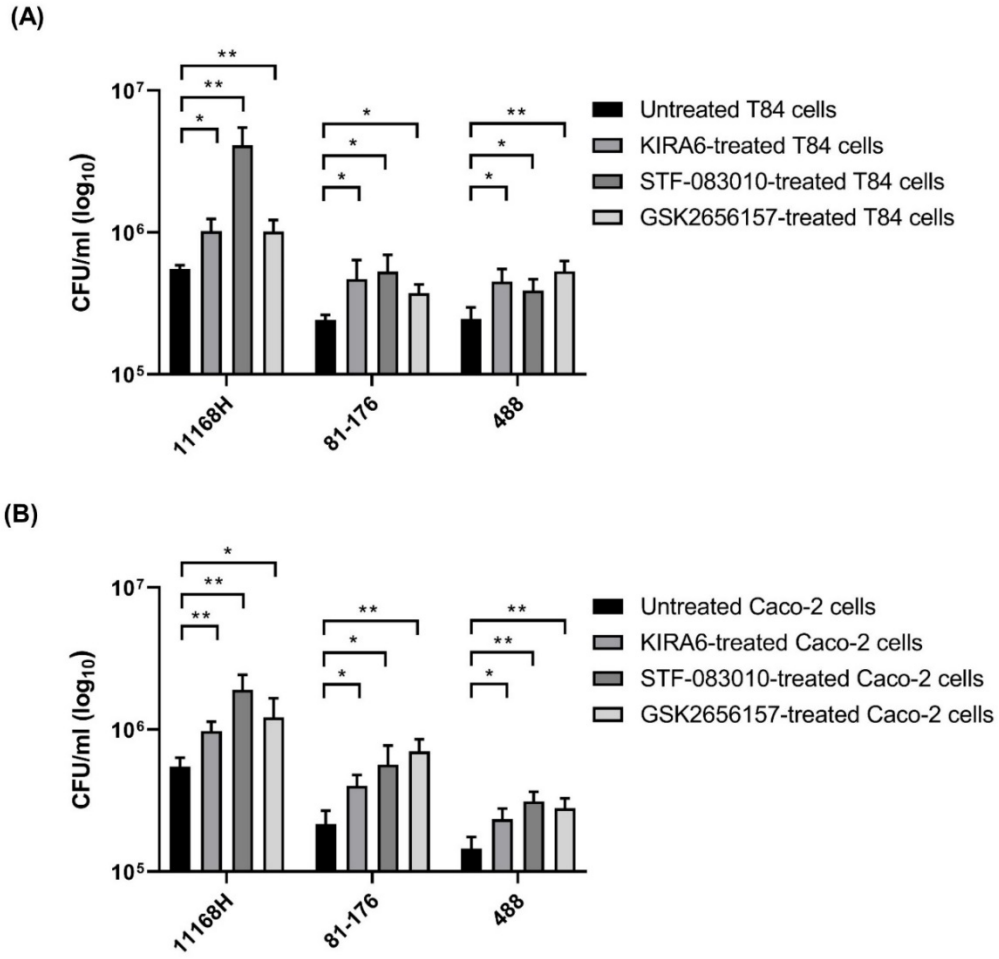


**Figure 5.7. The effect of UPR inhibitors on the number of intracellular *C. jejuni* in human intestinal epithelial cells.** (A) T84 or (B) Caco-2 cells were pre-treated with 3 µM of KIRA6, 100 µM of STF-083010 or 3 µM of GSK2656157 for 4 hours at 37°C in a 5% $CO_2$ incubator. T84 and Caco-2 cells were then infected with *C. jejuni* 11168H, 81-176 or 488 wild-type strains for 24 hours at 37°C in a 5% $CO_2$ incubator (MOI of 200:1). Human IECs were further treated with 3 µM of KIRA6 and 3 µM of GSK2656157 during *C. jejuni* infection. T84 and Caco-2 cells were washed with PBS and incubated with gentamicin (150 µg/ml) for 2 hours to kill extracellular bacteria and then lysed with 0.1% (v/v) Triton X-100 and CFU/ml were recorded after incubation. Three biological and three technical replicates were performed for each experiment. Asterisks denote a statistically significant difference (* = $p < 0.05$; ** = $p < 0.01$).

### 5.2.6. The effect of UPR inhibitors on induction of IL-8 secretion from T84 cells by *C. jejuni* wild-type strains and thapsigargin

Induction of IL-8 secretion from T84 cells by *C. jejuni* wild-type strains and thapsigargin was assessed. 11168H, 81-176 and 488 all induced IL-8 secretion at 24 hours post-infection; however, only 81-176 induced IL-8 secretion at 6 hours post-infection suggesting inter-strain variation in IL-8 induction (Figure 5.8). Thapsigargin induced IL-8 release from T84 cells at both 6- and 24-hours post-treatment indicating thapsigargin-induced UPR is implicated in inflammation (Figure 5.8). To determine if *C. jejuni*-induced inflammation is correlated to UPR activation, the effect of the UPR inhibitors on induction of IL-8 secretion from T84 cells by *C. jejuni* wild-type strains was investigated. Pre-treatment with KIRA6 and GSK2656157 significantly reduced *C. jejuni*- and thapsigargin-induced IL-8 secretion (Figure 5.9). In contrast, pre-treatment with STF-083010 significantly increased *C. jejuni*- induced IL-8 secretion whereas the treatment did not affect thapsigargin-mediated IL-8 release from T84 cells (Figure 5.9). Collectively, these data suggest there are differential effects of IRE1α inhibitors on IL-8 secretion. In addition, these observations imply that *C. jejuni*-mediated inflammation in human IECs might be linked to activation of PERK and IRE1α pathways.

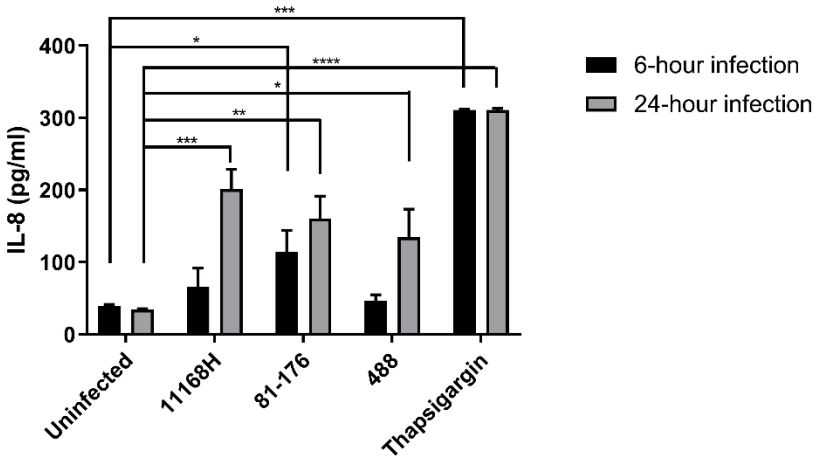


**Figure 5.8. IL-8 release from T84 cells infected with *C. jejuni* or treated with thapsigargin.** T84 cells in a 24-well plate were infected with *C. jejuni* 11168H, 81-176 or 488 wild-type strains (MOI 200:1) or treated with 2 μM of thapsigargin for 6 or 24 hours at 37°C in a 5% $CO_2$ incubator. Medium from each well was subjected to human IL-8 ELISA to measure the concentrations of IL-8. Three biological and two technical replicates were performed for each experiment. Asterisks denote a statistically significant difference (* = $p < 0.05$; ** = $p < 0.01$; *** = $p < 0.001$; **** = $p < 0.0001$).

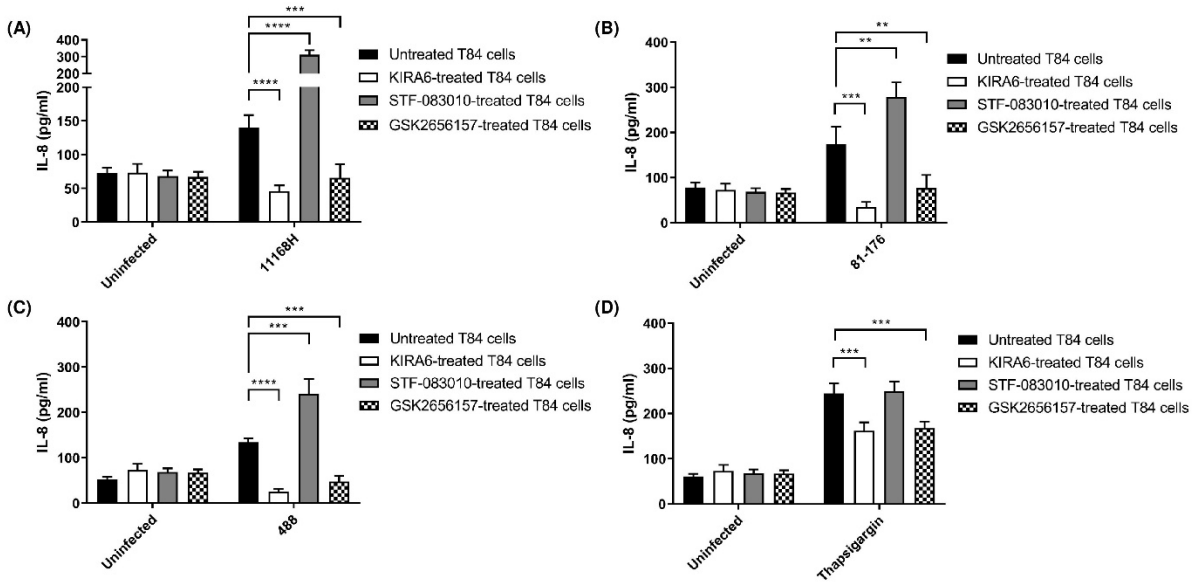


**Figure 5.9. The impact of UPR inhibitors on IL-8 release from T84 cells infected with *C. jejuni* or treated with thapsigargin.** T84 cells were pre-treated with 3 μM of KIRA6, 100 μM of STF-083010 or 3 μM of GSK2656157 for 4 hours at 37°C in a 5% $CO_2$ incubator. T84 cells were then infected with *C. jejuni* 11168H, 81-176 or 488 wild-type strains (MOI 200:1) or treated with 2 μM of thapsigargin for 24 hours at 37°C in a 5% $CO_2$ incubator. T84 cells were further treated with 3 μM of KIRA6 and 3 μM of GSK2656157 during *C. jejuni* infection. T84 cells in a 24-well plate were infected with *C. jejuni* (A) 11168H, (B) 81-176 or (C) 488 wild-type strains or treated with (D) thapsigargin for 6 or 24 hours at 37°C in a 5% $CO_2$ incubator. Medium from each well was subjected to human IL-8 ELISA to measure the concentrations of IL-8. Three biological and two technical replicates were performed for each experiment. Asterisks denote a statistically significant difference ** = $p < 0.01$; *** = $p < 0.001$; **** = $p < 0.0001$).

### 5.2.7. The NOD1 inhibitor ML130 does not affect *C. jejuni*- or thapsigargin-mediated UPR activation in human IECs

Given that *C. jejuni*-induced UPR might be responsible for inflammation in human IECs, further investigation of the relationship between NOD1 and *C. jejuni*-mediated UPR was conducted. Pre-treatment with ML130, a NOD1 inhibitor, did not affect *C. jejuni*- or thapsigargin-induced *CHOP* and spliced *XBP1* expression in either T84 or Caco-2 cells (Figure 5.10). These observations suggest *C. jejuni* and thapsigargin induce the UPR irrespective of NOD1 activity.

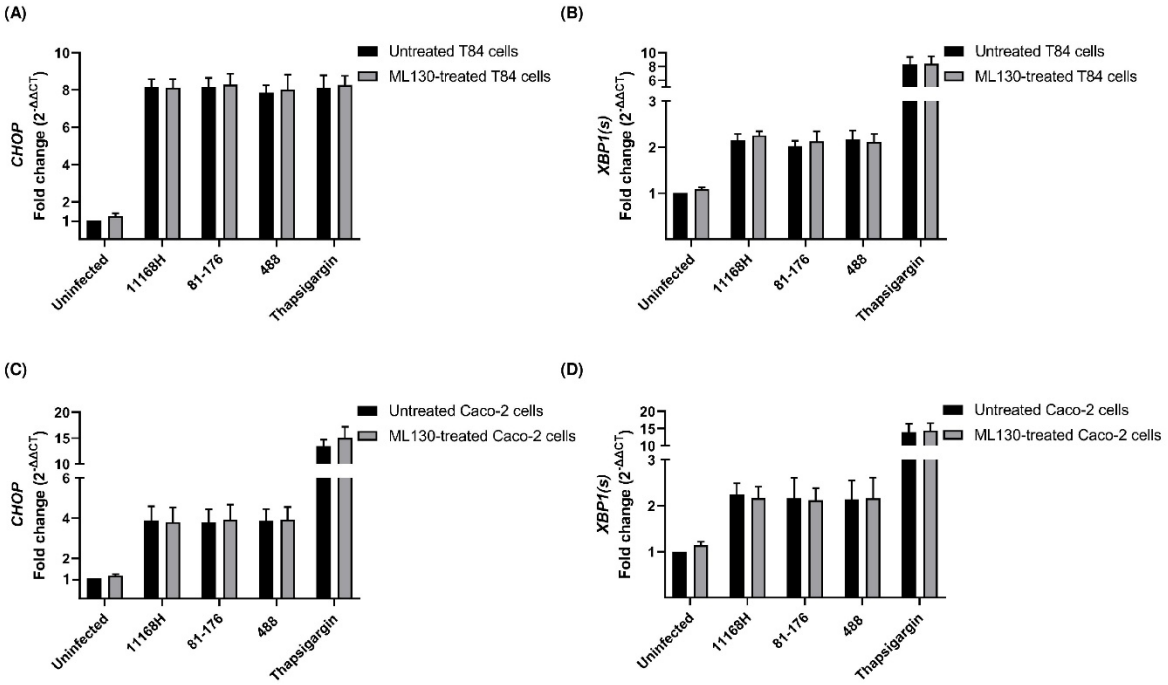


**Figure 5.10. UPR-related gene expression in T84 and Caco-2 cells treated with the NOD1 inhibitor ML130 followed by *C. jejuni* infection or thapsigargin treatment.** qRT-PCR showing expression of human (A, C) *CHOP* and (B, D) spliced *XBP1* [*XBP1(s)*] in T84 or Caco-2 cells infected with either *C. jejuni* 11168H, 81-176 or 488 wild-type strains (MOI of 200:1) or treated with 2 µM of thapsigargin for 24 hours at 37°C in a 5% $CO_2$ atmosphere. Prior to *C. jejuni* infection or thapsigargin treatment, T84 and Caco-2 cells were treated with 30 µM of ML130 for 4 hours at 37°C in a 5% $CO_2$ incubator. T84 and Caco-2 cells were further treated with 30 µM of ML130 during *C. jejuni* infection or thapsigargin treatment. *GAPDH* was used as an internal control. Three biological and three technical replicates were performed for each experiment.

### 5.2.8. The effect of ML130 on induction of IL-8 secretion from T84 cells by *C. jejuni* wild-type strains or thapsigargin

*C. jejuni* and thpaisgargin-mediated IL-8 induction from T84 cells with or without ML130 pre-treatment were measured to investigate whether ML130 affects induction of IL-8 secretion from T84 cells by *C. jejuni* wild-type strains and thapsigargin. T84 cells treated with ML130 exhibited a significant reduction in thapsigargin-mediated IL-8 secretion compared to the untreated control suggesting thapsigargin-induced IL-8 is dependent on NOD1 activity (Figure 5.11). In contrast, ML130 pre-treatment significantly increased *C. jejuni*-mediated IL-8 secretion from T84 cells (Figure 5.11). This suggests that *C. jejuni* infection involving the combined effects of different virulence determinants results in a more multifactorial response compared to thapsigargin treatment.

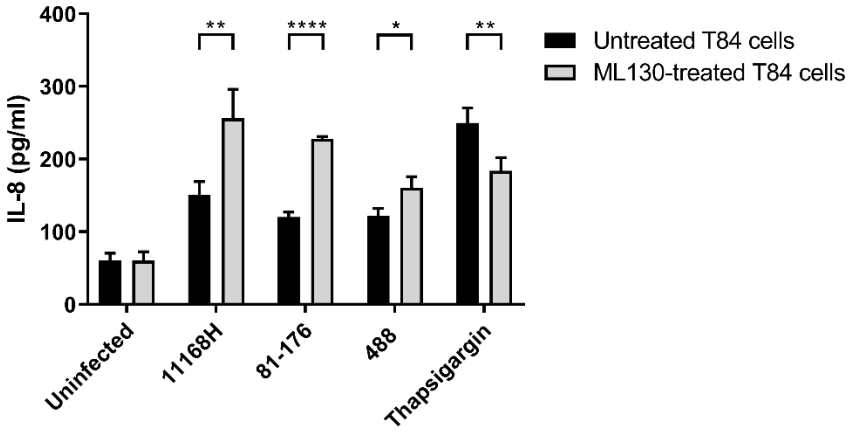


**Figure 5.11. The impact of the NOD1 inhibitor ML130 on IL-8 release from T84 cells infected with *C. jejuni* or treated with thapsigargin.** T84 cells were pre-treated with 30 μM of ML130 for 4 hours at 37°C in a 5% $CO_2$ incubator. T84 cells were then infected with *C. jejuni* 11168H, 81-176 or 488 wild-type strains (MOI of 200:1) or treated with 2 μM thapsigargin for 24 hours at 37°C in a 5% $CO_2$ incubator. T84 cells were further treated with 30 μM of ML130 for 4 hours during *C. jejuni* infection. Medium from each well was subjected to human IL-8 ELISA to measure the concentrations of IL-8. Three biological and two technical replicates were performed for each experiment. Asterisks denote a statistically significant difference (* = $p < 0.05$; ** = $p < 0.01$; **** = $p < 0.0001$).

### 5.2.9. Pre-treatment of human IECs with ML130 increases the number of intracellular *C. jejuni*

The impact of ML130 pre-treatment on intracellular *C. jejuni* survival within human IECs was investigated. Pre-treatment with ML130 significantly increased the number of intracellular *C. jejuni* in both T84 and Caco-2 cells compared to untreated human IECs indicating the antibacterial effect of NOD1 activity on intracellular *C. jejuni* within human IECs (Figure 5.12). In addition, these observations suggest the increased number of intracellular *C. jejuni* within human IECs pre-treated with ML130 might be responsible for the increased IL-8 secretion from human IECs pre-treated with ML130.

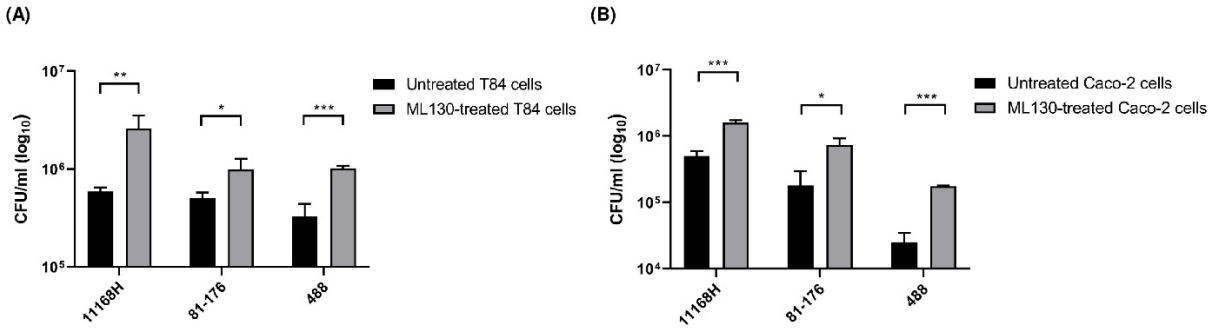


**Figure 5.12. The effect of the NOD1 inhibitor ML130 on intracellular *C. jejuni* in human intestinal epithelial cells.** (A) T84 or (B) Caco-2 cells were pre-treated with 30 µM of ML130 for 4 hours at 37°C in a 5% $CO_2$ incubator. T84 and Caco-2 cells were then infected with *C. jejuni* 11168H, 81-176 or 488 wild-type strains for 24 hours at 37°C in a 5% $CO_2$ incubator (MOI of 200:1). Human IECs were further treated with 30 µM of ML130 during *C. jejuni* infection. T84 and Caco-2 cells were washed with PBS then incubated with gentamicin (150 µg/ml) for 2 hours to kill extracellular bacteria and lysed 0.1% (v/v) Triton X-100. CFU/ml were recorded after incubation. Three biological and three technical replicates were performed for each experiment. Asterisks denote a statistically significant difference (* = $p < 0.05$; ** = $p < 0.01$; *** = $p < 0.001$).

### 5.2.10. Pre-treatment of BAPTA-AM decreases *C. jejuni*- or thapsigargin-mediated increases of intracellular $Ca^{2+}$ in T84 cells

Thapsigargin inhibits SERCA which transports $Ca^{2+}$ from the cytoplasm into the ER and consequently increases intracellular free $Ca^{2+}$ within the cytosol (Sehgal et al., 2017). Disruption of $Ca^{2+}$ homeostasis by thapsigargin induces ER stress and activates the UPR (Sehgal et al., 2017). To investigate if *C. jejuni* alters the concentration of intracellular free $Ca^{2+}$ within the cytosol, T84 cells were infected with *C. jejuni* wild-type strains and the concentration of intracellular free $Ca^{2+}$ within the cytosol was measured (Figure 5.13). All three *C. jejuni* wild-type strains and thapsigargin increased the concentration of intracellular free $Ca^{2+}$ within the cytosol compared to uninfected or untreated T84 cells (Figure 5.13). To investigate the impact of a $Ca^{2+}$ chelator BAPTA-AM on these increases in intracellular $Ca^{2+}$ resulted from *C. jejuni* infection or thapsigargin treatment, T84 cells were treated with BAPTA-AM prior to *C. jejuni* infection or thapsigargin treatment. BAPTA-AM pre-treatment significantly reduced the *C. jejuni*- or thapsigargin-mediated increases in intracellular $Ca^{2+}$ within the cytosol (Figure 5.13).

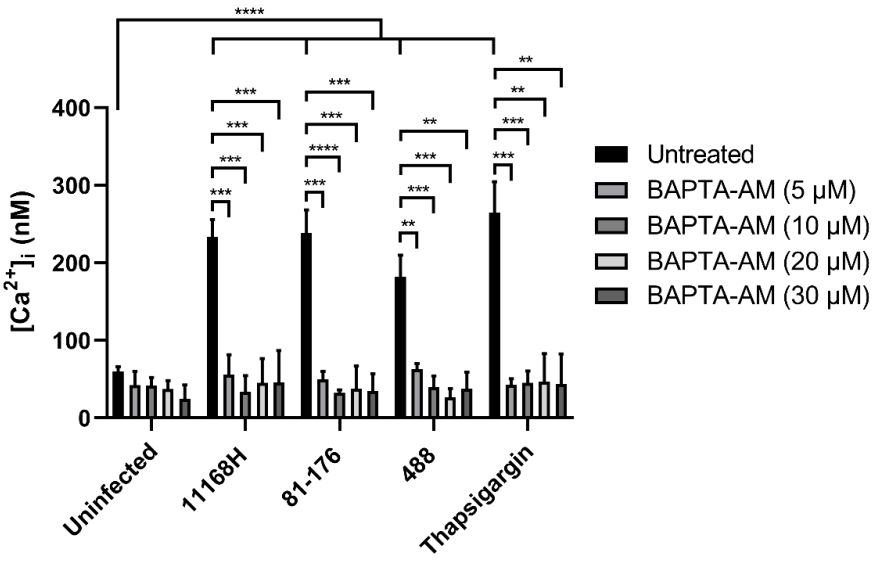


**Figure 5.13. The effect of the $Ca^{2+}$ chelator BAPTA-AM on the increases in intracellular $Ca^{2+}$ resulting from *C. jejuni* infection or thapsigargin treatment in human IECs.** T84 cells grown in a 96-well plate were pre-treated with 5, 10, 20 or 30 μM of BAPTA-AM for 1 hour at 37°C in a 5% $CO_2$ incubator. T84 cells were then infected with *C. jejuni* 11168H, 81-176 or 488 wild-type strains (MOI of 200:1) or treated with 2 μM thapsigargin for 24 hours at 37°C in a 5% $CO_2$ incubator. After infection or treatment, T84 cells were washed three times with HEPES BSS and treated with 5 μM of cell-permeable dye Fura-2, AM for 1 hour at 37°C in a 5% $CO_2$ incubator to detect intracellular $Ca^{2+}$. The two sets of fluorescence with 340 nm excitation and 510 nm emission ($\lambda_1$) and 380 nm excitation and 510 nm emission ($\lambda_2$) were recorded. Intracellular $Ca^{2+}$ concentration was calculated using the following equation; $[Ca^{2+}]_i = K_d \times Q \times (R - R_{min}) / (R_{max} - R)$. R represents the ratio of fluorescence intensity at $\lambda_1$ and $\lambda_2$. $\lambda_1$ detects $Ca^{2+}$-bound Fura-2 and $\lambda_2$ detects $Ca^{2+}$-free Fura-2. Q is the ratio of the minimal fluorescence intensity and the maximal fluorescence intensity at $\lambda_2$. $K_d$ is the dissociation of constant of the dye. The $K_d$ value of Fura-2 at 37°C is 224 nM (Grynkiewicz, Poenie, & Tsien, 1985). $R_{min}$ is the ratio of minimal fluorescence intensity at $\lambda_1$ and $\lambda_2$ and $R_{max}$ is the ratio of maximal fluorescence intensity at $\lambda_1$ and $\lambda_2$. Three biological and three technical replicates were performed for each experiment. Asterisks denote a statistically significant difference (** = $p < 0.01$; *** = $p < 0.001$; **** = $p < 0.0001$).

### 5.2.11. BAPTA-AM pre-treatment does not affect *C. jejuni*-mediated activation of PERK or IRE1α pathways in T84 cells

To investigate if *C. jejuni*-mediated UPR activation was correlated with the increase in intracellular $Ca^{2+}$ within the cytosol, T84 cells were pre-treated with BAPTA-AM to inhibit the increase in intracellular $Ca^{2+}$ by *C. jejuni* and transcriptional expression of *CHOP* and spliced *XBP1* were assessed. Pre-treatment with BAPTA-AM did not affect *C. jejuni*-mediated upregulation of *CHOP* and spliced *XBP1* (Figure 5.14A and 5.14B), suggesting that *C. jejuni*-mediated UPR activation is independent of any disruption of intracellular $Ca^{2+}$ homeostasis. In contrast, thapsigargin-mediated upregulation of *CHOP* and spliced *XBP1* was significantly reduced by BAPTA-AM pre-treatment (Figure 5.14A and 5.14B).

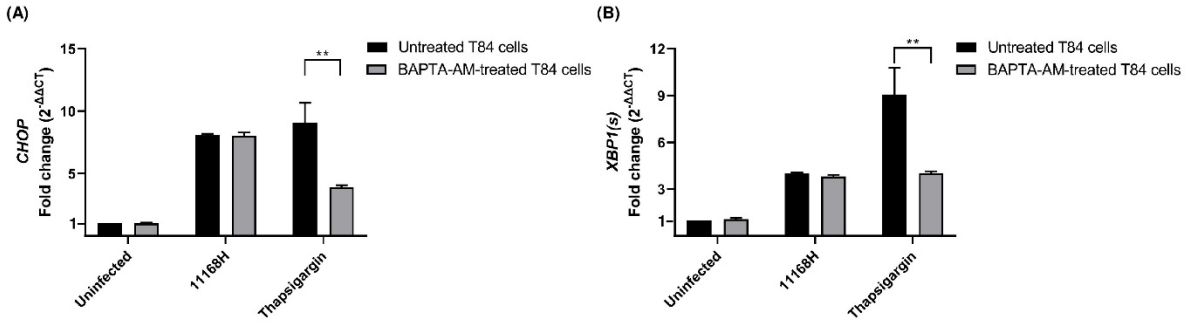


**Figure 5.14. UPR-related gene expression in T84 cells pre-treated with BAPTA-AM followed by *C. jejuni* infection or thapsigargin treatment.** qRT-PCR showing expression of human (A) *CHOP* and (B) spliced *XBP1* [*XBP1(s)*] in T84 cells infected with either *C. jejuni* 11168H wild-type strain (MOI of 200:1) or treated with 2 μM of thapsigargin for 24 hours at 37°C in a 5% $CO_2$ atmosphere. Prior to *C. jejuni* infection or thapsigargin treatment, T84 cells were pre-treated with 10 μM of BAPTA-AM for 1 hour at 37°C in a 5% $CO_2$ incubator. *GAPDH* was used as an internal control. Three biological and three technical replicates were performed for each experiment. Asterisks denote a statistically significant difference (** = $p < 0.01$).

### 5.2.12. Thapsigargin treatment downregulates *NOX1* expression

To investigate if thapsigargin-induced ER stress and the UPR affects *NOX1* expression in human IECs, T84 cells were treated with thapsigargin for 6 or 24 hours. After 6- and 24-hour treatment, thapsgiargin significantly downregulated *NOX1* expression in T84 cells (Figure 5.15A). *C. jejuni* 11168H, 81-176 and 488 wild-type strains also significantly reduced *NOX1* expression in T84 cells (Figure 5.15B). Collectively, these observations suggest that there might be a crosstalk between the UPR activation and *NOX1* expression.

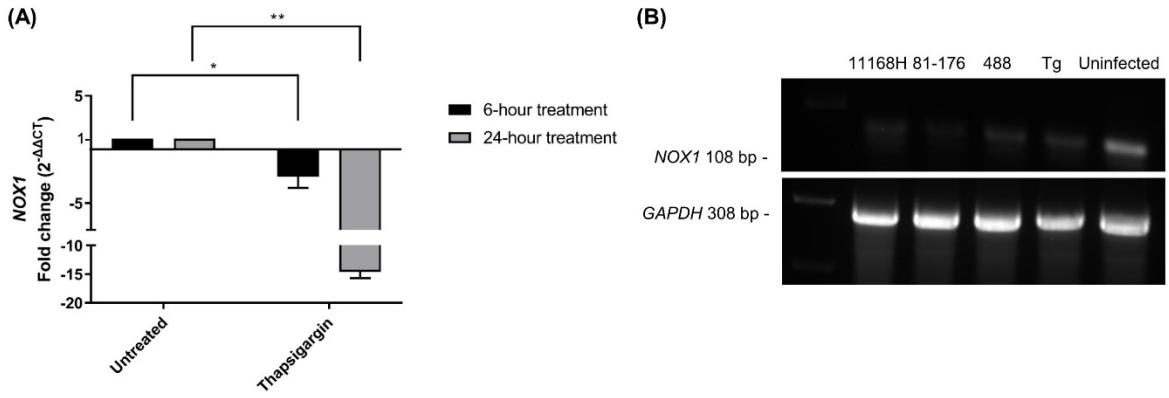


**Figure 5.15. Transcriptional levels of *NOX1* after thapsigargin treatment.** (A) qRT-PCR data showing expression of *NOX1*. T84 cells were treated with thapsigargin for 6 or 24 hours (B) RT-PCR showing expression of *NOX1* in T84 cells infected with *C. jejuni* (MOI of 200:1) or treated with thapsigargin (Tg) for 24 hours. *GAPDH* was used as an internal control. Three biological and three technical replicates were performed for each experiment. Asterisks denote a statistically significant difference (* = $p < 0.05$; ** = $p < 0.01$).

## 5.3. Discussion

### 5.3.1. UPR activation as a host defence mechanism against *C. jejuni* in human IECs

Some of the UPR-activating bacteria such as *S. enterica*, *B. melitensis* and *Chlamydia* spp. benefit from the UPR for intracellular replication (Antoniou et al., 2018; George et al., 2017; Smith et al., 2013). In contrast, as the UPR plays a role in bacterial clearance via crosstalk between UPR signalling and innate immune signalling resulting in inflammation (Choi & Song, 2019; Grootjans et al., 2016; Jean & Renée, 2014), some bacteria which replicate within host cells manipulate the UPR to evade UPR-induced host innate immunity (Alshareef, Hartland, & McCaffrey, 2021). For example, *L pneumophila* suppresses activation of the IRE1α pathway by secreting glucosyltransferases Lgt1, Lgt2 and Lgt3 which inhibit XBP1 splicing (Hempstead & Isberg, 2015; Sean & Shaeri, 2015). Unlike other UPR-modulating bacteria, the impact of the UPR on *C. jejuni* pathogenesis in human IECs has not yet been well-studied. The data presented in this chapter demonstrated that pre-activation of all three UPR pathways (PERK, IRE1α and ATF6) by treatment with thapsigargin prior to *C. jejuni* infection significantly reduced intracellular survival of *C. jejuni* within human IECs. In addition, selective inhibition of either the PERK or IRE1α pathways by different UPR inhibitors resulted in increased numbers of intracellular *C. jejuni* within human IECs. Further immunofluorescence microscopy can be used to visualise and ensure the reduction or increase of intracellular *C. jejuni* within human IECs with chemical treatments. Collectively, these results indicate each UPR pathway exhibits anti-bacterial effects on *C. jejuni* and that the UPR might be activated as a host defence mechanism. Unlike other intracellular bacteria which possess strategies to utilise or dampen UPR activation for replication inside the host cells, *C. jejuni* does not appear to replicate within human IECs but can survive within the host cell for more than 24 hours (Konkel et al., 1992; Watson & Galán, 2008). Given that the UPR is activated in human IECs upon *C. jejuni* infection and the UPR limits the number of intracellular *C. jejuni* within human IECs, it would be tempting to speculate that *C. jejuni* is not able to subvert the UPR and subsequent UPR-mediated proinflammation might inhibit *C. jejuni* replication and survival for extended periods of time within human IECs. In addition, different intracellular localisation of *C. jejuni* might be differentially affected by the UPR effects. For example, *C. jejuni* within CCVs might be more protected from the antibacterial effects of the UPR whereas *C. jejuni* free within the cytosol might be more susceptible to the UPR effects. Further investigation of the impact of the UPR-mediated inflammation on differentially localised *C. jejuni* within host cells will be necessary.

The Human IL-8 ELISA data presented in this chapter suggested *C. jejuni*-induced inflammation in human IECs is correlated with UPR activation. Significant reductions in *C. jejuni*- or thapsigargin-mediated IL-8 secretion was observed following inhibition of the IRE1α and PERK pathways by

KIRA6 and GSK2656157 respectively indicating involvement of these two UPR pathways in *C. jejuni* and thapsigargin-mediated inflammation. In innate immune signalling, TRAF2 interacts with phosphorylated IRE1α and induces inflammation by activating JNK and NF-κB signalling pathways (Hu et al., 2006; Jean & Renée, 2014). Given that STF-083010 inhibits only RNase activity but not kinase activity of IRE1α (Ghosh et al., 2014; Mahameed et al., 2019), the observation of no difference in thapsigargin-mediated IL-8 secretion in T84 cells treated with STF-083010 might be because IRE1α can still undergo autophosphorylation and can be recognised by TRAF2 resulting in inflammation. This result also indicates thapsigargin-mediated inflammation is dependent on the kinase activity of IRE1α rather than RNase activity which is consistent with data from a previous study (Keestra-Gounder et al., 2016). Intriguingly, data presented in this chapter also showed STF-083010 increased *C. jejuni*-mediated IL-8 secretion. There might be other cellular effects of STF-08310 on immune signalling in the context of *C. jejuni* infection. It is also possible that increased numbers of intracellular *C. jejuni* resulted from STF-083010 pre-treatment might lead to enhanced *C. jejuni*-induced IL-8 secretion. Unlike KIRA6 and GSK2656157, STF-083010 might produce an environment where a correlation between the *C. jejuni* bacterial burden within host cells and IL-8 secretion is significant. Further investigation is necessary to determine any additional effects of STF-083010 on immune signalling during *C. jejuni* infection.

In canonical signalling of NOD1, intracellular NOD1 detects bacterial peptidoglycan, recruits RIPK2 and interacts with TRAF2 for activation of NF-κB and JNK signalling pathways to induce proinflammation (Caruso et al., 2014; Heim, Stafford, & Nachbur, 2019). In contrast, non-canonical signalling of NOD1 is associated with IRE1α activation without any need for binding of peptidoglycan (Keestra-Gounder et al., 2016; Kuss-Duerkop & Keestra-Gounder, 2020). Upon UPR activation, phosphorylated IRE1α is detected by TRAF2 and TRAF2 interacts with NOD1 for NF-κB activation (Keestra-Gounder et al., 2016; Kuss-Duerkop & Keestra-Gounder, 2020). A previous study demonstrated there are no significant differences in thapsigargin-stimulated UPR activation in bone marrow-derived macrophages (BMDM) between NOD1/2$^{-/-}$ and wild-type mice (Keestra-Gounder et al., 2016). Consistent with the data in this previous study (Keestra-Gounder et al., 2016), qRT-PCR data presented in this chapter indicated NOD1 activity is not necessary for *C. jejuni*- and thapsigargin-mediated UPR activation in human IECs. However, NOD1 inhibition with ML130 pre-treatment reduced thapsigargin-mediated IL-8 secretion indicating thapsigargin-induced inflammation is dependent on NOD1 activity as demonstrated in the previous study (Keestra-Gounder et al., 2016). This observation also supports the concept that thapsigargin-induced inflammation is dependent on kinase activity of IRE1α so that TRAF2 recognises phosphorylated IRE1α and further interacts with NOD1 for inflammatory response (Keestra-Gounder et al., 2016; Kuss-Duerkop & Keestra-Gounder, 2020).

A previous study reported *C. jejuni* is recognised by NOD1 resulting in induction of IL-8 and human β-defensin 2 expression in Caco-2 cells (Zilbauer et al., 2007). NOD1 siRNA transfected Caco-2 cells exhibited an increased number of intracellular *C. jejuni* within Caco-2 cells compared to negative controls (Zilbauer et al., 2007). The data presented in this chapter also demonstrated that inhibition of NOD1 with ML130 pre-treatment resulted in enhanced numbers of intracellular *C. jejuni* within both T84 and Caco-2 cells, confirming the antibacterial effect of NOD1 on *C. jejuni*. In addition, even though ML130 pre-treatment reduced thapsigargin-induced IL-8 secretion, the pre-treatment increased *C. jejuni*-mediated IL-8 secretion from T84 cells which might be due to the increased numbers of intracellular *C. jejuni* within human IECs pre-treated with ML130. These observations also suggest that different virulence determinants are involved in *C. jejuni* infection resulting in more multifactorial effects compared to thapsigargin treatment. In contrast, Zilbauer et al. demonstrated NOD1 siRNA transfected cells exhibited reduced *C. jejuni*-induced IL-8 expression in Caco-2 cells compared to negative controls (Zilbauer et al., 2007). Such differing data in IL-8 secretion may be due to differences in the consequent physiological conditions which NOD1 siRNA and ML130 pre-treatment produce. NOD1 siRNA is designed to knockdown expression of *NOD1* (Zilbauer et al., 2007). The first step of siRNA-mediated knockdown of gene expression is introduction of long double-stranded RNA with 2 nucleotide 3' end overhangs into target cells (Dana et al., 2017). After internalisation, double-stranded RNA accumulates within the cytoplasm and then interacts with an RNase termed Dicer which cleaves long double-stranded RNA into short siRNA. siRNA then forms a complex with RNA-induced silencing complex (RISC). Separation of siRNA strands occurs and one strand with a less stable 5' end remains within RISC. The single-stranded siRNA within RISC binds to the complementary sequence of the target mRNA which is then degraded by an endonuclease termed Argonaute-2 of RISC resulting in reduced translation of the target mRNA (Dana et al., 2017).

In contrast to NOD1 siRNA transfection which degrades of *NOD1* mRNA, ML130 does not affect translation of NOD1 mRNA (Correa et al., 2011). ML130 directly interacts with NOD1 and may induce conformational changes which then interrupt intracellular trafficking of NOD1. Correa et al. demonstrated ML130 pre-treatment increases the localisation of NOD1 near the plasma membrane and reduces recruitment of RIPK2 (Correa et al., 2011). Alteration of the localisation of NOD1 and the downstream adapter protein RIPK2 might affect fine-tuned cellular immune system resulting in increased *C. jejuni*-mediated IL-8 secretion in response to increased bacterial burden within host cells. We speculate that increased NOD1 near the plasma membrane might enhance detection of invading *C. jejuni* in human IECs pre-treated with ML130. However, reduced RIPK2 recruitment might impair further downstream signalling of NOD1-induced inflammation resulting in reduced expression of antimicrobial peptides. Due to impaired antibacterial effects of NOD1, the number of intracellular *C.*

*jejuni* increased. A previous study demonstrated that binding of NOD1 ligand synergistically induces TLR-induced IL-8 production (Uehara et al., 2005). With ML130 pre-treatment, the increased detection of *C. jejuni* by NOD1 might synergistically induce TLR-mediated IL-8 secretion. Further investigation is required to determine the full cellular effects of ML130 on *C. jejuni*-induced inflammation in human IECs. In addition, given that the previous study demonstrated reduced *C. jejuni*-induced IL-8 expression with NOD1 siRNA transfection suggesting NOD1-dependent inflammation with *C. jejuni* infection (Zilbauer et al., 2007), it is also possible that UPR-induced inflammation with *C. jejuni* infection might be dependent on NOD1. Further works using NOD1 siRNA are necessary to investigate if NOD1 is necessary for UPR-mediated inflammation in human IECs infected with *C. jejuni*.

### 5.3.2. Possible mechanisms of *C. jejuni*-mediated UPR activation

$Ca^{2+}$ homeostasis within the ER is strictly regulated by $Ca^{2+}$-binding ER chaperones, SERCA pumps and $Ca^{2+}$ channels (Carreras-Sureda, Pihán, & Hetz, 2018). SERCA pumps import $Ca^{2+}$ into the ER and $Ca^{2+}$ channels release $Ca^{2+}$ into the cytosol (Carreras-Sureda, Pihán, & Hetz, 2018). As ER chaperones require a high concentration of $Ca^{2+}$ for proper folding of proteins entering the ER, disruption of $Ca^{2+}$ homeostasis within the ER leads to an increase in misfolded proteins within the ER resulting in activation of the UPR (Daverkausen-Fischer & Pröls, 2022). Some UPR-activating bacteria have been shown to induce ER stress by causing the release of $Ca^{2+}$ from the ER into the cytosol (H. H. Choi et al., 2010; Gekara et al., 2007; Grover et al., 2018; Pillich et al., 2012). A pore-forming toxin listeriolysin O secreted by *Listeria monocytogenes* induces $Ca^{2+}$ mobilisation from the ER into the cytosol in $Ca^{2+}$ channel-dependent and -independent manner (Gekara et al., 2007). In the $Ca^{2+}$ channel-independent mechanism, listeriolysin O impairs the ER membrane and induces $Ca^{2+}$ release from the store leading to activation of the UPR in murine bone marrow-derived mast cells (Gekara et al., 2007; Pillich et al., 2012). In addition, *Mycobacterium tuberculosis* secretes ESAT-6 protein via the Type VII secretion system (T7SS) and this pore-forming protein increases intracellular free $Ca^{2+}$ and activates the UPR in human alveolar epithelial A549 cells (H. Choi et al., 2010). A TLR4 ligand of *M. tuberculosis* antigen Rv0297 is also implicated in localisation of the ER, increase of intracellular free $Ca^{2+}$ and induction of the UPR in RAW 264.7 murine macrophage cells (Grover et al., 2018).

A previous study demonstrated an increase in cytosolic free $Ca^{2+}$ in INT407 cells infected with 81-176 via an unknown mechanism (Hu, Raybourne, & Kopecko, 2005). Consistent with this previous study (Hu, Raybourne, & Kopecko, 2005), data presented in this chapter showed that *C. jejuni* 11168H, 81-176 and 488 wild-type strains increased intracellular free $Ca^{2+}$ within the cytosol. Data presented in this chapter also showed the intracellular $Ca^{2+}$ increase resulting from *C. jejuni* infection was similar to the thapsigargin-induced increase in intracellular free $Ca^{2+}$. Thapsigargin-mediated activation of PERK and

IRE1α pathways was reduced by BAPTA-AM pre-treatment suggesting thapsigargin-induced UPR is dependent on $Ca^{2+}$ release. However, unlike thapsigargin, $Ca^{2+}$ release was not the cause of the UPR activation in 11168H-infected human IECs. In the previous chapter, we demonstrated 11168H and 488 induce activation of the PERK and IRE1α pathways but not the ATF6 pathway whereas thapsigargin activates all three UPR pathways. Collectively, the data indicates there might be other mechanisms for UPR activation by *C. jejuni* which are distinct from the mechanism of thapsigargin-induced UPR. Furthermore, given that 81-176 activates all three UPR pathways showing inter-strain variation in activation of the ATF6 pathway, it is also possible that 81-176 might in part activate the UPR via $Ca^{2+}$ release. Further experiments using 81-176 are needed to investigate whether 81-176-induced UPR activation is due in part to $Ca^{2+}$ release and whether the 81-176 T4SS encoded in the pVir plasmid is involved in the increase of intracellular free $Ca^{2+}$ (Bacon et al., 2000, 2002).

As $Ca^{2+}$ depletion increases misfolded proteins within the ER lumen and generally activates all three UPR pathways (Daverkausen-Fischer & Pröls, 2022), it is tempting to speculate that *C. jejuni*-mediated UPR activation may not be due to general stimuli which activate all three UPR pathways (PERK, IRE1α and ATF6). Consistent with this speculation, qRT-PCR data presented in the previous chapter also suggested that different *C. jejuni* virulence determinants are responsible for activation of each of the three UPR pathways. In addition, it is possible that *C. jejuni* might activate upstream cellular pathways which are directly or indirectly linked to each UPR pathway. For example, TLR2 and TLR4 stimulation by ligand binding in murine J774 macrophages leads to activation of the IRE1α pathway only but not the PERK and ATF6 pathways (Martinon et al., 2010). Another study demonstrated BMDM generated from $TLR2^{-/-}$ mice did not show differences in thapsigargin-mediated activation of the PERK pathway. However, BMDM obtained from $TLR4^{-/-}$ mice exhibited reduced activation of both the PERK and IRE1α pathways suggesting a connection between ER stress and TLR signalling (Mahadevan et al., 2011). Given that TLR2 and TLR4 detect *C. jejuni* and induce proinflammation (Friis, Keelan, & Taylor, 2009; Rathinam et al., 2009), further work is needed to investigate whether mechanisms of *C. jejuni*-mediated UPR activation in human IECs are related to TLR signalling.

### 5.3.3. The UPR activation and *NOX1* expression

ROS can be produced in the ER during protein folding processes (Cao & Kaufman, 2014). Protein disulphide isomerases (PDI) and ER oxidoreductase 1 (ERO1) are involved in protein disulphide bond formation in the ER lumen. During protein folding process, electrons are transferred from PDI to ERO1 and then to $O_2$ generating $H_2O_2$. An antioxidant in the ER, glutathione is involved in reduction of disulphide bonds through oxidisation to glutathione disulphide (Cao & Kaufman, 2014). As protein folding is a redox sensitive process, perturbation in redox homeostasis results in an increase of

misfolded proteins in the ER lumen and ER stress followed by UPR activation (Jean & Renée, 2014). As NOX is a major ROS producer in eukaryotic cells, studies have investigated a crosstalk between NOX and the UPR (Bhattarai et al., 2021; Laurindo, Araujo, & Abrahao, 2014). Previous studies have observed that NOX4 is upregulated during ER stress in specific cell types and UPR activation by tunicamycin is dependent on NOX4-mediated ROS production (Pedruzzi et al., 2004; Santos et al., 2009; Wu et al., 2010). NOX2 has also been implicated in the UPR (Li et al., 2010; Martinon et al., 2010). ER stress inducers such as cholesterol and 7-ketocholesterol induce NOX2 expression and ROS production. Cholesterol- and 7-ketocholesterol-mediated CHOP induction and TLR2- and TLR4-mediated XBP1 splicing are dependent on NOX2 in macrophages (Li et al., 2010; Martinon et al., 2010). These studies indicate that signalling between the UPR and NOX is bidirectional.

A previous study demonstrated that tunicamycin-induced ER stress significantly reduced *NOX1* expression in intestinal goblet cells (Tréton et al., 2014). In accordance with this previous study (Tréton et al., 2014), the data presented in this chapter shows that thapsigargin treatment downregulates *NOX1* expression in T84 cells. Considering that *C. jejuni* activates the UPR and downregulates NOX1 expression in human IECs as demonstrated in the previous chapters, the results suggest that thapsigargin- and tunicamycin-induced UPR results in downregulation of NOX1 and that *C. jejuni*-mediated downregulation of NOX1 might be due to UPR activation or other unknown mechanisms. Further investigation is required to elucidate mechanism(s) of *C. jejuni*-mediated downregulation of NOX1 and signalling between NOX1 and thapsigargin-induced UPR in human IECs.

## 5.4. Conclusion

In this chapter, the effect of the UPR activation on *C. jejuni* pathogenesis in human IECs was investigated. Data presented suggests that the UPR is activated as a host defence mechanism and exerts an antibacterial effect on intracellular *C. jejuni* within human IECs. This study also demonstrated that the *C. jejuni*-induced UPR was independent of NOD1 activity. This raises the possibility that *C. jejuni*-activated PERK and IRE1α pathways may be linked to *C. jejuni*-induced inflammation in human IECs. In addition, this study demonstrated *C. jejuni*-mediated UPR activation is independent of $Ca^{2+}$ release from the ER and suggesting that TLR2 and TLR4 detection of *C. jejuni* might be involved in *C. jejuni*-mediated UPR activation. This study also revealed thapsigargin treatment reduces *NOX1* expression in human IECs. Further investigation is required to determine the detailed mechanisms of *C. jejuni*-mediated activation of each UPR pathway and a crosstalk between the UPR activation and NOX1 expression in human IECs.

# CHAPTER SIX: Final Discussion

## 6.1. Summary

*C. jejuni* is classified as a microaerophilic bacterium, but is omnipresent in the environment and identified in various hosts emphasising the complexity of bacterial survival strategies possessed by this bacterium (Gundogdu et al., 2016). *C. jejuni* possesses distinctive features such as ability to evade the TLR5 surveillance system due to amino acid residues present in the *C. jejuni* flagella which exhibit reduced interaction with TLR5 and the lack of the classical stress response systems found in other enteric bacterial pathogens (Elmi et al., 2021). Bacterial pathogens have evolved the ability to establish successful infection of host cells in part by manipulating host cellular pathways to avoid host defence responses (Escoll et al., 2016). *C. jejuni* also modulates host defence systems to enhance bacterial fitness within host cells (Konkel et al., 1992; Watson & Galán, 2008). After internalisation into host cells, *C. jejuni* resides within CCVs which avoid fusion with lysosomes, protecting the bacteria from lysosomal degradation (Konkel et al., 1992; Watson & Galán, 2008). The aim of this study was to investigate *C. jejuni* modulation of the host defence machineries in human IECs involving NOX1-mediated ROS production and the UPR.

This study has demonstrated *C. jejuni*-mediated differential modulation of intracellular and extracellular ROS production from T84 and Caco-2 cells via downregulation of NOX1 expression (Figure 6.1). Reduction in NOX1 expression by *C. jejuni* was shown to be linked to a decrease in Rac1 activation at later infection time points. NOX1 inhibition experiments with DPI treatment and siRNA transfection demonstrated that NOX1 is necessary for *C. jejuni* pathogenesis in human IECs. These results suggest fine-tuned modulation of NOX1 expression by *C. jejuni* to ensure bacterial adherence and invasion to host cells during the early stages of infection. *C. jejuni* subsequently downregulates NOX1 to benefit from ROS reduction for enhanced survival during later stages of infection. Experiments with DPI treatment and NOX1 siRNA transfection showed reduced fibronectin expression with NOX1 inhibition, suggesting *C. jejuni* adherence and invasion may require NOX1 expression at earlier infection time points, given the well-established role of fibronectin in the initial stages of *C. jejuni* interaction with host cells (Eucker & Konkel, 2012; Konkel et al., 2020). In addition, downregulation of NOX1 expression by thapsigargin as well as *C. jejuni* indicated there might be a potential link between NOX1 and the UPR. Further mutation work could identify potential bacterial virulence determinants which are responsible for NOX1 modulation in human IECs.

Activation of the UPR in human IECs by *C. jejuni* wild-type strains was investigated (Figure 6.1). 11168H, 81-176 and 488 wild-type strains activated the PERK and IRE1α pathways in T84 and Caco-

2 cells whereas only 81-176 activated the ATF6 pathway in T84 cells suggesting both cell line- and strain-specific activation of the ATF6 pathway. To investigate the role of individual *C. jejuni* virulence determinants on UPR activation in human IECs, a *C. jejuni* 11168H *cdtABC* operon mutant was constructed and phenotypic assays were performed along with 11168H *cdtA*, *kpsM*, *flaA*, *htrA*, *cadF*, *flpA* mutants and a 11168H *cadF flpA* double mutant. Subsequently, activation of the UPR by individual mutants was investigated. The results indicated that live *C. jejuni* cells are required for UPR activation and that *C. jejuni* capsular polysaccharide, flagella and FlpA have a role in PERK pathway activation. Complementation works are required to confirm the phenotypes of the mutants in PERK pathway activation. In contrast, no significant differences in activation of the IRE1α pathway were observed with any of the 11168H mutants used in this study. Future studies should aim to identify potential bacterial virulence determinants which can activate the IRE1α pathway.

Next, the impact of the UPR activation on *C. jejuni* pathogenesis in human IECs was investigated (Figure 6.1). Experiments with thapsigargin and UPR inhibitors indicated that the UPR is activated as a host defence mechanism against *C. jejuni*, exerting an antibacterial effect on intracellular *C. jejuni* within human IECs. Cellular imaging analysis such as immunofluorescence microscopy can be further used to confirm the changes in the number of *C. jejuni* within human IECs with thapsigargin and UPR inhibitors. A NOD1-independent mechanism of *C. jejuni*-mediated UPR activation was demonstrated and *C. jejuni* activation of the PERK and IRE1α pathways were shown to be linked to *C. jejuni*-induced inflammation in human IECs. Further studies incorporating small animal models would provide better insight to the relationship between *C. jejuni*-mediated UPR activation and development of inflammatory diarrhoea. In addition, *C. jejuni*-mediated UPR activation is independent of $Ca^{2+}$ release from the ER, indicating that the mechanism of *C. jejuni*-mediated UPR activation is distinct from thapsigargin-mediated UPR activation. Lastly, the study demonstrated thapsigargin treatment significantly downregulates *NOX1* expression indicating that further investigation of the ER communication with NOX1 complex is necessary.

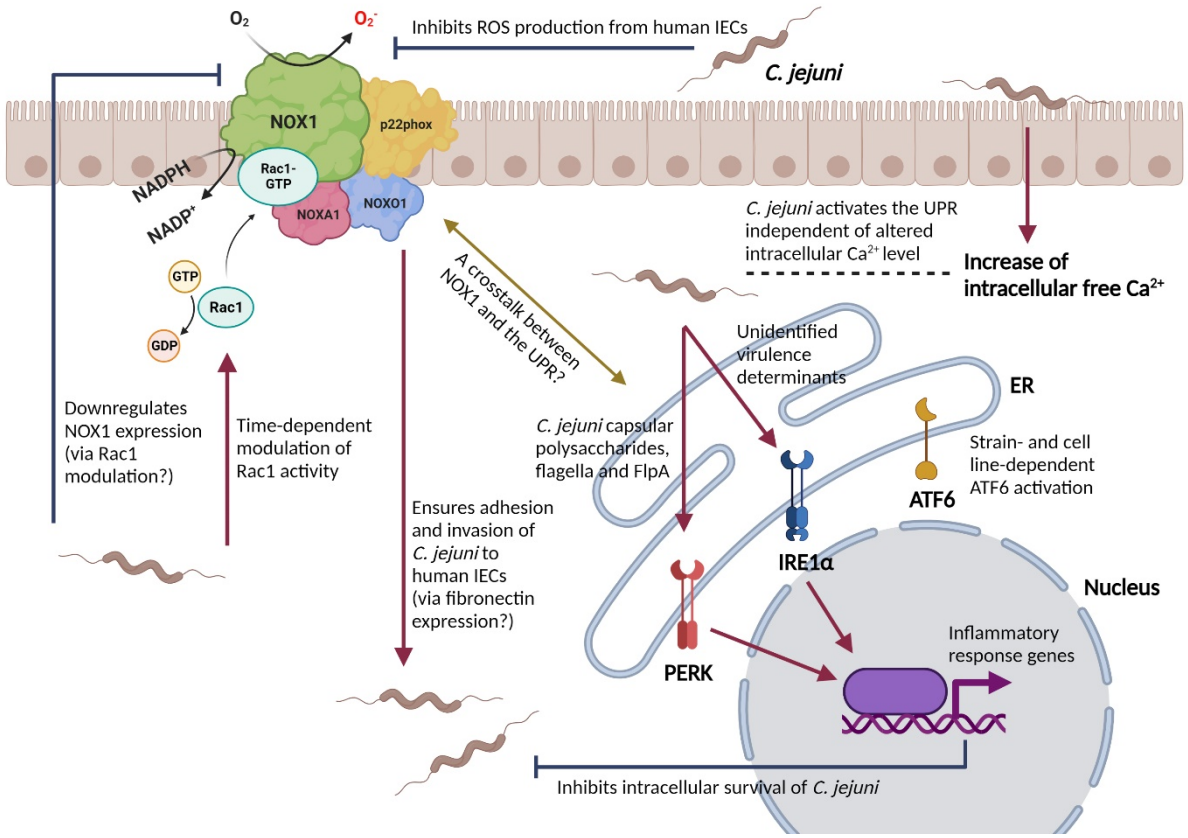


**Figure 6.1. Graphical summary of the main findings in this study.** *C. jejuni*-mediated modulation of extracellular ROS production in human IECs is strain-dependent at earlier infection time point. Whereas, all *C. jejuni* strains used in this study reduce both intracellular and extracellular ROS production in human IECs at later infection time point by downregulating NOX1 expression. *C. jejuni*-mediated modulation of NOX1 expression seems to be associated with time-dependent modulation of Rac1 activity by *C. jejuni*. NOX1 is necessary for adhesion and invasion of *C. jejuni* to human IECs at earlier infection time point. NOX1-dependent fibronectin expression might be involved in NOX1-dependent adhesion and invasion of *C. jejuni* to human IECs. All *C. jejuni* strains used in this study activate the PERK and IRE1α pathways and ATF6 pathway activation exhibits inter-strain variation. *C. jejuni* capsular polysaccharides, flagella and FlpA are shown to be responsible for PERK pathway activation. *C. jejuni*-mediated UPR activation is independent of increase in intracellular free $Ca^{2+}$ in human IECs. The UPR is activated as a host defence mechanism against *C. jejuni* by exerting an antibacterial effects such as inflammation. *C. jejuni*-mediated UPR activation is closely linked to *C. jejuni*-induced inflammation in human IECs. Created with BioRender.com

## 6.2. Future work

### 6.2.1. *C. jejuni*-mediated NOX2 expression in human macrophages and the UPR

Unlike IECs, macrophages engulf and kill microbial pathogens via rapid generation of ROS termed the oxidative burst which is regulated by NOX2 (Paiva & Bozza, 2014). In contrast to NOX1 which is mainly expressed in IECs, NOX2 is mainly found in immune cells (Brandes, Weissmann, & Schröder, 2014). *C. jejuni* can survive within human IECs by avoiding fusion with lysosomes but not within macrophages (Watson & Galán, 2008). Differential regulation of NOX1 and NOX2 might be linked to *C. jejuni* survival in different host cell types. NOX2 modulation in *C. jejuni*-infected human macrophages should also be investigated to understand the impact of NOX2 modulation on *C. jejuni* survival in human macrophages. A previous study demonstrated ER stress inducers upregulate *NOX2* expression along with ROS production in murine macrophages (Li et al., 2010). In addition, deficiency of NOX2 in murine macrophages resulted in reduced TLR2- and TLR4-mediated activation of IRE1α pathway, suggesting bidirectional signalling between the UPR and NOX2 (Martinon et al., 2010). Further experiments using UPR inhibitors and siRNA transfection targeting NOX2 and UPR-related components will be necessary to investigate crosstalk between the UPR activation and NOX2 modulation in human macrophages infected with *C. jejuni*.

### 6.2.2. Crosstalk between the UPR and NOX1 signalling in human IECs

In this study, downregulation of *NOX1* expression in human IECs infected with *C. jejuni* or treated with thapsigargin was demonstrated. Consistent with this observation, a previous study demonstrated that tunicamycin-induced UPR transcriptionally downregulated *NOX1* expression in intestinal goblet cells by an unknown mechanism (Tréton et al., 2014). Further studies using UPR inhibitors or siRNA transfection targeting NOX1 and UPR-related components are necessary to investigate whether there is bidirectional signalling between the *C. jejuni*- or thapsigargin-induced UPR activation and NOX1 expression in human IECs. In addition, expression of other components of the NOX1 complex such as NOXA1, NOXO1 and p22phox in human IECs infected with *C. jejuni* or treated with thapsigargin should also be explored to understand mechanisms of NOX1 downregulation and a potential crosstalk between the UPR and NOX1. Further work incorporating pull-down assay will allow to investigate if there are protein-protein interactions between UPR-related components and components of the NOX1 complex.

### 6.2.3. Characterisation of *C. jejuni* 81-176 T4SS in ROS production and UPR activation

The results from this study demonstrated that only *C. jejuni* 81-176, which possesses a putative T4SS, induced extracellular ROS from human IECs at 3 hours post-infection, suggesting a possible role for

the 81-176 T4SS in ROS production. *H. pylori* T4SS-mediated translocation of CagA has been associated with ROS production in immortalised mouse stomach epithelial cells (Chaturvedi et al., 2011). Chaturvedi et al. demonstrated CagA induces apoptosis by upregulating host spermine oxidase followed by $H_2O_2$ production during oxidation of spermine to spermidine (Chaturvedi et al., 2011). pVir of *C. jejuni* 81-176 encodes T4SS components and contains four genes which are orthologous to the *H. pylori* T4SS (Bacon et al., 2000, 2002; Kersulyte et al., 2003). However, there is little evidence of a full T4SS system and little is known about putative effector proteins of the 81-176 T4SS (Bacon et al., 2000, 2002; Kersulyte et al., 2003). Further studies are required to investigate the role of putative *C. jejuni* T4SS effector proteins in ROS production from host cells. In addition, unlike *C. jejuni* 11168H and 488 wild-type strains, 81-176 induced activation of the ATF6 pathway in T84 cells. Given that the T4SSs of *H. pylori*, *B. abortus* and *L. pneumophila* are implicated in UPR activation (de Jong et al., 2013; Ibe, Subramanian, & Mukherjee, 2021; Nami et al., 2020), future work should also explore the role of 81-176 T4SS in UPR activation. The impact of mutation of 81-176 T4SS components such as ComB1, ComB2, ComB3 and VirB11 on the UPR activation should be investigated.

#### 6.2.4. *C. jejuni* 488 T6SS and the UPR activation in human IECs

In addition to bacterial T4SSs, T6SSs have also been implicated in UPR activation (Jiang et al., 2016). Translocation of the TplE effector via the *P. aeruginosa* T6SS impairs the integrity of the ER membrane and activates the PERK and IRE1α pathways in human embryonic kidney HEK293T cells (Jiang et al., 2016). A T6SS cluster was identified in *C. jejuni* 488, containing genes encoding for all T6SS core components except for a ClpV ATPase (Liaw et al., 2019). Future works should examine whether the *C. jejuni* 488 T6SS gene cluster encodes ER-localising and/or ER-disrupting effector proteins and the effector proteins are responsible for UPR activation in human IECs. In addition, experiments with mutagenesis of structural components of the 488 T6SS should be conducted to investigate the role of structural components of T6SS in UPR activation in human IECs. Visualisation of the ER membrane in human IECs infected with a 488 wild-type strain with fluorescent-tagged effector proteins or structural components will help examine the localisation of effector proteins and/or structural components to investigate the interaction between the ER and *C. jejuni* T6SS.

#### 6.2.5. Relationship between *C. jejuni* invasion and the UPR activation in human IECs

The results from this study suggested that *C. jejuni* capsular polysaccharide, flagella and FlpA play a role during PERK pathway activation, indicating the possibility that PERK pathway activation might be dependent on adherence and invasion of *C. jejuni*. A previous study in our group demonstrated that microtubules, microfilaments, lipid rafts and/or PI3K pathway are necessary for *C. jejuni* invasion of human IECs (Hussein, 2018). Further studies using individual chemical inhibitors, such as colchicine,

cytochalasin D, methyl-beta-cyclodextrin and wortmannin, targeting each host component will allow an investigation of potential mechanisms of *C. jejuni* invasion-mediated UPR activation in human IECs. Furthermore, given that FlpA but not CadF is involved in PERK pathway activation, future work using chemical inhibitors can explore the differential impact of interaction between FlpA or CadF and human IECs on PERK pathway activation.

### 6.2.6. *C. jejuni* LOS and other possible bacterial virulence determinants and UPR activation in human IECs

This study demonstrated that no significant differences were observed in activation of the IRE1α pathway by *C. jejuni* 11168H *kpsM*, *flaA*, *flpA*, *cadF* mutants and the *cadF flpA* double mutant. Further studies are necessary to identify other *C. jejuni* virulence determinants which are responsible for IRE1α pathway activation. A previous study suggested *E. coli* LPS induces the IRE1α pathway but not the PERK pathway (Nakayama et al., 2010). As the structure of *C. jejuni* LOS is similar to LPS except for the lack of the O-antigen (Hameed et al., 2020), future work using purified *C. jejuni* LOS should investigate the involvement of *C. jejuni* LOS in activation of the IRE1α pathway in human IECs. Given that there is a large diversity in the LOS biosynthesis between *C. jejuni* strains (Bravo et al., 2021), inter-strain variation in LOS-mediated UPR activation should also be explored by using purified LOS from different *C. jejuni* strains. In addition, nuclear magnetic resonance (NMR) spectroscopy can also be used to identify other chemical and organic molecules within bacterial cell lysate or cell-free supernatant which might be responsible for UPR activation. Pull-down assay can also be performed to determine physical interactions between bacterial virulence determinants and components which are involved in UPR activation.

### 6.2.7. *C. jejuni* OMV-associated CDT and the UPR activation in human IECs

Proteomic studies revealed that *C. jejuni* OMVs contain adhesins CadF and FlpA, proteases HtrA and Cj0511 as well as *N*-linked glycoproteins (Elmi et al., 2012). As *C. jejuni* OMVs are associated with different bacterial virulence determinants, further works should be conducted to investigate whether *C. jejuni* OMVs can activate the UPR in human IECs. In addition, *C. jejuni* secretes CDT via OMVs and OMV-associated CDT exerts cytotoxicity on human IECs (Elmi et al., 2012; Lindmark et al., 2009). Data presented in this study demonstrated no significant differences observed in activation of either the PERK or IRE1α pathways by the *cdtABC* operon or *cdtA* mutants. A possible explanation for this observation is that the UPR is still activated via *C. jejuni* adherence and invasion which are independent of CDT activity. To exclude the effect of *C. jejuni* adherence and invasion on UPR activation and to investigate the effect of CDT alone, further studies using OMVs from the wild-type strain and *cdt* mutants will also be necessary to determine whether *C. jejuni* OMV-associated CDT is responsible for

the UPR activation in human IECs. In addition, as some *C. jejuni* isolates do not possess CDT (Jain et al., 2008), further work comparing CDT-positive and CDT-negative *C. jejuni* isolates in UPR activation in human IECs will be required.

### 6.2.8. TLR signalling and *C. jejuni*-mediated UPR activation and inflammation

TLR2 and TLR4 detection has been associated with UPR activation (Mahadevan et al., 2011; Martinon et al., 2010). Previous studies suggested that ligand binding of TLR2 and TLR4 induces UPR activation (Mahadevan et al., 2011; Martinon et al., 2010). The role in *C. jejuni* detection by TLR2 and TLR4 in UPR activation and subsequent UPR-induced inflammation in human IECs should be further investigated using siRNA transfection of TLR2 and TLR4. In addition, as *C. jejuni* activates TLR2 and TLR4 in Myd88- and TRIF-dependent manner (Friis, Keelan, & Taylor, 2009; Rathinam et al., 2009), the involvement of adapter proteins MyD88 and TRIF in *C. jejuni*-induced UPR activation should also be explored by using siRNA transfection targeting the adaptor proteins.

### 6.2.9. Identifying *C. jejuni*-mediated UPR activation using multi-omics profiling

Multi-omics profiling is an effective tool for comprehensive understanding of molecular and cellular responses (Lee, Hyeon, & Hwang, 2020). Multi-omics studies provide integrative insights of crosstalk between non-genetic modification, abundance of mRNA transcripts and protein expression under certain conditions via integrative analysis of transcriptome, proteome and epigenome in response to specific stimuli (Lee, Hyeon, & Hwang, 2020; Rohart et al., 2017). Multi-omics profiling incorporating different *C. jejuni* wild-type strains, mutants and siRNA transfection targeting UPR-related components or other cellular components will broaden the understanding of mechanisms of *C. jejuni*-mediated UPR activation and the crosstalk between the *C. jejuni*-activated UPR and inflammation. In addition, duel-RNA sequencing can be carried out to simultaneously sequence the transcriptome of host cells and infecting bacteria in the same biological sample (Damron et al., 2016; Marsh, Humphrys, & Myers, 2017). Dual-RNA sequencing can measure changes of transcriptome of human IECs and *C. jejuni* at the same time and compare the pathways human IECs are using to counteract *C. jejuni* infection. Therefore, dual-RNA sequencing will provide better insight into host-pathogen interactions which result in UPR activation.

### 6.2.10. NOX1 modulation and UPR activation in chickens

One of main routes of *Campylobacter* infection is consumption of undercooked chicken (Kaakoush et al., 2015). This is associated with *C. jejuni* colonisation in the avian ceca (Kaakoush et al., 2015). Even though a previous study demonstrated stressed broiler chickens can experience *C. jejuni*-induced enteritis, *C. jejuni* is considered as non-pathogenic to chickens (Humphrey et al., 2014; Kaakoush et al.,

2015). The variation in disease presentation in humans and chickens is related to differences in immune responses exerted by the two host species (de Zoete et al., 2010). *C. jejuni* induces TLR4 and MyD88-mediated IFN-β in human MM6 monocytic cells but not in chicken HD11 macrophages (de Zoete et al., 2010). This study demonstrated *C. jejuni*-mediated UPR activation is closely related to inflammation and there is a potential interplay between the UPR and NOX1. Therefore, further work comparing NOX1 modulation and UPR activation in human IECs and chicken IECs will be necessary to investigate if different disease outcomes of *C. jejuni* infection in the two host species are associated with differential NOX1 modulation and/or UPR activation.

In addition, a previous study compared virulence properties between *C. jejuni* strains isolated from human clinical samples and poultry (Van Deun et al., 2007). The authors showed there is no significant differences in invasiveness and IL-8 secretion in T84 cells between human clinical isolates and poultry isolates (Van Deun et al., 2007). However, compared to poultry isolates, human isolates are more tolerant to bile salt sodium deoxycholate suggesting increased bile salt-resistance might be linked to human disease outcomes of *C. jejuni* infection (Van Deun et al., 2007). Further studies are necessary to compare NOX1 modulation and UPR activation by human clinical isolates and poultry isolates in human IECs.

## References


Akazawa, Y., Isomoto, H., Matsushima, K., Kanda, T., Minami, H., Yamaghchi, N., . . . Nakao, K. (2013). Endoplasmic reticulum stress contributes to *Helicobacter pylori* VacA-induced apoptosis. *PLOS One, 8*(12), e82322. doi:10.1371/journal.pone.0082322

Alemka, A., Nothaft, H., Zheng, J., & Szymanski, C. M. (2013). N-glycosylation of *Campylobacter jejuni* surface proteins promotes bacterial fitness. *Infection and Immunity, 81*(5), 1674-1682. doi:10.1128/IAI.01370-12

Alshareef, M. H., Hartland, E. L., & McCaffrey, K. (2021). Effectors Targeting the Unfolded Protein Response during Intracellular Bacterial Infection. *Microorganisms (Basel), 9*(4), 705. doi:10.3390/microorganisms9040705

Amour, C., Gratz, J., Mduma, E., Svensen, E., Rogawski, E. T., McGrath, M., . . . Platts-Mills, J. A. (2016). Epidemiology and impact of *Campylobacter* infection in children in 8 low-resource settings: Results from the MAL-ED study. *Clinical infectious diseases, 63*(9), 1171-1179. doi:10.1093/cid/ciw542

Andersen-Nissen, E., Smith, K. D., Strobe, K. L., Barrett, S. L. R., Cookson, B. T., Logan, S. M., & Aderem, A. (2005). Evasion of Toll-like receptor 5 by flagellated bacteria. *Proceedings of the National Academy of Sciences - PNAS, 102*(26), 9247-9252. doi:10.1073/pnas.0502040102

Antoniou, A. N., Lenart, I., Kriston-Vizi, J., Iwawaki, T., Turmaine, M., McHugh, K., . . . Powis, S. J. (2018). *Salmonella* exploits HLA-B27 and host unfolded protein responses to promote intracellular replication. *Annals of the Rheumatic Diseases, 78*(1), 74-82. doi:10.1136/annrheumdis-2018-213532

Ashgar, S. S. A., Oldfield, N. J., Wooldridge, K. G., Jones, M. A., Irving, G. J., Turner, D. P. J., & Ala'Aldeen, D. A. A. (2007). CapA, an Autotransporter Protein of *Campylobacter jejuni*, Mediates Association with Human Epithelial Cells and Colonization of the Chicken Gut. *Journal of Bacteriology, 189*(5), 1856-1865. doi:10.1128/JB.01427-06

Aspinall, G. O., McDonald, A. G., Raju, T. S., Pang, H., Moran, A. P., & Penner, J. L. (1993). Chemical structures of the core regions of *Campylobacter jejuni* serotypes o:1, o:4, o:23, and o:36 lipopolysaccharides. *European Journal of Biochemistry*. doi:10.1111/j.1432-1033.1993.tb17849.x

Asrat, S., de Jesús, D. A., Hempstead, A. D., Ramabhadran, V., & Isberg, R. R. (2014). Bacterial pathogen manipulation of host membrane trafficking. *Annual review of cell and developmental biology, 30*(1), 79-109. doi:10.1146/annurev-cellbio-100913-013439

Aviello, G., & Knaus, U. (2017). ROS in gastrointestinal inflammation: rescue or sabotage? In (Vol. 174, pp. 1704-1718).

Aviello, G., & Knaus, U. G. (2018). NADPH oxidases and ROS signaling in the gastrointestinal tract. *Mucosal immunology, 11*(4), 1011-1023. doi:10.1038/s41385-018-0021-8

Avila-Calderón, E. D., Ruiz-Palma, M. D. S., Aguilera-Arreola, M. G., Velázquez-Guadarrama, N., Ruiz, E. A., Gomez-Lunar, Z., . . . Contreras-Rodríguez, A. (2021). Outer Membrane Vesicles of Gram-Negative Bacteria: An Outlook on Biogenesis. *Frontiers in Microbiology, 12*, 557902-557902. doi:10.3389/fmicb.2021.557902

Aya, T., Takaaki, S., Sho, H., Junko, K., Anh Quoc, N., Yuna, K., . . . Akira, T. (2018). Host cellular unfolded protein response signaling regulates *Campylobacter jejuni* invasion. *PLOS ONE, 13*(10), e0205865. doi:10.1371/journal.pone.0205865

Backert, S., Boehm, M., Wessler, S., & Tegtmeyer, N. (2013). Transmigration route of *Campylobacter jejuni* across polarized intestinal epithelial cells: paracellular, transcellular or both? *Cell communication and signaling, 11*(1), 72-72. doi:10.1186/1478-811X-11-72

Bacon, D. J., Alm, R. A., Burr, D. H., Hu, L., Kopecko, D. J., Ewing, C. P., . . . Guerry, P. (2000). Involvement of a plasmid in virulence of *Campylobacter jejuni* 81-176. *Infection and Immunity, 68*(8), 4384-4390. doi:10.1128/IAI.68.8.4384-4390.2000

Bacon, D. J., Alm, R. A., Burr, D. H., Hu, L., Kopecko, D. J., Ewing, C. P., . . . Guerry, P. (2002). DNA sequence and mutational analyses of the pVir plasmid of *Campylobacter jejuni* 81-176. *Infection and Immunity, 70*(11), 6242-6250. doi:10.1128/IAI.70.11.6242-6250.2002

Bacon, D. J., Szymanski, C. M., Burr, D. H., Silver, R. P., Alm, R. A., & Guerry, P. (2001). A phase-variable capsule is involved in virulence of *Campylobacter jejuni* 81-176. *Molecular microbiology, 40*(3), 769-777. doi:10.1046/j.1365-2958.2001.02431.x

Banerjee, T., Grabon, A., Taylor, M., & Teter, K. (2021). cAMP-Independent Activation of the Unfolded Protein Response by Cholera Toxin. *Infection and Immunity, 89*(2). doi:10.1128/IAI.00447-20

Basil, M. C., & Levy, B. D. (2016). Specialized pro-resolving mediators: endogenous regulators of infection and inflammation. *Nature reviews. Immunology, 16*(1), 51-67. doi:10.1038/nri.2015.4

Batchelor, R. A., Pearson, B. M., Friis, L. M., Guerry, P., & Wells, J. M. (2004). Nucleotide Sequences and Comparison of Two Large Conjugative Plasmids from Different *Campylobacter* species. *Microbiology, 150*, 3507-3517. doi:10.1099/mic.0.27112-0

Bereswill, S., Grundmann, U., Alutis, M. E., Fischer, A., & Heimesaat, M. M. (2017). *Campylobacter jejuni* infection of conventionally colonized mice lacking nucleotide-oligomerization-domain-2. *Gut Pathogens, 9*(1), 5-5. doi:10.1186/s13099-017-0155-3

Beumer, R. R., de Vries, J., & Rombouts, F. M. (1992). *Campylobacter jejuni* non-culturable coccoid cells. *International journal of food microbiology, 15*(1), 153-163. doi:10.1016/0168-1605(92)90144-R

Bhattacharyya, S., Sen, U., & Vrati, S. (2014). Regulated IRE1-dependent decay pathway is activated during Japanese encephalitis virus-induced unfolded protein response and benefits viral replication. *Journal of general virology, 95*(Pt 1), 71-79. doi:10.1099/vir.0.057265-0

Bhattarai, K. R., Riaz, T. A., Kim, H.-R., & Chae, H.-J. (2021). The aftermath of the interplay between the endoplasmic reticulum stress response and redox signaling. *Experimental & molecular medicine, 53*(2), 151-167. doi:10.1038/s12276-021-00560-8

Biram, A., & Shulman, Z. (2020). T cell help to B cells: Cognate and atypical interactions in peripheral and intestinal lymphoid tissues. *Immunological reviews, 296*(1), 36-47. doi:10.1111/imr.12890

Black, R. E., Levine, M. M., Clements, M. L., Hughes, T. P., & Blaser, M. J. (1988). Experimental *Campylobacter jejuni* infection in humans. *The Journal of infectious diseases, 157*(3), 472-479. doi:10.1093/infdis/157.3.472

Boehm, M., Hoy, B., Rohde, M., Tegtmeyer, N., Bæk, K. T., Oyarzabal, O. A., . . . Backert, S. (2012). Rapid paracellular transmigration of *Campylobacter jejuni* across polarized epithelial cells without affecting TER: role of proteolytic-active HtrA cleaving E-cadherin but not fibronectin. *Gut Pathogens, 4*(1), 3-3. doi:10.1186/1757-4749-4-3

Boesze-Battaglia, K., Brown, A., Walker, L., Besack, D., Zekavat, A., Wrenn, S., . . . Shenker, B. J. (2009). Cytolethal distending toxin-induced cell cycle arrest of lymphocytes is dependent upon recognition and binding to cholesterol. *The Journal of Biological Chemistry, 284*(16), 10650-10658. doi:10.1074/jbc.M809094200

Boll, J. M., & Hendrixson, D. R. (2013). A regulatory checkpoint during flagellar biogenesis in Campylobacter jejuni initiates signal transduction to activate transcription of flagellar genes. *mBio, 4*(5), e00432-e00413. doi:10.1128/mBio.00432-13

Bosman, F. T., & Stamenkovic, I. (2003). Functional structure and composition of the extracellular matrix. *The Journal of pathology, 200*(4), 423-428. doi:10.1002/path.1437

Brandes, R. P., Weissmann, N., & Schröder, K. (2014). Nox family NADPH oxidases: Molecular mechanisms of activation. *Free Radical Biology and Medicine, 76*, 208-226. doi:10.1016/j.freeradbiomed.2014.07.046

Bravo, V., Katz, A., Porte, L., Weitzel, T., Varela, C., Gonzalez-Escalona, N., & Blondel, C. J. (2021). Genomic analysis of the diversity, antimicrobial resistance and virulence potential of clinical *Campylobacter jejuni* and *Campylobacter coli* strains from Chile. *PLOS Neglected Tropical Diseases, 15*(2), e0009207-e0009207. doi:10.1371/journal.pntd.0009207

Bücker, R., Krug, S., Moos, V., Bojarski, C., Schweiger, M., Kerick, M., . . . Schulzke, J. (2018). *Campylobacter jejuni* impairs sodium transport and epithelial barrier function via cytokine release in human colon. *Mucosal immunology, 11*(2), 474-485. doi:10.1038/mi.2017.66

Buelow, D. R., Christensen, J. E., Neal-McKinney, J. M., & Konkel, M. E. (2011). *Campylobacter jejuni* survival within human epithelial cells is enhanced by the secreted protein CiaI. *Molecular microbiology, 80*(5), 1296-1312. doi:10.1111/j.1365-2958.2011.07645.x

Burgueño, J. F., Fritsch, J., Santander, A. M., Brito, N., Fernández, I., Pignac-Kobinger, J., . . . Abreu, M. T. (2019). Intestinal Epithelial Cells Respond to Chronic Inflammation and Dysbiosis by Synthesizing H2O2. *Frontiers in physiology, 10*, 1484-1484. doi:10.3389/fphys.2019.01484

Burnham, P. M., & Hendrixson, D. R. (2018). *Campylobacter jejuni*: collective components promoting a successful enteric lifestyle. *Nature reviews. Microbiology, 16*(9), 551-565. doi:10.1038/s41579-018-0037-9

Canonico, B., Di Sario, G., Cesarini, E., Campana, R., Luchetti, F., Zamai, L., . . . Papa, S. (2018). Monocyte Response to Different *Campylobacter jejuni* Lysates Involves Endoplasmic Reticulum Stress and the Lysosomal‐Mitochondrial Axis: When Cell Death Is Better Than Cell Survival. *Toxins, 10*(6), 239. doi:10.3390/toxins10060239

Cao, S. S., & Kaufman, R. J. (2014). Endoplasmic reticulum stress and oxidative stress in cell fate decision and human disease. *Antioxidants & Redox Signaling, 21*(3), 396-413. doi:10.1089/ars.2014.5851

Carreras-Sureda, A., Pihán, P., & Hetz, C. (2018). Calcium signaling at the endoplasmic reticulum: fine-tuning stress responses. *Cell calcium (Edinburgh), 70*, 24-31. doi:10.1016/j.ceca.2017.08.004

Caruso, R., Warner, N., Inohara, N., & Núñez, G. (2014). NOD1 and NOD2: Signaling, Host Defense, and Inflammatory Disease. *Immunity (Cambridge, Mass.), 41*(6), 898-908. doi:10.1016/j.immuni.2014.12.010

Celli, J., & Tsolis, R. M. (2014). Bacteria, the endoplasmic reticulum and the unfolded protein response: friends or foes? *Nature Reviews Microbiology, 13*(2), 73-82. doi:10.1038/nrmicro3393

Cerf-Bensussan, N., & Gaboriau-Routhiau, V. (2010). The immune system and the gut microbiota: friends or foes? *Nature reviews. Immunology, 10*(10), 735-744. doi:10.1038/nri2850

Cha, J. J., Min, H. S., Kim, K. T., Kim, J. E., Ghee, J. Y., Kim, H. W., . . . Cha, D. R. (2017). APX-115, a first-in-class pan-NADPH oxidase (Nox) inhibitor, protects db/db mice from renal injury. *Laboratory investigation; a journal of technical methods and pathology, 97*(4), 419–431.

Chandrashekhar, K., Kassem, I. I., & Rajashekara, G. (2017). *Campylobacter jejuni* transducer like proteins: Chemotaxis and beyond. *Gut microbes, 8*(4), 323-334. doi:10.1080/19490976.2017.1279380

Chaturvedi, R., Asim, M., Romero–Gallo, J., Barry, D. P., Hoge, S., de Sablet, T., . . . Wilson, K. T. (2011). Spermine oxidase mediates the gastric cancer risk associated with *Helicobacter pylori* CagA. *Gastroenterology (New York, N.Y. 1943), 141*(5), 1696-1708.e1692. doi:10.1053/j.gastro.2011.07.045

Chiang, J. Y. L. (2013). Bile Acid Metabolism and Signaling. *Comprehensive Physiology, 3*(3), 1191-1212. doi:10.1002/cphy.c120023

Choi, H., Shin, D.-M., Kang, G., Kim, K.-H., Park, J. B., Hur, G. M., . . . Song, C.-H. (2010). Endoplasmic reticulum stress response is involved in *Mycobacterium tuberculosis* protein ESAT-6-mediated apoptosis. *FEBS letters, 584*(11), 2445-2454. doi:10.1016/j.febslet.2010.04.050

Choi, H. H., Shin, D.-M., Kang, G., Kim, K.-H., Park, J. B., Hur, G. M., . . . Song, C.-H. (2010). Endoplasmic reticulum stress response is involved in *Mycobacterium tuberculosis* protein ESAT-6-mediated apoptosis. *FEBS letters, 584*(11), 2445-2454. doi:10.1016/j.febslet.2010.04.050

Choi, J.-A., & Song, C.-H. (2019). Insights Into the Role of Endoplasmic Reticulum Stress in Infectious Diseases. *Frontiers in Immunology, 10*, 3147-3147. doi:10.3389/fimmu.2019.03147

Cohen, E. J., Nakane, D., Kabata, Y., Hendrixson, D. R., Nishizaka, T., & Beeby, M. (2020). *Campylobacter jejuni* motility integrates specialized cell shape, flagellar filament, and motor, to coordinate action of its opposed flagella. *PLOS Pathogens, 16*(7), e1008620-e1008620. doi:10.1371/journal.ppat.1008620

Collatz, M. B., Rüdel, R., & Brinkmeier, H. (1997). Intracellular calcium chelator BAPTA protects cells against toxic calcium overload but also alters physiological calcium responses. *Cell calcium (Edinburgh), 21*(6), 453-459. doi:10.1016/S0143-4160(97)90056-7

Corcionivoschi, N., Alvarez, Luis A. J., Sharp, Thomas H., Strengert, M., Alemka, A., Mantell, J., . . . Bourke, B. (2012). Mucosal reactive oxygen species decrease virulence by disrupting *Campylobacter jejuni* phosphotyrosine signaling. *Cell Host & Microbe, 12*(1), 47-59. doi:10.1016/j.chom.2012.05.018

Correa, Ricardo G., Khan, Pasha M., Askari, N., Zhai, D., Gerlic, M., Brown, B., . . . Reed, John C. (2011). Discovery and Characterization of 2-Aminobenzimidazole Derivatives as Selective NOD1 Inhibitors. *Chemistry & biology, 18*(7), 825-832. doi:10.1016/j.chembiol.2011.06.009

Cui, J., Duizer, C., Bouwman, L. I., van Rooijen, K. S., Voogdt, C. G. P., van Putten, J. P. M., & de Zoete, M. R. (2021). The ALPK1 pathway drives the inflammatory response to *Campylobacter jejuni* in human intestinal epithelial cells. *PLOS Pathogens, 17*(8), e1009787-e1009787. doi:10.1371/journal.ppat.1009787

Damron, F. H., Oglesby-Sherrouse, A. G., Wilks, A., & Barbier, M. (2016). Dual-seq transcriptomics reveals the battle for iron during *Pseudomonas aeruginosa* acute murine pneumonia. *Scientific Reports, 6*(1), 39172-39172. doi:10.1038/srep39172

Dana, H., Chalbatani, G. M., Mahmoodzadeh, H., Karimloo, R., Rezaiean, O., Moradzadeh, A., . . . Gharagouzlo, E. (2017). Molecular Mechanisms and Biological Functions of siRNA. *International journal of biomedical science, 13*(2), 48-57.

Das, H., Koizumi, T., Sugimoto, T., Chakraborty, S., Ichimura, T., Hasegawa, K., & Nishimura, R. (2000). Quantitation of Fas and Fas ligand gene expression in human ovarian, cervical and

endometrial carcinomas using real-time quantitative RT-PCR. *British Journal of Cancer, 82*(10), 1682-1688. doi:10.1054/bjoc.2000.1118

Daverkausen-Fischer, L., & Pröls, F. (2022). Regulation of calcium homeostasis and flux between the endoplasmic reticulum and the cytosol. *The Journal of Biological Chemistry, 298*(7), 102061-102061. doi:10.1016/j.jbc.2022.102061

Davies, C., Taylor, A. J., Elmi, A., Winter, J., Liaw, J., Grabowska, A., . . . Dorrell, N. (2019). Sodium taurocholate stimulates *Campylobacter jejuni* outer membrane vesicle production via down-regulation of the maintenance of lipid asymmetry pathway. *Frontiers in Cellular and Infection Microbiology*. doi:10.3389/fcimb.2019.00177

de Jong, M. F., Starr, T., Winter, M. G., Den Hartigh, A. B., Child, R., Knodler, L. A., . . . Tsolis, R. M. (2013). Sensing of Bacterial Type IV Secretion via the Unfolded Protein Response. *mBio, 4*(1), e00418-00412. doi:10.1128/mBio.00418-12

De Nisco, N. J., Casey, A. K., Kanchwala, M., Lafrance, A. E., Coskun, F. S., Kinch, L. N., . . . Orth, K. (2021). Manipulation of IRE1-Dependent MAPK Signaling by a *Vibrio* Agonist-Antagonist Effector Pair. *mSystems, 6*(1). doi:10.1128/MSYSTEMS.00872-20

de Vries, S. P. W., Linn, A., Macleod, K., MacCallum, A., Hardy, S. P., Douce, G., . . . Everest, P. (2017). Analysis of Campylobacter jejuni infection in the gnotobiotic piglet and genome-wide identification of bacterial factors required for infection. *Scientific Reports, 7*(1), 44283. doi:10.1038/srep44283

de Zoete, M. R., Keestra, A. M., Roszczenko, P., & van Putten, J. P. M. (2010). Activation of Human and Chicken Toll-Like Receptors by *Campylobacter* spp. *Infection and Immunity, 78*(3), 1229-1238. doi:10.1128/IAI.00897-09

Del Rocio Leon-Kempis, M., Guccione, E., Mulholland, F., Williamson, M. P., & Kelly, D. J. (2006). The *Campylobacter jejuni* PEB1a adhesin is an aspartate/glutamate-binding protein of an ABC transporter essential for microaerobic growth on dicarboxylic amino acids. *Molecular microbiology, 60*(5), 1262-1275. doi:10.1111/j.1365-2958.2006.05168.x

DeMali, K. A., Wennerberg, K., & Burridge, K. (2003). Integrin signaling to the actin cytoskeleton. *Current opinion in cell biology, 15*(5), 572-582. doi:10.1016/S0955-0674(03)00109-1

den Hartog, G., Chattopadhyay, R., Ablack, A., Hall, E. H., Butcher, L. D., Bhattacharyya, A., . . . Blanke, S. R. (2016). Regulation of Rac1 and reactive oxygen species production in response to infection of gastrointestinal epithelia. *PLOS Pathogens, 12*(1), 1-20. doi:10.1371/journal.ppat.1005382

Deng, J., Lu, P. D., Zhang, Y., Scheuner, D., Kaufman, R. J., Sonenberg, N., . . . Ron, D. (2004). Translational Repression Mediates Activation of Nuclear Factor Kappa B by Phosphorylated Translation Initiation Factor 2. *Molecular and Cellular Biology, 24*(23), 10161-10168. doi:10.1128/MCB.24.23.10161-10168.2004

Devriese, S., Van den Bossche, L., Van Welden, S., Holvoet, T., Pinheiro, I., Hindryckx, P., . . . Laukens, D. (2017). T84 monolayers are superior to Caco-2 as a model system of colonocytes. *Histochemistry and Cell Biology, 148*(1), 85-93. doi:10.1007/s00418-017-1539-7

Di, X.-J., Wang, Y.-J., Han, D.-Y., Fu, Y.-L., Duerfeldt, A. S., Blagg, B. S. J., & Mu, T.-W. (2016). Grp94 Protein Delivers γ-Aminobutyric Acid Type A (GABAA) Receptors to Hrd1 Protein-mediated Endoplasmic Reticulum-associated Degradation. *The Journal of Biological Chemistry, 291*(18), 9526-9539. doi:10.1074/jbc.M115.705004

Dorrell, N., Mangan, J. A., Laing, K. G., Hinds, J., Linton, D., Al-Ghusein, H., . . . Wren, B. W. (2001). Whole genome comparison of *Campylobacter jejuni* human isolates using a low-cost microarray reveals extensive genetic diversity. *Genome research, 11*(10), 1706-1715. doi:10.1101/gr.185801

Duan, T., Du, Y., Xing, C., Wang, H. Y., & Wang, R.-F. (2022). Toll-Like Receptor Signaling and Its Role in Cell-Mediated Immunity. *Frontiers in Immunology, 13*, 812774-812774. doi:10.3389/fimmu.2022.812774

EFSA, & ECDC. (2021). The European Union one health 2019 zoonoses report. *EFSA journal, 19*(2), 286. doi:10.2903/j.efsa.2021.6406

Elatrech, I., Marzaioli, V., Boukemara, H., Bournier, O., Neut, C., Darfeuille-Michaud, A., . . . Marie, J.-C. (2015). *Escherichia coli* LF82 differentially regulates ROS production and mucin expression in intestinal epithelial T84 cells: implication of Nox1. *Inflammatory Bowel Disease, 21*, 1018-1026. doi:10.1097/MIB.0000000000000365

Elmi, A., Dorey, A., Watson, E., Jagatia, H., Gundogdu, O., Bajaj-Elliott, M., . . . Dorrell, N. (2017). *The bile salt sodium taurocholate induces Campylobacter jejuni outer membrane vesicle production and increases OMV-associated proteolytic activity*. Paper presented at the 19th International Workshop on Campylobacter, Helicobacter and Related Organisms, Nantes, France.

Elmi, A., Nasher, F., Dorrell, N., Wren, B., & Gundogdu, O. (2020). Revisiting Campylobacter jejuni Virulence and Fitness Factors: Role in Sensing, Adapting, and Competing. *Frontiers in cellular and infection microbiology, 10*, 607704-607704. doi:10.3389/fcimb.2020.607704

Elmi, A., Nasher, F., Dorrell, N., Wren, B., & Gundogdu, O. (2021). Revisiting *Campylobacter jejuni* Virulence and Fitness Factors: Role in Sensing, Adapting, and Competing. *Frontiers in Cellular and Infection Microbiology, 10*, 607704-607704. doi:10.3389/fcimb.2020.607704

Elmi, A., Nasher, F., Jagatia, H., Gundogdu, O., Bajaj-Elliott, M., Wren, B., & Dorrell, N. (2016). *Campylobacter jejuni* outer membrane vesicle-associated proteolytic activity promotes bacterial invasion by mediating cleavage of intestinal epithelial cell E-cadherin and occludin. *Cellular Microbiology, 18*(4), 561-572. doi:10.1111/cmi.12534

Elmi, A., Watson, E., Sandu, P., Gundogdu, O., Mills, D. C., Inglis, N. F., . . . Dorrell, N. (2012). *Campylobacter jejuni* Outer Membrane Vesicles Play an Important Role in Bacterial Interactions with Human Intestinal Epithelial Cells. *Infection and Immunity, 80*(12), 4089-4098. doi:10.1128/IAI.00161-12

Escoll, P., Mondino, S., Rolando, M., & Buchrieser, C. (2016). Targeting of host organelles by pathogenic bacteria: a sophisticated subversion strategy. *Nature reviews. Microbiology, 14*(1), 5-19. doi:10.1038/nrmicro.2015.1

Eshraghi, A., Dixon, S. D., Tamilselvam, B., Kim, E. J.-K., Gargi, A., Kulik, J. C., . . . Bradley, K. A. (2014). Cytolethal distending toxins require components of the ER-associated degradation pathway for host cell entry. *PLOS Pathogens, 10*(7), e1004295. doi:10.1371/journal.ppat.1004295

Eucker, T. P., & Konkel, M. E. (2012). The cooperative action of bacterial fibronectin-binding proteins and secreted proteins promote maximal *Campylobacter jejuni* invasion of host cells by stimulating membrane ruffling. *Cellular Microbiology, 14*(2), 226-238. doi:10.1111/j.1462-5822.2011.01714.x

Fischer, W., Püls, J., Buhrdorf, R., Gebert, B., Odenbreit, S., & Haas, R. (2001). Systematic mutagenesis of the *Helicobacter pylori cag* pathogenicity island: essential genes for CagA translocation in host cells and induction of interleukin-8. *Molecular microbiology, 42*(5), 1337-1348. doi:10.1046/j.1365-2958.2001.02714.x

Flanagan, R. C., Neal-McKinney, J. M., Dhillon, A. S., Miller, W. G., & Konkel, M. E. (2009). Examination of *Campylobacter jejuni* putative adhesins leads to the identification of a new protein, designated FlpA, required for chicken colonization. *Infection and Immunity, 77*(6), 2399-2407. doi:10.1128/IAI.01266-08

Fox, J. G., Rogers, A. B., Whary, M. T., Ge, Z., Taylor, N. S., Xu, S., . . . Erdman, S. E. (2004). Gastroenteritis in NF-κB-deficient mice is produced with wild-type *Camplyobacter jejuni* but not with *C. jejuni* lacking cytolethal distending toxin despite persistent colonization with both strains. *Infection and Immunity, 72*(2), 1116-1125. doi:10.1128/IAI.72.2.1116-1125.2004

Francois Watkins, L. K., Laughlin, M. E., Joseph, L. A., Chen, J. C., Nichols, M., Basler, C., . . . Friedman, C. R. (2021). Ongoing Outbreak of Extensively Drug-Resistant *Campylobacter jejuni* Infections Associated With US Pet Store Puppies, 2016-2020. *JAMA network open, 4*(9), e2125203-e2125203. doi:10.1001/jamanetworkopen.2021.25203

Fribley, A., Zhang, K., & Kaufman, R. J. (2009). Regulation of apoptosis by the unfolded protein response. *Methods in molecular biology (Clifton, N.J.), 559*, 191-191. doi:10.1007/978-1-60327-017-5_14

Friis, L. M., Keelan, M., & Taylor, D. E. (2009). Campylobacter jejuni Drives MyD88-Independent Interleukin-6 Secretion via Toll-Like Receptor 2. *Infection and Immunity, 77*(4), 1553-1560. doi:10.1128/IAI.00707-08

FSA. (2013). Annual report of the chief scientist 2012/2013. Retrieved 14.02.2022, from Food Standards Agency https://acss.food.gov.uk/sites/default/files/multimedia/pdfs/publication/cstar_2013.pdf

FSA. (2019). Major retailers publish campylobacter results for April-June 2019 [Online]. Food Standard Agency. Retrieved 10.02.2022, from Food Standards Agency https://www.food.gov.uk/print/pdf/node/2856

FSA. (2020). Foodborne disease estimates for the United Kingdom in 2018 [Online]. Food Standard Agency. Retrieved 14.02.2022, from Food Standard Agency https://webarchive.nationalarchives.gov.uk/ukgwa/20200803160512/https://www.food.gov.uk/sites/default/files/media/document/foodborne-disease-estimates-for-the-united-kingdom-in-2018.pdf

FSA. (2021). Enhanced molecular-based surveillance and source attribution of *Campylobacter* infections in the UK. Retrieved 10.02.2022, from Food Standard Agency https://www.food.gov.uk/sites/default/files/media/document/enhanced-molecular-based-surveillance-and-source-attribution-of-campylobacter-infections-in-the-uk.pdf

Fukuyama, S., & Kiyono, H. (2004). NALT- versus PEYER'S-patch-mediated mucosal immunity. *Nature reviews. Immunology, 4*(9), 699-710. doi:10.1038/nri1439

Futamura, Y., Tashiro, E., Hironiwa, N., Kohno, J., Nishio, M., Shindo, K., & Imoto, M. (2007). Trierixin, a novel Inhibitor of ER stress-induced XBP1 activation from *Streptomyces* sp. II. structure elucidation. *The Journal of Antibiotics (Tokyo), 60*(9). doi:10.1038/ja.2007.74.

Gallois, A., Klein, J. R., Allen, L.-A. H., Jones, B. D., & Nauseef, W. M. (2001). *Salmonella* pathogenicity island 2-Encoded type III secretion system mediates exclusion of NADPH oxidase assembly from the phagosomal membrane. *The Journal of immunology (1950), 166*(9), 5741.

Garg, A. D., Kaczmarek, A., Krysko, O., Vandenabeele, P., Krysko, D. V., & Agostinis, P. (2012). ER stress-induced inflammation: does it aid or impede disease progression? *Trends in Molecular Medicine, 18*(10), 589-598. doi:10.1016/j.molmed.2012.06.010

Gay, N. J., Symmons, M. F., Gangloff, M., & Bryant, C. E. (2014). Assembly and localization of Toll-like receptor signalling complexes. *Nature reviews. Immunology, 14*(8), 546-558. doi:10.1038/nri3713

Gaynor, E. C., Cawthraw, S., Manning, G., MacKichan, J. K., Falkow, S., & Newell, D. G. (2004). The Genome-Sequenced Variant of *Campylobacter jejuni* NCTC 11168 and the Original Clonal Clinical Isolate Differ Markedly in Colonization, Gene Expression, and Virulence-Associated Phenotypes. *Journal of Bacteriology, 186*(23), 8159-8159. doi:10.1128/JB.186.23.8159.2004

Gekara, N. O., Westphal, K., Ma, B., Rohde, M., Groebe, L., & Weiss, S. (2007). Multiple mechanisms of $Ca^{2+}$ signalling by listeriolysin O, the cholesterol-dependent cytolysin of *Listeria monocytogenes*. *Cellular Microbiology, 9*(8), 2008-2021. doi:10.1111/j.1462-5822.2007.00932.x

George, Z., Omosun, Y., Azenabor, A. A., Goldstein, J., Partin, J., Joseph, K., . . . Igietseme, J. U. (2019). The molecular mechanism of induction of unfolded protein response by *Chlamydia*. *Biochemical and Biophysical Research Communications, 508*(2), 421-429. doi:10.1016/j.bbrc.2018.11.034

George, Z., Omosun, Y., Azenabor, A. A., Partin, J., Joseph, K., Ellerson, D., . . . Igietseme, J. U. (2017). The Roles of Unfolded Protein Response Pathways in *Chlamydia* Pathogenesis. *The Journal of infectious diseases, 215*(3), 456-465. doi:10.1093/infdis/jiw569

Ghosh, R., Wang, L., Wang, Eric S., Perera, B. Gayani K., Igbaria, A., Morita, S., . . . Papa, Feroz R. (2014). Allosteric Inhibition of the IRE1α RNase Preserves Cell Viability and Function during Endoplasmic Reticulum Stress. *Cell, 158*(3), 534-548. doi:10.1016/j.cell.2014.07.002

Giallourou, N., Medlock, G. L., Bolick, D. T., Medeiros, P. H., Ledwaba, S. E., Kolling, G. L., . . . Guerrant, R. L. (2018). A novel mouse model of *Campylobacter jejuni* enteropathy and diarrhea. *PLOS Pathogens, 14*(3), e1007083. doi:10.1371/journal.ppat.1007083

Goodall, J. C., Wu, C., Zhang, Y., McNeill, L., Ellis, L., Saudek, V., & Gaston, J. S. H. (2010). Endoplasmic reticulum stress-induced transcription factor, CHOP, is crucial for dendritic cell IL-23 expression. *Proceedings of the National Academy of Sciences of the United States of America, 107*(41), 17698-17703. doi:10.1073/pnas.1011736107

Grant, C. C. R., Konkel, M. E., Cieplak, W. J., & Tompkins, L. S. (1993). Role of flagella in adherence, internalization, and translocation of *Campylobacter jejuni* in nonpolarized and polarized epithelial cell cultures. *Infection and Immunity, 61*(5), 1764-1771. doi:10.1128/iai.61.5.1764-1771.1993

Grootjans, J., Kaser, A., Kaufman, R., J. , & Blumberg, R., S. (2016). The unfolded protein response in immunity and inflammation. *Nature Reviews Immunology, 16*(8), 469-484. doi:10.1038/nri.2016.62

Grover, S., Sharma, T., Singh, Y., Kohli, S., P, M., Singh, A., . . . Hasnain, S. E. (2018). The PGRS Domain of *Mycobacterium tuberculosis* PE_PGRS Protein Rv0297 Is Involved in Endoplasmic Reticulum Stress-Mediated Apoptosis through Toll-Like Receptor 4. *mBio, 9*(3). doi:10.1128/mBio.01017-18

Grynkiewicz, G., Poenie, M., & Tsien, R. Y. (1985). A new generation of $Ca^{2+}$ indicators with greatly improved fluorescence properties. *The Journal of Biological Chemistry, 260*(6), 3440-3450. doi:10.1016/S0021-9258(19)83641-4

Guerra, L., Cortes-Bratti, X., Guidi, R., & Frisan, T. (2011). The biology of the cytolethal distending toxins. *Toxins, 3*(3), 172-190. doi:10.3390/toxins3030172

Guerry, P. (2007). *Campylobacter* flagella: not just for motility. *Trends in microbiology (Regular ed.), 15*(10), 456-461. doi:10.1016/j.tim.2007.09.006

Guerry, P., Alm, R. A., Power, M. E., Logan, S. M., & Trust, T. J. (1991). Role of two flagellin genes in Campylobacter motility. *Journal of Bacteriology, 173*(15), 4757-4764. doi:10.1128/JB.173.15.4757-4764.1991

Guerry, P., Ewing, C. P., Schirm, M., Lorenzo, M., Kelly, J., Pattarini, D., . . . Logan, S. (2006). Changes in flagellin glycosylation affect *Campylobacter* autoagglutination and virulence. *Molecular microbiology, 60*(2), 299-311. doi:10.1111/j.1365-2958.2006.05100.x

Guerry, P., Szymanski, C. M., Prendergast, M. M., Hickey, T. E., Ewing, C. P., Pattarini, D. L., & Moran, A. P. (2002). Phase Variation of *Campylobacter jejuni* 81-176 Lipooligosaccharide Affects Ganglioside Mimicry and Invasiveness In Vitro. *Infection and Immunity, 70*(2), 787-793. doi:10.1128/IAI.70.2.787-793.2002

Gundogdu, O., da Silva, D. T., Mohammad, B., Elmi, A., Mills, D. C., Wren, B. W., & Dorrell, N. (2015). The *Campylobacter jejuni* MarR-like transcriptional regulators RrpA and RrpB both influence bacterial responses to oxidative and aerobic stresses. *Frontiers in Microbiology, 6*, 1-12. doi:10.3389/fmicb.2015.00724

Gundogdu, O., da Silva, D. T., Mohammad, B., Elmi, A., Wren, B. W., van Vliet, A. H. M., & Dorrell, N. (2016). The *Campylobacter jejuni* oxidative stress regulator RrpB is associated with a genomic hypervariable region and altered oxidative stress resistance. *Frontiers in Microbiology, 7*, 2117-2117. doi:10.3389/fmicb.2016.02117

Gundogdu, O., Mills, D. C., Elmi, A., Martin, M. J., Wren, B. W., & Dorrell, N. (2011). The *Campylobacter jejuni* transcriptional regulator Cj1556 plays a role in the oxidative and aerobic stress response and is important for bacterial survival in vivo. *Journal of Bacteriology, 193*(16), 4238-4249. doi:10.1128/JB.05189-11

Halder, P., Datta, C., Kumar, R., Sharma, A. K., Basu, J., & Kundu, M. (2015). The secreted antigen, HP0175, of *Helicobacter pylori* links the unfolded protein response (UPR) to autophagy in gastric epithelial cells. *Cellular Microbiology, 17*(5), 714-729. doi:10.1111/cmi.12396

Hameed, A., Woodacre, A., Machado, L. R., & Marsden, G. L. (2020). An updated classification system and review of the lipooligosaccharide biosynthesis gene locus in *Campylobacter jejuni*. *Frontiers in Microbiology, 11*, 677-677. doi:10.3389/fmicb.2020.00677

Harrer, A., Bücker, R., Boehm, M., Zarzecka, U., Tegtmeyer, N., Sticht, H., . . . Backert, S. (2019). *Campylobacter jejuni* enters gut epithelial cells and impairs intestinal barrier function through cleavage of occludin by serine protease HtrA. *Gut Pathogens, 11*(1), 4-4. doi:10.1186/s13099-019-0283-z

Havelaar, A. H., van Pelt, W., Ang, C. W., Wagenaar, J. A., van Putten, J. P. M., Gross, U., & Newell, D. G. (2009). Immunity to Campylobacter: its role in risk assessment and epidemiology.

He, Z., Gharaibeh, R. Z., Newsome, R. C., Pope, J. L., Dougherty, M. W., Tomkovich, S., . . . Jobin, C. (2019). *Campylobacter jejuni* promotes colorectal tumorigenesis through the action of cytolethal distending toxin. *Gut, 68*(2), 289. doi:10.1136/gutjnl-2018-317200

Heim, V. J., Stafford, C. A., & Nachbur, U. (2019). NOD Signaling and Cell Death. *Frontiers in cell and developmental biology, 7*, 208-208. doi:10.3389/fcell.2019.00208

Helmcke, I., Heumüller, S., Tikkanen, R., Schröder, K., & P., B. R. (2009). Identification of Structural Elements in Nox1 and Nox4 Controlling Localization and Activity. *Antioxidants & Redox Signaling, 11*(6), 1279-1287. doi:10.1089/ars.2008.2383

Hempstead, A. D., & Isberg, R. R. (2015). Inhibition of host cell translation elongation by *Legionella pneumophila* blocks the host cell unfolded protein response. *Proceedings of the National Academy of Sciences - PNAS, 112*(49), E6790-E6797. doi:10.1073/pnas.1508716112

Hendrixson, D. R. (2006). A phase-variable mechanism controlling the *Campylobacter jejuni* FlgR response regulator influences commensalism. *Molecular microbiology, 61*(6), 1646-1659. doi:10.1111/j.1365-2958.2006.05336.x

Hendrixson, D. R., Akerley, B. J., & DiRita, V. J. (2001). Transposon mutagenesis of *Campylobacter jejuni* identifies a bipartite energy taxis system required for motility. *Molecular microbiology, 40*(1), 214-224. doi:10.1046/j.1365-2958.2001.02376.x

Hetz, C., & Papa, F. R. (2018). The unfolded protein response and cell fate control. *Molecular Cell, 69*(2), 169-181. doi:10.1016/j.molcel.2017.06.017

Hickey, T. E., Baqar, S., Bourgeois, A. L., Ewing, C. P., & Guerry, P. (1999). *Campylobacter jejuni*-Stimulated Secretion of Interleukin-8 by INT407 Cells. *Infection and Immunity, 67*(1), 88-93. doi:10.1128/iai.67.1.88-93.1999

Hickey, T. E., McVeigh, A. L., Scott, D. A., Michielutti, R. E., Bixby, A., Carroll, S. A., . . . Guerry, P. (2000). *Campylobacter jejuni* cytolethal distending toxin mediates release of interleukin-8 from intestinal epithelial cells. *Infection and Immunity, 68*(12), 6535-6541. doi:10.1128/IAI.68.12.6535-6541.2000

Hodge, R. G., & Ridley, A. J. (2016). Regulating Rho GTPases and their regulators. *Nature reviews. Molecular cell biology, 17*(8), 496-510. doi:10.1038/nrm.2016.67

Holmström, K. M., & Finkel, T. (2014). Cellular mechanisms and physiological consequences of redox-dependent signalling. *Nature reviews. Molecular cell biology, 15*(6), 411-421. doi:10.1038/nrm3801

Hong, G., Davies, C., Omole, Z., Liaw, J., Grabowska, A. D., Canonico, B., . . . Gundogdu, O. (2023). Campylobacter jejuni Modulates Reactive Oxygen Species Production and NADPH Oxidase 1 Expression in Human Intestinal Epithelial Cells. *Cellular Microbiology, 2023*, 1-14. doi:10.1155/2023/3286330

Hong, G., Davies, C., Omole, Z., Liaw, J., Grabowska, A. D., Canonico, B., . . . Gundogdu, O. (2022). *Campylobacter jejuni* modulates reactive oxygen species production and NADPH oxidase 1 expression in human intestinal epithelial cells. *bioRxiv*, 2022.2003.2004.482506. doi:10.1101/2022.03.04.482506

Horton, R. M., Cai, Z., Ho, S. N., & Pease, L. R. (2013). Gene Splicing by Overlap Extension: Tailor-Made Genes Using the Polymerase Chain Reaction. *BioTechniques, 54*(3), 129-133. doi:10.2144/000114017

Hu, L., Raybourne, R. B., & Kopecko, D. J. (2005). Ca2+ release from host intracellular stores and related signal transduction during *Campylobacter jejuni* 81-176 internalization into human intestinal cells. *Microbiology (Society for General Microbiology), 151*(9), 3097-3105. doi:10.1099/mic.0.27866-0

Hu, P., Han, Z., Couvillon, A. D., Kaufman, R. J., & Exton, J. H. (2006). Autocrine Tumor Necrosis Factor Alpha Links Endoplasmic Reticulum Stress to the Membrane Death Receptor Pathway through IRE1α-Mediated NF-κB Activation and Down-Regulation of TRAF2 Expression. *Molecular and Cellular Biology, 26*(8), 3071-3084. doi:10.1128/MCB.26.8.3071-3084.2006

Hughes, K. T., & Chevance, F. F. V. (2008). Coordinating assembly of a bacterial macromolecular machine. *Nature reviews. Microbiology, 6*(6), 455-465. doi:10.1038/nrmicro1887

Humphrey, S., Chaloner, G., Kemmett, K., Davidson, N., Williams, N., Kipar, A., . . . Wigley, P. (2014). *Campylobacter jejuni* is not merely a commensal in commercial broiler chickens and affects bird welfare. *mBio, 5*(4), e01364-e01314. doi:10.1128/mBio.01364-14

Hussein, M. (2018). *Further investigation of the roles of fibronectin-binding proteins CadF and FlpA during Campylobacter jejuni interactions with intestinal epithelial cells.*

Hwang, S., Kim, M., Ryu, S., & Jeon, B. (2011). Regulation of oxidative stress response by CosR, an essential response regulator in *Campylobacter jejuni*. *PLOS One, 6*(7), e22300. doi:10.1371/journal.pone.0022300

Ibe, N. U., Subramanian, A., & Mukherjee, S. (2021). Non-canonical activation of the ER stress sensor ATF6 by *Legionella pneumophila* effectors. *Life science alliance, 4*(12), e202101247. doi:10.26508/lsa.202101247

Jain, D., Prasad, K. N., Sinha, S., & Husain, N. (2008). Differences in virulence attributes between cytolethal distending toxin positive and negative Campylobacter jejuni strains. *Journal of medical microbiology, 57*(3), 267-272. doi:10.1099/jmm.0.47317-0

Janssens, S., Pulendran, B., & Lambrecht, B. N. (2014). Emerging functions of the unfolded protein response in immunity. *Nature Immunology, 15*(10), 910. doi:10.1038/ni.2991

Jean, C., & Renée, M. T. (2014). Bacteria, the endoplasmic reticulum and the unfolded protein response: friends or foes? *Nature Reviews Microbiology, 13*(2), 73-82. doi:10.1038/nrmicro3393

Jheng, J.-R., Ho, J.-Y., & Horng, J.-T. (2014). ER stress, autophagy, and RNA viruses. *Frontiers in Microbiology, 5*, 388-388. doi:10.3389/fmicb.2014.00388

Jiang, F., Wang, X., Wang, B., Chen, L., Zhao, Z., Waterfield, N. R., . . . Jin, Q. (2016). The *Pseudomonas aeruginosa* Type VI Secretion PGAP1-like Effector Induces Host Autophagy by Activating Endoplasmic Reticulum Stress. *Cell reports (Cambridge), 16*(6), 1502-1509. doi:10.1016/j.celrep.2016.07.012

Jin, S., Joe, A., Lynett, J., Hani, E. K., Sherman, P., & Chan, V. L. (2001). JlpA, a novel surface-exposed lipoprotein specific to *Campylobacter jejuni*, mediates adherence to host epithelial cells. *Molecular microbiology, 39*(5), 1225-1236. doi:10.1111/j.1365-2958.2001.02294.x

Jin, S., Song, Y. C., Emili, A., Sherman, P. M., & Chan, V. L. (2003). JlpA of *Campylobacter jejuni* interacts with surface-exposed heat shock protein 90α and triggers signalling pathways leading to the activation of NF-κB and p38 MAP kinase in epithelial cells. *Cellular Microbiology, 5*(3), 165-174. doi:10.1046/j.1462-5822.2003.00265.x

Joep, G., Arthur, K., Randal, J. K., & Richard, S. B. (2016). The unfolded protein response in immunity and inflammation. *Nature Reviews Immunology, 16*(8), 469-484. doi:10.1038/nri.2016.62

Johnson, W. M., & Lior, H. (1987a). Production of Shiga toxin and a cytolethal distending toxin (CLDT) by serogroups of *Shigella* spp. *FEMS Microbiology Letters, 48*(1-2), 235-238. doi:10.1111/j.1574-6968.1987.tb02548.x

Johnson, W. M., & Lior, H. (1987b). Response of Chinese hamster ovary cells to a cytolethal distending toxin (CDT) of *Escherichia coli* and possible misinterpretation as heat-labile (LT) enterotoxin. *FEMS Microbiology Letters, 43*(1), 19-23. doi:10.1111/j.1574-6968.1987.tb02091.x

Johnson, W. M., & Lior, H. (1988). A new heat-labile cytolethal distending toxin (CLDT) produced by *Campylobacter* spp. *Microbial Pathogenesis, 4*(2), 115-126. doi:10.1016/0882-4010(88)90053-8

Jones, M. A., Marston, K. L., Woodall, C. A., Maskell, D. J., Linton, D., Karlyshev, A. V., . . . Barrow, P. A. (2004). Adaptation of *Campylobacter jejuni* NCTC11168 to High-Level Colonization of the Avian Gastrointestinal Tract. *Infection and Immunity, 72*(7), 3769-3776. doi:10.1128/IAI.72.7.3769-3776.2004

Juhasz, A., Markel, S., Gaur, S., Liu, H., Lu, J., Jiang, G., . . . Doroshow, J. H. (2017). NADPH oxidase 1 supports proliferation of colon cancer cells by modulating reactive oxygen species-dependent signal transduction. *The Journal of Biological Chemistry, 292*, 7866-7887. doi:10.1074/jbc.M116.768283

Kaakoush, N. O., Castaño-Rodríguez, N., Mitchell, H. M., & Man, S. M. (2015). Global epidemiology of *Campylobacter* infection. *Clinical Microbiology Reviews, 28*(3), 687-720. doi:10.1128/CMR.00006-15

Kalischuk, L. D., Inglis, G. D., & Buret, A. G. (2007). Strain-dependent induction of epithelial cell oncosis by *Campylobacter jejuni* is correlated with invasion ability and is independent of cytolethal distending toxin. *Microbiology (Society for General Microbiology), 153*(9), 2952-2963. doi:10.1099/mic.0.2006/003962-0

Karlyshev, A. V., Everest, P., Linton, D., Cawthraw, S., Newell, D. G., & Wren, B. W. (2004). The *Campylobacter jejuni* general glycosylation system is important for attachment to human epithelial cells and in the colonization of chicks. *Microbiology (Society for General Microbiology), 150*(6), 1957-1964. doi:10.1099/mic.0.26721-0

Karlyshev, A. V., Henderson, J., Ketley, J. M., & Wren, B. W. (1999). Procedure for the investigation of bacterial genomes : Random shot-gun cloning, sample sequencing and mutagenesis of *Campylobacter jejuni*. *BioTechniques, 26*(1), 50-56. doi:10.2144/99261bm07

Karlyshev, A. V., Linton, D., Gregson, N. A., Lastovica, A. J., & Wren, B. W. (2000). Genetic and biochemical evidence of a *Campylobacter jejuni* capsular polysaccharide that accounts for Penner serotype specificity. *Molecular microbiology, 35*(3), 529-541. doi:10.1046/j.1365-2958.2000.01717.x

Karlyshev, A. V., Linton, D., Gregson, N. A., & Wren, B. W. (2002). A novel paralogous gene family involved in phase-variable flagella-mediated motility in Campylobacter jejuni. *Microbiology, 148*(2), 473-480. doi:10.1099/00221287-148-2-473

Karlyshev, A. V., McCrossan, M. V., & Wren, B. W. (2001). Demonstration of polysaccharide capsule in *Campylobacter jejuni* using electron microscopy. *Infection and Immunity, 69*(9), 5921-5924. doi:10.1128/IAI.69.9.5921-5924.2001

Karlyshev, A. V., Thacker, G., Jones, M. A., Clements, M. O., & Wren, B. W. (2014). *Campylobacter jejuni* gene *cj0511* encodes a serine peptidase essential for colonisation. *FEBS open bio, 4*(1), 468-472. doi:10.1016/j.fob.2014.04.012

Kawahara, T., Kohijima, M., Kuwano, Y., Mino, H., Teshima-Kondo, S., Takeya, R., . . . Rokutan, K. (2005). *Helicobacter pylori* lipopolysaccharide activates Rac1 and transcription of NADPH oxidse Nox1 and its organizer NoxO1. *The American Journal of Physiology-Cell Physiology, 288*, C450-C457. doi:10.1152/ajpcell.00319.2004

Kawahara, T., Kuwano, Y., Teshima-Kondo, S., Takeya, R., Sumimoto, H., Kishi, K., . . . Rokutan, K. (2016). Role of nicotinamide adenine dinucleotide phosphate oxidase 1 in oxidative burst responsse to toll-like receptor 5 signaling in large intestinal epithelial cells. *The Journal of Immunology, 172*, 3051-3058. doi:10.4049/jimmunol.172.5.3051

Kawai, T., & Akira, S. (2010). The role of pattern-recognition receptors in innate immunity: update on Toll-like receptors. *Nature Immunology, 11*(5), 373-384. doi:10.1038/ni.1863

Kay, E., Cuccui, J., & Wren, B. W. (2019). Recent advances in the production of recombinant glycoconjugate vaccines. *npj vaccines, 4*(1), 16-16. doi:10.1038/s41541-019-0110-z

Keestra-Gounder, A. M., Byndloss, M. X., Seyffert, N., Young, B. M., Chávez-Arroyo, A., Tsai, A. Y., . . . Tsolis, R. M. (2016). NOD1/NOD2 signaling links ER stress with inflammation. *Nature, 532*(7599), 394-397. doi:10.1038/nature17631

Kersulyte, D., Velapatino, B., Mukhopadhyay, A. K., Cahuayme, L., Bussalleu, A., Combe, J., . . . Berg, D. E. (2003). Cluster of Type IV Secretion Genes in *Helicobacter pylori*'s Plasticity Zone. *The Journal of Bacteriology, 185*(13), 3764-3772. doi:10.1128/JB.185.13.3764-3772.2003

Kim, S., Joe, Y., Surh, Y.-J., & Chung, H. T. (2018). Differential Regulation of Toll-Like Receptor-Mediated Cytokine Production by Unfolded Protein Response. *Oxidative Medicine and Cellular Longevity, 2018*, 9827312-9827318. doi:10.1155/2018/9827312

Konkel, M. E., Garvis, S. G., Tipton, S. L., Anderson, J. D. E., & Cieplak, J. W. (1997). Identification and molecular cloning of a gene encoding a fibronectin-binding protein (CadF) from *Campylobacter jejuni*. *Molecular microbiology, 24*(5), 953-963. doi:10.1046/j.1365-2958.1997.4031771.x

Konkel, M. E., Hayes, S. F., Joens, L. A., & Cieplak Jr, W. (1992). Characteristics of the internalization and intracellular survival of *Campylobacter jejuni* in human epithelial cell cultures. *Microbial Pathogenesis, 13*(5), 357-370. doi:10.1016/0882-4010(92)90079-4

Konkel, M. E., Kim, B. J., Rivera-Amill, V., & Garvis, S. G. (1999). Bacterial secreted proteins are required for the internaliztion of *Campylobacter jejuni* into cultured mammalian cells. *Molecular microbiology, 32*(4), 691-701.

Konkel, M. E., Klena, J. D., Rivera-Amill, V., Monteville, M. R., Biswas, D., Raphael, B., & Mickelson, J. (2004). Secretion of Virulence Proteins from *Campylobacter jejuni* Is Dependent on a Functional Flagellar Export Apparatus. *Journal of Bacteriology, 186*(11), 3296-3303. doi:10.1128/JB.186.11.3296-3303.2004

Konkel, M. E., Larson, C. L., & Flanagan, R. C. (2010). *Campylobacter jejuni* FlpA binds fibronectin and is required for maximal host cell adherence. *Journal of Bacteriology, 192*(1), 68-76. doi:10.1128/JB.00969-09

Konkel, M. E., Samuelson, D. R., Eucker, T. P., Shelden, E. A., & O'Loughlin, J. L. (2013). Invasion of epithelial cells by *Campylobacter jejuni* is independent of caveolae. *Cell communication and signaling, 11*(1), 100-100. doi:10.1186/1478-811X-11-100

Konkel, M. E., Talukdar, P. K., Negretti, N. M., & Klappenbach, C. M. (2020). Taking control: *Campylobacter jejuni* binding to fibronectin sets the stage for cellular adherence and invasion. *Frontiers in Microbiology, 11*, 564-564. doi:10.3389/fmicb.2020.00564

Korlath, J. A., Osterholm, M. T., Judy, L. A., Forfang, J. C., & Robinson, R. A. (1985). A point-source outbreak of campylobacteriosis associated with consumption of raw milk. *Journal of Infectious Diseases, 152*(3), 592-596. doi:10.1093/infdis/152.3.592

Krause-Gruszczynska, M., Boehm, M., Rohde, M., Tegtmeyer, N., Takahashi, S., Buday, L., . . . Backert, S. (2011). The signaling pathway of *Campylobacter jejuni*-induced Cdc42 activation: Role of fibronectin, integrin beta1, tyrosine kinases and guanine exchange factor Vav2. *Cell communication and signaling, 9*(1), 32-32. doi:10.1186/1478-811X-9-32

Krause-Gruszczynska, M., Rohde, M., Hartig, R., Genth, H., Schmidt, G., Keo, T., . . . Backert, S. (2007). Role of the small Rho GTPases Rac1 and Cdc42 in host cell invasion of *Campylobacter jejuni*. *Cellular Microbiology, 9*(10), 2431-2444. doi:10.1111/j.1462-5822.2007.00971.x

Kreutzberger, M. A. B., Ewing, C., Poly, F., Wang, F., & Egelman, E. H. (2020). Atomic structure of the *Campylobacter jejuni* flagellar filament reveals how ε Proteobacteria escaped Toll-like receptor 5 surveillance. *Proceedings of the National Academy of Sciences - PNAS, 117*(29), 16985-16991. doi:10.1073/pnas.2010996117

Kumar, S., & Dhiman, M. (2018). Inflammasome activation and regulation during *Helicobacter pylori* pathogenesis. *Microbial Pathogenesis, 125*, 468-474. doi:10.1016/j.micpath.2018.10.012

Kuss-Duerkop, S. K., & Keestra-Gounder, A. M. (2020). NOD1 and NOD2 Activation by Diverse Stimuli: a Possible Role for Sensing Pathogen-Induced Endoplasmic Reticulum Stress. *Infection and Immunity, 88*(7). doi:10.1128/IAI.00898-19

Lai, C.-K., Chen, Y.-A., Lin, C.-J., Lin, H.-J., Kao, M.-C., Huang, M.-Z., . . . Lai, C.-H. (2016). Molecular mechanisms and potential clinical applications of *Campylobacter jejuni* cytolethal distending toxin. *Frontiers in Cellular and Infection Microbiology, 6*, 1-8. doi:10.3389/fcimb.2016.00009

Lara-Tejero, M., & Galan, J. E. (2001). CdtA, CdtB, and CdtC Form a tripartite complex that is required for cytolethal distending toxin activity. *Infection and Immunity, 69*(7), 4358-4365. doi:10.1128/IAI.69.7.4358-4365.2001

Laurindo, F. R. M., Araujo, T. L. S., & Abrahao, T. B. (2014). Nox NADHPH Oxidases and the Endoplasmic Reticulum. *Antioxidants & Redox Signaling, 20*, 2755-2775. doi:10.1089/ars.2013.5605

Lavelle, E. C., Murphy, C., O'Neill, L. A. J., & Creagh, E. M. (2010). The role of TLRs, NLRs, and RLRs in mucosal innate immunity and homeostasis. *Mucosal immunology, 3*(1), 17-28. doi:10.1038/mi.2009.124

Lee, J., Hyeon, D. Y., & Hwang, D. (2020). Single-cell multiomics: technologies and data analysis methods. *Experimental & molecular medicine, 52*(9), 1428-1442. doi:10.1038/s12276-020-0420-2

Lee, R. B., Hassane, D. C., Cottle, D. L., & Pickett, C. L. (2003). Interactions of *Campylobacter jejuni* cytolethal distending toxin subunits CdtA and CdtC with HeLa cells. *Infection and Immunity, 71*(9), 4883-4890. doi:10.1128/IAI.71.9.4883-4890.2003

Leoni, G., Alam, A., Neumann, P.-A., Lambeth, J. D., Cheng, G., McCoy, J., . . . Nusrat, A. (2013). Annexin A1, formyl peptide receptor, and Nox1 orchestrate epithelial repair. *The Journal of Clinical Investigation, 123*, 443-454. doi:10.1172/JCI65831

Li, G., Scull, C., Ozcan, L., & Tabas, I. (2010). NADPH oxidase links endoplasmic reticulum stress, oxidative stress, and PKR activation to induce apoptosis. *The Journal of Cell Biology, 191*(6), 1113-1125. doi:10.1083/jcb.201006121

Li, Y., & Trush, M. A. (1998). Diphenyleneiodonium, an NAD(P)H Oxidase Inhibitor, also Potently Inhibits Mitochondrial Reactive Oxygen Species Production. *Biochemical and Biophysical Research Communications, 253*(2), 295-299. doi:10.1006/bbrc.1998.9729

Liaw, J., Hong, G., Davies, C., Elmi, A., Sima, F., Stratakos, A., . . . Dorrell, N. (2019). The Campylobacter jejuni Type VI Secretion System Enhances the Oxidative Stress Response and Host Colonization. *Frontiers in Microbiology, 10*, 2864. doi:10.3389/fmicb.2019.02864

Lindmark, B., Rompikuntal, P. K., Vaitkevicius, K., Song, T., Mizunoe, Y., Uhlin, B. E., . . . Wai, S. N. (2009). Outer membrane vesicle-mediated release of cytolethal distending toxin (CDT) from *Campylobacter jejuni*. *BMC microbiology, 9*(1), 220-220. doi:10.1186/1471-2180-9-220

Lindsay Davis, & DiRita, V. (2008). Growth and laboratory maintenance of *Campylobacter jejuni*. *Current Protocols in Microbiology, 10*(1), Chapter 8 Unit 8A.1.1-8A.1.7. doi:10.1002/9780471729259.mc08a01s10

Linton, D., Dorrell, N., Hitchen, P. G., Amber, S., Karlyshev, A. V., Morris, H. R., . . . Wren, B. W. (2005). Functional analysis of the Campylobacter jejuni N-linked protein glycosylation pathway. *Molecular microbiology, 55*(6), 1695-1703. doi:10.1111/j.1365-2958.2005.04519.x

Linton, D., Gilbert, M., Hitchen, P. G., Dell, A., Morris, H. R., Wakarchuk, W. W., . . . Wren, B. W. (2000). Phase variation of a β-1,3 galactosyltransferase involved in generation of the ganglioside GM1-like lipo-oligosaccharide of *Campylobacter jejuni*. *Molecular microbiology, 37*(3), 501-514. doi:10.1046/j.1365-2958.2000.02020.x

Lipinski, S., Petersen, B.-S., Barann, M., Piecyk, A., Tran, F., Mayr, G., . . . Rosenstiel, P. (2019). Missense variants in NOX1 and p22phox in a case of very-early-onset inflammatory bowel disease are functionally linked to NOD2. *Cold Spring Harbor Molecular Case Studies, 5*(1). doi:10.1101/mcs.a002428

Liu, J., Ibi, D., Taniguchi, K., Lee, J., Herrema, H., Akosman, B., . . . Ozcan, U. (2016). Inflammation Improves Glucose Homeostasis through IKKβ-XBP1s Interaction. *Cell, 167*(4), 1052-1066.e1018. doi:10.1016/j.cell.2016.10.015

Logan, S. M., Kelly, J. F., Thibault, P., Ewing, C. P., & Guerry, P. (2002). Structural heterogeneity of carbohydrate modifications affects serospecificity of *Campylobacter* flagellins. *Molecular microbiology, 46*(2), 587-597. doi:10.1046/j.1365-2958.2002.03185.x

Ma, M., Li, H., Wang, P., Yang, W., Mi, R., Zhuang, J., . . . Shen, H. (2021). ATF6 aggravates angiogenesis-osteogenesis coupling during ankylosing spondylitis by mediating FGF2 expression in chondrocytes. *iScience, 24*(7), 102791-102791. doi:10.1016/j.isci.2021.102791

Mabbott, N., Donaldson, D., Ohno, H., Williams, I. R., & Mahajan, A. (2013). Microfold (M) cells: important immunosurveillance posts in the intestinal epithelium. *Mucosal immunology, 6*, 666-667. doi:https://doi.org/10.1038/mi.2013.30

Macpherson, A. J., McCoy, K. D., Johansen, F. E., & Brandtzaeg, P. (2008). The immune geography of IgA induction and function. *Mucosal immunology, 1*(1), 11-22. doi:10.1038/mi.2007.6

Mahadevan, N. R., Rodvold, J., Sepulveda, H., Rossi, S., Drew, A. F., & Zanetti, M. (2011). Transmission of endoplasmic reticulum stress and pro-inflammation from tumor cells to myeloid cells. *Proceedings of the National Academy of Sciences - PNAS, 108*(16), 6561-6566. doi:10.1073/pnas.1008942108

Mahameed, M., Wilhelm, T., Darawshi, O., Obiedat, A., Tommy, W.-S., Chintha, C., . . . Tirosh, B. (2019). The unfolded protein response modulators GSK2606414 and KIRA6 are potent KIT inhibitors. *Cell death & disease, 10*(4), 300. doi:10.1038/s41419-019-1523-3

Maly, D. J., & Papa, F. R. (2014). Druggable sensors of the unfolded protein response. *Nature chemical biology, 10*(11), 892-901. doi:10.1038/nchembio.1664

Manea, S. A., Todirita, A., Raicu, M., & Manea, A. (2014). C/EBP transcription factors regulate NADPH oxidase in human aortic smooth muscle cells. *Journal of Cellular and Molecular Medicine, 18*(7), 1467-1477. doi:10.1111/jcmm.12289

Mantis, N. J., Rol, N., & Corthésy, B. (2011). Secretory IgA's complex roles in immunity and mucosal homeostasis in the gut. *Mucosal immunology, 4*(6), 603-611. doi:10.1038/mi.2011.41

Marsh, J. W., Humphrys, M. S., & Myers, G. S. A. (2017). A Laboratory Methodology for Dual RNA-Sequencing of Bacteria and their Host Cells In Vitro. *Frontiers in Microbiology, 8*, 1830-1830. doi:10.3389/fmicb.2017.01830

Martinon, F., Chen, X., Lee, A.-H., & Glimcher, L. H. (2010). TLR activation of the transcription factor XBP1 regulates innate immune responses in macrophages. *Nature Immunology, 11*(5), 411-418. doi:10.1038/ni.1857

Márton, M., Bánhegyi, G., Gyöngyösi, N., Kálmán, E. É., Pettkó-Szandtner, A., Káldi, K., & Kapuy, O. (2022). A systems biological analysis of the ATF4-GADD34-CHOP regulatory triangle upon endoplasmic reticulum stress. *FEBS open bio, 12*(11), 2065-2082. doi:10.1002/2211-5463.13484

Matziouridou, C., Rocha, S. C., Haabeth, O., Rudi, K., Carlsen, H., & Kielland, A. (2018). iNOS- and Nox1-dependent ROS production maintains bacterial homeostasis in the ileum of mice. *Mucosal immunology, 11*, 774-784. doi:10.1038/mi.2017.106

Maue, A. C., Mohawk, K. L., Giles, D. K., Poly, F., Ewing, C. P., Jiao, Y., . . . Guerry, P. (2013). The polysaccharide capsule of *Campylobacter jejuni* modulates the host immune response. *Infection and Immunity, 81*(3), 665-672. doi:10.1128/IAI.01008-12

Maurel, M., Chevet, E., Tavernier, J., & Gerlo, S. (2014). Getting RIDD of RNA: IRE1 in cell fate regulation. *Trends in Biochemical Sciences, 39*(5), 245-254. doi:10.1016/j.tibs.2014.02.008

Mehat, J. W., Park, S. F., van Vliet, A. H. M., & La Ragione, R. M. (2018). CapC, a Novel Autotransporter and Virulence Factor of *Campylobacter jejuni*. *Applied and Environmental Microbiology, 84*(16). doi:10.1128/AEM.01032-18

Mehlitz, A., Karunakaran, K., Herweg, J. A., Krohne, G., Linde, S., Rieck, E., . . . Rudel, T. (2014). The chlamydial organism *Simkania negevensis* forms ER vacuole contact sites and inhibits ER-stress. *Cellular Microbiology, 16*(8), 1224-1243. doi:10.1111/cmi.12278

Misiewicz, M., Déry, M.-A., Foveau, B., Jodoin, J., Ruths, D., & LeBlanc, A. C. (2013). Identification of a Novel Endoplasmic Reticulum Stress Response Element Regulated by XBP1. *The Journal of Biological Chemistry, 288*(28), 20378-20391. doi:10.1074/jbc.M113.457242

Miyamoto, S., Kathz, B.-Z., Lafrenie, R. M., & Yamada, K. M. (1998). Fibronectin and integrins in cell adhesion, signaling, and morphogenesis. *Annals of the New York Academy of Sciences, 857*(1), 119-129. doi:10.1111/j.1749-6632.1998.tb10112.x

Moran, A. P. (1997). Structure and conserved characteristics of *Campylobacter jejuni* lipopolysaccharides. *The Journal of infectious diseases, 176*(Supplement-2), S115-S121. doi:10.1086/513781

Morinaga, N., Yahiro, K., Matsuura, G., Moss, J., & Noda, M. (2008). Subtilase cytotoxin, produced by Shiga-toxigenic *Escherichia coli,* transiently inhibits protein synthesis of Vero cells via degradation of BiP and induces cell cycle arrest at G1 by downregulation of cyclin D1. *Cellular Microbiology, 10*(4), 921-929. doi:10.1111/j.1462-5822.2007.01094.x

Mowat, A. M. (2003). Anatomical basis of tolerance and immunity to intestinal antigens. *Nature reviews. Immunology, 3*(4), 331-341. doi:10.1038/nri1057

Musch, M. W., Clarke, L. L., Mamah, D., Gawenis, L. R., Zhang, Z., Ellsworth, W., . . . Barrett, T. A. (2002). T cell activation causes diarrhea by increasing intestinal permeability and inhibiting epithelial Na+/K+-ATPase. *The Journal of Clinical Investigation, 110*(11), 1739-1747. doi:10.1172/JCI0215695

Nakayama, Y., Endo, M., Tsukano, H., Mori, M., Oike, Y., & Gotoh, T. (2010). Molecular mechanisms of the LPS-induced non-apoptotic ER stress-CHOP pathway. *Journal of biochemistry (Tokyo), 147*(4), 471-483. doi:10.1093/jb/mvp189

Nam Shin, J. E., Ackloo, S., Mainkar, A. S., Monteiro, M. A., Pang, H., Penner, J. L., & Aspinall, G. O. (1997). Lipo-oligosaccharides of *Campylobacter jejuni* serotype O:10. Structures of core oligosaccharide regions from a bacterial isolate from a patient with the Miller-Fisher

syndrome and from the serotype reference strain. *Carbohydrate research, 305*(2), 223-232. doi:10.1016/S0008-6215(97)00259-0

Nami, B., Azzawri, A., Ucar, V. B., & Acar, H. (2020). Recombinant *Helicobacter pylori* CagA protein induces endoplasmic reticulum stress and autophagy in human cells. *bioRxiv*, 2020.2006. 2026.174615.

Neal-McKinney, J. M., & Konkel, M. E. (2012). The *Campylobacter jejuni* CiaC virulence protein is secreted from the flagellum and delivered to the cytosol of host cells. *Frontiers in Cellular and Infection Microbiology, 2*, 31. doi:10.3389/fcimb.2012.00031

Negretti, N. M., Gourley, C. R., Talukdar, P. K., Clair, G., Klappenbach, C. M., Lauritsen, C. J., . . . Konkel, M. E. (2021). The *Campylobacter jejuni* CiaD effector co-opts the host cell protein IQGAP1 to promote cell entry. *Nature Communications, 12*(1), 1339-1339. doi:10.1038/s41467-021-21579-5

Newell, D. G. (2001). Animal models of *Campylobacter jejuni* colonization and disease and the lessons to be learned from similar Helicobacter pylori models. *Journal of applied microbiology, 90*(S6), 57S-67S. doi:10.1046/j.1365-2672.2001.01354.x

Nisimoto, Y., Tsubouchi, R., Diebold, B. A., Qiao, S., Ogawa, H., Ohara, T., & Tamura, M. (2008). Activation of NADPH oxidase 1 in tumour colon epithelial cells. *Biochemical Journal, 415*, 57-65. doi:10.1042/BJ20080300

Noah, T. K., Donahue, B., & Shroyer, N. F. (2011). Intestinal development and differentiation. *Experimental cell research, 317*(19), 2702-2710. doi:10.1016/j.yexcr.2011.09.006

Nougayrède, J. P., Fernandes, P. J., & Donnenberg, M. S. (2003). Adhesion of enteropathogenic *Escherichia coli* to host cells. *Cellular Microbiology, 5*(6), 359-372. doi:10.1046/j.1462-5822.2003.00281.x

Nowakowska-Gołacka, J., Sominka, H., Sowa-Rogozińska, N., & Słomińska-Wojewódzka, M. (2019). Toxins Utilize the Endoplasmic Reticulum-Associated Protein Degradation Pathway in Their Intoxication Process. *International Journal of Molecular Sciences, 20*(6), 1307. doi:10.3390/ijms20061307

Nowshin Papri, Zhahirul Islam, Sonja E. Leonhard, Quazi D. Mohammad, Hubert P. Endtz, & Jacobs, B. C. (2021). Guillain–Barré syndrome in low-income and middle-income countries: challenges and prospects. *Nature Reviews Neurology, 17*, 285-296. doi:https://doi.org/10.1038/s41582-021-00467-y

Nunoshiba, T., Hidalgo, E., Amabile Cuevas, C. F., & Demple, B. (1992). Two-stage control of an oxidative stress regulon: the *Escherichia coli* SoxR protein triggers redox-inducible expression of the soxS regulatory gene. *Journal of Bacteriology, 174*(19), 6054-6060. doi:10.1128/jb.174.19.6054-6060.1992

O'Malley, Y. Q., Reszka, K. J., Rasmussen, G. T., Abdalla, M. Y., Denning, G. M., & Britigan, B. E. (2003). The *Pseudomonas* secretory product pyocyanin inhibits catalase activity in human

lung epithelial cells. *Am J Physiol Lung Cell Mol Physiol, 285*, L1077–L1086,. doi:https://doi.org/10.1152/ajplung.00198.2003

O Cróinín, T., & Backert, S. (2012). Host epithelial cell invasion by *Campylobacter jejuni:* trigger or zipper mechanism? *Frontiers in Cellular and Infection Microbiology, 2*, 25-25. doi:10.3389/fcimb.2012.00025

Paerhati, P., Liu, J., Jin, Z., Jakoš, T., Zhu, S., Qian, L., . . . Yuan, Y. (2022). Advancements in Activating Transcription Factor 5 Function in Regulating Cell Stress and Survival. *International Journal of Molecular Sciences, 23*(13), 7129. doi:10.3390/ijms23137129

Paiva, C. N., & Bozza, M. T. (2014). Are reactive oxygen species always detrimental to pathogens? *Antioxidants & Redox Signaling, 20*, 1000-1037. doi:10.1089/ars.2013.5447

Palyada, K., Sun, Y.-Q., Flint, A., Butcher, J., Naikare, H., & Stintzi, A. (2009). Characterization of the oxidative stress stimulon and PerR regulon of *Campylobacter jejuni*. *BMC Genomics, 10*(1), 481-481. doi:10.1186/1471-2164-10-481

Park, S. F. (2002). The physiology of *Campylobacter* species and its relevance to their role as foodborne pathogens. *International journal of food microbiology, 74*(3), 177-188. doi:10.1016/S0168-1605(01)00678-X

Parkhill, J., Wren, B. W., Mungall, K., Ketley, J. M., Churcher, C., Basham, D., . . . Barrell, B. G. (2000). The genome sequence of the food-borne pathogen *Campylobacter jejuni* reveals hypervariable sequences. *Nature, 403*(6770), 665. doi:10.1038/35001088

Paton, A. W., Beddoe, T., Thorpe, C. M., Whisstock, J. C., Wilce, M. C. J., Rossjohn, J., . . . Paton, J. C. (2006). AB5 subtilase cytotoxin inactivates the endoplasmic reticulum chaperone BiP. *Nature (London), 443*(7111), 548-552. doi:10.1038/nature05124

Pedron, T., Parsot, C., Kim, D. W., Mateescu, B., Sansonetti, P. J., Arbibe, L., . . . Batsche, E. (2007). An injected bacterial effector targets chromatin access for transcription factor NF-κB to alter transcription of host genes involved in immune responses. *Nature Immunology, 8*(1), 47-56. doi:10.1038/ni1423

Pedruzzi, E., Guichard, C., Ollivier, V., Driss, F., Fay, M., Prunet, C., . . . Ogier-Denis, E. (2004). NAD(P)H Oxidase Nox-4 mediates 7-ketocholesterol-induced endoplasmic reticulum stress and apoptosis in human aortic smooth muscle cells. *Molecular and Cellular Biology, 24*(24), 10703. doi:10.1128/MCB.24.24.10703-10717.2004

Pei, Z., Burucoa, C., Grignon, B., Baqar, S., Huang, X. Z., Kopecko, D. J., . . . Blaser, M. J. (1998). Mutation in the peb1A locus of *Campylobacter jejuni* reduces interactions with epithelial cells and intestinal colonization of mice. *Infection and Immunity, 66*(3), 938-943. doi:10.1128/IAI.66.3.938-943.1998

Penner, J. L., Hennessy, J. N., & Congi, R. V. (1983). Serotyping of *Campylobacter jejuni* and *Campylobacter coli* on the basis of thermostable antigens. *European journal of clinical microbiology, 2*(4), 378–383. doi:https://doi.org/10.1007/BF02019474

Pickett, C. L., Pesci, E. C., Cottle, D. L., Russell, G., Erdem, A. N., Zeytin, H., & O'Brien, A. (1996). Prevalence of cytolethal distending toxin production in *Campylobacter jejuni* and relatedness of *Campylobacter* sp. *cdtB* genes. *Infection and Immunity, 64*(6), 2070-2078.

Pillich, H., Loose, M., Zimmer, K. P., & Chakraborty, T. (2012). Activation of the unfolded protein response by *Listeria monocytogenes*. *Cellular Microbiology, 14*(6), 949-964. doi:10.1111/j.1462-5822.2012.01769.x

Pizarro-Cerdá, J., & Cossart, P. (2006). Bacterial adhesion and entry into host cells. *Cell, 124*(4), 715-727. doi:10.1016/j.cell.2006.02.012

Platts-Mills, J. A., & Kosek, M. (2014). Update on the burden of *Campylobacter* in developing countries. *Current opinion in infectious diseases, 27*(5), 444-450. doi:10.1097/QCO.0000000000000091

Radomska, K. A., Wösten, M. M. S. M., Ordoñez, S. R., Wagenaar, J. A., & van Putten, J. P. M. (2017). Importance of *Campylobacter jejuni* FliS and FliW in flagella biogenesis and flagellin secretion. *Frontiers in Microbiology, 8*, 1060-1060. doi:10.3389/fmicb.2017.01060

Rathinam, V. A. K., Appledorn, D. M., Hoag, K. A., Amalfitano, A., & Mansfield, L. S. (2009). *Campylobacter jejuni*-Induced Activation of Dendritic Cells Involves Cooperative Signaling through Toll-Like Receptor 4 (TLR4)-MyD88 and TLR4-TRIF Axes. *Infection and Immunity, 77*(6), 2499-2507. doi:10.1128/IAI.01562-08

Reeser, R. J., Medler, R. T., Billington, S. J., Jost, B. H., & Joens, L. A. (2007). Characterization of *Campylobacter jejuni* biofilms under defined growth conditions. *Applied and Environmental Microbiology, 73*(6), 1908-1913. doi:10.1128/AEM.00740-06

Rehwinkel, J., & Gack, M. U. (2020). RIG-I-like receptors: their regulation and roles in RNA sensing. *Nature reviews. Immunology, 20*(9), 537-551. doi:10.1038/s41577-020-0288-3

Ren, F., Li, X., Tang, H., Jiang, Q., Yun, X., Fang, L., . . . Jiao, X.-A. (2018). Insights into the impact of flhF inactivation on *Campylobacter jejuni* colonization of chick and mice gut. *BMC microbiology, 18*(1), 149-149. doi:10.1186/s12866-018-1318-1

Rhyu, D. Y., Yang, Y., Ha, H., Lee, G. T., Song, J. S., Uh, S. T., & Lee, H. B. (2005). Role of reactive oxygen species in TGF-beta1-induced mitogen-activated protein kinase activation and epithelial-mesenchymal transition in renal tubular epithelial cells. *Journal of the American Society of Nephrology, 16*(3), 667-675.

Riganti, C., Gazzano, E., Polimeni, M., Costamagna, C., Bosia, A., & Ghigo, D. (2004). Diphenyeleneiodonium inhibits the cell redox metabolism and induces oxidative stress. *The Journal of Biological Chemistry, 279*, 47726-47731. doi:10.1074/jbc.M406314200

Robinson, L., Liaw, J., Omole, Z., Xia, D., van Vliet, A. H. M., Corcionivoschi, N., . . . Gundogdu, O. (2021). Bioinformatic Analysis of the *Campylobacter jejuni* Type VI Secretion System and Effector Prediction. *Frontiers in Microbiology, 12*, 694824-694824. doi:10.3389/fmicb.2021.694824

Rohart, F., Gautier, B., Singh, A., & Lê Cao, K.-A. (2017). mixOmics: An R package for 'omics feature selection and multiple data integration. *PLoS computational biology, 13*(11), e1005752-e1005752. doi:10.1371/journal.pcbi.1005752

Rosenberger, C. M., Brumell, J. H., & Finlay, B. B. (2000). Microbial pathogenesis: Lipid rafts as pathogen portals. *Current biology, 10*(22), R823-R825. doi:10.1016/S0960-9822(00)00788-0

Rudel, T., Kepp, O., & Kozjak-Pavlovic, V. (2010). Interactions between bacterial pathogens and mitochondrial cell death pathways. *Nature reviews. Microbiology, 8*(10), 693-705. doi:10.1038/nrmicro2421

Samuelson, D. R., & Konkel, M. E. (2013). Serine phosphorylation of cortactin is required for maximal host cell invasion by *Campylobacter jejuni*. *Cell communication and signaling, 11*(1), 82-82. doi:10.1186/1478-811X-11-82

Santos, C. X. C., Tanaka, L. Y., Wosniak, J. J., & Laurindo, F. R. M. (2009). Mechanisms and implications of reactive oxygen species generation during the unfolded protein response: roles of endoplasmic reticulum oxidoreductases, mitochondrial electron transport, and NADPH oxidase. *Antioxidants & Redox Signaling, 11*(10), 2409-2427. doi:https://doi.org/10.1089/ars.2009.2625

Schmittgen, T. D., & Livak, K. J. (2008). Analyzing real-time PCR data by the comparative $C_T$ method. *Nature Protocols, 3*(6), 1101-1108. doi:10.1038/nprot.2008.73

Schneider, C. A., Rasband, W. S., & Eliceiri, K. W. (2012). NIH Image to ImageJ: 25 years of image analysis. *Nature methods, 9*(7), 671-675. doi:10.1038/nmeth.2089

Schwarz, D. S., & Blower, M. D. (2015). The endoplasmic reticulum: structure, function and response to cellular signaling. doi:10.1007/s00018-015-2052-6

Schwerd, T., Bryant, R. V., Pandey, S., Capitani, M., Meran, L., Cazier, J. B., . . . Uhlig, H. H. (2018). NOX1 loss-of-function genetic variants in patients with inflammatory bowel disease. *Mucosal immunology*, 562-574. doi:10.17863/CAM.18641

Sean, T.-A., & Shaeri, M. (2015). *Legionella* suppresses the host unfolded protein response via multiple mechanisms. *Nature Communications, 6*(1), 1-10. doi:10.1038/ncomms8887

Sehgal, P., Szalai, P., Olesen, C., Praetorius, H. A., Nissen, P., Christensen, S. B., . . . Møller, J. V. (2017). Inhibition of the sarco/endoplasmic reticulum (ER) Ca2+-ATPase by thapsigargin analogs induces cell death via ER Ca2+ depletion and the unfolded protein response. *The Journal of Biological Chemistry, 292*(48), 19656-19673. doi:10.1074/jbc.M117.796920

Sharafutdinov, I., Esmaeili, D. S., Harrer, A., Tegtmeyer, N., Sticht, H., & Backert, S. (2020). *Campylobacter jejuni* serine protease HtrA cleaves the tight junction component claudin-8. *Frontiers in Cellular and Infection Microbiology, 10*, 590186-590186. doi:10.3389/fcimb.2020.590186

Silva, J., Leite, D., Fernandes, M., Mena, C., Gibbs, P. A., & Teixeira, P. (2011). *Campylobacter* spp. as a Foodborne Pathogen: A Review. *Frontiers in Microbiology, 2*, 1-12. doi:10.3389/fmicb.2011.00200

Smith, J. A., Khan, M., Magnani, D. D., Harms, J. S., Durward, M., Radhakrishnan, G. K., . . . Splitter, G. A. (2013). *Brucella* Induces an Unfolded Protein Response via TcpB That Supports Intracellular Replication in Macrophages ( Brucella Induces UPR in Macrophages). *PLOS Pathogens, 9*(12), e1003785. doi:10.1371/journal.ppat.1003785

Song, Y. C., Jin, S., Louie, H., Ng, D., Lau, R., Zhang, Y., . . . Chan, V. L. (2004). FlaC, a protein of *Campylobacter jejuni* TGH9011 (ATCC43431) secreted through the flagellar apparatus, binds epithelial cells and influences cell invasion. *Molecular microbiology, 53*(2), 541-553. doi:10.1111/j.1365-2958.2004.04175.x

Spiller, R., & Garsed, K. (2009). Postinfectious Irritable Bowel Syndrome. *Gastroenterology, 136*(6), 1979-1988. doi:10.1053/j.gastro.2009.02.074

Stahl, M., Butcher, J., & Stintzi, A. (2012). Nutrient acquisition and metabolism by *Campylobacter jejuni*. *Frontiers in Cellular and Infection Microbiology, 2*, 5-5. doi:10.3389/fcimb.2012.00005

Stahl, M., Ries, J., Vermeulen, J., Yang, H., Sham, H. P., Crowley, S. M., . . . Vallance, B. A. (2014). A Novel Mouse Model of *Campylobacter jejuni* Gastroenteritis Reveals Key Pro-inflammatory and Tissue Protective Roles for Toll-like Receptor Signaling during Infection. *PLOS Pathogens, 10*(7). doi:10.1371/journal.ppat.1004264

Stengel, S. T., Fazio, A., Lipinski, S., Jahn, M. T., Aden, K., Ito, G., . . . Rosenstiel, P. (2020). Activating Transcription Factor 6 Mediates Inflammatory Signals in Intestinal Epithelial Cells Upon Endoplasmic Reticulum Stress. *Gastroenterology (New York, N.Y. 1943), 159*(4), 1357-1374.e1310. doi:10.1053/j.gastro.2020.06.088

Stolfi, C., Maresca, C., Monteleone, G., & Laudisi, F. (2022). Implication of Intestinal Barrier Dysfunction in Gut Dysbiosis and Diseases. *Biomedicines, 10*(2), 289. doi:10.3390/biomedicines10020289

Sumimoto, H., Miyano, K., & Takeya, R. (2005). Molecular composition and regulation of the Nox family NAD(P)H oxidases. *Biochemical and Biophysical Research Communications, 338*(1), 677-686. doi:10.1016/j.bbrc.2005.08.210

Szegezdi, E., Logue, S. E., Gorman, A. M., & Samali, A. (2006). Mediators of endoplasmic reticulum stress-induced apoptosis. *EMBO reports, 7*(9), 880-885. doi:10.1038/sj.embor.7400779

Szymanski, C. M., Logan, S. M., Linton, D., & Wren, B. W. (2003). *Campylobacter* – a tale of two protein glycosylation systems. *Trends in microbiology (Regular ed.), 11*(5), 233-238. doi:10.1016/S0966-842X(03)00079-9

Szymanski, C. M., Yao, R., Ewing, C. P., Trust, T. J., & Guerry, P. (1999). Evidence for a system of general protein glycosylation in *Campylobacter jejuni*. *Molecular microbiology, 32*(5), 1022-1030. doi:10.1046/j.1365-2958.1999.01415.x

Tamura, M., Gu, J., Danen, E. H., Takino, T., Miyamoto, S., & Yamada, K. M. (1999). PTEN Interactions with Focal Adhesion Kinase and Suppression of the Extracellular Matrix-dependent Phosphatidylinositol 3-Kinase/Akt Cell Survival Pathway. *The Journal of Biological Chemistry, 274*(29), 20693-20703. doi:10.1074/jbc.274.29.20693

Tentaku, A., Shimohata, T., Hatayama, S., Kido, J., Nguyen, A. Q., Kanda, Y., . . . Takahashi, A. (2018). Host cellular unfolded protein response signaling regulates *Campylobacter jejuni* invasion. *PLOS One, 13*(10), e0205865. doi:10.1371/journal.pone.0205865

Thibault, P., Logan, S. M., Kelly, J. F., Brisson, J.-R., Ewing, C. P., Trust, T. J., & Guerry, P. (2001). Identification of the carbohydrate moieties and glycosylation motifs in *Campylobacter jejuni* flagellin. *The Journal of Biological Chemistry, 276*(37), 34862-34870. doi:10.1074/jbc.M104529200

Thornley, J. P., Jenkins, D., Neal, K., Wright, T., Brough, J., & Spiller, R. C. (2001). Relationship of *Campylobacter* toxigenicity in vitro to the development of postinfectious irritable bowel syndrome. *Journal of Infectious Diseases, 184*(5), 606-609. doi:10.1086/322845

Tréton, X., Pedruzzi, E., Guichard, C., Ladeiro, Y., Sedghi, S., Vallée, M., . . . Ogier-Denis, E. (2014). Combined NADPH oxidase 1 and interleukin 10 deficiency induces chronic endoplasmic reticulum stress and causes ulcerative colitis-like disease in mice. *PLOS One, 9*(7), e101669. doi:10.1371/journal.pone.0101669

Uehara, A., Yang, S., Fujimoto, Y., Fukase, K., Kusumoto, S., Shibata, K., . . . Takada, H. (2005). Muramyldipeptide and diaminopimelic acid-containing desmuramylpeptides in combination with chemically synthesized Toll-like receptor agonists synergistically induced production of interleukin-8 in a NOD2- and NOD1-dependent manner, respectively, in human monocytic cells in culture. *Cellular Microbiology, 7*(1), 53-61. doi:10.1111/j.1462-5822.2004.00433.x

Ueyama, T., Geiszt, M., & Leto, T. L. (2006). Involvement of Rac1 in activation of multicomponent Nox1- and Nox3-based NADPH oxidases. *Molecular and Cellular Biology, 26*(6), 2160-2174. doi:10.1128/MCB.26.6.2160-2174.2006

van der Flier, L. G., & Clevers, H. (2009). Stem cells, self-renewal, and differentiation in the intestinal epithelium. *Annual review of physiology, 71*(1), 241-260. doi:10.1146/annurev.physiol.010908.163145

van der Post, S., Birchenough, G. M. H., & Held, J. M. (2021). NOX1-dependent redox signaling potentiates colonic stem cell proliferation to adapt to the intestinal microbiota by linking EGFR and TLR activation. *Cell reports (Cambridge), 35*(1), 108949-108949. doi:10.1016/j.celrep.2021.108949

Van Deun, K., Haesebrouck, F., Heyndrickx, M., Favoreel, H., Dewulf, J., Ceelen, L., . . . Pasmans, F. (2007). Virulence properties of Campylobacter jejuni isolates of poultry and human origin. *Journal of medical microbiology, 56*(10), 1284-1289. doi:10.1099/jmm.0.47342-0

Vandamme, P. (2000). Taxonomy of the family Campylobacteraceae. In Irving Nachamkin & M. J. Blaser (Eds.), *Campylobacter* (2nd ed., pp. 3-26). Washington, DC, USA: ASM Press.

Vandamme, P., Dewhirst, F. E., Paster, B. J., & On, S. L. W. (2015). *Campylobacter*. In *Bergey's Manual of Systematics of Archaea and Bacteria* (pp. 1-27).

Vareechon, C., Zmina, S. E., Karmakar, M., Pearlman, E., & Rietsch, A. (2017). *Pseudomonas aeruginosa* effector ExoS inhibits ROS production in human neutrophils. *Cell Host & Microbe, 21*(5), 611-618.e615. doi:10.1016/j.chom.2017.04.001

Wacker, M., Linton, D., Aebi, M., Hitchen, P. G., Nita-Lazar, M., Haslam, S. M., . . . Wren, B. W. (2002). N-Linked glycosylation in *Campylobacter jejuni* and its functional transfer into *E. coli*. *Science (American Association for the Advancement of Science), 298*(5599), 1790-1793. doi:10.1126/science.298.5599.1790

Wang, C., & Eskiw, C. H. (2019). Cytoprotective effects of Avenathramide C against oxidative and inflammatory stress in normal human dermal fibroblasts. *Scientific Reports, 9*(1), 2932-2912. doi:10.1038/s41598-019-39244-9

Watson, R. O., & Galán, J. E. (2008). *Campylobacter jejuni* survives within epithelial cells by avoiding delivery to lysosomes (*C. jejuni* intracellular survival). *PLOS Pathogens, 4*(1), e14. doi:10.1371/journal.ppat.0040014

Whitehouse, C. A., Balbo, P. B., Pesci, E. C., Cottle, D. L., Mirabito, P. M., & Pickett, C. L. (1998). *Campylobacter jejuni* cytolethal distending toxin causes a G2-phase cell cycle block. *Infection and Immunity, 66*(5), 1934-1940.

Willison, H. J., Jacobs, B. C., & van Doorn, P. A. (2016). Guillain-Barré syndrome. *The Lancet, 388*(10045), 717-727. doi:10.1016/S0140-6736(16)00339-1

Wooldridge, K. G., Williams, P. H., & Ketley, J. M. (1996). Host signal transduction and endocytosis of *Campylobacter jejuni*. *Microbial Pathogenesis, 21*(4), 299-305. doi:10.1006/mpat.1996.0063

Wu, R.-F., Ma, Z., Liu, Z., & Terada, L. S. (2010). Nox4-derived $H_2O_2$ mediates endoplasmic reticulum signaling through local Ras activation. *Molecular and Cellular Biology, 30*(14), 3553-3568. doi:10.1128/MCB.01445-09

Yamazaki, H., Hiramatsu, N., Hayakawa, K., Tagawa, Y., Okamura, M., Ogata, R., . . . Kitamura, M. (2009). Activation of the Akt-NF-κB Pathway by Subtilase Cytotoxin through the ATF6 Branch of the Unfolded Protein Response. *The Journal of immunology (1950), 183*(2), 1480-1487. doi:10.4049/jimmunol.0900017

Young, K. T., Davis, L. M., & DiRita, V. J. (2007). *Campylobacter jejuni*: molecular biology and pathogenesis. *Nature Reviews Microbiology, 5*(9), 665-679. doi:10.1038/nrmicro1718

Zhang, C., Bai, N., Chang, A., Zhang, Z., Yin, J., Shen, W., . . . Liu, C. (2013). ATF4 is directly recruited by TLR4 signaling and positively regulates TLR4-trigged cytokine production in human monocytes. *Cellular & molecular immunology, 10*(1), 84-94. doi:10.1038/cmi.2012.57

Zhang, J., Wang, X., Vikash, V., Ye, Q., Wu, D., Liu, Y., & Dong, W. (2016). ROS and ROS-mediated cellular signaling. *Oxidative Medicine and Cellular Longevity, 2016*, 1-18. doi:10.1155/2016/4350965

Zhang, K., Shen, X., Wu, J., Sakaki, K., Saunders, T., Rutkowski, D. T., . . . Kaufman, R. J. (2006). Endoplasmic reticulum stress activates cleavage of CREBH to induce a systemic inflammatory response. *Cell, 124*(3), 587-599. doi:10.1016/j.cell.2005.11.040

Zhang, X. L., Tsui, I. S. M., Yip, C. M. C., Fung, A. W. Y., Wong, D. K. H., Xiaoyun, D. A. I., . . . Morris, C. (2000). *Salmonella enterica* serovar Typhi uses Type IVB pili to enter human intestinal epithelial cells. *Infection and Immunity, 68*(6), 3067-3073. doi:10.1128/IAI.68.6.3067-3073.2000

Zheng, J., Meng, J., Zhao, S., Singh, R., & Song, W. (2008). *Campylobacter*-Induced Interleukin-8 Secretion in Polarized Human Intestinal Epithelial Cells Requires *Campylobacter*-Secreted Cytolethal Distending Toxin- and Toll-Like Receptor-Mediated Activation of NF-κB. *Infection and Immunity, 76*(10), 4498-4508. doi:10.1128/IAI.01317-07

Zheng, M., Åslund, F., & Storz, G. (1998). Activation of the OxyR Transcription Factor by Reversible Disulfide Bond Formation. *Science (American Association for the Advancement of Science), 279*(5357), 1718-1721. doi:10.1126/science.279.5357.1718

Zilbauer, M., Dorrell, N., Boughan, P. K., Harris, A., Wren, B. W., Klein, N. J., & Bajaj-Elliott, M. (2005). Intestinal Innate Immunity to *Campylobacter jejuni* Results in Induction of Bactericidal Human Beta-Defensins 2 and 3. *Infection and Immunity, 73*(11), 7281-7289. doi:10.1128/IAI.73.11.7281-7289.2005

Zilbauer, M., Dorrell, N., Elmi, A., Lindley, K. J., Schüller, S., Jones, H. E., . . . Bajaj-Elliott, M. (2007). Major role for intestinal epithelial nucleotide oligomerization domain 1 (NOD1) in eliciting host bactericidal immune responses to *Campylobacter jejuni*. *Cellular Microbiology, 9*(10), 2404-2416. doi:10.1111/j.1462-5822.2007.00969.x

# Appendices

## Appendix 1: Chapter 3 publication - *Campylobacter jejuni* modulates reactive oxygen species production and NADPH oxidase 1 expression in human intestinal epithelial cells.

Hindawi
Cellular Microbiology
Volume 2023, Article ID 3286330, 14 pages
https://doi.org/10.1155/2023/3286330

WILEY | Hindawi

*Research Article*

# *Campylobacter jejuni* Modulates Reactive Oxygen Species Production and NADPH Oxidase 1 Expression in Human Intestinal Epithelial Cells

**Geunhye Hong,[1] Cadi Davies,[1] Zahra Omole,[1] Janie Liaw,[1] Anna D. Grabowska,[2] Barbara Canonico,[3] Nicolae Corcionivoschi,[4,5] Brendan W. Wren,[1] Nick Dorrell,[1] Abdi Elmi,[1] and Ozan Gundogdu[1]**

[1]*Faculty of Infectious and Tropical Diseases, London School of Hygiene & Tropical Medicine, Keppel Street, London WC1E 7HT, UK*
[2]*Department of Biophysics, Physiology and Pathophysiology, Medical University of Warsaw, Warsaw 02-004, Poland*
[3]*Department of Biomolecular Sciences, University of Urbino Carlo Bo, Urbino 61029, Italy*
[4]*Bacteriology Branch, Veterinary Sciences Division, Agri-Food and Biosciences Institute (AFBI), Belfast BT9 5PX, UK*
[5]*Faculty of Bioengineering of Animal Resources, University of Life Sciences King Mihai I from Timisoara, Timisoara 300645, Romania*

Correspondence should be addressed to Nick Dorrell; nick.dorrell@lshtm.ac.uk, Abdi Elmi; abdi.elmi@lshtm.ac.uk, and Ozan Gundogdu; ozan.gundogdu@lshtm.ac.uk

Received 8 March 2022; Revised 9 December 2022; Accepted 14 December 2022; Published 30 January 2023

Academic Editor: Shiek Ahmed



*Campylobacter jejuni* is the major bacterial cause of foodborne gastroenteritis worldwide. Mechanistically, how this pathogen interacts with intrinsic defence machinery of human intestinal epithelial cells (IECs) remains elusive. To address this, we investigated how *C. jejuni* counteracts the intracellular and extracellular reactive oxygen species (ROS) in IECs. Our work shows that *C. jejuni* differentially regulates intracellular and extracellular ROS production in human T84 and Caco-2 cells. *C. jejuni* downregulates the transcription and translation of nicotinamide adenine dinucleotide phosphate (NAPDH) oxidase (NOX1), a key ROS-generating enzyme in IECs and antioxidant defence genes *CAT* and *SOD1*. Furthermore, inhibition of *NOX1* by diphenylene iodonium (DPI) and siRNA reduced *C. jejuni* ability to interact, invade, and intracellularly survive within T84 and Caco-2 cells. Collectively, these findings provide mechanistic insight into how *C. jejuni* modulates the IEC defence machinery.

## 1. Introduction

Microbial pathogens have evolved to possess subversion strategies to alter the functionality of host cells upon infection [1]. These include modulation of host cell functions that involve vesicle trafficking, apoptosis, and immune activation [2–4]. Crucially, these host cell functions are essential for elimination of foreign pathogens. The evolving battle between pathogen and host adds to the complexity of the pathogenesis of infection [1].

*Campylobacter jejuni* is the leading foodborne bacterial cause of human gastroenteritis worldwide [5]. *C. jejuni* causes watery or bloody diarrhoea, abdominal pain, and fever. *C. jejuni* infection can also lead to Guillain-Barré syndrome (GBS), a rare but severe postinfectious autoimmune complication of the peripheral nervous system [5–7]. Importantly, campylobacteriosis in low-income countries is associated with child growth impairment and can be fatal in children [8]. Although *C. jejuni* is a microaerophilic bacterium, its omnipresence in the environment and various

hosts is mitigated by regulatory mechanisms against oxidative stress [9]. Upon adhering and invading human intestinal epithelial cells (IECs), *C. jejuni* manipulates host cytoskeleton regulation to maximise its invasion [10]. Following invasion, *C. jejuni* resides in cytoplasmic vacuoles named *Campylobacter* containing vacuoles (CCVs) which can escape the canonical endocytic pathway and avoid fusion with lysosomes [11, 12]. These findings demonstrate that modulation and invasion of host IECs are a prerequisite for human intestinal disease caused by *C. jejuni*.

A vital mechanism used by host cells in response to pathogens is the production of reactive oxygen species (ROS) which are highly reactive molecules, such as oxygen radicals and nonradicals, produced by the partial reduction of oxygen [13]. When phagocytes such as macrophages detect and engulf pathogens using the respiratory burst, ROS are rapidly generated to eradicate the engulfed pathogens through oxidative damage [14]. Interestingly, the level of ROS produced by human IECs is lower in comparison to resident macrophages and blood leukocytes (neutrophils and monocytes); however, ROS in IECs can also exhibit antimicrobial activity by inducing inflammation [14–16]. The precarious nature of ROS production by IECs is demonstrated by exhibiting both deleterious and beneficial host effects; thus, homeostasis of ROS is essential. To counter the damaging effects of ROS, host IECs possess antioxidant components that neutralise ROS, such as catalase, superoxide dismutase, and glutathione peroxidase. Nicotinamide adenine dinucleotide phosphate oxidase (NADPH oxidase; NOX) and mitochondria have central roles as predominant sources of ROS in human IECS [13].

NOX is an essential multicomponent enzyme which catalyses production of superoxide ($O_2^-$) [17, 18]. In IECs, the most abundant types of NOX are NOX1 and NOX4. Intriguingly, NOX4 is constitutively active, whereas NOX1 is not. The NOX1 complex is composed of NOX1, p22phox, NOX organiser 1 (NOXO1), NOX activator (NOXA1), and small GTPase Rac1. NOX1 is the catalytic subunit of the complex on the plasma membrane, and its activation is dependent on supplementary cytosolic subunits. Following this, p22phox is transported to the plasma membrane promoted by NOX1 expression [17]. Upon activation, NOXO1 binds to both NOXA1 and p22phox targeting NOXA1 to the plasma membrane. In turn, NOXA1 binds to guanosine triphosphate- (GTP-) bound Rac1 and promotes electron flow through flavocytochrome in NOX1 in a GTP-dependent manner. Studies have shown that GTP-bound Rac1 is essential for activity of NOX1 [19, 20]. Electrons travel from NADPH initially to flavin adenine dinucleotide (FAD), then through the NOX heme groups and finally to oxygen, forming $O_2^-$ [19]. Notably, NOX1-mediated ROS play important roles in IECs including regulation of growth and proliferation, epithelial wound healing, intestinal host defence, and maintenance of bacterial homeostasis in the GI tract [21–23].

How *C. jejuni* interacts with the inherent defence machinery of human IECs remains unclear. To explore this further, we examined the mechanisms *C. jejuni* uses to counteract the intracellular and extracellular ROS in IECs. Previous findings demonstrated the upregulation of NOX1 in IECs by enteric pathogens such as *Escherichia coli* [24], *Salmonella* enteritidis [25], and *Helicobacter pylori* [26, 27]. *C. jejuni* lacks classical stress response regulators such as OxyR and SoxRS that are found in other enteric bacteria [28, 29]. Instead, it possesses unique strategies to counteract oxidative stress such as CosR, PerR, and MarR-type regulators RrpA and RrpB [9, 30, 31]. Given these survival properties of *C. jejuni*, we hypothesised that *C. jejuni* may have distinct host cell modulation mechanisms in play. In this study, we show that diverse *C. jejuni* strains downregulate both intracellular and extracellular ROS production in human IECs by modulating the expression of NOX1. We demonstrate inhibition of NOX1 by diphenylene iodonium (DPI), and siRNA reduced the ability of *C. jejuni* to interact, invade, and intracellularly survive within T84 and Caco-2 cells. Our results highlight a unique strategy of *C. jejuni* survival and emphasise the importance of NOX1 in *C. jejuni*-IEC interactions. This represents a distinctive mechanism that *C. jejuni* uses to modulate IEC defence machinery.

## 2. Experimental Procedures

*2.1. Bacterial Strains and Growth Conditions. C. jejuni* wild-type strains used in this study are listed in Table S1. For general growth, all *C. jejuni* strains were grown on Columbia Blood Agar (CBA) plates (Oxoid, UK) supplemented with 7% (*v*/*v*) horse blood (TCS Microbiology, UK) and *Campylobacter* selective supplement Skirrow (Oxoid) at 37°C under microaerobic conditions (10% $CO_2$, 5% $O_2$, and 85% $N_2$) (Don Whitley Scientific, UK).

*2.2. Human Intestinal Epithelial Cell Culture.* T84 cells (ECACC 88021101) and Caco-2 cells (ECACC 86010202) were obtained from European Collection of Authenticated Cell Cultures (ECACC). T84 and Caco-2 cells were cultured in a 1 : 1 mixture of Dulbecco's modified Eagle's medium and Ham's F-12 medium (DMEM/F-12; Thermo Fisher Scientific, USA) with 10% fetal bovine serum (FBS; Labtech, UK), 1% nonessential amino acid (Sigma-Aldrich, USA), and 1% penicillin-streptomycin (Sigma-Aldrich). Both cell lines were cultured at 37°C in a 5% $CO_2$-humidified environment. DMEM/F-12 without penicillin-streptomycin was used for the coculture assays. DMEM/F-12 without phenol red was used for the ROS detection assays.

*2.3. T84 and Caco-2 Cell Infection Assays.* Human IECs were counted using hemocytometer (Thermo Fisher Scientific, USA), and for general infection assays, approximately $10^5$ cells were seeded in 24-well tissue culture plates 7 days prior to initiation of the *C. jejuni* infection. The plates were incubated at 37°C in a 5% $CO_2$ atmosphere. For Western blotting, approximately $2 \times 10^5$ cells were seeded in 6-well tissue culture plates. Prior to the infection, IECs were washed with phosphate-buffered saline (PBS; Thermo Fisher Scientific) three times and the medium was replaced with DMEM/F-12 without penicillin-streptomycin. *C. jejuni* strains grown on CBA plates for 24 hours were resuspended in PBS, and bacterial suspension with appropriate $OD_{600}$

was then incubated with IECs for various time periods giving a multiplicity of infection (MOI) of 200 : 1. In some experiments, T84 and Caco-2 cells were pretreated with 10 $\mu$M DPI for 1 hour, washed three times with PBS, and then infected with *C. jejuni*. As with our previous infection assays [32, 33], we primarily focus on relatively early time points as many of the transcriptional and translational changes that we observe in the crosstalk between *C. jejuni* and IECs in our *in vitro* assays are ephemeral in nature, and so our focus is to detect these subtle deviations that lead to mechanistic impact.

*2.4. DCFDA Measurement of Intracellular Reactive Oxygen Species (ROS).* To analyse the levels of intracellular ROS production in human IECs under experiments conditions, DCFDA Cellular ROS Detection Assay Kit (Abcam, UK) was used according to the manufacturer's instructions. Briefly, IECs grown in 96-well cell culture plates were washed three times with PBS and incubated with *C. jejuni* for 3 or 24 hours (MOI 200 : 1). For positive controls, IECs were treated with 500 $\mu$M $H_2O_2$ for 45 minutes. 45 minutes prior to completion of the infection, 100 $\mu$M 2′,7′-dichlorofluorescin diacetate (DCFDA) was added into each well giving a final concentration of 50 $\mu$M. After *C. jejuni* infection, the fluorescence was detected using SpectraMax M3 Multi-Mode Microplate Reader (Molecular Devices, USA) with 485 nm excitation and 535 nm emission.

*2.5. Measurement of Extracellular $H_2O_2$.* Amplex® Red Hydrogen Peroxide/Peroxidase Assay Kit (Invitrogen, USA) was used to measure extracellular $H_2O_2$ in culture media after incubation with *C. jejuni*. Briefly, Amplex® Red reagent (10-acetyl-3,7-dihydroxyphenoxazine) with horseradish peroxidase (HRP) reacts with $H_2O_2$ in a 1 : 1 stoichiometry producing a fluorescent product called resorufin. After incubation with *C. jejuni* for 3 or 24 hours, 100 $\mu$l of culture media was transferred to a 96-well plate and 100 $\mu$l of reaction mixture containing 50 $\mu$M Amplex® Red reagent was added followed by incubation for 10 minutes at 37°C in a 5% $CO_2$-humidified environment. Using SpectraMax M3 Multi-Mode Microplate Reader, fluorescence was measured at 530 nm excitation and 590 nm emission.

*2.6. Real-Time Quantitative Polymerase Chain Reaction (qRT-PCR) Analysis.* For qRT-PCR, RNA was isolated from infected and uninfected IECs using PureLink™ RNA Mini Kit (Thermo Fisher Scientific) and contaminating DNA was removed using TURBO DNA-free kit (Ambion, USA) according to the manufacturer's instructions. Concentration and purity of RNA samples were determined in a NanoDrop ND-1000 spectrophotometer (Thermo Fisher Scientific). 400 ng of RNA per sample were first denatured at 65°C for 5 minutes and snap cooled on ice. Complementary DNA (cDNA) was generated with random hexamers and SuperScript III Reverse Transcriptase (Thermo Fisher Scientific). Each reaction had 10 $\mu$l of SYBR Green PCR Master Mix (Applied Biosystems, USA), 1 $\mu$l of primer (20 pmol), 1 $\mu$l of cDNA, and 10 $\mu$l of HyClone™ water (Thermo Fisher Scientific). The sequence of each primer is described in Table S2. All reactions were run in triplicate on an ABI-PRISM 7500 instrument (Applied Biosystems). Relative expression changes were calculated using the comparative $C_T$ cycle ($2^{-\Delta\Delta CT}$) method [34]. Expression levels of all target genes were normalised to *gapdh* expression determined in the same sample as an internal control. A minimum of three biological replicates were always analysed, each with three technical replicates.

*2.7. Semiquantitative Reverse Transcription (RT-PCR) Analysis.* Each PCR reaction had 50 $\mu$l of FasTaq PCR master mix (Qiagen, Netherlands), 2 $\mu$l of primer (0.4 nmol) described in Table S2, and 1.5 $\mu$l of cDNA. For PCR reactions, Tetrad-2 Peltier thermal cycler (Bio-Rad, UK) was used. One cycle of PCR programme performs 95°C for 15 seconds after 2 minutes in the first cycle, annealing at 50°C for 20 seconds, and extension at 72°C for 30 seconds. Total 36 cycles were repeated. The PCR products were loaded on the 1% agarose gel, and the gel was running for 1 hour at 120 V. The gel was imaged using G:BOX Chime XRQ (Syngene, USA). Quantification of relative mRNA level was performed using ImageJ software [35].

*2.8. SDS-PAGE and Western Blot Analysis.* After infection, IECs were washed three times with PBS and lysed with cold RIPA lysis and extraction buffer (Thermo Fisher Scientific) with cOmplete™ Mini EDTA-free Protease Inhibitor Cocktail (Roche, Switzerland) and cleared by centrifugation (4°C, 13,000 × *g*, 20 min). Protein concentration was determined using Pierce™ Bicinchoninic acid (BCA) Protein Assay Kit (Thermo Fisher Scientific) according to the manufacturer's instructions. Afterward, samples were diluted to a desired concentration in HyClone™ water and 4× Laemmli sample buffer (Sigma-Aldrich) and incubated for 5 minutes at 95°C. 30 $\mu$g of protein samples was separated using 4-12% NuPAGE™ Bis-Tris gel in 1× NuPAGE™ MES buffer or MOPS buffer (Thermo Fisher Scientific). Proteins were transferred from the gel using the iBlot® 2 transfer stacks (Life Technologies, USA) using the iBlot® Gel Transfer Device (Invitrogen). These stacks were integrated with nitrocellulose transfer membrane. After the transfer, membranes were blocked with 1× PBS containing 2% (*w*/*v*) milk. Membranes were then probed with primary antibodies overnight as described previously [32]. The following primary antibodies were used: GAPDH (ab181602, Abcam), NOX1 (ab101027, Abcam), or NOX1 (NBP-31546, Novus Biologicals). Blots were developed using LI-COR infrared secondary antibody (IRDye 800CW Donkey anti-rabbit IgG) and imaged on a LI-COR Odyssey Classic (LI-COR Biosciences, USA). Quantification of relative protein levels normalised to GAPDH expression was performed using ImageJ software [35].

*2.9. Detection of GTP-Bound Active Rac1.* The levels of active GTP-bound Rac1 were measured by using Rac1 G-LISA kit (Cytoskeleton Inc., USA) according to the manufacturer's instructions. Briefly, before the infection, IECs were incubated with reduced serum (0.1% FBS) for 24 hours. Infected or uninfected human IECs were washed with 1× PBS and

lysed using the supplied 1× lysis buffer. Cell lysates were centrifuged for 1 minute at 10,000 × *g* at 4°C and adjusted to 1 mg/ml for the further process of the assay. As a positive control, constitutively active Rac1 (RCCA) was provided in the kit. Three biological replicates were conducted in all experiments, along with two technical replicates for each assay.

*2.10. Inhibition of NOX1 with Diphenyleneiodonium Chloride (DPI).* A stock solution of 3.25 mM DPI (Sigma-Aldrich) in dimethyl sulfoxide (DMSO, Sigma-Aldrich) was prepared and stored at -20°C. For treatment, the DPI stock solution was diluted to 10 $\mu$M DPI in culture media without antibiotics and then incubated with IECs for 1 hour at 37°C in a 5% $CO_2$ atmosphere. After treatment, IECs were washed with PBS for three times before coincubation with *C. jejuni* for various time points.

*2.11. Small Interfering (si) RNA Transfection.* On the day of reverse transfection, 500 $\mu$l of Caco-2 cells ($10^5$ cells/ml) was seeded in 24-well plates and treated for 24 hours with 30 pmol siRNA from either NOX1 siRNA (sc-43939; Santa Cruz Biotechnology Inc., USA) or Ambion® Silencer Negative Control #1 siRNA (Invitrogen) for the negative control. For preparation of siRNA transfection reagent complex, 3 $\mu$l of 10 $\mu$M stock siRNA was diluted with 100 $\mu$l of Opti-MEM® Reduced-Serum Medium (Thermo Fisher Scientific) and mixed with 1.5 $\mu$l of Lipofectamine® RNAiMAX Transfection Reagent (Thermo Fisher Scientific). After 24 hours transfection, media was replaced with DMEM/F-12 containing 10% FBS. After additional 48 or 72 hours, RNA and protein were extracted to check efficacy of transfection.

*2.12. Adhesion, Invasion, and Intracellular Survival Assay.* Adherence, invasion, and intracellular assays were performed as described previously with minor modifications [32, 33]. T84 and Caco-2 cells seeded in a 24-well plate were washed three times with PBS and treated with 10 $\mu$M DPI for 1 hour or transfected with NOX1 siRNA as described above. Then, IECs were inoculated with *C. jejuni* with $OD_{600}$ 0.2 at a MOI of 200 : 1 and incubated for 3 hours at 37°C in 5% $CO_2$. For the interaction (adhesion and invasion) assay, monolayers were washed three times with PBS to remove unbound extracellular bacteria and then lysed with PBS containing 0.1% (*v*/*v*) Triton X-100 (Sigma-Aldrich) for 20 min at room temperature. The cell lysates were diluted and plated on blood agar plates to determine the number of interacting bacteria (CFU/ml).

Invasion assays were performed by additional step of treatment of gentamicin (150 $\mu$g/ml) for 2 hours to kill extracellular bacteria, washed three times with PBS, lysed, and plated as described above. For intracellular survival assays, after infection with *C. jejuni* for 3 hours, T84 and Caco-2 cells were treated with gentamicin (150 $\mu$g/ml) for 2 hours to kill extracellular bacteria followed by further 18 hours incubation with gentamicin (10 $\mu$g/ml). Cell lysis and inoculation were performed as described above.

*2.13. Cytotoxicity Assay with Trypan Blue Exclusion Methods.* After treatment with DPI and gentamicin or transfection with siRNA as previously described, IECs were washed three times with PBS and were detached using trypsin-EDTA (Thermo Fisher Scientific) and resuspended with culture media. 50 $\mu$l of cell suspension was added into 50 $\mu$l of 0.4% trypan blue solution (Thermo Fisher Scientific), and the numbers of viable and dead cells were counted using hemocytometer under a microscope.

*2.14. Campylobacter jejuni Viability Test with DPI Treatment.* T84 cells were treated with 10 $\mu$M DPI for 1 hour, and the cells were washed three times with PBS. After DPI treatment for 1 hour, *C. jejuni* strains ($OD_{600}$ 0.2) were coincubated for 1 hour with PBS from the last wash. After incubation, serial dilution was performed and each dilution was spotted on to blood agar plates. The plates were incubated under microaerobic condition at 37°C for 48 hours. CFU of each spot was recorded.

*2.15. Statistical Analysis and Graphing.* At least three biological replicates were performed in all experiments. Each biological replicate was performed in three technical replicates. For statistical analysis and graphing, GraphPad Prism 8 for Windows (GraphPad Software, USA) was used. One sample *t*-test or unpaired *t*-test was used to compare two data sets for significance with $*$ indicating $p < 0.05$, $**$ indicating $p < 0.01$, $***$ indicating $p < 0.001$, and $****$ indicating $p < 0.0001$.

## 3. Results

*3.1. Campylobacter jejuni Modulates Intracellular and Extracellular ROS in T84 and Caco-2 Cells in a Time- and Strain-Dependent Manner.* As *C. jejuni* possesses distinct physiological characteristics compared to more studied enteric pathogens, we assessed the ability of three distinct *C. jejuni* strains to modulate intracellular and extracellular ROS in T84 and Caco-2 cells [28]. We observed strain-specific ROS modulation at 3- and 24-hour postinfection (Figure 1). All three *C. jejuni* strains reduced the levels of intracellular ROS in T84 and Caco-2 cells compared to the uninfected control (Figures 1(a), 1(b), 1(e), and 1(f)). A similar pattern was observed for extracellular ROS where all *C. jejuni* strains reduced the levels of extracellular ROS in T84 and Caco-2 cells compared to the uninfected control (Figures 1(c), 1(d), 1(g), and 1(h)). A distinct pattern was observed when assessing levels of extracellular ROS for *C. jejuni* 81-176 strain at a 3-hour postinfection (Figures 1(c) and 1(g)). At this early time point, extracellular ROS is increased in T84 and Caco-2 cells infected with *C. jejuni* 81-176, although we observed similar reduced levels of ROS at 24 hours. As controls, *C. jejuni* infection did not affect viability of both T84 and Caco-2 cells (Figure S1) and levels of ROS were unchanged when *C. jejuni* was resuspended in DMEM in the absence of IECs (Figure S2). Collectively, these results indicate a strain- and time-specific pattern linking the ability of different *C. jejuni* strains to modulate intracellular and extracellular ROS levels in T84 and Caco-2 cells.

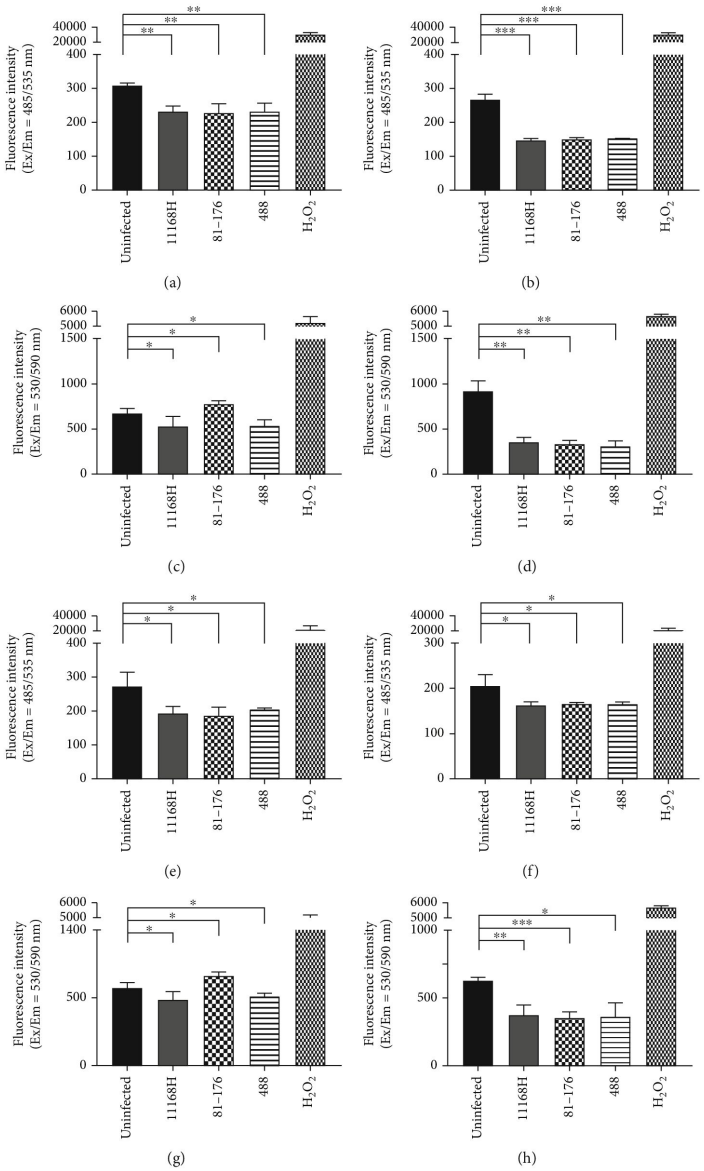


Figure 1: Detection of intracellular and extracellular ROS in T84 and Caco-2 cells after infection with *C. jejuni* 11168H, 81-176, or 488 strains. Intracellular ROS in T84 cells after infection with *C. jejuni* for (a) 3 hours or (b) 24 hours and extracellular ROS from T84 cells after infection with *C. jejuni* for (c) 3 hours or (d) 24 hours were measured. Intracellular ROS in Caco-2 cells after infection of *C. jejuni* for (e) 3 hours or (f) 24 hours and extracellular ROS from Caco-2 cells after infection for (g) 3 hours or (h) 24 hours were measured. For detection of intracellular ROS, DCFDA was used. For detection of extracellular ROS, Amplex® Red reagent with HRP was used. $H_2O_2$ was used as a positive control. Experiments were repeated in three biological and three technical replicates. Asterisks denote a statistically significant difference ($^*p < 0.05$; $^{**}p < 0.01$; $^{***}p < 0.001$).

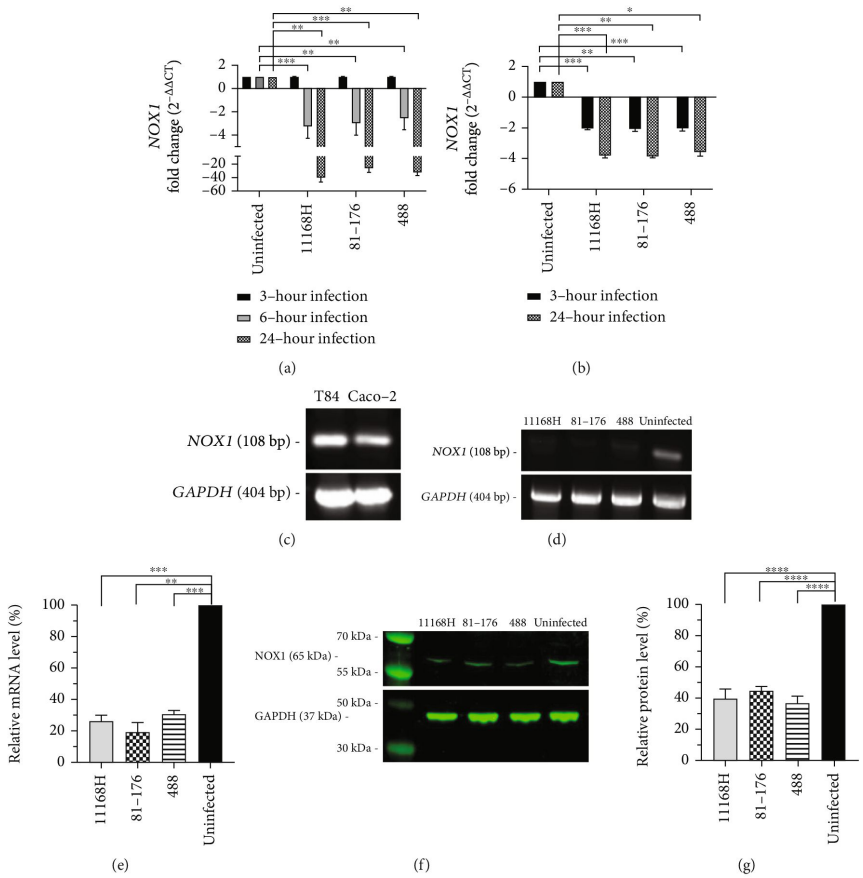


FIGURE 2: *C. jejuni* modulates NOX1 expression in T84 and Caco-2 cells. qRT-PCR showing expression of *NOX1* in (a) T84 and (b) Caco-2 cells. (c) RT-PCR showing expression of *NOX1* in uninfected T84 and Caco-2 cells. *GAPDH* was used as an internal control. (d) RT-PCR showing expression of *NOX1* in T84 cells infected with *C. jejuni* for 24 hours and (e) relative mRNA levels as a percentage from RT-PCR data. (f) Western blotting showing NOX1 in T84 cells infected with *C. jejuni* for 24 hours and (g) relative protein level as a percentage from Western blotting. Asterisks denote a statistically significant difference ($^{*}p < 0.05$; $^{**}p < 0.01$; $^{***}p < 0.001$).

*3.2. Campylobacter jejuni Modulates Intracellular and Extracellular ROS in T84 and Caco-2 Cells via the Downregulation of NOX1 Complex.* Given the observed modulation of intracellular and extracellular ROS in T84 and Caco-2 cells, we next explored the mechanism by which *C. jejuni* strains orchestrate ROS modulation. We analysed the transcription and translation of NOX1 which is the main source of ROS production in IECs [17, 18]. As shown in Figure 2, NOX1 transcription and translation levels were significantly reduced in both T84 (Figure 2(a)) and Caco-2 cells (Figure 2(b)) infected with *C. jejuni* when compared to uninfected cells. Notably, at a 24-hour postinfection, mRNA levels of *NOX1* in T84 cells are significantly reduced compared with *C. jejuni*-infected Caco-2 cells. We measured the relative levels of mRNA between T84 and Caco-2 cells and identified T84 cells expressed a higher basal level of *NOX1* mRNA compared to Caco-2 cells (Figure 2(c)). As a result of this higher basal level of *NOX1* mRNA in T84 cells, we validated our qRT-PCR data using RT-PCR where less expression of *NOX1* in *C. jejuni*-infected T84 cells was observed (Figures 2(d) and 2(e)). Reduction in the translational level of NOX1 in *C. jejuni*-infected T84 cells was confirmed independently by Western blotting (Figures 2(f) and 2(g)).

*3.3. Campylobacter jejuni Modulates Activity of Small GTPase Rac1 in T84 and Caco-2 Cells in a Time-Dependent Manner.* To gain further insight into the mechanism that

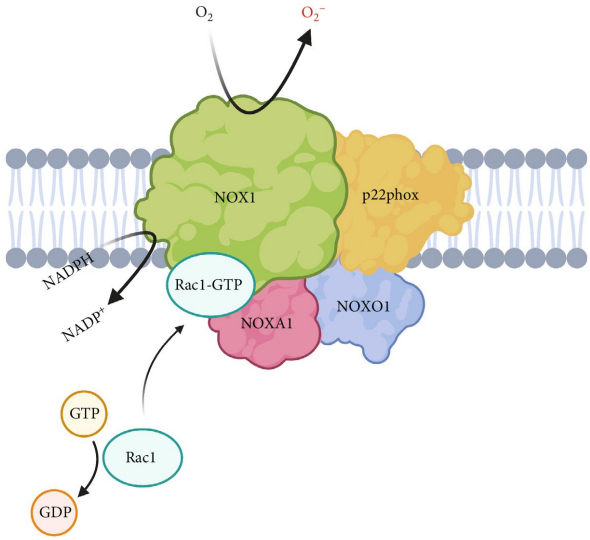


Figure 3: Proposed structure of the NOX1 complex consisting of NOX1, p22phox, GTP-bound Rac1, NOXA1, and NOXO1. p22phox and other subcellular subunits are assembled to activate catalytic subunit NOX1 which results in the generation of $O_2^-$ by oxidising NADPH [17]. Created with http://BioRender.com.

leads to *C. jejuni* modulation of ROS in T84 and Caco-2 cells, we examined the ability of *C. jejuni* to activate Rac1, a member of the Rho family of small GTPases. Rac1 undergoes cycling between active GTP- and inactive GDP-bound form which switches activation of cellular response upon stimuli [36]. Although GTP-bound Rac1 is implicated in NOX1 activation in several eukaryotic cell lines [19, 20], the contribution of Rac1 in *C. jejuni*-mediated NOX1 modulation is unknown. As shown in Figure 3, active GTP-bound Rac1 is an integral part of the NOX1 complex. Given that *C. jejuni* activates Rac1 in human INT 407 cells via *Campylobacter* invasion antigen D (CiaD) [10, 37] and that Rac1 supports NOX1 activity only in its GTP-bound active form, we examined the abundance of GTP-bound Rac1 to investigate if downregulation of NOX1 is linked to modulation of Rac1 by *C. jejuni*. Interestingly, *C. jejuni* 11168H strain induced Rac1 1 and 3 hours after infection in T84 cells (Figure 4(a)). After 24 hours of infection, Rac1 activity was reduced (though not statistically significant; $p = 0.0714$) (Figure 4(a)). Similarly, *C. jejuni* 11168H induced Rac1 activity after 1 hour of infection in Caco-2 cells (Figure 4(b)). However, this activity was reduced after 3- and 24-hours of infection (Figure 4(b)). These results suggest that the downregulation of NOX1 by *C. jejuni* is inversely correlated with an increase in Rac1 GTPase activity.

*3.4. Campylobacter jejuni Modulates Transcription of Antioxidant-Related Genes in T84 and Caco-2 Cells.* To gain further insight into the ability of *C. jejuni* to modulate intracellular and extracellular ROS in T84 and Caco-2 cells, we sought to understand if *C. jejuni* modulates the expression of two important antioxidant genes, superoxide dismutase 1 (*SOD1*) and catalase (*CAT*). SOD1 decomposes $O_2^-$ to $H_2O_2$, and CAT breaks down $H_2O_2$ to $H_2O$ and $O_2$ [13]. Intriguingly, as shown in Figures 5(a) and 5(b), there is a significant downregulation of the mRNA levels of *CAT* and *SOD1* at 24 hours of postinfection in T84 cells. A similar pattern was observed when compared with Caco-2 cells where the expression of *CAT* and *SOD1* at 24 hours of post-infection is significantly downregulated (Figures 5(c) and 5(d)). In contrast, the expression of *CAT* and *SOD1* at 3 hours of postinfection is unaffected. These results may indicate *C. jejuni*-mediated reduction in intracellular and extracellular ROS is independent of modulation of *CAT* and *SOD1*.

*3.5. Chemical Inhibition of NOX1 Activity by DPI Impairs Campylobacter jejuni Interaction, Invasion, and Intracellular Survival of T84 and Caco-2 Cells in vitro.* Having established that *C. jejuni* significantly reduced the transcription and translation of NOX1 in T84 and Caco-2 cells in a time-dependent manner, and that Rac1 is not only known as a key component of the NOX1 complex, but also implicated in cell dynamic morphology [19, 20], we hypothesised Rac1-mediated NOX1 might modulate membrane ruffling and cytoskeleton rearrangement which might in turn affect *C. jejuni* interaction with IECs. Therefore, we investigated the role of NOX1 in *C. jejuni* interaction, invasion, and intracellular survival in IECs by transiently pretreating T84 and Caco-2 cells with DPI (10 $\mu$M) which is known to inhibit activity of flavoenzymes including NOX complex [38]. First, we demonstrated that DPI reduced ROS in T84 and Caco-2 cells (Figure S3). As

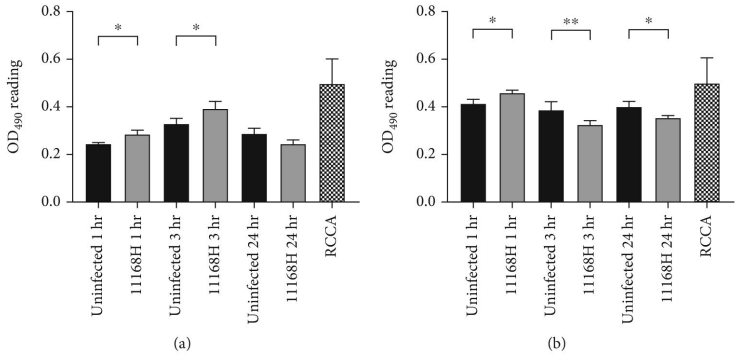


FIGURE 4: *C. jejuni* modulates activity of small GTPase Rac1 in T84 and Caco-2 cells. (a) T84 and (b) Caco-2 cells were infected with *C. jejuni* 11168H strain for 1, 3, and 24 hours, and the activation of small GTPase Rac1 in each time point was measured. Constitutively, active Rac1 (RCCA) was used as a positive control. Experiments were repeated in three biological and three technical replicates. Asterisks denote a statistically significant difference ($^{*}p < 0.05$; $^{**}p < 0.001$).

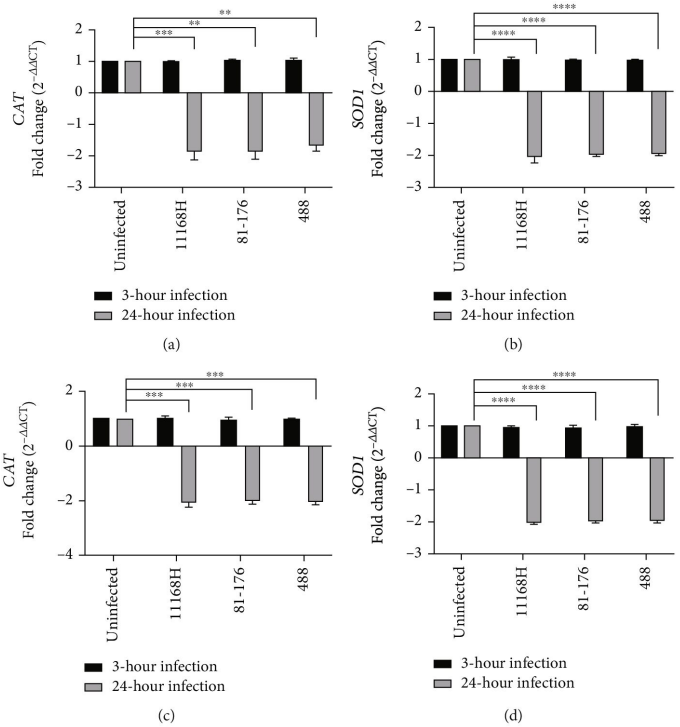


FIGURE 5: qRT-PCR showing expression of human catalase (*CAT*) and superoxide dismutase 1 (*SOD1*) in T84 and Caco-2 cells. (a, b) T84 and (c, d) Caco-2 cells were infected with *C. jejuni* for 3 or 24 hours, and transcriptional levels of *CAT* and *SOD1* were measured. *GAPDH* was used as an internal control. Experiments were repeated in three biological and three technical replicates. Asterisks denote a statistically significant difference ($^{**}p < 0.01$; $^{***}p < 0.001$; $^{****}p < 0.0001$).

shown in Figures 6(a), 6(c), and 6(e), pretreatment of T84 cells by DPI significantly reduced the ability of *C. jejuni* to interact, invade, and survive intracellularly in T84 cells. Similarly, as shown in Figures 6(b), 6(d), and 6(f), *C. jejuni* infected with DPI-treated Caco-2 cells showed significant reduction in interaction, invasion, and intracellular survival compared to untreated Caco-2 cells. Since our data revealed *C. jejuni* reduced interaction, invasion, and intracellular survival between the control- and DPI-treated T84 and Caco-2 cells, we next evaluated the viability of *C. jejuni*, T84, and Caco-2 cells coincubated with DPI. Treatment with DPI did not affect viability of IECs (Figure S4) or *C. jejuni* (Figure S5). Thus, our observations suggest further inhibition of NOX1 with DPI is detrimental to *C. jejuni* interaction, invasion, and intracellular survival in IECs.

*3.6. NOX1 Silencing by siRNA Impairs Campylobacter jejuni Interaction, Invasion, and Intracellular Survival in Caco-2 Cells in vitro.* As DPI is a pan-NOX inhibitor, we silenced NOX1 expression in Caco-2 cells by delivering specific small interfering RNA (siRNA) into cultured Caco-2 cells. We used siRNA sequence which targets regions of NOX1 for silencing. As a negative control, we used a nontargeting scrambled RNA sequence which is not complementary to the *NOX1* mRNA. As shown in Figures 7(a) and 7(b), transcriptional and translational levels of NOX1 were significantly decreased in cells treated with NOX1 siRNA, relative to that in mock-treated Caco-2 controls. We further confirmed reduced activity of NOX1 by demonstrating significant reduction in extracellular ROS (Figure 7(c)). We showed that NOX1 siRNA transfection did not affect viability of Caco-2 cells (Figure S6). Based on these results, we further investigated interaction, invasion, and intracellular survival of *C. jejuni* within Caco-2 cells (Figures 7(d)–7(f)). Our result showed significant decrease in *C. jejuni* interaction, invasion, and intracellular survival when compared to nontransfected controls. This result highlights a correlation between reduced NOX1 expressions with a reduction in *C. jejuni* infection. Taken together, our results demonstrate that NOX1 is a critical host factor for *C. jejuni* interaction, invasion, and intracellular survival.

## 4. Discussion

Upon infection, host cells induce a range of cellular responses to remove offending pathogens. However, bacterial pathogens often target host organelle(s), signalling pathway(s), or immune responses to evade host defence mechanisms [1]. Disruption of ROS production in host cells by bacterial pathogens has been previously reported [39, 40]. *S. typhimurium* pathogenicity island-2 encoding Type III Secretion System (T3SS) inhibits ROS production in human macrophages by preventing NOX2 assembly [39, 41]. In addition, *Pseudomonas aeruginosa* T3SS effector, ExoS, disrupts ROS production in human neutrophils by ADP-ribosylating Ras and inhibiting its activity which is essential for NOX2 assembly [40].

We have characterised the ability of distinct *C. jejuni* strains to modulate intracellular and extracellular ROS from human IECs *in vitro*. ROS production by human IECs is a major defence mechanism, yet how *C. jejuni* evades ROS remains unclear. Our work establishes that in contrast to other enteric pathogens, *C. jejuni* uses a different mechanism involving downregulation of NOX1 expression to modulate ROS in human IECs [24–27]. We examined three different *C. jejuni* strains using two different human IECs and showed that *C. jejuni* strains modulate intracellular and extracellular ROS from human IECs via the differential regulation of the transcription and translation of NOX1 which is a major ROS source in IECs [13]. Interestingly, a previous study demonstrated that *C. jejuni* 81-176 induces extracellular ROS production through NOX1 activation in human ileocecal adenocarcinoma-derived HCT-8 cells [42]. To further understand the implications of *C. jejuni* transcriptional and translational downregulation of NOX1 in T84 and Caco-2 cells, we revealed similarities with some other enteropathogens and also differences amongst others including the *C. jejuni* strain 81-176 [24–27]. Enteropathogens such as *E. coli*, *Salmonella* spp., and *H. pylori* upregulate expression of NOX1 and ROS production in infected IECs [24–27]. Our findings confirmed downregulation of ROS production by *C. jejuni* is strain dependent. In contrast to *C. jejuni* 11168H and 488 strains, *C. jejuni* 81-176 induced extracellular ROS in T84 and Caco-2 cells at 3 hours of postinfection. Induction of extracellular ROS by *C. jejuni* 81-176 at this earlier infection time point was also observed previously [42]. We hypothesise *C. jejuni* 81-176 might have additional bacterial determinants which may induce host extracellular ROS independent of NOX1 modulation (*e.g.*, the pVir and pTet plasmids which encode putative Type IV Secretion Systems (T4SS)) [43, 44]. We also noted a difference between the ability of *C. jejuni* strains to regulate expression of NOX1 in T84 and Caco-2 cells. This difference could be due to variations between the two cell lines. Caco-2 cells possess characteristic enterocytes, whereas T84 cells possess characteristic colonocytes throughout differentiation [45]. In addition, previous studies have shown that reduced *NOX1* mRNA was present in the ileum than in the colon of healthy patients suggesting there is a gradient in NOX1 expression from the small intestine to large intestine [46]. In our study, the lower expression of *NOX1* mRNA detected in Caco-2 cells compared to T84 cells was also observed.

As ROS homeostasis in the GI tract is regulated by multiple antioxidant enzymes [13], *C. jejuni*-mediated modulation of *CAT* and *SOD1* at the transcriptional level was investigated. Our data demonstrated C. *jejuni* strains did not affect transcriptional levels of *CAT* and *SOD1* in T84 and Caco-2 cells after 3 hours of infection, but they significantly downregulated expression of both genes after 24 hours. To our knowledge, this is the first data on *C. jejuni* modulation of antioxidant-related genes in human IECs *in vitro*. Our observations imply *C. jejuni* might modulate intracellular or extracellular ROS after 3 hours of infection without modulating expression of *CAT* and *SOD1*. These results also suggest that there could be additional mechanisms of *C. jejuni*-mediated reduction of ROS because *C. jejuni* was able to reduce ROS after 24 hours of infection even though transcription levels of antioxidant-related genes

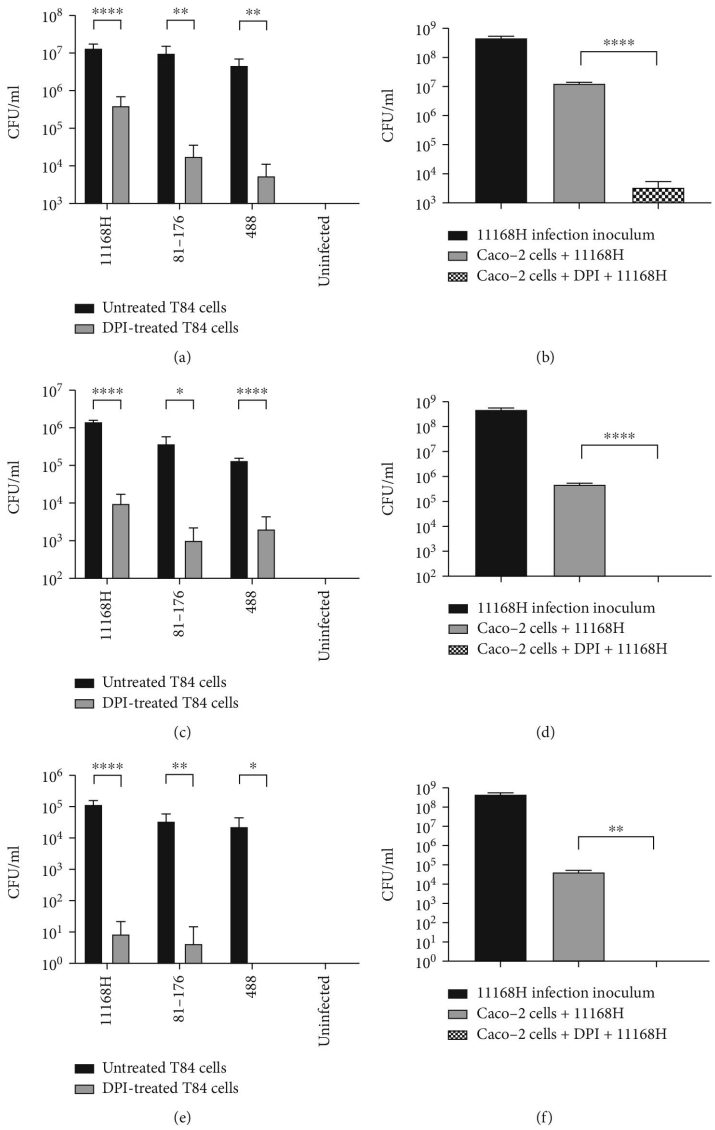


Figure 6: The effect of DPI on *C. jejuni* interaction, invasion, and intracellular survival. T84 and Caco-2 cells were pretreated with 10 $\mu$M of DPI for 1 hour and infected with *C. jejuni* for 3 hours. (a) T84 and (b) Caco-2 cells were washed with PBS and lysed, and the numbers of interacting bacteria were assessed. (c, d) For invasion assay, after infection with *C. jejuni*, *IECs* were incubated with gentamicin (150 $\mu$g/ml) for 2 hours to kill extracellular bacteria and then lysed, and the numbers of intracellular bacteria were assessed. (e, f) For intracellular survival assay, 2 hours of gentamicin treatment was followed by further incubation with gentamicin (10 $\mu$g/ml) for 18 hours. Then, cells were lysed, and the numbers of intracellular bacteria were assessed. Experiments were repeated in three biological and three technical replicates. Asterisks denote a statistically significant difference ($^{*}p < 0.05$; $^{**}p < 0.01$; $^{****}p < 0.0001$).

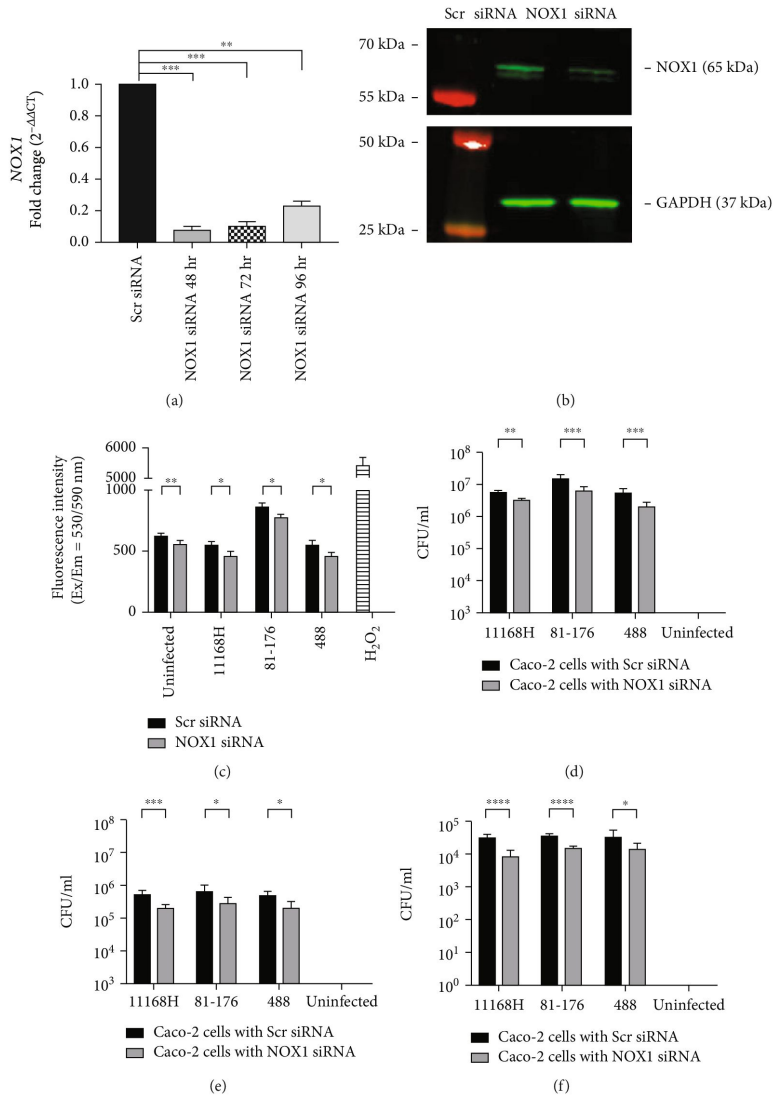


FIGURE 7: The effect of NOX1 silencing on *C. jejuni* interaction, invasion, and intracellular survival. Caco-2 cells were transfected with NOX1 siRNA or scrambled siRNA (Scr siRNA). (a) qRT-PCR showing expression of *NOX1* after siRNA transfection. (b) Western blotting showing expression of NOX1 after 72 hours of siRNA transfection. (c) Detection of extracellular ROS from Caco-2 cells after 72 hours of siRNA transfection followed by coincubation of *C. jejuni* for 3 hours. (d) After 72 hours of siRNA transfection followed by *C. jejuni* infection for 3 hours, Caco-2 cells were washed with PBS and lysed and the numbers of interacting bacteria were assessed or (e) for invasion assay, the cells were incubated with gentamicin (150 $\mu$g/ml) for 2 hours to kill extracellular bacteria and then lysed, and the numbers of intracellular bacteria were assessed. (f) For intracellular survival assay, 2 hours of gentamicin treatment was followed by further incubation with gentamicin (10 $\mu$g/ml) for 18 hours. Then, the cells were lysed, and the number of intracellular bacteria was determined. Experiments were repeated in three biological and three technical replicates. Asterisks denote a statistically significant difference ($^{*}p < 0.05$; $^{**}p < 0.01$; $^{***}p < 0.001$; $^{****}p < 0.0001$).

*CAT* and *SOD1* were downregulated. However, we cannot disregard the possibilities that *C. jejuni* might secrete its own antioxidant-related proteins that may mitigate host cellular ROS and/or *C. jejuni* might induce expression of other host antioxidant genes such as mitochondrial superoxide dismutase (SOD2), extracellular superoxide dismutase (SOD3), and glutathione peroxidase [13]. A previous study demonstrated *Pseudomonas* pyocyanin decreased expression of human CAT but not SOD1 in the human A549 alveolar type II epithelial cells [47]. *C. jejuni* might produce pyocyanin-like metabolites but this is not yet investigated. In addition, downregulation of genes encoding CAT and SOD1 might be a host cellular strategy to produce ROS for clearance of *C. jejuni*.

Upon adhering to host cells, *C. jejuni* modulates small GTPase Rac1 resulting in actin filament reorganisation to promote invasion. Activation of Rac1 in human embryonic INT 407 cells was observed between 45 minutes and 4 hours after *C. jejuni* infection [10, 37]. In accordance with previous studies, we demonstrated *C. jejuni* activates Rac1 at early infection time points. In contrast, a decrease of active Rac1 was detected at the later infection time point. Given the association of the active GTP-bound Rac1 and NOX1 activity, the early activation of Rac1 in IECs suggests that *C. jejuni* uses an intriguing system which we hypothesise could have temporally nonoverlapping mechanisms. The GTP-bound Rac1 observed in early time points may be linked to the requirement for *C. jejuni* to establish adhesion/invasion utilising a distinct mechanism in its infection cycle. Although the inactive GDP-bound Rac1 observed at the later time point of 24 hours, this suggests *C. jejuni* clearly possesses yet-to-be discovered mechanisms that enable differential regulation of NOX1 relative to modulation of Rac1. We also observe the pattern of active GTP-bound Rac1 in Caco-2 cells that is different to T84 cells. Such a difference may be due to the signalling cues between the cells and *C. jejuni* preference to efficiently interact with individual cells by binding, invading, and intracellularly surviving from distinct states during its infection.

The impact of differential regulation of NOX1 on *C. jejuni* interaction, invasion, and intracellular survival in human IECs remains unclear. Surprisingly, chemical inhibition of NOX1 significantly reduced the ability of *C. jejuni* to interact, invade, and survive intracellularly in T84 and Caco-2 cells. It is possible that DPI may inadvertently affect local cellular receptors that *C. jejuni* uses to bind human IECs. Since DPI is not a specific inhibitor of NOX1 [38], we repeated these experiments using siRNA silencing of *NOX1* which demonstrated similar findings, suggesting that NOX1 is indirectly necessary for *C. jejuni* interaction, invasion, and intracellular survival. Previous studies have demonstrated that DPI treatment reduced fibronectin expression in rat renal tubular epithelial cells [48], and a pan-NOX inhibitor APX-115 reduced fibronectin production in mesangial cells [49]. As fibronectin has been demonstrated as a key host receptor that *C. jejuni* uses to bind and invade human IECs [50], we hypothesise that silencing *NOX1* might also affect expression of a key receptor fibronectin as is the case following DPI treatment, and this might be responsible for the reduced interaction and invasion of *C. jejuni* strains. We hypothesise that *C. jejuni* fine-tunes the modulation of NOX1 in a cell-specific manner, so that there is no impact on its ability to adhere and invade at early infection time points and then subsequently downregulates NOX1 to obtain the potential benefits of ROS reduction for its enhanced survivability at later infection time points. However, the broader nonspecificity of DPI and siRNA silencing experiments means that there could be alternative mechanisms in play.

We have demonstrated that *C. jejuni* modulates intracellular and extracellular ROS in human T84 and Caco-2 cells. Our observations link *C. jejuni* ROS modulation to the transcriptional and translational downregulation of NOX1. These findings also point to a further role of Rac1 in NOX1 modulation and downstream interaction. Based on chemical inhibition and silencing of NOX1 expression and translation, our findings suggest an indirect role of NOX1 for adhesion, invasion, and intracellular survival of *C. jejuni*. In this context, further understanding *C. jejuni* determinants that lead to ROS and/or NOX1 modulation in IECs will provide greater insights into how *C. jejuni* manipulate host defence mechanisms and cause diarrhoeal disease.

## Data Availability

The raw data used to support the findings of this study are available from the corresponding authors upon request.

## Disclosure

This manuscript is available as a preprint on bioRxiv [51].

## Conflicts of Interest

The authors declare that they have no conflicts of interest.

## Authors' Contributions

Abdi Elmi and Ozan Gundogdu share joint senior authorship.

## Acknowledgments

We would like to acknowledge Marta Mauri for kind advice on siRNA transfection. This research was performed as part of the employment of the authors at the London School of Hygiene & Tropical Medicine.

## Supplementary Materials

*Supplementary 1*. Supplementary Figure S1: trypan blue exclusion assay with *C. jejuni* infection.

*Supplementary 2*. Supplementary Figure S2: detection of extracellular ROS in DMEM inoculated with *C. jejuni*.

*Supplementary 3*. Supplementary Figure S3: detection of intracellular ROS and extracellular ROS in T84 and Caco-2 cells with or without DPI pretreatment followed by *C. jejuni* infection.

*Supplementary 4.* Supplementary Figure S4: assessment of cell viability using trypan blue exclusion assay with DPI and/or gentamicin treatment.

*Supplementary 5.* Supplementary Figure S5: *C. jejuni* viability assay with DPI treatment.

*Supplementary 6.* Supplementary Figure S6: assessment of cell viability using trypan blue exclusion assay with NOX1 siRNA transfection.

*Supplementary 7.* Supplementary Table S1: *C. jejuni* strains used in this study.

*Supplementary 8.* Supplementary Table S2: primers used in this study.

## References


[1] P. Escoll, S. Mondino, M. Rolando, and C. Buchrieser, "Targeting of host organelles by pathogenic bacteria: a sophisticated subversion strategy," *Nature Reviews. Microbiology*, vol. 14, no. 1, pp. 5–19, 2016.

[2] S. Asrat, D. A. de Jesús, A. D. Hempstead, V. Ramabhadran, and R. R. Isberg, "Bacterial pathogen manipulation of host membrane trafficking," *Annual Review of Cell and Developmental Biology*, vol. 30, no. 1, pp. 79–109, 2014.

[3] L. Arbibe, D. W. Kim, E. Batsche et al., "An injected bacterial effector targets chromatin access for transcription factor NF-κB to alter transcription of host genes involved in immune responses," *Nature Immunology*, vol. 8, no. 1, pp. 47–56, 2007.

[4] T. Rudel, O. Kepp, and V. Kozjak-Pavlovic, "Interactions between bacterial pathogens and mitochondrial cell death pathways," *Nature Reviews. Microbiology*, vol. 8, no. 10, pp. 693–705, 2010.

[5] J. Silva, D. Leite, M. Fernandes, C. Mena, P. A. Gibbs, and P. Teixeira, "*Campylobacter* spp. as a foodborne pathogen: a review," *Frontiers in Microbiology*, vol. 2, pp. 1–12, 2011.

[6] N. O. Kaakoush, N. Castaño-Rodríguez, H. M. Mitchell, and S. M. Man, "Global epidemiology of *Campylobacter* infection," *Clinical Microbiology Reviews*, vol. 28, no. 3, pp. 687–720, 2015.

[7] H. J. Willison, B. C. Jacobs, and P. A. van Doorn, "Guillain-Barre syndrome," *The Lancet*, vol. 388, no. 10045, pp. 717–727, 2016.

[8] C. Amour, J. Gratz, E. Mduma et al., "Epidemiology and impact of *Campylobacter* infection in children in 8 low-resource settings: results from the MAL-ED study," *Clinical Infectious Diseases*, vol. 63, no. 9, pp. 1171–1179, 2016.

[9] O. Gundogdu, D. T. da Silva, B. Mohammad et al., "The *Campylobacter jejuni* oxidative stress regulator RrpB is associated with a genomic hypervariable region and altered oxidative stress resistance," *Frontiers in Microbiology*, vol. 7, pp. 2117–2117, 2016.

[10] N. M. Negretti, C. R. Gourley, P. K. Talukdar et al., "The *Campylobacter jejuni* CiaD effector co-opts the host cell protein IQGAP1 to promote cell entry," *Nature Communications*, vol. 12, no. 1, pp. 1339–1339, 2021.

[11] M. E. Konkel, S. F. Hayes, L. A. Joens, and W. Cieplak Jr., "Characteristics of the internalization and intracellular survival of Campylobacter jejuni in human epithelial cell cultures," *Microbial Pathogenesis*, vol. 13, no. 5, pp. 357–370, 1992.

[12] R. O. Watson and J. E. Galán, "*Campylobacter jejuni* survives within epithelial cells by avoiding delivery to lysosomes," *PLoS Pathogens*, vol. 4, no. 1, article e14, 2008.

[13] G. Aviello and U. Knaus, "ROS in gastrointestinal inflammation: rescue or sabotage?," *British Journal of Pharmacology*, vol. 174, no. 12, pp. 1704–1718, 2017.

[14] C. N. Paiva and M. T. Bozza, "Are reactive oxygen species always detrimental to pathogens?," *Antioxidants & Redox Signaling*, vol. 20, no. 6, pp. 1000–1037, 2014.

[15] J. F. Burgueño, J. Fritsch, A. M. Santander et al., "Intestinal epithelial cells respond to chronic inflammation and dysbiosis by synthesizing $H_2O_2$," *Frontiers in Physiology*, vol. 10, pp. 1484–1484, 2019.

[16] K. M. Holmström and T. Finkel, "Cellular mechanisms and physiological consequences of redox-dependent signalling," *Nature Reviews. Molecular Cell Biology*, vol. 15, no. 6, pp. 411–421, 2014.

[17] R. P. Brandes, N. Weissmann, and K. Schröder, "Nox family NADPH oxidases: molecular mechanisms of activation," *Free Radical Biology and Medicine*, vol. 76, pp. 208–226, 2014.

[18] H. Sumimoto, K. Miyano, and R. Takeya, "Molecular composition and regulation of the Nox family NAD(P)H oxidases," *Biochemical and Biophysical Research Communications*, vol. 338, no. 1, pp. 677–686, 2005.

[19] Y. Nisimoto, R. Tsubouchi, B. A. Diebold et al., "Activation of NADPH oxidase 1 in tumour colon epithelial cells," *Biochemical Journal*, vol. 415, no. 1, pp. 57–65, 2008.

[20] T. Ueyama, M. Geiszt, and T. L. Leto, "Involvement of Rac1 in activation of multicomponent Nox1- and Nox3-based NADPH oxidases," *Molecular and Cellular Biology*, vol. 26, no. 6, pp. 2160–2174, 2006.

[21] A. Juhasz, S. Markel, S. Gaur et al., "NOX1 modulates colon cancer growth and angiogenesis," *The Journal of Biological Chemistry*, vol. 292, no. 19, pp. 7866–7887, 2017.

[22] S. Lipinski, B. S. Petersen, M. Barann et al., "Missense variants in NOX1 and p22phox in a case of very-early-onset inflammatory bowel disease are functionally linked to NOD2," *Cold Spring Harbor Molecular Case Studies*, vol. 5, no. 1, article a002428, 2019.

[23] C. Matziouridou, S. D. C. Rocha, O. A. Haabeth, K. Rudi, H. Carlsen, and A. Kielland, "iNOS- and Nox1-dependent ROS production maintains bacterial homeostasis in the ileum of mice," *Mucosal Immunology*, vol. 11, no. 3, pp. 774–784, 2018.

[24] I. Elatrech, V. Marzaioli, H. Boukemara et al., "*Escherichia coli LF82* differentially regulates ROS production and mucin expression in intestinal epithelial T84 cells: implication of Nox 1," *Inflammatory Bowel Disease*, vol. 21, no. 5, pp. 1018–1026, 2015.

[25] T. Kawahara, Y. Kuwano, S. Teshima-Kondo et al., "Role of nicotinamide adenine dinucleotide phosphate oxidase 1 in oxidative burst response to Toll-like receptor 5 signaling in large intestinal epithelial cells," *The Journal of Immunology*, vol. 172, no. 5, pp. 3051–3058, 2004.

[26] G. Den Hartog, R. Chattopadhyay, A. Ablack et al., "Regulation of Rac 1 and reactive oxygen species production in response to infection of gastrointestinal epithelia," *PLoS Pathogens*, vol. 12, no. 1, article e1005382, 2016.

[27] T. Kawahara, M. Kohjima, Y. Kuwano et al., "*Helicobacter pylori* lipopolysaccharide activates Rac1 and transcription of NADPH oxidase Nox1 and its organizer NoxO1 in guinea

pig gastric mucosal cells," *The American Journal of Physiology-Cell Physiology*, vol. 288, no. 2, pp. C450–C457, 2005.

[28] P. M. Burnham and D. R. Hendrixson, "Campylobacter jejuni: collective components promoting a successful enteric lifestyle," *Nature Reviews. Microbiology*, vol. 16, no. 9, pp. 551–565, 2018.

[29] A. Elmi, F. Nasher, N. Dorrell, B. Wren, and O. Gundogdu, "Revisiting Campylobacter jejuni virulence and fitness factors: role in sensing, adapting, and competing," *Frontiers in Cellular and Infection Microbiology*, vol. 10, article 607704, 2020.

[30] S. Hwang, M. Kim, S. Ryu, and B. Jeon, "Regulation of oxidative stress response by CosR, an essential response regulator in *Campylobacter jejuni*," *PLoS One*, vol. 6, no. 7, article e22300, 2011.

[31] K. Palyada, Y.-Q. Sun, A. Flint, J. Butcher, H. Naikare, and A. Stintzi, "Characterization of the oxidative stress stimulon and PerR regulon of Campylobacter jejuni," *BMC Genomics*, vol. 10, no. 1, pp. 481–481, 2009.

[32] A. Elmi, F. Nasher, H. Jagatia et al., "*Campylobacter jejuni* outer membrane vesicle-associated proteolytic activity promotes bacterial invasion by mediating cleavage of intestinal epithelial cell E-cadherin and occludin," *Cellular Microbiology*, vol. 18, no. 4, pp. 561–572, 2016.

[33] O. Gundogdu, D. C. Mills, A. Elmi, M. J. Martin, B. W. Wren, and N. Dorrell, "The *Campylobacter jejuni* transcriptional regulator Cj1556 plays a role in the oxidative and aerobic stress response and is important for bacterial survival in vivo," *Journal of Bacteriology*, vol. 193, no. 16, pp. 4238–4249, 2011.

[34] T. D. Schmittgen and K. J. Livak, "Analyzing real-time PCR data by the comparative $C_T$ method," *Nature Protocols*, vol. 3, no. 6, pp. 1101–1108, 2008.

[35] C. A. Schneider, W. S. Rasband, and K. W. Eliceiri, "NIH Image to ImageJ: 25 years of image analysis," *Nature Methods*, vol. 9, no. 7, pp. 671–675, 2012.

[36] R. G. Hodge and A. J. Ridley, "Regulating Rho GTPases and their regulators," *Nature Reviews. Molecular Cell Biology*, vol. 17, no. 8, pp. 496–510, 2016.

[37] M. Krause-Gruszczynska, M. Rohde, R. Hartig et al., "Role of the small Rho GTPases Rac1 and Cdc42 in host cell invasion of *Campylobacter jejuni*," *Cellular Microbiology*, vol. 9, no. 10, pp. 2431–2444, 2007.

[38] C. Riganti, E. Gazzano, M. Polimeni, C. Costamagna, A. Bosia, and D. Ghigo, "Diphenyleneiodonium inhibits the cell redox metabolism and induces oxidative stress," *The Journal of Biological Chemistry*, vol. 279, no. 46, pp. 47726–47731, 2004.

[39] A. Gallois, J. R. Klein, L.-A. H. Allen, B. D. Jones, and W. M. Nauseef, "Salmonella pathogenicity island 2-encoded type III secretion system mediates exclusion of NADPH oxidase assembly from the phagosomal membrane," *The Journal of Immunology*, vol. 166, no. 9, pp. 5741–5748, 2001, 5741.

[40] C. Vareechon, S. E. Zmina, M. Karmakar, E. Pearlman, and A. Rietsch, "Pseudomonas aeruginosa effector ExoS inhibits ROS production in human neutrophils," *Cell Host & Microbe*, vol. 21, no. 5, pp. 611–618.e5, 2017.

[41] A. N. Antoniou, I. Lenart, J. Kriston-Vizi et al., "*Salmonella* exploits HLA-B27 and host unfolded protein responses to promote intracellular replication," *Annals of the Rheumatic Diseases*, vol. 78, no. 1, pp. 74–82, 2019.

[42] N. Corcionivoschi, L. A. Alvarez, T. H. Sharp et al., "Mucosal Reactive Oxygen Species Decrease Virulence by Disrupting *Campylobacter jejuni* Phosphotyrosine Signaling," *Cell Host & Microbe*, vol. 12, no. 1, pp. 47–59, 2012.

[43] D. J. Bacon, R. A. Alm, L. Hu et al., "DNA sequence and mutational analyses of the pVir plasmid of *Campylobacter jejuni* 81-176," *Infection and Immunity*, vol. 70, no. 11, pp. 6242–6250, 2002.

[44] R. A. Batchelor, B. M. Pearson, L. M. Friis, P. Guerry, and J. M. Wells, "Nucleotide sequences and comparison of two large conjugative plasmids from different *Campylobacter* species," *Microbiology*, vol. 150, no. 10, pp. 3507–3517, 2004.

[45] S. Devriese, L. Van den Bossche, S. Van Welden et al., "T84 monolayers are superior to Caco-2 as a model system of colonocytes," *Histochemistry and Cell Biology*, vol. 148, no. 1, pp. 85–93, 2017.

[46] T. Schwerd, R. V. Bryant, S. Pandey et al., "NOX1 loss-of-function genetic variants in patients with inflammatory bowel disease," *Mucosal Immunology*, vol. 11, 2018.

[47] Y. Q. O'Malley, K. J. Reszka, G. T. Rasmussen, M. Y. Abdalla, G. M. Denning, and B. E. Britigan, "The *Pseudomonas* secretory product pyocyanin inhibits catalase activity in human lung epithelial cells," *American Journal of Physiology. Lung Cellular and Molecular Physiology*, vol. 285, no. 5, pp. L1077–L1086, 2003.

[48] D. Y. Rhyu, Y. Yang, H. Ha et al., "Role of reactive oxygen species in TGF-beta1-induced mitogen-activated protein kinase activation and epithelial-mesenchymal transition in renal tubular epithelial cells," *Journal of the American Society of Nephrology*, vol. 16, no. 3, pp. 667–675, 2005.

[49] J. J. Cha, H. S. Min, K. T. Kim et al., "APX-115, a first-in-class pan-NADPH oxidase (Nox) inhibitor, protects *db*/*db* mice from renal injury," *Laboratory Investigation*, vol. 97, no. 4, pp. 419–431, 2017.

[50] M. E. Konkel, P. K. Talukdar, N. M. Negretti, and C. M. Klappenbach, "Taking control: *Campylobacter jejuni* binding to fibronectin sets the stage for cellular adherence and invasion," *Frontiers in Microbiology*, vol. 11, pp. 564–564, 2020.

[51] G. Hong, C. Davies, Z. Omole et al., "*Campylobacter jejuni* modulates reactive oxygen species production and NADPH oxidase 1 expression in human intestinal epithelial cells," *bioRxiv*, 2022.